Universidad de Málaga

Escuela Técnica Superior de Ingeniería de Telecomunicación

TESIS DOCTORAL

Optimization of Mobility Parameters using Fuzzy Logic and Reinforcement Learning in Self-Organizing Networks

Autor:

Pablo Muñoz Luengo

Directora:

Raquel Barco Moreno

AUTOR: Pablo Muñoz Luengo

http://orcid.org/0000-0002-3265-5728

EDITA: Publicaciones y Divulgación Científica. Universidad de Málaga

Dra. Dª Raquel Barco Moreno, profesora doctora del Departamento de Ingeniería de Comunicaciones de la Universidad de Málaga

CERTIFICA:

Que **D. Pablo Muñoz Luengo**, Ingeniero de Telecomunicación, ha realizado en el Departamento de Ingeniería de Comunicaciones de la Universidad de Málaga, bajo su dirección el trabajo de investigación correspondiente a su TESIS DOCTORAL titulada:

Optimization of Mobility Parameters using Fuzzy Logic and Reinforcement Learning in Self-Organizing Networks

En dicho trabajo se han propuesto aportaciones originales para diversos problemas de optimización en redes móviles, en particular, el balance de carga mediante movilidad, la optimización del procedimiento de traspaso así como su coordinación con el balance de carga y, por último, el direccionamiento de tráfico en escenarios de redes heterogéneas. También se ha propuesto un modelo de abstracción para un simulador de la tecnología celular LTE que ha permitido la evaluación y validación de las técnicas propuestas. Los resultados expuestos han dado lugar a publicaciones en revistas y aportaciones a congresos internacionales.

Por todo ello, considera que esta Tesis es apta para su presentación al Tribunal que ha de juzgarla. Y para que conste a efectos de lo establecido en el Artículo 8º del Real Decreto 778/1998, Real Decreto 56/2005 y Real Decreto 1393/2007, reguladores de los Estudios de Tercer Ciclo-Doctorado, AUTORIZA la presentación de esta Tesis en la Universidad de Málaga.

Málaga a _____ de _____ de _____

Fdo: Dra. Dª. Raquel Barco Moreno

UNIVERSIDAD DE MÁLAGA
ESCUELA TÉCNICA SUPERIOR DE INGENIERÍA DE TELECOMUNICACIÓN

Reunido el tribunal examinador en el día de la fecha, constituido por:

Presidente: Dr. D. _____

Secretario: Dr. D. _____

Vocales: Dr. D. _____

Dr. D. _____

Dr. D. _____

para juzgar la Tesis Doctoral titulada *Optimization of Mobility Parameters using Fuzzy Logic and Reinforcement Learning in Self-Organizing Networks* realizada por D. Pablo Muñoz Luengo y dirigida por la Dra. D.ª Raquel Barco Moreno, acordó por

_____ otorgar la calificación de

_____ y para que conste,

se extiende firmada por los componentes del tribunal la presente diligencia.

Málaga a _____ de _____ del _____

El Presidente: El Secretario:

Fdo.: _____ Fdo.: _____

El Vocal: El Vocal: El Vocal:

Fdo.: _____ Fdo.: _____ Fdo.: _____

A mis padres, mi hermano
y Mari Ángeles.

"Men build too many walls and not enough bridges."

Isaac Newton.

Acknowledgements

I still remember the first day I came into the office room in the second block, third floor... and I realized that it was surprisingly empty, "yes, I am opening the lab", I thought. Fortunately, people were gradually arriving and, four years later, I can say that the lab where I have spent an important part of my life has become a comfortable and peaceful working place with very friendly people. Thus, as it could not be otherwise, the first ripe fruit of such a nice atmosphere has been this thesis, and I really hope that it is only the first of many theses.

Firstly, I would like to express my profound gratitude to my supervisor, Raquel Barco, for giving me the opportunity to work in this department, for encouraging me to be self-motivated and ambitious about my career, for her support in crucial moments and for assisting me in writing papers and reviews. I especially appreciate her hard-working attitude.

I would like to thank the other "senior" members of my group. Thanks Matías, who I estimate for his dedication to the students, for lending a hand regardless the workload he is carrying, for the clarity of his explanations and for the vast knowledge he shares with the group. Thanks Salva for being an example to follow. I appreciate his honesty, sympathy and closeness to the people, which are so essential for the working environment. Thanks also go to Fernando, Mariano, Pedro and Marta for their assistance during the meetings.

I wish to thank the people I had the great opportunity to meet beyond the borders. Especially, thanks Daniela Laselva for teaching me to infer and reason properly. She helped me in developing Traffic Steering techniques for heterogeneous networks. I would highlight her ability to transmit, her empathy, her great capacity for work and, more important, her kindness and goodness. Thanks Thomas Jansen for his hospitality, his technical assistance and his positive attitude. He helped me in developing the indoor mobility model. Thanks Preben Mogensen and Thomas Kürner for their attention and for allowing me to work in international environments. Thanks Lisbeth Schiønning for generously assisting me in managing a lot of issues. Thanks also to my office mates abroad, among which are Dennis, Michele, Pannos and Beatriz.

I would like to thank all my office mates in the lab. Special mention to Isa, seated next to me since almost the beginning, she developed the main simulation tool used in this thesis, also participated actively in technical discussions and she has become someone to trust, share my concerns with and whom I would clearly go to for advice. Thanks Jose María for his sympathy, his optimism and his ability to judge well in practical matters. He included the femtocell scenario

in the simulation tool. Thanks Ana Belén for her trust placed in me and for encouraging me when I needed it. Thanks José Ángel and Rocio A. for joining in the lunch and having good times (this also includes Simone and Cristina, from the adjacent lab). Thanks also to Ale, Sergio, Victor, Emil, Ana, Rocio P., Estela, Maite, Jaime, Gonzalo and anyone who has been through the lab contributing to keep a wonderful atmosphere.

I must also acknowledge the financial support given by the projects mentioned below, together with the research group TIC-102 Ingeniería de Comunicaciones and the University of Málaga, which have been equally important to make possible this work and allowed me to present results and exchange knowledge and skills in conferences, journals, workshops and research stays abroad.

Finally, I would like to strongly thank my family for the support they have provided me through my entire life. In particular, thanks to my parents (words are not enough to thank them) for their love and never-ending support and for always encouraging me to do the best for my studies. Thanks to my brother for his tolerance and endurance since I was a baby. Special thanks, of course, to my closer friends since I started this adventure at the university, in particular, to Lucas, Laura D., María, Selu, Laura G., Josema, Sabi, Carlos G., Laura L., Germán, Patri A., Mar, Pablo, Carlos R., Almu, Patri G., Carmen, Fida, Elena, Lydia, Carlos C., Ramón, Cristian and Esther for sharing moments with me to enjoy, clear the mind and recharge batteries. I would also like to express my most sincere gratitude to Mari Ángeles for her love and patience. She inspired me to complete this book. And thanks to God for the impact He has had in my life.

This work has been partially supported by the Junta de Andalucía (Excellence Research Program, project P08-TIC-4052) and by the Spanish Ministry of Science and Innovation (grants TEC2009-13413 and IPT-2011-1272-430000).

Contents

Abstract

In the last years, cellular networks have experienced a large increase in size and complexity. As a result, mobile operators have focused attention on reducing capital expenditures (CAPEX) and operational expenditures (OPEX) of their networks. This fact has stimulated strong research activity in the field of Self-Organizing Networks (SON), which is a set of principles and concepts defined for automating network management while improving network quality. Increasing automation in cellular networks means significant OPEX reduction as fewer personnel are necessary to maintain a network. In addition, network performance is enhanced as the number of human errors is diminished, also taking advantage of the analytical capabilities of computers to introduce more efficient procedures in the network.

The main benefits derived from applying SON functionalities are especially valuable in the Radio Access Network (RAN) segment, since this part of the network usually forms the bottleneck due to its operational complexity and network costs. In particular, the SON functions are classified into three terms: Self-Configuration, Self-Healing and Self-Optimization. The first term, Self-Configuration, attempts to automate network deployment and parameter configuration, e.g. when a new resource is added to the existing infrastructure. Self-Healing is related to failure detection, diagnosis, compensation and recovery in order to cope with major service outages and degradations. Lastly, Self-Optimization aims to dynamically adapt network parameters to improve network quality.

In the context of Self-Optimization, certain functions have been identified as key enablers in the literature, among which are Mobility Load Balancing (MLB) and Mobility Robustness Optimization (MRO). The former is an automated function where cells suffering occasional congestion can transfer load to neighboring cells, which have spare resources, by adjusting mobility parameters. The latter is a solution for automatic detection and correction of errors and suboptimal settings in the mobility configuration, which may lead to a degradation of user performance. In addition, due to the fact that these two functions can adjust the same mobility parameters, a conflict may happen if MLB and MRO tune the parameters in opposite directions. The coordination of these two functions is also an important issue in the context of SON.

On the other hand, the large investments on infrastructure to cope with the growing demand of traffic has led to a heterogeneous network deployment characterized by the presence of different technologies, cell sizes, frequencies, etc. However, these solutions are expected to be insufficient,

meaning that the existing networks will also play a key role in facing that enormous traffic demand. In this context, Traffic Steering (TS) becomes a powerful mechanism in which user distributions across the different operator's networks are modified according to a policy or specific objectives, mainly related to cost, user satisfaction, power consumption, coverage, etc. As a result of applying those TS techniques, the overall network performance is improved.

In this thesis, several optimization techniques for next-generation wireless networks are proposed to solve different problems in the field of SON and heterogeneous networks. The common basis of these problems is that network parameters are automatically tuned to deal with the specific problem. As the set of network parameters is extremely large, this work mainly focuses on parameters involved in mobility management. In addition, the proposed self-tuning schemes are based on Fuzzy Logic Controllers (FLC), whose potential lies in the capability to express the knowledge in a similar way to the human perception and reasoning. In addition, in those cases in which a mathematical approach has been required to optimize the behavior of the FLC, the selected solution has been Reinforcement Learning, since this methodology is especially appropriate for learning from interaction, which becomes essential in complex systems such as wireless networks.

Taking this into account, firstly, a new MLB scheme is proposed to solve persistent congestion problems in next-generation wireless networks, in particular, due to an uneven spatial traffic distribution, which typically leads to an inefficient usage of resources. A key feature of the proposed algorithm is that not only the parameters are optimized, but also the parameter tuning strategy. Secondly, a novel MLB algorithm for enterprise femtocells scenarios is proposed. Such scenarios are characterized by the lack of a thorough deployment of these low-cost nodes, meaning that a more efficient use of radio resources can be achieved by applying effective MLB schemes. As in the previous problem, the optimization of the self-tuning process is also studied in this case. Thirdly, a new self-tuning algorithm for MRO is proposed. This study includes the impact of context factors such as the system load and user speed, as well as a proposal for coordination between the designed MLB and MRO functions. Fourthly, a novel self-tuning algorithm for TS in heterogeneous networks is proposed. The main features of the proposed algorithm are the flexibility to support different operator policies and the adaptation capability to network variations. Finally, with the aim of validating the proposed techniques, a dynamic system-level simulator for Long-Term Evolution (LTE) networks has been designed.

Resumen

En los últimos años, las redes celulares han experimentado un gran crecimiento tanto en tamaño como en complejidad. Como resultado, los operadores móviles han centrado su atención en reducir los gastos de capital (CAPEX) y operacionales (OPEX) de sus redes. Este hecho ha suscitado una fuerte actividad investigadora en el campo de las redes auto-organizativas (*Self-Organizing Networks*, SON), las cuales presentan una serie de principios y conceptos definidos para automatizar la gestión de redes a la vez que se mejora su calidad. La automatización de las redes móviles implica una reducción significativa de los gastos operacionales, debido a que se requiere menos personal para mantener y administrar la red. Además, se mejoran las prestaciones de la red puesto que se disminuye el número de errores humanos y se aprovechan las ventajas de las capacidades de cálculo de los computadores para introducir procedimientos más eficientes en la red.

La aplicación de funcionalidades SON permite obtener grandes beneficios, especialmente en la red de acceso radio (*Radio Access Network*, RAN), debido a que esta parte de la red normalmente es el "cuello de botella" dada su complejidad desde el punto de vista operacional y los costes asociados. Las funciones SON se clasifican en tres categorías: auto-configuración, auto-curación y auto-optimización. La primera categoría, auto-configuración, trata de automatizar el despliegue de la red y la configuración de parámetros, por ejemplo, cuando un nuevo elemento de red se añade a la infraestructura existente. La auto-curación está relacionada con la detección, diagnosis, compensación y recuperación de fallos con el objetivo de hacer frente a cortes y degradaciones de servicio importantes. Por último, la auto-optimización trata de adaptar dinámicamente los parámetros de red para mejorar su calidad.

Dentro de la categoría de auto-optimización, ciertas funciones han adquirido gran relevancia en la bibliografía, entre las que se encuentran el balance de carga mediante movilidad (*Mobility Load Balancing*, MLB) y la optimización de la movilidad (*Mobility Robustness Optimization*, MRO). La primera de ellas, MLB, es una función automática en la que las celdas que sufren congestión pueden transferir, mediante un correcto ajuste de los parámetros de movilidad, parte de la carga a sus celdas vecinas, las cuales deben disponer de suficientes recursos libres. MRO es una función que permite detección y corrección automática de errores y ajustes sub-óptimos en la configuración de movilidad, los cuales pueden llevar a una degradación de las prestaciones de usuario. Además, debido a que estas dos funciones pueden ajustar los mismos parámetros de

movilidad, podría existir un conflicto si MLB y MRO ajustan dichos parámetros en direcciones opuestas. Por tanto, la coordinación de ambas funciones es también una cuestión importante en el contexto de SON.

Por otro lado, la enorme inversión en infraestructura realizada por los operadores para satisfacer la creciente demanda de tráfico ha dado lugar al despliegue de redes heterogéneas, las cuales están caracterizadas por la presencia de diferentes tecnologías, tamaños de celdas, frecuencias de uso, etc. Sin embargo, es probable que estas soluciones sean insuficientes, de manera que las redes que ya han sido desplegadas con anterioridad también jueguen un papel esencial para hacer frente al fuerte crecimiento de la demanda de tráfico. En este contexto, el direccionamiento de tráfico (*Traffic Steering*, TS) es un potente mecanismo consistente en modificar la distribución de usuarios en las diferentes redes pertenecientes al operador con la intención de satisfacer una determinada política u objetivo, principalmente relacionado con los costes, la satisfacción de usuario, el consumo de potencia, la cobertura, etc. Como resultado de aplicar estas técnicas, se mejoran las prestaciones globales de red.

En la presente tesis se proponen diversas técnicas de optimización para redes inalámbricas de próxima generación con el objetivo de resolver diferentes problemas en el campo de SON y redes heterogéneas. El fundamento básico de todas las técnicas propuestas es que los parámetros de red son ajustados automáticamente para resolver un problema específico. Puesto que el conjunto de parámetros de red existente es muy grande, este trabajo se centra fundamentalmente en aquellos parámetros que forman parte de la gestión de movilidad. Además, los esquemas de auto-ajuste propuestos están basados en controladores de lógica difusa (*Fuzzy Logic Controller*, FLC), cuyo potencial radica en la capacidad de poder expresar el conocimiento de una manera similar al razonamiento y la percepción humana. Por otra parte, en aquellos casos en los que se requiere una herramienta matemática para optimizar el comportamiento del FLC, en esta tesis la solución adoptada ha sido el uso de aprendizaje por refuerzo, debido a que esta metodología es especialmente apropiada para el aprendizaje mediante interacción, el cual se hace esencial en sistemas complejos como es el caso de las redes inalámbricas.

Teniendo en cuenta esto, en primer lugar, se ha propuesto un esquema para MLB con la finalidad de resolver problemas de congestión persistente en redes de inalámbricas de próxima generación, en particular, debidos a una distribución espacial de tráfico desigual, la cual típicamente conlleva un uso ineficiente de los recursos. Una característica clave del algoritmo propuesto es que no solo se optimizan los parámetros, sino también la propia estrategia de ajuste de parámetros. En segundo lugar, se ha propuesto un esquema para MLB aplicable en escenarios de femtoceldas de oficina o corporativos. Estos escenarios se caracterizan por la falta de un riguroso análisis en la etapa de despliegue, de manera que es posible realizar un uso más eficiente de los recursos radio en la etapa de explotación mediante la aplicación de técnicas efectivas de MLB. Al igual que en el problema anterior, en este caso la optimización del proceso de auto-ajuste también forma parte del estudio. En tercer lugar, se ha propuesto un algoritmo de auto-ajuste para MRO. Este estudio incluye un análisis del impacto de factores contextuales tales como la carga del sistema y la velocidad de usuario, así como una propuesta para la coordinación de los esquemas de MLB y MRO diseñados. En cuarto lugar, se ha propuesto un algoritmo de auto-ajuste para TS en el contexto de redes heterogéneas. Las principales características del algoritmo propuesto son la

flexibilidad para soportar diferentes políticas del operador y la capacidad de adaptación a variaciones en la red. Finalmente, con el objetivo de validar las técnicas propuestas, se ha diseñado un simulador dinámico de nivel de sistema para redes *Long-Term Evolution* (LTE).

List of Contributions

The following list presents the publications related to this thesis.

Journals

Arising from this thesis

[I] P. Muñoz, R. Barco, D. Laselva and P. Mogensen. Mobility-based Strategies for Traffic Steering in Heterogeneous Networks. *IEEE Communications Magazine*, vol. 51, no. 5, pp 54-62, May 2013.

[II] P. Muñoz, R. Barco and I. de la Bandera, Optimization of Load Balancing using Fuzzy Q-Learning for Next Generation Wireless Networks, *Expert Systems With Applications* (Elsevier), vol. 40, no. 4, pp 984-994, March 2013.

[III] P. Muñoz, D. Laselva, R. Barco and P. Mogensen. Adjustment of mobility parameters for traffic steering in multi-RAT multi-layer wireless networks, *EURASIP Journal on Wireless Communication and Networking*, 2013:133, May 2013.

[IV] P. Muñoz, R. Barco and I. de la Bandera. On the Potential of Handover Parameter Optimization for Self-Organizing Networks. *IEEE Transactions on Vehicular Technology*, accepted in 2013.

[V] P. Muñoz, R. Barco, J. M. Ruiz, I. de la Bandera and A. Aguilar. Fuzzy Rule-based Reinforcement Learning for Load Balancing Techniques in Enterprise LTE Femtocells. *IEEE Transactions on Vehicular Technology*, accepted in 2012.

[VI] J. M. Ruiz, S. Luna-Ramírez, M. Toril, F. Ruiz, I. de la Bandera, P. Muñoz, R. Barco, P. Lázaro and V. Buenestado, Design of a Computationally Efficient Dynamic System-Level Simulator for Enterprise LTE Femtocell Scenarios, *Journal of Electrical and Computer Engineering*, vol. 2012, Dec. 2012.

[VII] P. Muñoz, I. de la Bandera, F. Ruiz, S. Luna-Ramírez, R. Barco, M. Toril, P. Lázaro and J. Rodríguez, Computationally-Efficient Design of a Dynamic System-Level LTE Simulator, *International Journal of Electronics and Telecommunications*, vol. 57, no. 3, pp 347-358, Sep. 2011.

Related to this thesis

[VIII] R. Barco, P. Lázaro and P. Muñoz. A Unified Framework for Self-Healing in Wireless Networks. *IEEE Communications Magazine*, Vol.50 (12), pp.134-142. Dec. 2012.

Conferences and Workshops

Arising from this thesis

[IX] P. Muñoz, I. de la Bandera, R. Barco, M. Toril, S. Luna-Ramírez and J.M. Ruiz, "Sensitivity Analysis and Self-Optimization of LTE Intra-Frequency Handover", *6th Scientific Meeting, COST action IC1004*, Málaga (Spain), February 2013.

[X] P. Muñoz, R. Barco, I. de la Bandera, M. Toril and S. Luna-Ramírez, "Optimization of a Fuzzy Logic Controller for Handover-based Load Balancing", *Int. Workshop on Self-Organising Networks (IWSON), IEEE Vehicular Technology Conference (VTC) Spring*, Budapest, Hungary, May 2011.

[XI] P. Muñoz, I. de la Bandera, R. Barco, F. Ruiz, M. Toril and S. Luna-Ramírez, "Estimation of Link-Layer Quality Parameters in a System-Level LTE Simulator", *5th International Conference on Broadband and Biomedical Communications* (IB2COM) 2010. Málaga (Spain). December, 2010.

[XII] P. Muñoz, I. de la Bandera, R. Barco, M. Toril and S. Luna-Ramírez, "Optimización del balance de carga en redes LTE mediante el algoritmo de Q-Learning difuso", *XXVI Simposio de la Unión Científica Internacional de Radio* (URSI 2011), Leganés (Spain), September, 2011.

[XIII] I. de la Bandera, P. Muñoz, R. Barco, M. Toril and S. Luna-Ramírez, "Auto-ajuste del margen de handover en redes LTE", *XXVI Simposio de la Unión Científica Internacional de Radio* (URSI 2011), Leganés (Spain), September, 2011.

[XIV] P. Muñoz, I. de la Bandera, R. Barco, F. Ruiz, M. Toril and S. Luna-Ramírez, "Diseño del Nivel de Enlace para un Simulador LTE", *XXV Simposio de la Unión Científica Internacional de Radio* (URSI 2010), Bilbao (Spain). September, 2010.

Related to this thesis

[XV] J.M. Ruiz, S. Luna-Ramírez, M. Toril, F. Ruiz, I. de la Bandera and P. Muñoz, "Analysis of Load Sharing Techniques in Enterprise LTE Femtocells", *Int. Workshop on Femtocells, Wireless Advanced* 2011, London, UK, June 2011.

[XVI] J. Rodríguez, I. de la Bandera, P. Muñoz and R. Barco, "Load Balancing in a Realistic Urban Scenario for LTE Networks", *Int. Workshop on Self-Organising Networks (IWSON), IEEE Vehicular Technology Conference (VTC) Spring*, Budapest, Hungary, May 2011.

[XVII] J. Rodríguez, I. de la Bandera, P. Muñoz and R. Barco, "Balance de carga en red LTE en un entorno urbano realista", *XXVI Simposio de la Unión Científica Internacional de Radio* (URSI 2011), Leganés (Spain), September, 2011.

[XVIII] G. Jiménez, R. Barco, P. Muñoz and M. Toril, "Optimización del Umbral de Traspaso para Femtoceldas LTE", *XXVI Simposio de la Unión Científica Internacional de Radio* (URSI 2011), Leganés (Spain), September, 2011.

[VI, VII, XI, XIV] are devoted to the simulation tools that allow the performance of the proposed algorithms to be evaluated. [II, X, XII, XVI, XVII] are devoted to the load balancing problem in macrocell scenarios, while that problem in femtocell scenarios is addressed in [V, XV, XVIII]. The problem of handover optimization is tackled in [IV, IX, XIII]. [VIII] is devoted to Self-Healing in the field of Self-Organizing Networks. In [I, III], the proposed techniques for Traffic Steering in the context of Heterogeneous Networks are described. The author has been the primary author of all the contributions "arising from this thesis" except [VI, XIII], being there a key contributor. In [VI], the author wrote the section dedicated to the indoor mobility model and helped with the design of the link layer. In [XIII], the author was involved in the design, analysis and writing stages. Finally, the author helped with the writing and review of the papers "related to this thesis".

Several research projects have been involved in these contributions. In particular, the following publications were developed in the frame of these projects:

- P08-TIC-4052 grant from the Junta de Andalucía: [I-VII, IX-XVIII].
- TEC2009-13413 grant from the Spanish Ministry of Science and Innovation: [II, V-VII, IX-XIV, XV, XVIII].
- IPT-2011-1272-430000 grant from the Spanish Ministry of Science and Innovation: [V].

In addition, [I, III] were also developed in collaboration with Nokia Siemens Networks in Aalborg, Denmark.

Acronyms

3GPP	3rd Generation Partnership Project
ACK	Acknowledge
AMC	Adaptive Modulation and Coding
ANFIS	Adaptive Network Fuzzy Inference System
ANR	Automatic Neighbor Relation
AP	Absolute Priority
ARP	Allocation and Retention Priority
ARQ	Automatic Repeat Request
AWGN	Additive White Gaussian Noise
B3G	Beyond-3rd-Generation
BC	Best Channel
BCCCH	Broadcast Control Channel
BCH	Broadcast Channel
BEE	Balanced Exploration and Exploitation
BLER	Block Error Rate
CAPEX	Capital Expenditures

CBR	Call Blocking Ratio
CCCH	Common Control Channel
CDF	Cumulative Distribution Function
CDR	Call Dropping Ratio
CFI	Control Format Indicator
CI	Confidence Interval
CPICH	Common Pilot Channel
CQI	Channel Quality Indicator
DCCH	Dedicated Control Channel
DCI	Downlink Control Information
DL-SCH	Downlink Shared Channel
DR	Directed Retry
DTCH	Dedicated Traffic Channel
E^3	End-to-End Efficiency
E-DCH	Enhanced-Dedicated Channel
E-UTRAN	Evolved Universal Terrestrial Radio Access Network
Ec/No	Energy per chip divided by the power density in the band
EH	Extremely High
EIA	Extended Indoor A
EL	Extremely Low
EN	Extremely Negative
eNB	evolved Node B
EP	Extremely Positive
EPC	Evolved Packet Core

EPA	Extended Pedestrian A
EPS	Evolved Packet System
ETU	Extended Typical Urban
EVA	Extended Vehicular A
FDD	Frequency-Division Duplex
FLC	Fuzzy Logic Controller
FoM	Figure-of-Merit
FRLS	Fuzzy rule-based Reinforcement Learning System
FTP	File Transfer Protocol
GoS	Grade-of-Service
GPRS	General Packet Radio Service
GSM	Global System for Mobile communications
H	High
HARQ	Hybrid Automatic Repeat Request
HetNets	Heterogeneous Networks
HI	HARQ Indicator
HLB	Handover Margin Load Balancing
HO	Handover
HO PP	Handover Ping-Pong
HOM	Handover margin
HOR	Handover Ratio
HS-DPCCH	High Speed-Dedicated Physical Control Channel
HS-DSCH	High-Speed Downlink-Shared Channel
HS-SCCH	High Speed-Shared Control Channel

HSDPA	High-Speed Downlink Packet Access
HSPA	High-Speed Packet Access
HSUPA	High-Speed Uplink Packet Access
IAT	Inter-Arrival Time
IntHO	Interference Handover
IP	Internet Protocol
KPI	Key Performance Indicator
L	Low
LevHO	Minimum Level Handover
LDF	Large Delay First
LTE	Long-Term Evolution
LTE-A	LTE-Advanced
M	Medium
MAC	Medium Access Control
MBMS	Multimedia Broadcast/Multicast Service
MBSFN	Multimedia Broadcast/Multicast service Single Frequency Network
MCCH	Multicast Control Channel
MCH	Multicast Channel
MCS	Modulation and Coding Scheme
MDP	Markov Decision Process
MIMO	Multiple-Input and Multiple-Output
MLB	Mobility Load Balancing
MME	Mobility Management Entity

MRO	Mobility Robustness Optimization
MTCH	Multicast Traffic Channel
N	Negative
NACK	Not Acknowledge
NAS	Non-access stratum
NGMN	Next Generation Mobile Networks
OAM	Operations, Administration, and Maintenance
OFDM	Orthogonal Frequency Division Multiplexing
OFDMA	Orthogonal Frequency-Division Multiple Access
OPEX	Operational Expenditures
OR	Outage Ratio
P	Positive
PAPR	Peak-to-average power ratio
PBCH	Physical Broadcast Channel
PBGT_HO	Power Budget Handover
PCCH	Paging Control Channel
PCH	Paging Channel
PDCCH	Physical Downlink Control Channel
PDCP	Packet Data Convergence Protocol
PDSCH	Physical Downlink Shared Channel
PF	Proportional Fair
PHICH	Physical HARQ Indicator Channel
PLB	Power Load Balancing
PRACH	Physical Random Access Channel

PRB	Physical Resource Block
PUCCH	Physical Uplink Control Channel
PUSCH	Physical Uplink Shared Channel
QCI	QoS Class Identifier
QHLB	Q-Learning Handover Margin Load Balancing
QoS	Quality-of-Service
QPLB	Q-Learning Power Load Balancing
QualHO	Quality Handover
RACH	Random Access Channel
RAN	Radio Access Network
RAT	Radio Access Technology
RL	Reinforcement Learning
RLC	Radio Link Control
RLF	Radio Link Failure
RNC	Radio Network Controller
RR	Round Robin
RRC	Radio Resource Control
RRM	Radio Resource Management
RSCP	Received Signal Code Power
RSRP	Reference Signal Received Power
RSRQ	Reference Signal Received Quality
RSSI	Received Signal Strength Indicator
S-GW	Serving Gateway
SC-FDMA	Single-Carrier Frequency Division Multiple Access

SINR	Signal to Interference-plus-Noise Ratio
SIR	Signal-to-Interference Ratio
SON	Self-Organizing Network
SWG	Sub-Working Group
TDD	Time-Division Duplex
TS	Traffic Steering
TTI	Transmission Time Interval
TTT	Time-To-Trigger
TXP	Transmit Power
UCI	Uplink Control Information
UDR	User Dissatisfaction Ratio
UE	User Equipment
UEE	Unbalanced Exploration and Exploitation
UL-SCH	Uplink Shared Channel
UMA	University of Málaga
UMTS	Universal Mobile Telecommunications Service
US	Uncorrelated Scattering
VH	Very High
VL	Very Low
VN	Very Negative
VP	Very Positive
VoIP	Voice over Internet Protocol
WCDMA	Wideband Code Division Multiple Access
WG	Working Group

WiMAX	Worldwide Interoperability for Microwave Access
WLAN	Wireless Local Area Network
WSS	Wide-Sense Stationary
WSSUS	Wide-Sense Stationary Uncorrelated Scattering
Z	Zero

Chapter 1

Introduction

This chapter aims to explain the purpose of this thesis and its motivation, present its objectives and describe the document structure.

1.1 Motivation

In the last few years, mobile networks have significantly changed the way people communicate. In particular, there has been a clear shift from fixed to mobile cellular telephony and the mobile industry has experienced an enormous growth both in terms of mobile technology and its subscribers. In 2011, global penetration of mobile-cellular technology reached 87% with almost six billion mobile-cellular subscriptions. Furthermore, mobile-broadband subscriptions have grown 45% annually over the last years and currently, there are twice as many mobile-broadband as fixed-broadband subscriptions [1].

Since the first generation of cellular networks was introduced in the 1980s, the traffic demand has grown dramatically. Due to this, mobile operators have been investing heavily in infrastructure upgrades in order to support such a traffic demand. The first generation, based on analog telecommunications standards, provided the basic mobile voice. This generation continued until being replaced by the second generation, known as Global System for Mobile communications (GSM). The second generation was characterized by introducing capacity and coverage. Later, the third generation known as Universal Mobile Telecommunications Service (UMTS) provided data services at higher speeds as a first approach to mobile-broadband experience, which will be further developed by the fourth generation. Currently, migration towards the fourth generation of mobile networks is considered one of the main goals of mobile operators. Such a migration, also known as Long-Term Evolution (LTE), will provide access to a wide range of telecommunication services, most of them supported by both mobile and fixed networks. In addition, many

networking technologies will also be available to enable true ubiquitous mobile access, which means that many technologies will become available to provide different wireless solutions (e.g. wireless sensor networks, enhanced third generation) and networking protocols will connect users to the best available network. Furthermore, mobile terminals (or smartphones) will benefit from major advances in technology developments in areas such as semiconductors, nanotechnology, processing power and storage capacity, thus enabling the emergence of smaller, complex and intelligent devices.

The problem of the increasing traffic demand in current cellular networks is further aggravated by considering financial constraints from the operator perspective, as higher capacity and enhanced user experience should be provided at the expense of higher capital expenditures (CAPEX) and operational expenditures (OPEX). Since users may be reluctant to pay proportionally higher bills for improved services, minimizing CAPEX and OPEX while providing better user experience and capacity becomes a crucial consideration for mobile operators. For this reason, operators attempt to achieve a trade-off between providing improved services and retaining reasonable profits to make the business model commercially viable.

To cope with the enormous increase in traffic demand in a cost effective way, new technology should not only increase the speed of data transfer in the network, but also increase automation of network management. Such a requirement has triggered research to add intelligence and autonomy to future cellular networks, resulting in a new paradigm known as Self-Organizing Networks (SONs) [2]. The development of SON techniques is motivated by several factors [3]. Firstly, due the mobility of users and the unpredictable nature of the radio channel, cellular networks do not fully utilize the available resources, thus leading to potential congestion situations and suboptimal performance. Secondly, the recent deployment of smaller cells (e.g. femtocells) and outdoor relays in order to provide more capacity has brought a significant increase in the number of network elements, making configuration and maintenance tasks more tedious. In this case, classic manual and field trial based design approaches may lead to suboptimal solutions. This is of special interest in femtocell scenarios, as this type of cells is typically deployed without following a rigorous planning approach. This practice can lead to a waste of network resources or, even worse, it can cause severe interference to neighboring cells of higher sizes, thus degrading the overall performance. Thirdly, with the classic approach for periodic manual optimization, the increasing complexity of future systems (e.g. in technology, protocols) will result in higher number of human errors, which in turn will result in longer recovery and restoration times. Finally, an important benefit derived from automation of network management is that human effort can be freed from mundane and tedious tasks, so that expertise can be focused on new areas, bringing additional value to the operator.

Thus, introducing automation in cellular networks means significant OPEX reduction and improved customer experience. To achieve this, the SON proposal aims to enable a set of functionalities for automated management of cellular networks, so that human intervention is minimized in the planning, deployment, optimization and maintenance tasks. In 2006, the Next Generation Mobile Networks (NGMN) Alliance identified excessive dependence on manual operational effort as a potential problem [4]. With the aim of increasing operational efficiency, the

new paradigm SON was translated into particular functionalities, which later were grouped by the 3rd Generation Partnership Project (3GPP) into three categories, Self-Configuration, Self-Optimization and Self-Healing [5]. In particular, Self-Configuration refers to the dynamic 'plug and play' behavior of newly deployed base stations, which configure radio parameters (e.g. the transmission frequency and power) in an autonomous manner, leading to faster cell planning and rollout. Self-Optimization aims to dynamically adapt network parameters to improve network quality, including optimization of coverage, capacity, handover and interference. Self-Healing is related to failure detection, diagnosis, compensation and recovery in order to cope with major service outages and degradations which significantly decrease user performance. Not all of the SON functionalities considered by the 3GPP have received the same attention in the research field. Moreover, certain functions in Self-Optimization have been identified as key enablers, among which are those addressed in this thesis, Mobility Load Balancing (MLB) and Mobility Robustness Optimization (MRO) [6]. This fact has stimulated research activity in the field of parameter self-tuning for both MLB [7][8][9][10][11] and MRO [12][13][14][15][16].

MLB is a function where cells suffering occasional congestion can transfer load to neighboring cells, which have spare resources. This is achieved by adjusting mobility parameters in order to relieve the congestion in the affected area. MLB includes load reporting between base stations to exchange information such as cell load levels and available capacity. The development of MLB algorithms is motivated by some issues. Firstly, in the case of intra-system load balancing, when a user is handed over to another cell, the propagation conditions could get worse if the user is located near the cell edge because of the interference caused by neighboring cells. Thus, the degradation of signal quality for these users should be considered in the process. Secondly, in the case of inter-system load balancing, a proper interface to exchange load information in a heterogeneous scenario and additional intelligence to compare and weigh the capacities of the different radio technologies should be necessary. Thirdly, although a handover due to load balancing is carried out as a regular handover (i.e. the procedure that preserves the connection when the user moves around the network), it may be necessary to amend parameters so that the mobile terminal does not return to the congested cell. Such a correction must take place in both cells, so that the handover settings remain coherent in both sides.

MRO is a solution for automatic detection and correction of errors in the mobility configuration, which may lead to a degradation of user performance. In particular, this function mainly focuses on errors causing dropped calls due to handovers that are carried out too late or early when the user moves between cells. MRO must also take into account handovers performed to a wrong cell. As LTE is being deployed with a frequency reuse of one (i.e. the same frequency is shared by all cells), the inter-cell interference becomes an important issue, especially in the cell-edge. Such interference typically results in dropped calls and failures related to handovers. Supposing that this issue is counteracted or at least reduced, another challenging issue is to cope with unnecessary handovers, among which are the so-called ping-pong handovers. A ping-pong handover occurs when a user is handed over to a cell and then it comes back to the first cell in a short time interval. Finally, another interesting challenge is the coordination with MLB, which can cooperate on the problem of a high number of dropped calls, since in the intra-frequency case, MLB may lead to an increase in the number of dropped calls.

On the other hand, the large increase in both size and complexity experienced by cellular networks has led to a heterogeneous environment characterized by the presence of networks with different cell sizes, technologies, carrier frequencies, etc. In this context, the coverage area of these networks is usually overlapped. Thus, operators have some degree of freedom to steer traffic across the networks with the aim of optimizing the usage of radio resources. Some early studies in this field are [17][18][19][20][21]. The potential of traffic steering in heterogeneous networks brings new challenges to operators since the task of selecting a more suitable network can be made to achieve a goal or a combination of goals, for instance, related to cost, user satisfaction, power consumption, coverage, securing Quality-of-Service (QoS) for the requested service, etc. In practice, the operator needs to decide which performance indicators derived from network measurements must be optimized to improve some aspect of the network. Because of the lack of studies related to this new paradigm, this thesis is also devoted to traffic steering in heterogeneous networks, focusing on the development of automated techniques based on adjustment of mobility parameters.

1.2 Preliminaries

The Mobile Network Optimization team [22], belonging to the *Ingeniería de Comunicaciones* Group (TIC-102), is a research group dedicated to the improvement of current and future mobile telecommunications networks. The group was created in 2003 by six associate professors from the Communications Engineering Department of the University of Málaga (UMA). The aim was to take advantage of the know-how acquired in a 4-year contract with Nokia Networks to develop a mobile system engineering centre at the *Parque Tecnológico de Andalucía*. Since then, the group has largely grown, having participated in several projects in regional, national and international calls. In addition, the group has worked in projects with the main international operators and vendors: Nokia-Siemens, Ericsson, Alcatel-Lucent, Telefónica, Orange-France Telecom, etc.

The group is one of the pioneers in SON, having started to work in optimization and auto-diagnosis in second generation networks even before the term SON was created. The CELTIC-EUREKA project called Gandalf (CP2-014 EUREKA/GANDALF: Monitoring and self-tuning of radio resource management parameters in a multi-system network, 2005-2007), in which the group participated, is a reference as one of the first international projects in the topic. In particular, the aim of Gandalf was to develop self-optimization techniques for networks with multiple radio access technologies and auto-diagnosis tools. The partners were France Telecom R+D, Ericsson R+D Ireland, Moltsen Intelligent SW, Telefónica R+D and University of Limerick.

In 2009, the *Junta de Andalucía* funded a research project of the Communication Engineering Department named "Adaptive techniques for radio resource management in Beyond Third Generation networks", which has been in place during five years and has supported this PhD. The main lines of this project are the development and evaluation of algorithms for self-tuning of joint radio resource management parameters, the development and evaluation of optimization algorithms for the self-tuning parameter process and the impact assessment of these proposed techniques on the global QoS. The main simulation tool used in this thesis has also been deve-

loped in the context of this project.

Other research projects closely related with thesis are the project entitled "Self-optimizing heterogeneous mobile radio access networks", funded by the Spanish Ministry of Science and Innovation, and the project "Localization and self-organization in femtocell environments (MONOLOC)", funded by the Spanish Ministry of Science and Innovation and the European Regional Development Fund. One of the lines of these two projects in common with this thesis is the development of self-tuning algorithms for adjusting radio resource management parameters in LTE femtocells.

Finally, among the current projects of this team, the most important ones are three contracts with Ericsson to develop SON techniques and tools for current and future mobile communication networks (2012-1015). It is foreseen that more than 40 engineers are going to be hired within this project.

1.3 Research objectives

The main goal of this thesis is the design of optimization techniques for mobile networks, by self-tuning network parameters. Such a goal is applied to different problems:

- A self-tuning method to solve **persistent congestion problems in next-generation wireless networks**, in particular, due to an uneven spatial traffic distribution, e.g. when the center of a city becomes crowded. Following the 3GPP guidelines, in which the load balancing problem is referred to as MLB, mobility parameters will take precedence for the self-tuning mechanism. In addition, the optimization of the self-tuning process must be addressed. Such an optimization will provide certain adaptation capacity to the self-tuning algorithm. Hence, not only the parameters, but also the parameter tuning strategy will be optimized.
- A scheme to solve **persistent congestion problems in enterprise femtocells scenarios**, in which the lack of a thorough deployment of these low-cost nodes calls for algorithms that make a more efficient use of radio resources. The self-tuning process will be characterized by tuning specific parameters of femtocells, such as the transmit power or handover margins. In addition, as in the previous problem, the optimization of the self-tuning process must also be studied.
- A proposal for **handover optimization in next-generation wireless networks**. The aim of this function, referred to as MRO in 3GPP terminology, is to reduce the number of dropped calls and avoid unnecessary handovers. In this study, the impact of context factors such as the system load and user speed must be addressed. Furthermore, the need for an optimization of this process, which depends on the complexity of the proposed self-tuning algorithm, must also be considered.
- A proposal for **SON coordination** between the proposed MLB and MRO functions. Since these two functions adjust the same parameters, a method for conflict avoidance must be

proposed.

- A self-tuning algorithm for **traffic steering in heterogeneous networks**, which eases operators the flexibility to choose a specific policy. The scenario under study must be representative of a realistic network deployment that combines the presence of different technologies, cell sizes, frequencies, hotspots, etc. deployed in a rational manner. In addition to the flexibility to support different operator policies, the adaptation capability to network variations must also be a key feature of the proposed scheme.

With the aim of validating the proposed techniques, a **simulation tool for next-generation wireless networks** tailored to the proposed methods and procedures will also be necessary. The design of such a simulator will therefore constitute a key part of this thesis.

1.4 Document structure

This thesis is divided into those problems to be solved, and they will be treated independently. The structure of this document reflects that division in separated chapters, except for the first two problems, which share the same topic (i.e. load balancing) and thus, they have been included into the same chapter. For an easier understanding, the different problems have been treated with an unified structure.

This document consists of eight chapters. The first chapter corresponds to this introduction to the thesis, which gives a general view of automated network management and main use cases. Chapters 2 and 3 include the required background to follow the rest of the report. In particular, Chapter 2 provides an introduction to the SON paradigm and a review of the state-of-the-art of the problems and techniques addressed in this thesis, while Chapter 3 provides a review of the theoretical basis of the mathematical techniques suitable for parameters self-tuning and its optimization. In Chapter 4, the simulation tools used to validate the proposed algorithms are described, focusing on the dynamic system-level LTE simulator, whose design has been part of this thesis. The following chapters, which are devoted to the design of self-tuning schemes, have a similar structure, beginning with a brief introduction of the problem to be solved, then, describing the proposed scheme as a solution to the problem in an additional section, and, finally, presenting the main results of the analysis. More specifically, Chapter 5 is dedicated to the load balancing problem in both macrocell and enterprise femtocell scenarios, for which self-optimizing schemes are proposed. In Chapter 6, a self-tuning algorithm for handover optimization and a method for coordination between load balancing and handover optimization are proposed. Chapter 7 is devoted to the development of traffic steering techniques in heterogeneous networks. It is worth noting that, although the previous chapters are mainly focused on LTE networks, the proposed techniques are also valid for other existing and future cellular networks. Finally, Chapter 8 summarizes the main conclusions of the research and future lines of action are proposed.

This report also includes as appendix A a brief summary of the thesis in Spanish.

Chapter 2

Self-Organization in Radio Access Networks

This chapter introduces the key concepts involved in the automatic management of current and future Radio Access Networks (RANs). In the last years, network operators have focused attention on reducing CAPEX and OPEX of the cellular networks. An effective manner to achieve this objective is by means of automatic management, which allows to remove several human interventions from network operation and maintenance. In this area, the concept of SONs involves different mechanisms and methods to enhance the operations of complex networks. As a result of applying SON techniques, not only the manual intervention is minimized, but also network efficiency and service quality are increased. Those benefits derived from SON functionalities are especially valuable in the RAN segment, since this part of the network usually forms the bottleneck in wireless networks due to its operational complexity and network costs.

The potential of SON techniques can be further exploited if they are applied in the context of heterogeneous networks (HetNets). HetNets involve a diverse network deployment characterized by the presence of networks with different architectures, technologies, frequencies, cell sizes, elements, etc., whose objective is to cope with the increasing traffic demand which cannot be served by conventional cellular networks. In this context, since the coverage area of those networks are typically overlapped, mobile users can be steered to a particular network in order to satisfy different operator policies related to costs, user satisfaction, power consumption, coverage, securing QoS for the requested service, etc. Those actions, known as Traffic Steering (TS), can be seen as SON mechanisms if they are automatically executed with the aim of both reducing operational costs and enhancing network performance.

This chapter is divided into two parts. For clarity, the first part begins by describing the RANs that are assumed in this work, focusing on LTE, which plays an important role in the

evaluation part of this thesis. Subsequently, the concept of SON is analyzed in detail regarding the main use cases concerning pre-operational parameter planning, radio parameter optimization, and troubleshooting in cellular networks. Special attention is devoted to radio parameter optimization, since some of the related use cases are addressed in this thesis. The second part of the chapter describes the state of the art in radio parameter optimization, focusing on automated techniques related to the SON use cases addressed in this thesis and the coordination of those techniques. In addition, the state of the art in TS is summarized.

2.1 Preliminaries

2.1.1 Radio Access Technologies

Cellular systems are an extremely popular solution to provide voice and data communication for mobile users. The key feature behind cellular systems is that the signal power decreases with distance, meaning that the same frequency spectrum can be reused from a certain location. As a result, the geographic area can be divided into different cells where some radio resources (or channels) are allocated to each cell. Such resources are managed by a base station, which is the network element owned by the operator that acts as a wireless access point for users. Then, the User Equipment (UE) can connect to the base station to initiate a connection.

The infrastructure of mature cellular networks must evolve to cope with the increasing demand for mobile-broadband services. This need of extra capacity comes from the increasing complexity in the UEs (commonly called smartphones), the growing demand for online applications (such as video and music streaming services) and the increasing number of hotspots (small areas with high demand of traffic). Currently, the most widely used wireless technology in the world is the second generation of telecommunication systems, known as GSM. However, since the data-handling capabilities of GSM systems are very limited, the third generation, known as UMTS was developed to provide higher data-rates. The air interface of UMTS is based on Wideband Code Division Multiple Access (WCDMA), which initially offered data speeds up to 384 Kbps. Later, to enhance WCDMA networks, newer upgrades to WCDMA providing much faster data speeds were developed, such as High-Speed Packet Access (HSPA) and its evolution, HSPA+. In particular, HSPA+ increases peak data-rates to 168 Mbps in the downlink and 22 Mbps in the uplink. Such values are technically achieved through the use of higher order modulation and multiple antennas on the receiver and transmitter. Finally, the evolution towards the fourth generation has brought new technologies to the markets, such as LTE and LTE-Advanced (LTE-A), which are expected to significantly improve user experience. The air interface of those new technologies assume Orthogonal Frequency-Division Multiple Access (OFDMA), which in the case of LTE provides peak data-rates up to 299.6 Mbps in the downlink and 75.4 Mbit/s in the uplink. Since the SON methods and algorithms proposed in this thesis have been designed for HSPA and LTE systems, the rest of this section is an overview of those technologies.

Overview of the HSPA system

The standardization organization responsible for producing the specifications that define HSPA and also other technologies such as LTE and LTE-A is the 3GPP. In particular, Release 5 and Release 6 of the 3GPP specifications are devoted to HSPA, while Release 7 is devoted to HSPA+. The HSPA system improves the performance of existing WCDMA network architecture, being a cost-effective solution for UMTS networks compared to LTE and LTE-A, which would require a substantial change in the architecture. The first step in the specification of HSPA (Release 5) was to improve the downlink by introducing High-Speed Downlink Packet Access (HSDPA), while the second step (Release 6) was to improve the uplink by introducing High-Speed Uplink Packet Access (HSUPA). Thus, the implementation of both technologies is known as HSPA.

The two main features of UMTS systems are variable spreading factor and fast power control [23]. With the former, the transmitted signal is spread over a wide spectrum range to adjust the bit rate of dedicated physical channels, while, with the latter, the received power is maintained constant in order to achieve the Block Error Rate (BLER) target. In contrast, some of the main features of HSPA systems include the following:

- *Channel-dependent scheduling.* The aim of this feature is to allocate resources to users with favorable instantaneous channel conditions, which provides a gain known as multi-user diversity.
- *Adaptive Modulation and Coding* (AMC). With this feature, the modulation and the coding rate are adapted to the instantaneous channel quality instead of using power control. AMC is especially more efficient for services that tolerate short-term variations in the data-rate. In addition, data-rates can be increased in HSPA by using spectral-efficient 16QAM modulation when channel conditions are good.
- *Hybrid Automatic Repeat Request and soft-combining* (HARQ). These methods provide robustness against link adaptation errors. With HARQ, the transport block retransmission process is significantly faster, since this functionality is now located in the base station (Node B) instead of the Radio Network Controller (RNC) as in UMTS. With soft-combining, data from the original transmission can be combined with data from the later transmission, before attempting to decode the message. As a result, the probability of successful decoding would be increased.
- *Short Transmission Time Interval.* In UMTS, Transmission Time Interval (TTI) refers to the duration of a transmission on the radio link. TTI values of 10 ms, 20 ms and 40 ms are typically used. Conversely, in HSPA, the TTI is reduced to 2 ms. A short TTI improves the tracking of channel variations, which is exploited by AMC and channel-dependent scheduling features.

Regarding the system architecture, both UMTS and HSPA can share all the network elements in the core network and also in the RAN segment, including the Node B sites, antennas and antenna lines. Hence, the cost of upgrading from UMTS to HSPA is lower than deploying a new standalone cellular network. However, there are significant architectural changes between

these two technologies which are necessary to bring the control for link adaptation and retransmissions closer to the air interface. In HSDPA [24], an important architectural change for this purpose is that the transport channel carrying the user data in the downlink, named as High-Speed Downlink-Shared Channel (HS-DSCH), is directly terminated at the Node B, which is different from all the transport channels adopted in UMTS. Another key upgrade is that the Medium Access Control (MAC) layer is now located in the Node B. Such a change also carries some implications to the network architecture. The first implication is that the MAC layer can control the resources of the HS-DSCH. Secondly, the new location of this layer allows to execute the HARQ functionality on the physical layer, meaning that faster retransmissions are provided. Lastly, recent channel quality reports can be acquired in order to track the instantaneous signal quality for low-speed users.

In HSDPA, the transmission power is kept constant over the TTI and shared when transmission to multiple users occurs in parallel. Code and transmission power are dynamically allocated to users in the time domain. The transport channel HS-DSCH utilizes a fixed spreading factor equal to 16, while the maximum number of codes used for transmission is 16. The signaling of this channel is supported by the High Speed-Shared Control Channel (HS-SCCH) in downlink, and the High Speed-Dedicated Physical Control Channel (HS-DPCCH) in uplink. To illustrate the general functionality of these channels, Fig. 2.1 shows an example in which a certain UE is connected to a Node B. Firstly, the UE reports in the HS-DPCCH the Channel Quality Indicator (CQI), which contains an estimation of the channel quality. Secondly, from the CQI report and other sources such as HARQ acknowledgements and buffer size, the Node B determines which Modulation and Coding Scheme (MCS) will be used in the downlink. Thirdly, the user data is sent to the UE in the HS-DSCH, together with the information for HS-DSCH demodulation in the HS-SCCH. Finally, the UE sends the Acknowledge (ACK)/Not Acknowledge (NACK) by using the HS-DPCCH to ensure correct decoding of packet data.

To efficiently make use of the limited radio spectrum resources and radio network infrastructure, Radio Resource Management (RRM) is a set of functionalities that involve strategies and algorithms for controlling parameters such as transmit power, channel allocation, MCS, etc. Some of these functionalities, such as AMC and HARQ, have already been mentioned in this

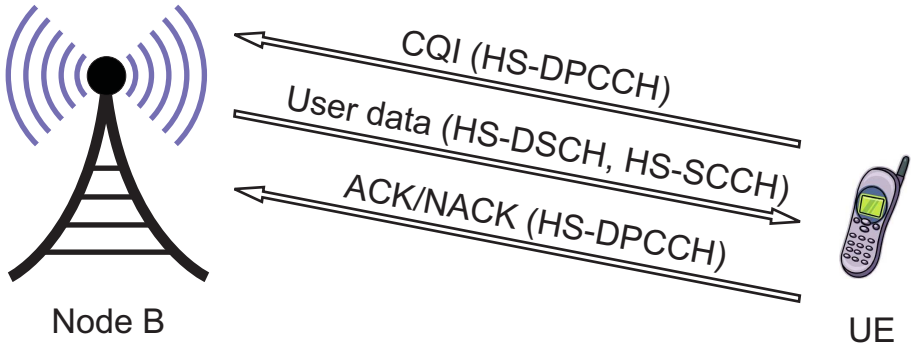

Figure 2.1: General operation of HSDPA transmission scheme

section. However, RRM also includes other mechanisms for resource sharing, such as packet scheduling, admission control, cell reselection and handover control [25]. The following paragraphs provides a brief overview of the main RRM functions [23].

Firstly, packet scheduling is responsible for allocating resources among users at each time interval. As other functionalities in HSDPA, scheduling has also been moved to Node B, meaning that faster reallocations of resources and faster adaptation to channel variations can be achieved. To allocate resources, the packet scheduler can use the information reported in the CQI, so that the scheduling decision can be made on the basis of scheduling users with the best instantaneous channel conditions. However, there are some other strategies that can be used by the packet scheduler to assign resources. For instance, a simple approach would be the *Round Robin* method, where users are sequentially served, so that all users receive the same average allocation time. Another well-known policy is named as *proportional fair* scheduling, which attempts to maximize network throughput while at the same time some fairness between users is ensured.

The admission control decides whether or not to admit a new user given that the service is provided without worsening the connections of already active users. Depending on the service type, resources can be critical or not. For example, a Voice over Internet Protocol (VoIP) call established in the HS-DSCH may limit the resources available for new calls if the maximum end-to-end delay of the VoIP call could not be ensured. In contrast, for non-real-time services such as File Transfer Protocol (FTP) downloads, the limitation would be given by the bit rate. A simple model for admission control is based on thresholds. In this model, the amount of occupied resources Z is calculated at each time instant. When a new call is generated, the network estimates how many resources ΔZ are needed to support it. Then, the call is accepted if the following expression is fulfilled:

$$Z + \Delta Z < Z_{th}, \tag{2.1}$$

where Z_{th} is the maximum threshold of used resources, which can be static or dynamic. Other, more complex, admission control models can be based on position and user mobility information, as well as QoS indicators.

Mobility management is also an RRM functionality that comprises two basic procedures carried out when the UE is in idle state (not on a call) and connected mode (on a call) [25]. In idle state, the cell reselection is the procedure performed when the UE moves from one cell to another. As the UE is camped on a cell, it could be commanded to detect, synchronize and monitor intra-frequency, inter-frequency and inter-RAT cells in order to select a more suitable cell on which camp. Typically, the measurement process starts if the signal power received from the camping cell is below a specific threshold. In addition, cells are considered detectable if they exceed certain absolute power level. Then, the reselection decision is made by comparing power measurements between the target and source cells. In some cases, the source cell provides a neighbor list for the intra-frequency and inter-frequency cells, but, at other times, only the carrier frequency and bandwidth are provided. The advantage of having a neighbor list is that the UE can limit its measurement activity in complex situations. In connected mode, the handover

(HO) is the procedure that preserves the connection (e.g. a call) when the user moves around the network. In UMTS, soft-HOs allows the UE to be simultaneously connected to two or more cells during a call. However, in HSPA, this kind of HOs is not possible, since data transmission is done by one shared channel, HS-DSCH. Thus, in contrast, those HOs in which the UE can only be connected to one cell are called hard-HOs. Prior to performing a hard-HO, measurement reports are sent from the UE to the RNC, which makes the decision and initiates the HO process. If the HO is carried out between cells belonging to the same Node B, then the MAC layer can forward the data flow from the source cell to the target cell, maintaining HARQ process. Conversely, if the HO is carried out between different Node B's, then the MAC layer resets buffers in the source cell, while at the same time the target cell starts to send data to the UE. Once the UE has changed the cell, data transmission is terminated from the previous cell and all MAC functions of the UE are reset. In addition, there are some HO parameters which can be adjusted to modify the behavior of the HO procedure, for instance, to minimize the unnecessary changes of serving cell due to fast variations in the received power. Those parameters will be explained in detail in later chapters of this thesis, since they will play a key role in the proposed SON algorithms.

Therefore, measurements at the UE and network are necessary to support mobility. To initiate a specific UE measurement, the network sends a control message to the UE including an identifier, the measurement objects and the reporting criterion, which can be periodical or event-triggered. When the reporting criterion is fulfilled, the UE replies with a measurement report message to the network including the identifier and the results. In HSPA, the main physical layer measurements are the following [26]:

- *Common Pilot Channel* (CPICH) *Received Signal Code Power* (RSCP). The CPICH is a downlink channel whose transmitted bit sequence is known and broadcast by Node B's with constant power. The aim of this channel is to synchronize the UE to the Node B. There are two types of CPICH, the Primary and Secondary CPICH, differing in their use and physical limitations. The CPICH RSCP is the received power on one code measured on the Primary CPICH. The reference point for the RSCP is the antenna connector at the UE.

- *Received Signal Strength Indicator* (RSSI). The RSSI is the received wideband power, including thermal noise and noise generated in the receiver, within the bandwidth defined by the receiver pulse shaping filter. The reference point for this measurement is the antenna connector at the UE.

- CPICH *Ec/No*. It is the received energy per chip (Ec) divided by the power density in the band (No). If receiver diversity is not in use by the UE, the CPICH Ec/No is identical to the CPICH RSCP divided by the RSSI. Measurement shall be performed on the Primary CPICH. The reference point for the CPICH Ec/No is the antenna connector at the UE.

In HSUPA [27], solutions similar to HSDPA have been designed to improve uplink packet data performance. In particular, there are three key features for HSUPA: multi-code transmission, fast physical layer retransmission combining and fast scheduling at the Node B. Firstly, the multi-code transmission means that the new uplink channel, called Enhanced-Dedicated Channel (E-DCH) can support up to four codes to increase the uplink data-rate. Secondly, the fast

HARQ protocol, similar to the one used for HSDPA, enables that the Node B can rapidly request retransmission of erroneously received data. As a result, better robustness and lower retransmission latencies are provided. Thirdly, the fast scheduling at the Node B enables rapid resource reallocation between UEs, so that a larger number of high data-rate users can be admitted and better adaptation to interference variations can be achieved. Other features are that HSUPA retains the uplink power control and variable spreading factor from UMTS (unlike HSDPA), and soft-HOs are also possible in HSUPA, meaning that a UE can, for instance, be scheduled from just one Node B or from several Node B's at the same time. The general functionality of HSUPA is as follows. Firstly, the Node B estimates the data-rate transmission for each active UE based on the device-specific feedback. Then, the scheduler, which is located in the Node B, reports the uplink data-rate to the UE with a frequency that depends on the received feedback, the scheduling algorithm and the user prioritization scheme. Finally, the retransmissions are initiated by the Node B feedback.

Overview of the LTE system

To ensure that the third generation UMTS remains competitive in the future, 3GPP began a project to define the long-term evolution of UMTS cellular technology, which is commonly referred by the project name LTE [28]. This standard is documented in Release 8 of the 3GPP specifications, with minor enhancements described in Release 9. Although LTE has been marketed as the fourth generation of wireless technology, Releases 8 and 9 do not satisfy the technical requirements adopted by the 3GPP consortium for its new standard generation. In this sense, only LTE-A is the standard that formally satisfies the requirements to be considered as the fourth generation.

The aim of LTE is to provide high data-rates, low latency, low power consumption, spectral flexibility and reduced OPEX [29]. The network architecture has also been redesigned and simplified to an IP-based system with significantly reduced latency compared to the third generation architecture [5]. The LTE air interface supports both Frequency-Division Duplex (FDD) and Time-Division Duplex (TDD) modes, each of which has its own frame structure. Downlink and uplink transmission in LTE are based on OFDMA and Single-Carrier Frequency Division Multiple Access (SC-FDMA), respectively. Thanks to OFDMA and SC-FDMA access schemes, flexible bandwidths can be supported in LTE. With 20 MHz bandwidth, the system supports peak data-rates up to 326 Mbps in the downlink and 86.4 Mbps in the uplink. The basis of Orthogonal Frequency Division Multiplexing (OFDM) is to split the available spectrum into several narrowband channels referred to as subcarriers. Thus, multiple access in OFDMA is achieved by allocating subsets of those subcarriers to individual users, so that simultaneous low data-rate transmission from several users can be supported. In the uplink, SC-FDMA is used to provide increased uplink coverage due to low peak-to-average power ratio (PAPR) relative to OFDMA. As the transmission power at the UE is limited, a reduction in signal peaks would provide increased transmit power enabling higher data-rates. The 3GPP also defines variable channel bandwidths selectable from 1.4 to 20 MHz, with subcarrier spacing of 15 kHz. The smallest amount of radio resources that can be allocated to a user by the scheduler in the uplink or the downlink is called

a Physical Resource Block (PRB). A PRB occupies 180 kHz in the frequency domain and 0.5 ms in the time domain [30]. As previously mentioned, downlink transmission in LTE is based on OFDM, which makes use of a large number of closely spaced orthogonal subcarriers that are transmitted in parallel. In particular, a PRB comprises 12 subcarriers at a 15 kHz spacing. Each subcarrier is modulated at a low symbol rate by using a conventional modulation scheme, e.g. QPSK, 16-QAM or 64-QAM. The combination of all the subcarriers in the time domain creates an OFDM symbol, which is then transmitted after including guard intervals to prevent inter-symbol interference at the receiver. As a result, the data-rate generated by using OFDM is similar to conventional single-carrier modulation schemes for the same bandwidth.

On the one hand, OFDM provides significant benefits when compared to WCDMA systems. For example, multi-path propagation is a typical phenomenon commonly found in cellular environments. In this context, codes in WCDMA are no longer orthogonal and interfere with each other resulting in inter-user and inter-symbol interference. Such a problem is more pronounced for larger bandwidths (e.g. 10 and 20 MHz required for support of higher data rates). Conversely, OFDM provides the greatest advantage over WCDMA networks in those situations, since a cyclic extension of the OFDM signal is used to avoid this interference. More specifically, the last part of the OFDM signal is added as cyclic prefix in the beginning of the OFDM signal. Some other advantages are that OFDM can easily be scaled up to wide channels (which are more resistant to fading), OFDM is more attractive for Multiple-Input and Multiple-Output (MIMO) antenna configurations, and channel equalizers are much simpler to implement in LTE than in WCDMA, since the channel for each OFDM subcarrier experiences almost flat-fading. On the other hand, OFDM also has some disadvantages. The subcarriers are closely spaced, meaning that OFDM is more sensitive to frequency errors, phase noise and Doppler effect. In addition, as the OFDM symbol is formed by simply adding the modulated subcarrier signals, this signal has much larger signal amplitude variations than the individual subcarriers. Such a characteristic of the OFDM signal creates high peak-to-average signals, which is the main reason why SC-FDMA is used in the uplink.

Thus, in the uplink, SC-FDMA is implemented to avoid the high PAPR associated with OFDM. Such a different transmission scheme offers not only the low PAPR from techniques of single-carrier transmission systems, but also the multi-path resistance and flexible frequency allocation from OFDMA. The main difference between these two schemes is that OFDMA transmits the data symbols in parallel, one per subcarrier, while SC-FDMA transmits them in series at a higher rate and also occupying more bandwidth. Therefore, visually, the OFDMA signal is clearly multi-carrier with one data symbol per subcarrier, while the SC-FDMA signal is more similar to a single-carrier in which the data symbol is represented by one wideband signal. As previously stated, in OFDMA, the transmission in parallel of multiple symbols causes the undesirable high PAPR. Conversely, in SC-FDMA systems, by transmitting L data symbols in series at a rate L times higher, the occupied bandwidth is the same as in OFDMA but the PAPR is the same as that used for the original data symbols, regardless of the value of L. Thus, by using SC-FDMA in the LTE uplink, low signal peaks comparable to OFDM signal peaks can be achieved. It is also worth mentioning that SC-FDMA is resistant to multi-path when the data symbols are still short. In particular, to provide resistance to delay spread, it is necessary

that each subcarrier is maintained constant in the frequency domain during the symbol period. In SC-FDMA, even though the symbols are not constant in the time domain over the symbol period, the associated spectrum remains constant. This is because the time-varying SC-FDMA symbol composed of L serial data symbols is equivalent to L time-invariant subcarriers in the frequency domain. As a result, SC-FDMA benefits from multi-path protection despite its short data symbols.

One of the main advantages of OFDM lies in its suitability to MIMO application. MIMO is a key technology to increase the capacity of wireless networks, based on the use of multiple antennas at both the transmitter and receiver. More specifically, multiple antennas allow to achieve the diversity gain, since radiated signals will take different physical paths. Such a diversity gain improves the link performance when the channel quality cannot be tracked at the transmitter, as it happens for high mobility UEs. When multiple transmission antennas and only one receiver antenna are implemented in the system (i.e. multiple-input and single-output), the data-rates cannot be increased, but the same data-rates can be supported by using less power. This MIMO configuration can also provide greater robustness of the signal to fading and better performance in low quality conditions. To achieve this, data is sent on both transmitting antennas but coded such that the receiver can identify each transmitter. In addition, higher peak data rates can be achieved by using more complex MIMO schemes in which multiple transmission antennas at the base station are combined with multiple receiver antennas at the UE. In particular, this configuration takes advantage of the MIMO spatial multiplexing, where multiple data stream are transmitted between the base station and the UE. All these characteristics highlight that MIMO is an important part of modern wireless communication standards, such as LTE, IEEE 802.11n (Wi-Fi) and Worldwide Interoperability for Microwave Access (WiMAX).

The LTE network architecture is designed to support packet-switched traffic with seamless mobility, QoS and low latency. While the RAN segment is divided into the Node B and the RNC in UMTS/HSPA networks, the architecture is greatly simplified in LTE (see Fig. 2.2), resulting in a new network element, called evolved Node B (eNB), which provides the user plane and control plane protocol terminations toward the UE [5]. Thus, the RNC is removed from the network architecture and its functionality is shared between the eNB and the mobility management entity/serving gateway (MME/S-GW), located in the core network. The eNBs are connected between each other by means of the X2 interface and they can also be connected to the core network by means of the S1 interface. The following functions are covered at the eNB:

- Radio resource management.
- Internet Protocol (IP) header compression and encryption.
- Selection of MME at UE attachment.
- Routing of user plane data towards S-GW.
- Scheduling and transmission of paging messages and broadcast information.
- Measurement and measurement reporting configuration for mobility and scheduling.

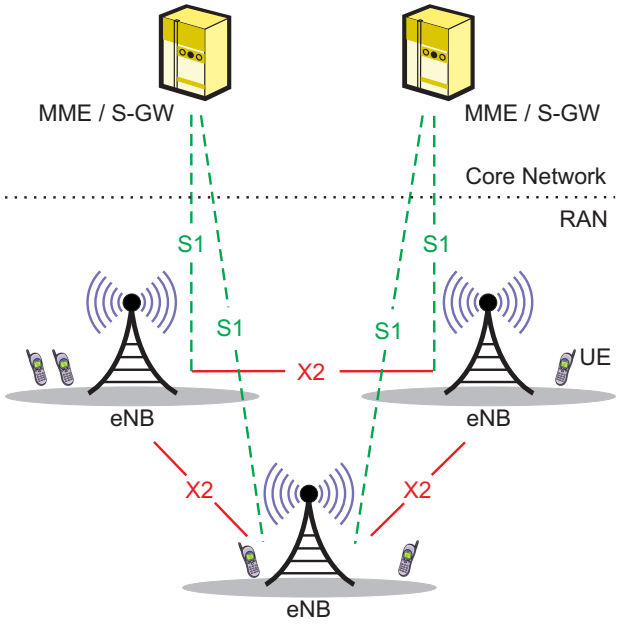

Figure 2.2: LTE network architecture [5]

The most important functions of the MME are the following:

- Non-access stratum (NAS) signaling and NAS signaling security.
- Access stratum security control.
- Idle state mobility handling.
- S-GW and MME selection (for HOs with MME change).
- Bearer management control.

Finally, the S-GW includes these functions:

- Mobility anchor point for inter-eNB HOs and inter-3GPP mobility.
- Packet routing and forwarding.
- Transport level packet marking in the uplink and the downlink.

The RAN segment in LTE is also called Evolved Universal Terrestrial Radio Access Network (E-UTRAN). The radio protocol architecture of E-UTRAN is represented in Fig. 2.3 for the user-plane and the control-plane. Both the user-plane, which terminates in the eNB on the network side, and the control-plane include the following layers:

- *Physical layer.* This layer offers data transport services to the next higher level through the so-called transport channels [31]. In addition, it handles coding/decoding, modulation/demodulation, multiple antenna transmission, etc.
- *MAC layer.* It handles the mapping between logical channels and transport channels [32].

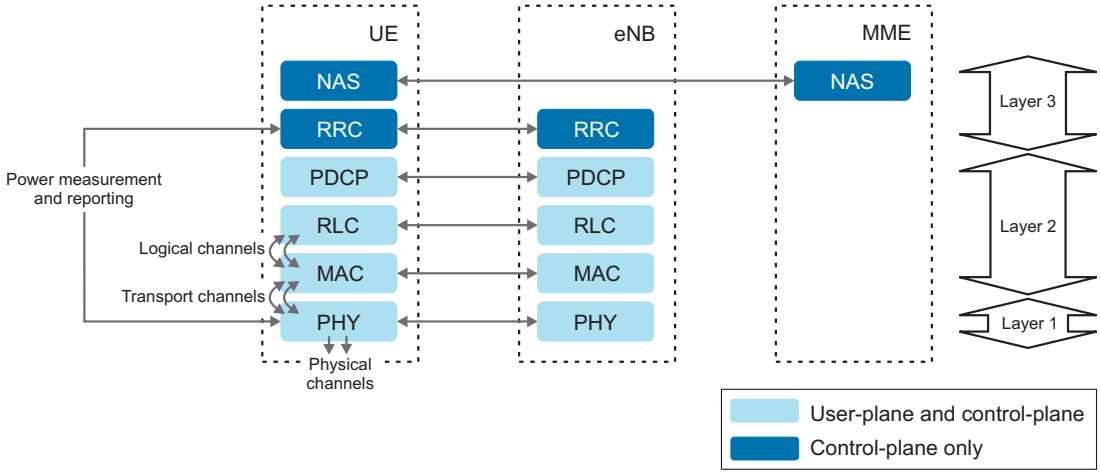

Figure 2.3: User-plane and control-plane protocol stack and radio channels overview

MAC offers services to the next higher level through the so-called logical channels. It is also responsible for error correction through HARQ and uplink and downlink scheduling. The scheduling functionality is located in the eNB.

- *Radio Link Control* (RLC) *layer.* RLC is in charge of concatenation, segmentation and reassembly of RLC service data units, error correction through Automatic Repeat Request (ARQ), in sequence delivery of messages to higher layers and duplicate detection [33]. RLC offers services to the next higher level through radio bearers, which are then mapped to bearers belonging to the core network.

- *Packet Data Convergence Protocol* (PDCP) *layer.* The main services and functions of this layer for the user-plane include IP header compression and decompression, ciphering and deciphering, in sequence delivery of messages to higher layers and duplicate detection [34]. The main functions for the control-plane are ciphering and integrity protection and transfer of control-plane data.

- *Radio Resource Control* (RRC) *layer.* This layer is responsible for broadcast of System Information and paging, RRC connection management, radio bearer control, security and QoS management functions, UE measurement reporting and mobility functions including cell (re-)selection and HO [35].

- *NAS layer.* NAS protocols support the UE mobility and bearer management. This layer also defines the rules for a mapping between parameters during inter-system mobility with 3GPP and non-3GPP access networks. In addition, it provides the NAS security by integrity protection and ciphering of NAS signaling messages.

By taking a closer look at the physical layer, both the signals and channels generated by this layer can be identified. On the one hand, the physical signals include the reference signals and the primary and secondary synchronization signals. The reference signals are used for channel estimation, meaning that, without the use of these signals, phase and amplitude shifts in the

received signal would make demodulation unreliable. In the uplink, the reference signals are also used for synchronization to the UE. The primary and secondary synchronization signals are used for cell search and identification by the UE. This allows the UE to identify and synchronize with the network. On the other hand, the physical channels carry data from higher layers including control, scheduling, and user payload. More specifically, in the downlink, the main physical channels and their functionalities are the following:

- *Physical Broadcast Channel* (PBCH) carries cell-specific information.
- *Physical Downlink Control Channel* (PDCCH) informs the UE about resource scheduling and HARQ information.
- *Physical Downlink Shared Channel* (PDSCH) carries the user payload.
- *Physical HARQ Indicator Channel* (PHICH) carries HARQ ACK/NACKs in response to uplink transmissions.

In the uplink, the main physical channels are:

- *Physical Random Access Channel* (PRACH) carries the random access preamble.
- *Physical Uplink Control Channel* (PUCCH) carries CQI reports and HARQ ACK/NACKs in response to downlink transmission.
- *Physical Uplink Shared Channel* (PUSCH) carries the user payload.

Although the LTE downlink and uplink use different multiple access schemes, a common frame structure is shared. The frame structure defines the frame, slot, and symbol in the time domain. In the downlink, the primary and secondary synchronization signals, reference signals, PBCH, PDCCH and PDSCH are almost always present in a downlink radio frame. Each physical signal and channel are also associated with a specific modulation scheme. For instance, PBCH and PDCCH can only use QPSK, while PDSCH can use QPSK, 16QAM or 64QAM, depending on the AMC functionality.

The next layer in the protocol stack, i.e. the MAC layer, makes use of the data transport services provided by the physical layer through transport channels and control information channels. On the one hand, the transport channels are as follows:

- *Downlink Shared Channel* (DL-SCH) is mapped to PDSCH and characterized by supporting HARQ, dynamic link modulation and dynamic/semi-static resource allocation.
- *Broadcast Channel* (BCH) is mapped to PBCH, it is required to be broadcast in the entire coverage area of the cell and it has pre-defined transport format.
- *Paging Channel* (PCH) is mapped to PDSCH and it provides support for UE discontinuous reception, which is a feature to keep the UE in a sleep mode during certain periods (enabling UE power saving).
- *Multicast Channel* (MCH) provides support for Multimedia Broadcast/Multicast service Single Frequency Network (MBSFN) and semi-static resource allocation.

- *Uplink Shared Channel* (UL-SCH) is mapped to PUSCH and characterized by supporting HARQ, dynamic link adaptation and dynamic/semi-static resource allocation.
- *Random Access Channel* (RACH) is mapped to PRACH and characterized by limited control information and collision risk.

On the other hand, the control information channels are as follows:

- *Control Format Indicator* (CFI) defines the number of PDCCH symbols per subframe.
- *HARQ Indicator* (HI) represents a NACK with value '0' and an ACK with value '1'.
- *Downlink Control Information* (DCI) contains information including DL-SCH resource allocation.
- *Uplink Control Information* (UCI) contains scheduling requests and acknowledgement responses or retransmission requests.

The transport channels are encoded and decoded using channel coding schemes. The turbo coding is used for UL-SCH, DL-SCH, PCH and MCH, since these channels carry large data packets. A tail biting convolutional coding is used for downlink and uplink control as well as BCH.

The MAC layer provides the logical channels to the next layer RLC. A logical channel is defined by the type of information which is carried. According to this, logical channels are classified into control channels and traffic channels for control-plane and user-plane information transfer, respectively. In particular, the control channels are the following:

- *Broadcast Control Channel* (BCCCH) is a downlink channel used for broadcasting system control information.
- *Paging Control Channel* (PCCH) is a downlink channel used for paging information and system information change notifications. Paging is the procedure that allows the network to request the establishment of a NAS signaling connection to the UE. PCCH is used for paging when the network has no knowledge about the location cell of the UE.
- *Common Control Channel* (CCCH) transmits control information between UEs and the network. It is used for UEs having no RRC connection with the network.
- *Multicast Control Channel* (MCCH) is a point-to-multipoint downlink channel used for the transmission of Multimedia Broadcast/Multicast Service (MBMS) control information.
- *Dedicated Control Channel* (DCCH) is a point-to-point bi-directional channel used for the transmission of dedicated control information between a UE and the network. It is used for UEs having an RRC connection with the network.

The traffic channels used by the RLC layer are:

- *Dedicated Traffic Channel* (DTCH) is a point-to-point channel dedicated to a single UE for the transmission of user information. It is defined for both uplink and downlink.

- *Multicast Traffic Channel* (MTCH) is a point-to-multipoint downlink channel used for the transmission of user traffic to UEs that receive MBMS.

The RRC layer handles the control-plane signaling of Layer 3 between the UEs and the E-UTRAN. At this layer, information is carried by bearers, which are classified into radio bearers, S1 bearers and Evolved Packet System (EPS) bearers. Radio bearers, which are established by using RRC protocol, carry information on the radio interface. S1 bearers are defined between the eNB and the MME/S-GW, while EPS bearers are defined between the MME and the S-GW. There exists one-to-one mapping between radio, S1 and EPS bearers. An EPS bearer also has an associated QoS profile including some parameters, among which are the following:

- *QoS Class Identifier* (QCI) is a scalar denoting the kind of service that can be supported by the bearer (e.g. bearer with/without guaranteed bit rate, priority, packet delay budget and packet error loss rate). This parameter is used as a reference to access node-specific parameters that control bearer-level packet forwarding treatment (e.g. scheduling weights, admission thresholds and queue management thresholds).
- *Allocation and Retention Priority* (ARP) determines whether a bearer can be accepted or needs to be rejected in case of network congestion during the bearer establishment. In addition, this parameter is used for bearer modification and, occasionally, for bearer dropping. Once that the bearer has successfully been established, ARP has no impact on packet level forwarding.

At Layer 3, two RRC states namely RRC_IDLE and RRC_CONNECTED are defined. In the RRC_IDLE state, the main functions are broadcast of system information, paging, cell measurement, cell selection/reselection and UE discontinuous reception. In the RRC_CONNECTED state, the UE has an E-UTRAN RRC connection, so that unicast data to/from the UE and broadcast/multicast data to the UE can be transferred. Other functions in RRC_CONNECTED are control channel monitoring to determine if data has been scheduled for the UE, CQI reporting, cell measurement, measurement reporting and system information acquisition. A UE changes from RRC_IDLE to RRC_CONNECTED state when an RRC connection is successfully established, while the UE returns to RRC_IDLE state by releasing the RRC connection. Unlike the RRC_IDLE state, in which mobility is controlled by the UE, the RRC_CONNECTED state involves network-controlled mobility. In LTE, fast and seamless HOs are of particular interest for delay-sensitive services such as VoIP. The simplified network architecture allows that HOs occur more frequently across eNBs than across core networks because the area covered by a MME/S-GW is generally much larger than the area covered by a single eNB. In addition, the signaling on X2 interface between eNBs is used for HO preparation, while the S-GW acts as anchor for inter-eNB HOs.

To make proper HOs and cell reselections, decisions require knowledge of the environment. By taking and reporting measurements of the radio environment, the UE provides the information necessary to the network in order to make the correct mobility decisions. Thus, the UE and the eNB are required to make physical layer measurements of the radio characteristics. In particular, the main physical layer measurements in LTE are the following [36]:

- *Reference Signal Receive Power* (RSRP). The RSRP is the linear average over the power contributions of the resource elements that carry cell-specific reference signals within the considered measurement frequency bandwidth. In both the downlink and the uplink there are reference signals, also known as pilot signals, which are used by the receiver to estimate, for example, the path loss.
- *Reference Signal Receive Quality* (RSRQ). The RSRQ is defined as the ratio N $\times$ RSRP/(E-UTRA carrier RSSI), where N is the number of resource blocks of the E-UTRA carrier RSSI measurement bandwidth. The E-UTRA carrier RSSI comprises the linear average of the total received power observed only in OFDM symbols containing reference symbols, in the measurement bandwidth, over the N resource blocks by the UE from all sources, including co-channel serving and non-serving cells, adjacent channel interference, thermal noise etc.

2.1.2 Self-Organizing Networks

During the last years, the growing demand of smartphones, online applications and multimedia services has led operators to upgrade their networks and use these resources more efficiently. With the extensive deployment of GSM, mobile networks are now available for a large number of people in the world. However, GSM is mainly intended for carrying voice traffic, while the capability devoted to data is rather limited. The increase in traffic demand comes from the emergence of new data services such as video and music streaming via web, social networking, location-based services, free applications markets, etc. Furthermore, the improved data processing and storage capabilities of the new terminals encourage the development of such services and user applications. In this sense, together with the existing smartphones, the recent so-called tablets are also taking place within the market for mobile terminals. Such devices include high resolution displays, whose touch interface eases the handling, and powerful processors that allow to display high-definition video and high-quality games. To cope with such a demand for data traffic, upgrading mature networks by increasing the number of macrocells would not be sufficient. Instead, to provide the desired capacity, the introduction of incoming and future technologies such as LTE and its evolution LTE-A will be necessary. One implication of this is that, to provide seamless connectivity and mobility across the network, a more complex control-plane would be needed, since the network infrastructure will become more complex and heterogeneous.

Upgrading the network infrastructure poses many challenges to operators in terms of reducing both CAPEX and OPEX [2]. CAPEX is related to the costs of adding new network resources to the existing network, while OPEX is related to the ongoing costs for network operation. To cope with the huge, necessary investment on infrastructure and taking into account that the average revenue per user has been decreasing during the last years, operators have paid special attention to cost savings, especially the OPEX. For this reason, the SON concept establishes a new paradigm for network management whose principal objective is to substantially reduce OPEX by decreasing human effort devoted to network operational tasks while at the same time optimizing network efficiency and service quality. In practice, SON means a set of functionalities for automated network planning, deployment, optimization and maintenance activities of these networks. As shown in Fig. 2.4, those functionalities are typically based on adaptive algorithms

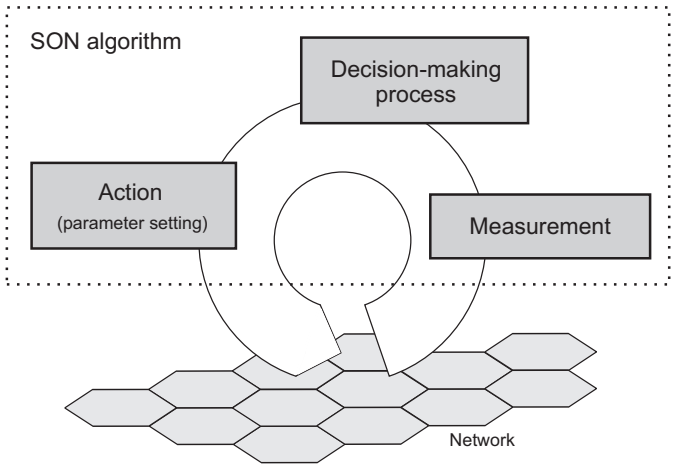

Figure 2.4: Typical phases in a SON functionality

which continuously execute a loop involving an initial measurement activity, a decision-making process and, lastly, a phase in which one or more actions are applied to the network. Firstly, the measurement phase implies a continuous activity where a lot of network measurements are collected and processed. According to the nature of the data, the information used as input for the SON algorithms can be classified into the following types [37]:

- *Configuration parameters.* They represent the actual configuration of network elements and network resources.
- *Counters.* This type of metric includes measurements from the network elements, which can be reported periodically or on-demand. Examples of counters are the traffic load, resource availability, the number of dropped calls, etc.
- *Alarms.* An alarm is a message generated by a network element when there is a failure.
- *Mobile traces.* This is information from specific UEs, which can be collected from most network elements (e.g. eNB).
- *Real-time monitoring.* It includes online measurements of specific items, such as traffic load and HOs performed in a certain network element.
- *Drive tests.* This refers to field measurements, e.g. related to coverage and interference, performed in a certain area by specialized equipment, which can also provide precise location information.
- *Key Performance Indicators* (KPIs). They are derived from other measurements, e.g. through a specific formula of counters, with the aim of providing a meaningful performance measure. An example of KPI is the blocking ratio, defined as the ratio between the number of blocked calls and the number of offered calls.
- *Context information.* This information is related to the environment, such as type of area (e.g. rural area), UE distribution (e.g. uniform), etc.

Secondly, the processed measurements are used by the SON algorithm to make a decision, which is usually a variation in a network parameter. Roughly, the algorithm analyzes the incoming information and compares the actual with the desired behavior of the network. If any parameter changes are necessary, then an updated set of radio parameters is derived. Finally, the new parameter configuration is applied to the network. Examples of network parameters are antenna tilts, power settings, neighbor cell lists, HO thresholds, etc. As shown in Fig. 2.5, the implementation of the SON solution approach can be either centralized or distributed [6]. In the first case, all SON algorithms are executed in a central node (e.g. a server), which reasonably should be located close to or within the Operations, Administration, and Maintenance (OAM) system. A disadvantage of this approach is that the fault-tolerance is low, since a failure in the central node would make the system inoperative. In the second case, the SON algorithms are located on each network element, e.g. eNB. The eNBs would communicate with each other via the X2 interface in order to exchange information. The main drawback of this approach is that more communication bandwidth is needed, as well as coordination between many nodes would be also a complex task.

Presently, network management consists of the processes and activities involved with planning, configuration, optimization and maintenance of networks, which are performed centrally from an OAM system. Some of these tasks are accomplished manually (e.g. adjustment of antenna tilt), while others are typically semi-automated and need to be supervised by human operators (e.g. adjustment of mobility parameters). Such a human effort is often expensive, slow and subject to errors. Thus, automation of network management allows operators to face the increasing complexity of mobile networks in order to use more efficiently resources while at the same time diminishing human involvement. In addition, SON capabilities can be further exploited in a context of multi-technology scenarios. Extending the SON concept to all RATs allows

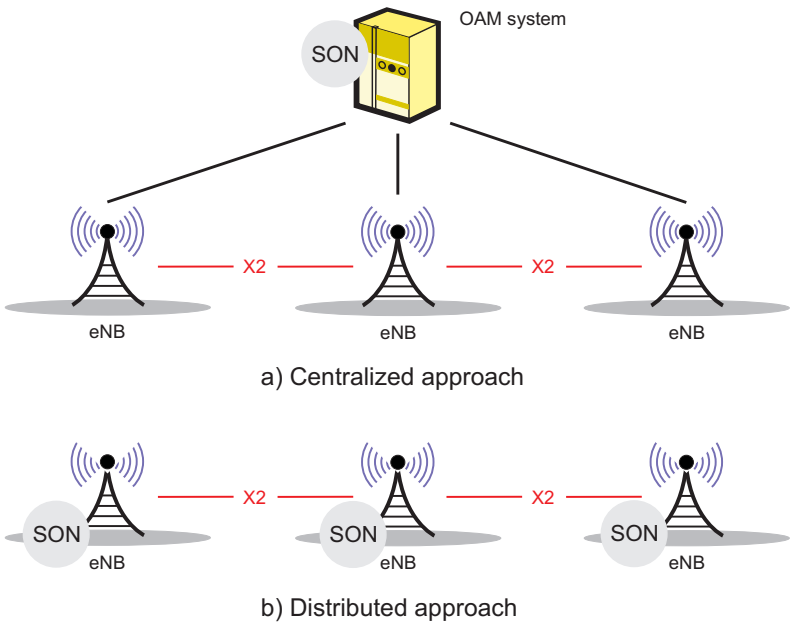

Figure 2.5: Implementation schemes for SON functions

operators to perform powerful optimization mechanisms in order to harmonize the whole network management and increase operational efficiency, as well as maximizing operational savings.

The SON concept was firstly introduced by the NGMN Alliance in [4], where a set of general use cases was derived from the operators' knowledge about problems in mobile network deployment and operation. Subsequently, the 3GPP translated this concept into more specific functionalities and use cases [5], which are part of the Release 8 together with the specifications of LTE, but this does not necessarily imply that SON can only be applied to LTE networks. Instead, 3GPP SON features can be extended to other Radio Access Technologies (RATs) as well (e.g. LTE-A). The classification of SON use cases adopted in this thesis is illustrated in Fig. 2.6. In particular, the proposed use cases are grouped into the following categories, denoted as self-X:

- *Self-Configuration.* It attempts to automate network parameter configuration according to the 'plug and play' behavior, e.g., when a new resource is added to the existing infrastructure [38]. This functionality allows network elements to autonomously launch, run setup routines, configure initial parameters, etc.
- *Self-Healing.* It is related to failure detection, diagnosis, compensation and recovery in order to cope with major service outages and degradations which significantly decrease user performance [39]. Self-Healing also includes those actions that prevent potential problems from arising.
- *Self-Optimization.* It aims to dynamically adapt network parameters to improve network quality [40]. Generally, the Self-Optimization algorithm recalculates the optimal parameter settings when traffic and network conditions change.

This classification is made according to the 3GPP guidelines. Other classifications, such as the one in [4], also include a fourth category, named Self-Planning, which is devoted to the derivation of the settings for a new network node, including the selection of the site location and configuration of the antenna settings. However, these tasks are typically associated with the deployment phase rather than with the operational phase of cellular networks. For this reason, the classification adopted in this thesis has been based on the 3GPP specification. In the following paragraphs, an overview of the SON functionalities and their related use cases is provided [5][41][42].

Firstly, Self-Configuration comprises all the activities related to the preparation, installation and setting up of a new eNB prior to its operation. After the initial configuration, this functionality also includes the periodical updates of the corresponding network elements. The following tasks belong to this category:

- *Hardware installation and initial configuration.* This refers to the physical installation of the new eNB and cabling for antennas and networking. In this case, the term Self-Configuration means 'plug and play' behavior for the hardware, so that it requires minimum human intervention. Examples of this behavior are autonomous measurement of antenna loss and initial parameter configuration of the database.

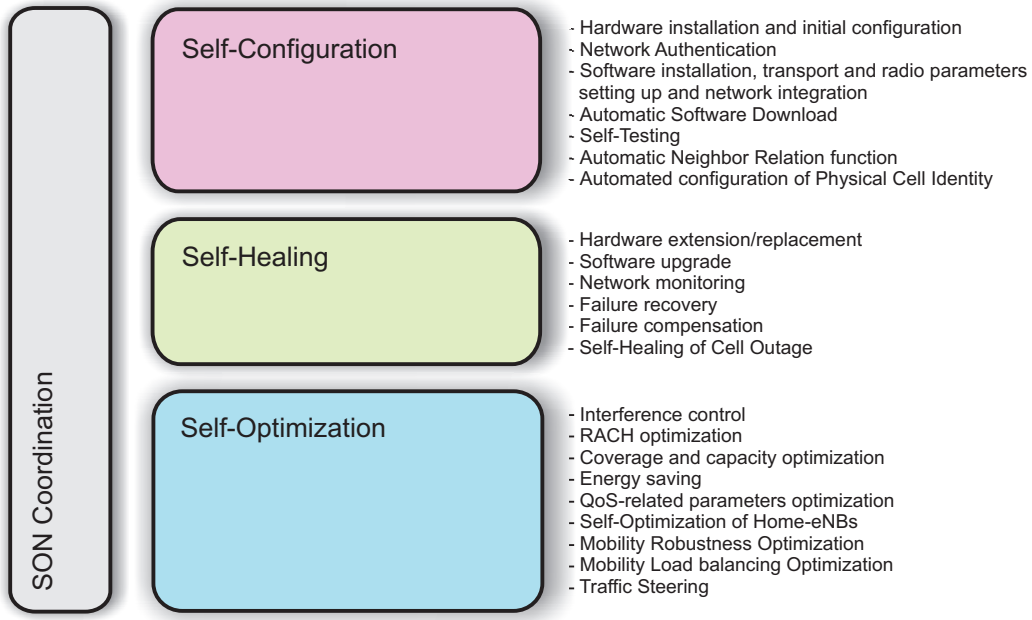

Figure 2.6: Classification of the SON use cases [5][41][42]

- *Network Authentication.* After the physical installation, the new eNB needs to discover the Network Element Manager and perform the authentication process.
- *Software installation, transport and radio parameters setting up and network integration.* Once the new eNB has been successfully authenticated, it needs to download relevant parameter settings and software packages, set up transport and radio parameters and modify the neighbor network elements (e.g. eNBs, MMEs and S-GW) according to the new situation in the network.
- *Automatic Software Download.* This functionality allows the eNB to autonomously download the new software packages and firmware. The update process can be initiated by either the eNB or the management server.
- *Self-Testing.* Before the eNB is operating in the network, Self-Testing ensures reliable operation of the network element. It involves Self-Testing of the hardware and software and checking whether the eNB will have the expected behavior or not. Self-tuning can be also commanded when the eNB is already operating in the network.

The 3GPP has defined two important use cases related to Self-Configuration [5][43], which are:

- *Automatic Neighbor Relation function* (ANR). The purpose of the ANR function is to remove human interventions from the management of neighbor cell relations. A bad neighbor relation configuration would cause HO failures and dropped calls. For this reason, neighbor relations need to be carefully known and planned. In addition, the large number of neighbor relations in a real network makes the manual neighbor planning time consuming and expensive, being the automatic solution more appropriate in this context. The ANR function can be applied not only to cells that are already deployed, but also to new cells,

for which completely new neighbor lists need to be generated.

The ANR function is located in the eNB and it manages the Neighbor Relation Table by means of two functions: the Neighbor Detection function, which finds new neighbors and adds them to the table, and the Neighbor Removal function, which removes outdated relations from the table. In addition, such a table contains some attributes to indicate for example if a relation should not be removed from the table or not be used for HO reasons, or if an X2 interface corresponding to a relation should not be used. In the case of the intra-frequency ANR, the procedure is as follows: firstly, the eNB commands each UE to perform measurements on neighbor cells; after this, the UE reports to the eNB the information necessary to identify the neighbor cells; finally, the eNB adds the neighbor relation to the Neighbor Relation Table. In the case of inter-RAT/inter-frequency ANR, each cell contains a search list containing all frequencies that should be searched.

- *Automated configuration of Physical Cell Identity.* The Physical Cell Identity is an essential configuration parameter of a radio cell. This parameter is divided into the Physical Layer Cell Group and Physical Layer Identity numbers. The former defines what group the cell belongs to, while the latter defines the identity. The total number of possible values is limited to 504, so that reuse of this parameter in different cells is unavoidable. This means that, when a new eNB is deployed, a Physical Cell Identity has to be allocated to each of its supported cells, avoiding collision with neighbor cells. If the selected Physical Cell Identity is already being used by another cell, then the identification of these cells will be hindered.

  Typically, the Physical Cell Identity has been derived from radio network planning, being part of the initial configuration of the node. The SON technique that implements automatic configuration of this parameter must fulfill that the value assigned to this parameter is unique in the area covered by the cell and there is no neighbor cell with identical value.

Secondly, Self-Healing mechanisms aim to mitigate as far as possible the performance degradation caused by a problem in a cell (e.g. a transceiver out of order). Self-Healing is different from the traditional fault management, whose objective is to detect failures as soon as they occur and to minimize their effects on the user performance. The main difference lies in the fact that Self-Healing performs fault management activities in an autonomous way. In addition, Self-Healing algorithms analyze not only alarms generated by network elements, but also KPIs and configuration parameters when trying to isolate network faults. More specifically, Self-Healing covers the following functions:

- *Hardware extension/replacement.* This refers to the replacement of hardware due to a fault in a network element which causes minimum service outage and the extension of hardware to provide more capacity when needed. Those tasks should require minimal operator intervention.

- *Software upgrade.* This activity also requires minimum operator attention. It includes automatic software download to the eNB and automatic upgrade for the Network Element Manager. As a result of these processes, software failures should be minimized. Note

that some tasks in this sub-group can be overlapped with others, e.g. Self-Configuration activities.

- *Network monitoring.* This function is responsible for collecting and analyzing network measurements in order to identify potential failures that can occur during the operation. This function also includes failure detection and diagnosis. In this context, inter-vendor scenarios should be supported and sophisticated trace functionality should be available. The more complete the information is, the faster the failures are identified and solved. A typical example for this category is the cell outage detection.
- *Failure recovery.* This function executes the repair actions for a identified problem. Those actions can be performed remotely (e.g. rebooting a system or changing a parameter) or locally (e.g. technicians replacing a piece of equipment). Recovery of a network element should require minimum intervention by an expert.
- *Failure compensation.* The aim of this function, which is performed while the recovery action to solve the abnormal behavior is being identified, is to minimize the degradation in network performance caused by the failure. That is, when a problem cannot be solved immediately, the affected cell and neighboring cells cooperate to minimize quality degradation. Failure compensation includes cell outage compensation (i.e. when a cell is in outage) and cell degradation compensation (i.e. when its service is degraded).

The 3GPP has defined an important use case related to Self-Healing, which is known as Self-Healing of Cell Outage [39]. The objective of this use case is to detect, compensate and recover a cell outage (e.g. sleeping, out-of-service). The cell compensation attempts to automatically maintain as much as possible normal services to the network users while the cell outage is being recovered.

Although Self-Healing is distinctly defined, sometimes the scope of self-X functions can be overlapped, causing some confusion. This is especially the case for parameter setting, in which the same parameter can be adjusted by different self-X functions. For instance, the transmit power can be a network parameter tuned by the Self-Optimization function, but if a bad configuration of the transmit power is causing major problems in a cell, the Self-Healing function will also change the conflicting network parameter in order to solve the problems. Since some use cases can adjust the same parameters, a SON coordination (Fig. 2.6) is also needed to maintain a good level of performance in the network [6].

Lastly, to describe Self-Optimization, the following section is entirely devoted for this purpose, since this functionality includes the SON use cases addressed in this thesis.

2.1.3 Self-Optimization

The deployment of mobile networks is a dynamic process, where continuously new sites are deployed, in order to adapt to traffic and context variations. Due to these variations, networks will have hardly the optimal configuration at a certain moment, so that certain network optimization

would be needed. In addition, the increasing level of competition has led operators to face the challenge of minimizing costs while at the same time providing high-quality services. In practice, instead of making large investments to update the existing infrastructure, these challenges can be accomplished by optimizing network parameters. In this context, Self-Optimization includes those optimization tasks which are carried out automatically.

As other self-X functions, Self-Optimization is a continuous process which comprises the following phases: collecting network measurements, calculating the parameter modification from the performance evaluation and, lastly, updating the parameter setting in the real network. This optimization is based on tuning parameters with the aim of achieving a well-defined goal, which can be expressed in terms of coverage, capacity or quality through the KPIs (key variables derived from network measurements). A combination of KPIs can also be used during the optimization process, since this activity usually involves implicit trade-offs between those indicators. The main Self-Optimization functions are shown in Fig. 2.6. The last part of this section provides a brief description of each of those functions [44].

Interference control

In mobile radio networks, interference is one of the main limiting factors for the system performance. A thorough management of interference can increase the system capacity and improve the QoS. In LTE, the scheduler allocates different radio resources to each user, so that the intra-cell interference between users is not an issue. However, this does not occur for inter-cell interference, which will be high at the cell-edge for loaded cells if assuming frequency reuse of one. As a result, low throughput and unsatisfactory QoS could be experienced by users at the cell-edge. Although there are features in LTE systems such as frequency-selective scheduling, which allocates PRBs with low interference to the users, SON techniques can also be used to further improve performance.

The interference control can be performed in both the uplink and the downlink. In the former, the interference coordination is carried out by controlling the usage of PRBs in different sectors, while in the latter, it is carried out by mainly controlling the transmit power patterns. These procedures, of course, require the exchange of certain information through the X2 interface in order to facilitate interference-aware scheduling and other SON techniques.

RACH optimization

The RACH is a transport channel characterized by limited control information and collision risk. Thus, its configuration has critical impact to system performance. In particular, the RACH collision probability becomes a critical factor for call setup delays, data resuming delays from the uplink unsynchronized state and HO delays. It also affects the call setup success rate and HO success rate.

In the uplink, resources need to be allocated exclusively for RACH, meaning that the amount of allocated resources has a direct impact on the system capacity. If few resources are allocated to RACH, it may result in low preamble detection probability and limited capacity. Therefore,

RACH parameter optimization should improve the operating grade of the RACH in order to provide significant benefits to the deployed network.

The optimal setting of RACH parameters depends on a multitude of factors, such as the uplink inter-cell interference from the PUSCH, RACH load, PUSCH load, uplink and downlink imbalance, etc. These are in turn affected by network parameters, such as the antenna tilt, transmit power and HO thresholds. For instance, if the antenna tilt of a cell is modified, the coverage of the neighbor cells will be changed, thus affecting the call arrival rate and HO rate. As a result, the RACH usage in each cell will also be changed and a new optimization iteration should be performed.

Coverage and capacity optimization

Coverage and capacity optimization is a typical operational task in mobile networks. Due to variations in the environment, planning tools, which are based on theoretical models, are not sufficient to provide the best performance in terms of coverage and capacity. For this reason, optimization is based on measurements and KPIs, which are derived directly from the network and provide a better estimation of the network state. For example, call drop rates give a first indication for areas with coverage holes, while traffic counters are used to identify capacity problems. In this sense, the main objective of a SON algorithm would be, a priori, to maximize coverage, since it typically has higher priority than capacity optimization. However, since coverage and capacity are linked, a trade-off between these two characteristics is also suitable for optimization.

The need for automatic optimization of coverage and capacity also comes from those variations in the environment, since manual optimization in such cases would be very expensive and time consuming. Changes affecting coverage and capacity are diverse. For instance, a change of season, a new building, a new deployed eNBs or a wrong parameter setting in the planning phase could lead to a reduction of capacity or coverage. As observed, the variation of these changes along the time is relatively slow. For instance, traffic distribution might be different in the day than in the night, leading to a waste of network resources and lower quality if network parameters are not changed, e.g. twice daily, to cope with such traffic variations. Thus, algorithms related to this use case are executed over long intervals, only when changes are large enough to have impact on system performance.

Energy saving

Initially, the major goal for wireless networks was to increase spectral efficiency (i.e. provide the highest data-rate with a given spectrum) without concerning the power consumption. In the UE side, reductions in energy use were focused on prolonging stand-by time and talk time. However, presently energy expenses have become a critical issue for operators. Reductions in energy use should be made only if the capacity offered by the network matches as much as possible the traffic demand. For example, those cells that provide additional capacity in a certain deployment should be switched off when its capacity is no longer needed.

The main reasons for implementing the energy saving functionality is that energy costs have been enormously increased in the last years, electricity costs are already an important component

of the OPEX, and some environmental aspects, such as the CO_2 emission, have become strong arguments from the perspective of the current governments and corporations.

QoS-related parameters optimization

The QoS refers to several related aspects of the services calls that allow the transport of traffic with special requirements, e.g. ensuring a specific frame error rate, delay or throughput. The optimization of QoS-related parameters deals with the trade-off between the QoS and the Grade-of-Service (GoS). The latter refers to performance metrics associated with call accessibility and maintainability, which are basically related to how many calls the system can handle simultaneously. Accessibility is usually measured in terms of call blocking (it happens when a call request is rejected), while maintainability is usually measured in terms of call dropping (it happens when a ongoing call is aborted). The following use cases attempt to find a good trade-off between QoS and GoS:

- *Admission control parameter optimization.* The basic operation of the admission control is to admit or reject new calls and incoming calls from other cells. This decision takes into account different aspects such as the current capacity, the system load, desired QoS of the newly requested and ongoing calls. In this sense, the objective of this use case is to self-optimize the admission control thresholds in order to minimize call blocking while at the same time fulfilling the QoS requirements of the admitted calls with sufficient likelihood, which is related to uncontrollable factors, such as the user mobility and variations in radio conditions and system load.

- *Congestion control parameter optimization.* While the admission control operates under normal conditions, the congestion control works in extreme conditions in order to cope with e.g. overload situations and prolonged bad radio conditions. In those cases, the admission control, which is of a proactive nature, cannot deal with unacceptable values of QoS requirements. In contrast, the congestion control, which is of a reactive nature, have to get the system back to a feasible load situation. Thus, the objective of this use case is to self-optimize the congestion control parameters in order to maximize resource utilization provided that certain QoS degradation due to congestion problems is allowed.

- *Packet scheduling parameter optimization.* This use case is mainly applied to LTE networks. Since LTE is optimized for packet data transfer, the packet scheduling plays a critical role. More specifically, the packet scheduler coordinates the access to shared channel resources and operates in two dimensions, the time and the frequency domain. The objective of the packet scheduling parameter optimization is to achieve the individual QoS requirements of the ongoing calls in the most efficient way, i.e. finding a good trade-off between fairness and spectral efficiency.

Self-Optimization of Home-eNBs

The concept of home-eNB refers to a small base station designed to increase capacity and coverage in indoor environments, e.g. residential and small business areas. These low-power nodes allow to create cells of small size which are called femtocells. A home-eNB may be turned on and off frequently or moved to a different geographical position, it may have closed or open access and

it is not physically accessible for operators. All these features transform the Self-Optimization of home-eNBs into a challenging task, which is different from the optimization related to macrocells.

The home-eNBs need to be physically installed by the customer and connected to the operator network through the customer's fixed Internet line. Since the customer usually does not have the knowledge needed to install software on home-eNBs, the configuration of these devices need to be performed in an automatic manner. Although the management of home-eNBs includes certain elements of Self-Configuration, it is more related with Self-Optimization, since these small nodes need to be constantly adapted to context variations.

The objectives of this use case are various. For instance, a home-eNB should automatically detect neighboring eNBs (including other home-eNBs) in order to have seamless mobility between eNodeBs. The neighboring cell list should also be maintained and optimized throughout the time, especially because home-eNBs are switched on and off arbitrary and more frequently. In addition, the radio parameters (e.g. the transmit power) should be optimized in order to minimize coverage holes or interference. Regarding the user mobility, the decision of performing or not an HO (between macrocell and femtocell) should also be optimized in order to avoid unnecessary HOs.

Mobility Robustness Optimization

The MRO aims to minimize the occurrence of undesirable effects (e.g. dropped calls) due to the HO process, which is the procedure that allows the user to freely move around the network. Since recent technologies (e.g. LTE) are being deployed with a frequency reuse of 1, the interference in adjacent cells becomes an important issue, especially in the cell-edge. This typically results in dropped calls and failures related to HOs. Furthermore, sub-optimal settings of HO parameters under poor radio conditions are more sensitive to call dropping and HO signaling load, which may lead to a redundant waste of network resources. Thus, the main objective of MRO should be to reduce the number of dropped calls due to suboptimal adjustment of HO parameters, while the secondary objective would be to reduce the inefficient usage of network resources due to unnecessary HOs.

The importance of this use case lies on the fact mobility management is crucial for operators, since sub-optimal settings of the mobility procedures directly affect the user performance. In particular, the call dropping is key from the operator perspective, since a reduction in this indicator can involve a significant loss of customer confidence and thus, important revenue losses for the operators.

Mobility Load Balancing Optimization

The MLB optimization deals with congestion situations in which some cells in the network are more heavily loaded than their neighbors e.g. due to an uneven spatial distribution of the offered traffic. In these situations, some traffic could be shifted from the heavily loaded cell towards the more lightly loaded cell by adjusting mobility parameters in order to relieve the congestion.

This use case is strongly linked to the MRO use case, since the MLB aims at dynamically

adapting mobility parameters according to the current traffic load of the cell and that of neighboring cells. The potential of sending users towards non-optimal cells from the radio perspective (e.g. signal strength) may lead to a decrease in the radio conditions of those users transferred to neighboring cells, meaning that the MRO should also take care of such an issue. However, as a result of a better matching between the spatial distribution of traffic demand and network resources, it is expected that more users can be accepted in the crowded area and more capacity is provided to the ongoing connections.

Traffic Steering

The evolution of next-generation wireless networks is envisioned to satisfy the growing traffic demand of new services. The increasing complexity and capability of terminals (or smartphones) has encouraged the development of new applications with higher requirements of bandwidth. To deal with this traffic demand, multiple RANs will be deployed covering the same area. HetNets will be characterized by the presence of networks with different technologies, frequencies, cell sizes, etc. Future RATs must co-exist and co-operate with existing technologies to provide high data rates and good QoS. In addition, hierarchical cellular structures involving cells with different sizes (e.g. macro, micro, pico and femtocells) allow to provide more capacity in crowded areas or hotspots.

In this context, since the coverage area of the deployed networks in HetNets are partially or totally overlapped, mobile operators can send users towards a specific network with the aim of utilizing resources more efficiently. This concept, known as TS, can be performed by using mechanisms of mobility management, which are standardized by the 3GPP in the case of mobile networks, providing support for interoperability with other systems [5]. In addition, such a task of selecting a more suitable network can be made to achieve a goal or a combination of goals, for instance, related to cost, user satisfaction, power consumption, coverage, etc. For this reason, the potential of TS in HetNets due to the widespread deployment of overlapping wireless networks brings many challenges to the operators.

2.2 State of the Art

This section presents the state of the art in SON, focusing on the use cases studied in this thesis as well as a survey on adaptive techniques for network parameter optimization. According to the 3GPP guidelines, certain use cases have received special attention in the research field, in particular, the MRO and the MLB Optimization [6]. Moreover, enhancements for these two use cases have recently become a requirement in 3GPP Release 10. Due to this, the MRO and MLB use cases have been addressed in this thesis. In addition, the coordination of SON techniques has also become of special interest in Release 11 [6]. Since there are multiple use cases, one challenging issue arising from the application of SON techniques is that some of these use cases are strongly coupled, needing to be coordinated. For instance, the two previous example use cases (MRO and MLB) can cooperate on the problem of a high number of dropped calls. Thus, the network performance could benefit from the SON coordination in these situations. For this

reason, the coordination of MRO and MLB has also been addressed in this thesis. On the other hand, to cope with the increasing mobile-broadband traffic in the last years, HetNets has become an effective solution to provide higher data rates and seamless connectivity and mobility across the network. In this sense, TS is a challenging Self-Optimizing use case from the operator perspective [45]. The concept of TS involves a powerful mechanism based on sending users to a specific subnetwork in the HetNet with the aim of optimizing the usage of radio resources. Due to this, the potential of TS techniques has also been studied in this work.

After presenting a survey on international projects related to SON, the rest of the section is devoted to the bibliography related with the specific SON use cases addressed in this thesis, i.e. MLB, MRO, SON coordination and TS in HetNets. In addition, a survey on adaptive optimization techniques for these use cases is also provided.

2.2.1 International projects

The introduction of new air interface technologies and network topologies due to the growing demand of smartphones and multimedia services has increased the complexity of network operation. The only feasible option for operators to cope with rapid technological changes and maintain the level of competition is by increasing the level of automation in the network [46]. In this context, there are certain areas especially attractive to offer a cost-effective implementation, especially those involving heavy calculations or signal processing. The benefit of a higher level of automation is an increase in network performance since those tasks can be executed faster and applied on a wide scale, i.e. a large number of cells. Another positive side effect is that human effort can be freed from mundane and tedious tasks and, instead, expertise can be applied in new areas, which bring additional value to the operator. As a result, the staff will be working on challenging tasks, which results in more motivation and productivity. For these reasons, the automation of network operation has gained attention in the research community, which is evident from several completed and ongoing international projects. The main public research projects and consortiums which are related with the area of automated network management and SON are the following:

- The *GANDALF* project (2005-2007), being part of the initiative EUREKA CELTIC, was aimed at developing automatic optimization tools for wireless networks with multiple RATs, in particular, GSM, General Packet Radio Service (GPRS), UMTS and Wireless Local Area Network (WLAN). This project covered automated diagnosis for troubleshooting, auto-tuning of network parameters and joint RRM between the networks [47].
- The *End-to-End Efficiency* (E^3) project (2008-2009) was focused on integrating cognitive wireless systems in the Beyond-3rd-generation (B3G) world, evolving current heterogeneous wireless system infrastructures into an integrated, scalable and efficiently managed B3G cognitive system framework [48]. One of the main E^3 objectives was to optimize the use of the radio resources and spectrum, following cognitive radio and cognitive network paradigms. To achieve this, the purpose was firstly to build a unique and generic architectural framework which was network and equipment agnostic and was mapped onto existing

and future network topologies. Then, autonomic and self-X concepts were incorporated in the system architecture to increase the efficiency of network operation. Finally, self-learning capabilities were included to improve the targets of the self-optimization processes in the management system.

- *COST 2100* (2006-2010) was the Action on pervasive mobile and ambient wireless communications belonging to the European, inter-governmental, scientific and technical cooperation framework COST. The Sub-Working Group (SWG) 3.1 focused on mobile wireless network optimization. As network models together with simulated environment models usually do not satisfy the operator's requirements, SWG 3.1 aimed at substituting artificially generated data by the measured data taken from the real system. The continuation of this Action, known as *COST IC1004*, is currently ongoing. Its Working Group (WG) 3 is similar to the SWG 3.1 previously mentioned.

- The *SOCRATES* project (2008-2011) developed SON algorithms to enhance the operations of wireless access networks, by integrating network planning, configuration and optimization into a single, mostly automated process requiring minimal manual intervention [2]. In this context, a functional architecture for SON coordination has also been proposed in order to avoid conflicts due to the simultaneous operation of different SON functions. The use cases considered by the SOCRATES project are listed in [44]. For each use case, the required input data, the desired output parameters, the actions to be performed, possible dependencies on further standardization and potential gain in terms of OPEX and CAPEX reduction were firstly analyzed. Later, aspects such as the implementation and interdependencies among the use cases were also studied.

- The *SELF-NET* project (2008-2010) aimed at designing, developing and validating an innovative paradigm for cognitive self-managed elements of the future internet [49]. One of the main objectives was to incorporate new management capabilities into network elements in order to take advantage of the increasing knowledge that characterizes the daily operation of mobile users. In addition, another key objective of Self-NET was to provide a holistic architectural and validation framework that unifies networking operations and service facilities of the future internet.

- The *UniverSelf* project (2010-2013) aims at overcoming the growing management complexity of future networking systems and reducing the barriers that complexity and ossification pose to further growth [50]. To achieve these objectives, UniverSelf presents a unified management framework for the different architectures and all required functions to achieve self-management. The impact on the industry and the push of European research into the direction of exploitation is another of the main goals.

- The *SEMAFOUR* project (2012-2015), considered as the continuation of the SOCRATES project, will design and develop a unified self-management system, which enables the network operators to holistically manage and operate their complex heterogeneous mobile networks [51]. The first objective is to develop multi-RAT and multi-layer SON functions that provide a closed control loop for the configuration, optimization and failure recovery of the network across different RATs (e.g. UMTS, LTE, WLAN) and cell layers (e.g.

macro, micro, pico, femto). The second objective is to design and develop an integrated SON management system, which acts as interface between operator policies and the SON functions.

2.2.2 Mobility load balancing

Load balancing copes with congestion situations where neighboring cells with spare resources are utilized for offloading the congested cells. Load balancing is considered by the 3GPP as an important issue in SON due to its effectiveness to increase network capacity. Firstly, the concept of SON is widely addressed in next-generation networks, being part of the specification of LTE [52]. Secondly, the MLB use case is introduced in [43] together with other Self-Optimization use cases. Later, the MLB, as part of SON, is recognized as one of the key enablers in LTE-A [53], where enhancements for this use case are proposed to be investigated. Finally, the application of MLB to HetNets and inter-RAT scenarios is proposed in [6].

The load balancing problem can be solved by sharing traffic between adjacent cells. MLB is tackled here as a Self-Optimizing task that can be solved by tuning specific network parameters, in particular, those involved in the HO process. The HO process is responsible for transferring an ongoing call from one cell to another. By adjusting HO parameters settings, the service area of a cell can be modified to send users to neighboring cells. Thus, the size of the congested cell is reduced while adjacent cells increase in size taking users from the congested cell edge. As a result of a better matching between the spatial distribution of traffic demand and network resources, more users could be accepted in the crowded area so that the call blocking probability would be reduced [54].

A significant research effort has been devoted to the load balancing problem. In [54], a method for determining the best traffic share between cells in a GSM network is presented, where a closed-form expression for the optimal traffic sharing criterion is derived by solving a classical optimization problem. In [55], it was shown that the number of unnecessary HO attempts and failures can be significantly reduced by tuning the load-based HO thresholds in a GSM/WCDMA scenario, where it is assumed that a sufficient number of users are handed over to less loaded cells when the load exceeds the threshold. In [56], the decision of triggering inter-system HOs for load balancing between UMTS and GSM depends on the load in the target and the source cell, the QoS, the time elapsed from the last HO and the HO overhead. The studies in [56] show that both the capacity and the provided QoS could be notably improved in overload situations. In [7], the proposed load balancing scheme tunes HO thresholds in the soft-HO algorithm for UMTS networks, where a user can be simultaneously connected to two or more cells. In the case of LTE networks, several studies about load balancing can also be found in the literature. In [8][9][10], similar algorithms for MLB are proposed. In particular, these algorithms automatically adjust the HO margins until the load or the load difference between cells is below a threshold. In [57], load balancing is formulated as a multi-objective optimization problem. More specifically, the proposed algorithm maximizes both load balance for real-time constant bit rate users and a utility function based on QoS requirements for best effort users. In [58], the authors propose a method inspired by the flowing water algorithm that creates an HO

margin adjusting scheme from load measurements. In [59], a game theoretic scenario for load balancing is proposed. In [60], the load balancing problem is simplified to a single aggregate objective function optimization problem, which takes into account the physical resource limits and the QoS requirements.

Some of the previous references are focused on inter-system load balancing, where propagation conditions are not necessarily a problem because the coverage areas of different radio technologies are typically overlapped. In the case of intra-system load balancing, when a user is handed over to another cell, the propagation conditions could get worse if the user is located near the cell edge because of the interference caused by neighboring cells. In LTE, the previous references analyze the performance of load balancing mostly in terms of achievable throughput for data services, neglecting the dropping rate, which is an important performance indicator in real-time traffic (voice, video, etc.). Also it is noted that controlling those quality indicators (e.g., dropping rate) for real-time traffic is not considered by the previous references as only performance evaluation is carried out without any further impact on the indicators. In [10], it is remarked that the trade-off between enhanced blocking and degraded dropping can be adjusted by restricting the maximum achievable HO margin. However, further study of load balancing effects on quality indicators for real-time traffic would be necessary. In this sense, an important contribution of this thesis with respect to the MLB use case is the design of an algorithm to control quality performance for real-time traffic during the load balancing process.

On the other hand, the vertiginous increase in mobile-broadband traffic experienced in the last years has led operators to deploy cells of lower sizes to cope with such an increase in traffic demand. The reason for this is to keep the users closer to the base station as well as to allocate a lower number of users per cell. In this context, femtocells are envisioned to cope with such a demand of capacity in indoor environments [61]. Since those small cells are low-cost nodes, a thorough deployment is not typically performed, especially in enterprise scenarios. As a result, the matching between traffic demand and network resources is rarely the optimal. This means that the application of load balancing techniques are especially attractive in those cases. In addition, most of the tasks involved in the installation, operation and maintenance of femtocells have to be done in an automatic manner, since the customer cannot be assumed to have the knowledge necessary to manage femtocells. For this reason, SON is also a key concept for femtocell management.

The challenges in femtocell self-organizing has gained attention in the research community, which is evident from several international projects (e.g. *HOMESNET* [62], *BeFEMTO* [63], *FREEDOM* [64]). Most efforts have been paid to the design of advanced Radio Resource Management algorithms to reduce inter-cell interference [65][66][67]. In [68], a self-tuning algorithm for selecting femtocell pilot power and antenna pattern is proposed to improve the coverage and minimize the total number of HO attempts. In [69], an adaptive algorithm for selecting the hysteresis margin based on user position is presented. In [70], an accurate model for simulating femtocells is proposed, where different levels of complexity in the prediction of femtocells and their effects on HOs as well as on call drops are also investigated. In addition, recent studies have considered networked femtocell environments, among which is the enterprise scenario [71].

However, few studies have addressed load balancing in enterprise femtocells with legacy equipment, which is of relevant interest for operators [72][11][73]. Many challenges arise from the fact that those scenarios often include three-dimensional structures, unequal distribution of traffic load is very common (e.g., crowded/uncrowded offices), the user mobility pattern is different (probably more intense) than at home and open access is usually employed instead of closed access. Thus, further study of load balancing in enterprise scenarios would be necessary. In particular, this thesis investigates the potential of different load balancing techniques to solve persistent congestion problems in enterprise LTE femtocells.

2.2.3 Mobility robustness optimization

Roughly, MRO is the optimization of the HO process, which typically involves a trade-off between the amount of signaling load due to HOs and the quality of the active connections in the network. As in the case of MLB, MRO has been considered by the 3GPP as a key functionality in the field of SON. The basics of MRO are introduced in [43], while enhancements for this use case and its application to HetNets and inter-RAT scenarios are addressed in [53] and [6], respectively. Following the 3GPP guidelines [6], the main objective of MRO should be to reduce the number of dropped calls due to suboptimal adjustment of HO parameters, while the secondary objective would be to reduce the inefficient usage of network resources due to unnecessary HOs.

The MRO has gained attention in the research community, which is evident from several international recently finalized projects (e.g., *SOCRATES* [2] and *E3* [48]). Thus, several techniques for HO optimization applied to different RATs can be found in the literature. In [74][75], the optimization of the so-called soft-HO in WCDMA has been addressed. However, next-generation wireless networks are based on hard-HOs, meaning that the UE is attached to a single cell at a specific time. In this field, some performance analyses for intra-frequency LTE HOs are described in [76][77], but no SON algorithms are provided to find an optimal setting of HO parameters in those papers. Other works that propose a SON algorithm only consider one HO parameter in the analysis, [12][13][14]. In [15][16], techniques for modifying both the HO margin (HOM) and the Time-To-Trigger (TTT) are proposed, but no further impact on user speed is analyzed. Finally, the inter-system HO optimization has been addressed in [78][79].

Unlike previous work in this area, a significant contribution of this thesis is to study performance analysis considering both HO parameters (i.e. the HOM and the TTT) for different situations, highlighting the variation of the user speed. The impact on the GoS (e.g., call dropping and call blocking) for future services such as VoIP calls is also studied. In addition, an important contribution in the area of SON is the proposal of a novel MRO algorithm, which has several benefits over other existing approaches. For instance, in [15], the optimal values of the HO parameters are selected from a diagonal through the grid of HOM and TTT values, based on a previous sensitivity analysis derived from system performance simulations, thus limiting the results to the used, realistic, simulated scenario. Conversely, in this work, the proposed SON algorithm optimizes HOMs independently of the simulated scenario.

2.2.4 SON coordination

In Section 2.1.2, the development of stand-alone SON functions has been addressed. It is noted that, with the growing deployment of SON functions, the number of conflicts and dependencies between them increases. A conflict can happen if, for example, two different individual SON functions (e.g. the MLB and MRO) optimize the same parameter (e.g. the HOM) with different goals at a network element. The interaction between SON functions also exists if the modification of a parameter affects the operation of other SON functions. Those conflicts may have a negative impact on network performance, which is far from the operator's objectives when the SON functions are implemented. Thus, the avoidance and resolution of conflicts and dependencies between these functions become an important issue for operators.

The study of SON coordination is a recent topic addressed in the bibliography. In [80], a generic mathematical model for the interaction of multiple SON mechanisms running in parallel, along with a practically implementable coordination mechanism, are proposed. The SOCRATES project has also defined a general framework approach for SON coordination that addresses the avoidance, detection and resolution of conflicts that can occur between different individual SON functions [81][82]. However, in the SOCRATES project, minor attention has been devoted to specific SON use cases that have a strong interrelation regarding the involved control parameters. In particular, the coordination between macro and femtocell HO optimization [83], admission control and HO optimization [84], and load balancing and HO optimization [85] have been investigated. Related to this thesis, special attention has been devoted to the coordination between load balancing and HO optimization (i.e. MLB and MRO, respectively), addressed by the SOCRATES project. However, in that project, the study assumes the control parameters of the MLB and MRO algorithms to be independent of each other, i.e. the two algorithms do not tune the same parameters. In particular, the MLB function adjusts the HOM, while the MRO function adjusts the TTT and hysteresis parameters. The interactions exist because these two functions influence the same KPIs that are used as input for the optimization algorithms. Unlike this design, the MRO function proposed in this thesis do not adjust the hysteresis parameter of the HO procedure, since it cannot be adjusted per cell-basis or adjacency-basis, which is a severe limitation in mobile networks due to the variant nature of the radio environment. This consideration makes the coordination problem different from the approach studied by the SOCRATES project. The coordination between MLB and MRO has been also investigated in some other works. In [86], a constraint for the connection quality more restrictive than the one assumed in the SOCRATES project is considered. In this sense, the MLB function is restrained in favor of the HO performance optimization. However, as in the SOCRATES project, the MRO function also consider the hysteresis parameter, which is a limitation as it cannot be defined at cell level. Furthermore, the impact of the user speed on the coordination algorithm is disregarded. The user speed is an important factor as the HO signaling significantly increases with the user speed. In [87], to avoid the conflict between MLB and MRO, the HOM range of MLB is dynamically adjusted according to the TTT and the hysteresis parameters, which are first adjusted considering the effect of the user speed. However, such an optimization is related with a fast adaptation (i.e. on-line) of HO parameters, which is not the problem addressed in this thesis. In particular, the parameters in [87] are considered to be UE specific. Such UE specific

properties are not available on the level of the OAM system, so this kind of optimization can only be done in the eNB. In addition, that approach requires velocity estimates which are not easy to obtain [41]. Conversely, in this thesis, the variations of HO parameters are performed to adapt to slower changes (e.g. hours, days) in the environment and they are adjusted per cell-basis or adjacency-basis.

2.2.5 Traffic steering

Currently, large investments on infrastructure are needed to cope with the growing demand of traffic. In this sense, operators can choose from various alternatives, such as deploying cells of lower sizes and making use of newer technologies (e.g. LTE and LTE-A). However, these solutions are expected to be insufficient, meaning that the existing networks will also play a key role in coping with that enormous traffic demand. In this context, HetNets are shown as an effective solution to provide higher data rates and seamless connectivity and mobility across the network. To achieve these goals, HetNets involve not only deploying e.g. different RATs, cell sizes, and carrier frequencies, but also managing the hybrid network as a unified whole. In HetNets, the concept of TS involves a powerful mechanism based on sending users to the correct subnetwork with the aim of optimizing the usage of radio resources. Since the coverage area of the deployed subnetworks are partially or totally overlapped, network operators could determine toward which network a user connection should be routed to utilize resources more efficiently.

The potential of steering a user connection towards a specific network layer in HetNets brings new challenges to the operators. Such a challenging task of selecting the *best* network due to the widespread deployment of overlapping wireless networks has been addressed in the literature. In [17], a policy-enabled HO to express policies on what is the *best* wireless system is proposed. These policies allow to establish different trade-offs among indicators related to cost, performance, power consumption, etc. In [18], an analytical approach to define a wide range of RAT selection policies taking into account several allocation criteria such as service type, load, etc. is proposed. Users can also use simultaneously services through different RATs. Such a problem is addressed in [19][20], where different strategies in a multi-RAT, multicellular and multiservice scenario are designed to indicate the suitability of selecting a specific RAT. Similarly, the problem of allocating multiple services onto different subsystems in multiaccess wireless systems is addressed in [21], where some principles for how this service allocation should be done to maximize the resulting combined capacity are discussed.

There are also many references focused on particular cases showing the benefits of TS. For instance, a network layer suffering from a temporary traffic congestion can offload some users to a non-loaded layer (load balancing) [9][56]. High speed users can be connected to a so-called umbrella layer to avoid a frequent number of HOs [88]. Other factors contributing to the preferred choice of the access technology are addressed in [89], where aspects such as coverage, securing QoS for the requested service, minimizing the cost of delivering the service to the end user and maximizing the spectrum utilization by traffic packaging are considered to select the access technology. Potentials of dynamic TS algorithms are also addressed in [45].

As shown in the previous references, the specific objectives of TS depend on the operator policy and they are achieved by utilizing mechanisms of mobility management, which usually are standardized by organizations such as the 3GPP [5]. In idle mode, no dedicated resources have been established for the UE and the procedure for changing of camping cell is called cell reselection. A TS policy can be used in this case to determine the preferred layer for camping [19][90]. In connected mode, an HO is typically carried out when the UE moves between two cells to preserve the user connection. However, this is not necessarily the only reason for triggering an HO. Since the coverage area of the layers is overlapped, a UE could trigger an HO due to TS reasons [17][91]. An important issue that arises from using both cell reselection and HO procedures for TS is the need of aligning these two mechanism to avoid ping-pong effects.

Most of the previous references are focused on selecting the preferred RAT disregarding the fact that heterogeneity of future networks also includes networks with different frequencies, cell sizes, etc. In addition, the RATs used as examples for assessing the TS techniques typically have been GSM, UMTS and WLAN, so that further study of future networks such as LTE and LTE-A would be necessary. For these reasons, in this thesis, novel TS techniques for HetNets based on adjustment of mobility parameters are investigated.

2.2.6 Adaptive techniques for network parameter optimization

Concerning the second broad topic of the thesis, automatic self-tuning has been widely applied in the literature to wireless network parameter optimization. Proactive approaches formulate the tuning problem as a classical optimization problem, which can be solved exactly [92][93]. Unfortunately, the required analysis tool is rarely available for cost reasons. Therefore, operators have to solve the problem by heuristic methods. In this sense, self-tuning fuzzy systems are shown as an effective solution, where, in most cases, a Fuzzy Logic Controller (FLC) is designed to tune a specific network parameter (e.g., HOMs, transmit power) with the objective of improving performance (e.g. maximizing throughput). With regard to the SON use cases addressed in this thesis, various FLC designs can be found in the bibliography for MLB [11][73][91][94][95][96] as well as for MRO [75]. All these references prove that FLCs are very useful for automatic network parameter optimization. Fuzzy Logic benefits come from their ability to translate human knowledge into a set of basic rules.

The design of FLCs requires the definition of a rule base, or knowledge base, containing the fuzzy rules that represent the mapping of the input to the output in linguistic terms. Such rules are derived from the knowledge and experience of a human expert of the system. In cellular networks, the experience is extracted from network operators, which are used to manually adjust many network parameters. However, knowledge is not always available so that performance is usually limited by the behavior imposed to the FLC. In those cases, increasing the number of rules is not an effective solution, since the human expert may find difficulty in defining many rules. For this reason, different strategies have been investigated to create, adapt or refine rules, e.g. through learning using neural networks [97][98], genetic algorithms [99] and Reinforcement Learning (RL) [9][19][100]. Thus, mathematical techniques have been successfully applied in wireless network optimization problems. In Chapter 3, a brief overview of these techniques will

be provided. Among these solutions, fuzzy Q-Learning is an RL method particularly appropriate for learning from interaction, when it is often impractical to obtain representative examples of desired behavior for all the situations (e.g. in wireless networks) in which the controller has to act [101].

Different works applying Q-Learning in wireless network optimization problems can also be found in the bibliography [102][103][104][105][106][107][108]. Related to this thesis, the inter-system load balancing problem is addressed in [9] by designing an FLC optimized by the fuzzy extension of Q-Learning algorithm in a UMTS network with WLAN hotspots. Concerning TS, in [109], the Nash-Stackelberg fuzzy Q-learning is used for decision-making in heterogeneous cognitive networks, with the network as leader that aims at maximizing its utility (revenue) and the mobiles as followers that have their individual objectives (maximizing their QoS). Therefore, the combination of FLCs and the fuzzy Q-Learning algorithm is a powerful Self-Optimization mechanism where the FLC facilitates the modeling at a higher level of abstraction (i.e. human reasoning) and the Q-Learning allows to train/adapt the controller. For this reason, the solution adopted in this thesis is based on the fuzzy Q-Learning algorithm. More details about this method will be provided in Chapter 3.

2.3 Conclusions

In this chapter, firstly, the RANs that are assumed in this thesis have been described. While HSPA supports increased peak data rates and reduced latency compared to original WCDMA protocols, LTE also provides low power consumption, spectral flexibility and reduced OPEX. Both technologies are envisioned to play a key role in coping with the growing demand of traffic in the next years.

Secondly, the concept of SON has been analyzed in detail, showing the importance of this paradigm to enhance network performance and reduce operational costs. In addition, within this broad concept, the main use cases concerning Self-Configuration, Self-Healing and Self-Optimization have been discussed. Regarding Self-Optimization, certain use cases have received special attention in the research field, in particular, the MRO and the MLB. These functions cope with mobility problems and congestion situations, respectively. In addition to these use cases, TS is a powerful mechanism in the context of HetNets which allow to utilize resources more efficiently, benefiting operators and users. The operational process of such functionalities is based on executing a loop including the following steps: collecting network measurements, calculating the parameter modification and applying it to the network. Thus, by dynamically optimizing the network, improved end-user experience and increased network capacity are provided.

Thirdly, the State of the Art on the field of SON and the mentioned use cases has been presented through a study of recent and ongoing research. The conclusion is that further efforts are needed to find more effective solutions, especially those based on self-learning approaches.

Chapter 3

Adaptive optimization techniques

The first part of this chapter summarizes the principles of Fuzzy Logic, which is the theoretical basis on which the techniques proposed in this thesis are based. The analysis focuses on FLCs, which provide an effective means of converting a linguistic control strategy based on expert knowledge into an automatic control strategy. The second part of the chapter is devoted to several techniques which are especially suitable for optimizing FLCs. Special attention is drawn to RL, which in this thesis, has been the selected method amongst the previously described ones.

3.1 Parameter self-tuning

3.1.1 Introduction

In recent years, network management automation has become very important. To cope with the enormous investment on infrastructure made in the last decade, operators have paid special attention to cost savings, where the concept of SON is of relevant interest. In this context, self-X functions (e.g. Self-Optimization) typically involve network parameter tuning. On the one hand, the set of network parameters that can be optimized in a wireless network is extremely large, as there are lots of algorithms running and some parameters are defined on a per-cell or per-adjacency basis. In addition, even if the optimization process is only performed on a few relevant parameters, the relationship between parameter settings and network performance is not straightforward. For this reason, network parameter optimization should be performed in an automated manner. As a result, the network would be able to adjust its parameters in order to achieve optimal performance without human effort. On the other hand, not all parameters are equally easy to change. For instance, those radio parameters requiring site visit and climbing the antenna would be excluded from the definition of self-X functions executed during the operational

phase. However, there are many parameters that can be changed remotely from the OAM system. Even in this category, some parameters can be changed on the fly, while others may require locking the network element. From the operator perspective, modifying network parameters that do not require time scheduling is the preferred alternative.

Different approaches can be followed to face the problem of automatically modifying parameters in a wireless network [110]. The first classification, shown in Fig. 3.1, is made according to whether a simplified model of the system is used (or not) to search the optimal configuration. If such a model is used [see Fig. 3.1(a)], firstly, it should properly describe the relationship between input and output variables. For this purpose, the system inputs and outputs need to be previously defined. The inputs can be network parameters and uncontrollable uncertainties, while the outputs consist of a set of measurements, which are used to build the KPIs. In ad-

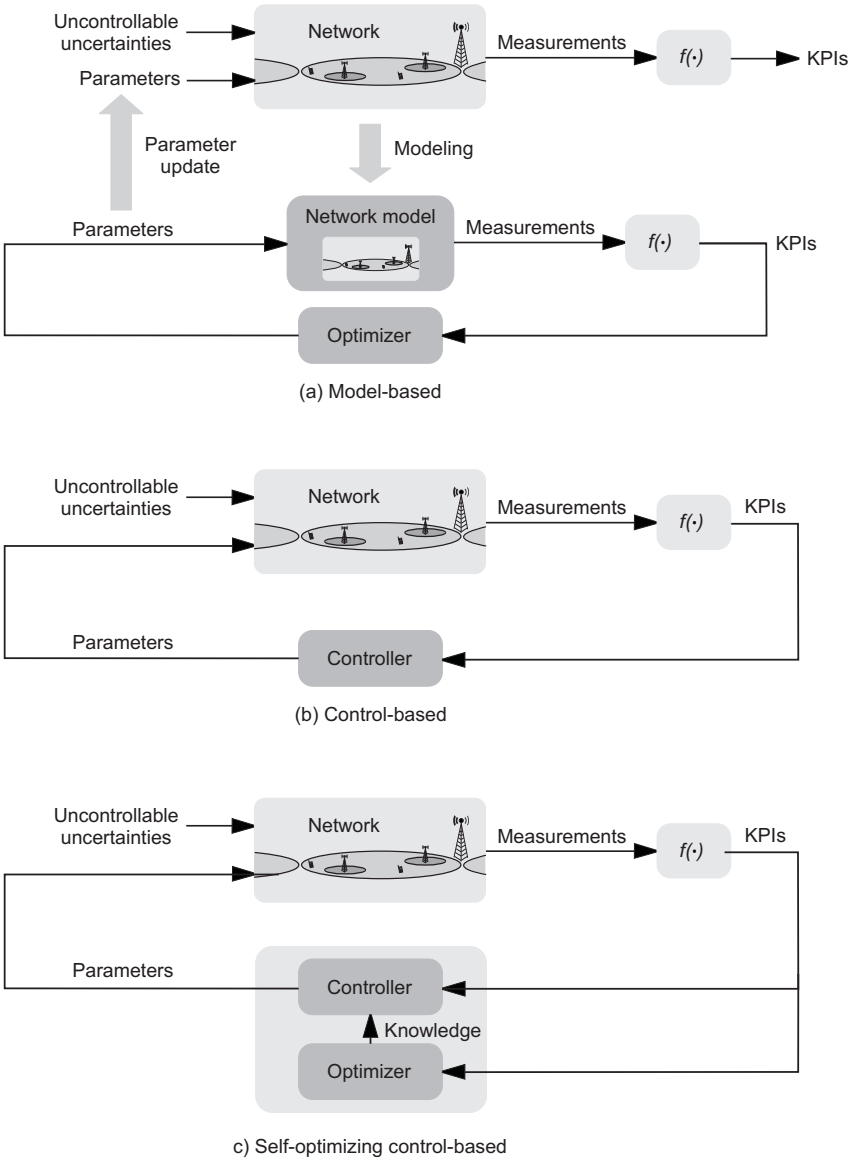

Figure 3.1: Self-tuning approaches for wireless networks

dition, several KPIs can be combined to generate a Figure-of-Merit (FoM), based on operator's requirements and targets. The relationship between parameters and KPIs/FoMs (i.e. the network model) is established by means of an analytical or simulation-based model. Once the model is defined, the next step is to find the optimal parameter settings. If the search space is large, as it usually happens in wireless networks, an optimization method is normally used (denoted in the figure as the optimizer). This process can require some iterations to find the optimal solution. Finally, the best parameter settings found in the model are applied to the real network. The potential of this approach lies on the construction of a network model that is accurate and manageable. In general, an analytical model that accurately describes the relationship between network performance and parameters cannot be built because of the complexity needed. Instead, simulation models are a more suitable solution since the dynamic behavior and randomness in the system can be easily described. Unfortunately, the accuracy of these models is not always sufficient. In wireless networks, the lack of accuracy typically comes from the complexity of propagation models and traffic distribution in both the time and space domains. As a result, the self-tuning process might lead to sub-optimal network performance. In this case, the simulation model should not be used to find the optimal settings of a particular network, but it could be used to assess optimization methods before including them in the real network. To refine the network model, network measurements can be collected during the operational stage. Thus, it is more likely that the network model is closer to the optimal solution. However, even in this situation, the network is subject to changes caused by uncontrollable factors. For instance, re-configuration of another set of parameters carried out by the operator can cause the parameter settings found by the network model become ineffective. To cope with this issue, the network model must be updated periodically, as well as the optimization process must also be run periodically.

When a network model is not possible (e.g. for complexity reasons), the self-tuning entity can interact directly with the network. In this case, a closed-loop structure is used to find the optimal parameter settings. In Fig. 3.1(b) the basic structure of a closed-loop control system is shown. This scheme is based on a controller that typically adjusts network parameters by comparing the values of KPIs with some reference values (e.g. to maintain call blocking below 5%). On the one hand, a distinct advantage of this approach is that the sensitivity to external inputs is reduced with the use of feedback. Thus, good performance is achieved regardless of uncontrollable uncertainties and variations in the traffic distribution or propagation environment. On the other hand, this approach has several limitations. Firstly, the search space is much smaller than in the model-based approach. The reason for this is that, as operators do not accept service degradation during operation, only small variations to the default parameter settings are allowed in the network. Secondly, if the reference values previously mentioned are not properly selected, optimal performance is not guaranteed. Nevertheless, a reasonable choice of reference values usually leads to a better solution than the initial one and, in many situations, such a solution is enough for operators. In spite of these limitations, the control-based approach is widely used by operators due to its simplicity.

To overcome some of the limitations inherent in the previous approach, a third scheme shown in Fig. 3.1(c) is proposed. The principles of this approach are basically the same as in the second approach, i.e. a closed-loop control system is implemented. The only difference is

that the controller is improved by an optimization method (i.e. the optimizer) to cope with the context variations in the environment, or to refine the controller when knowledge is not (or partially) available. The latter case is of special interest in wireless networks, since the presence of many context factors makes the definition of the controller more difficult. In addition, if the reference values of the controller have not been properly selected, they can be adjusted by the optimizer, thus being more likely to find the optimal solution. Finally, as in the second approach, the main drawback is that the search space is small, as no service degradation during operation is accepted.

Based on the previous statements, in this thesis, the second and third schemes shown in Fig. 3.1 are used for network parameter optimization. In particular, the control-based approach is implemented when the configuration of the controller is simple and knowledge is available. In this case, a trial-and-error strategy is typically performed to find the best configuration of the controller. Conversely, the self-optimizing control-based approach is applied in those cases in which the complexity of defining the behavior of the controller is high or knowledge is not available. In this context, Fuzzy Logic is a mathematical discipline especially appropriate to design controllers, as its potential lies in the capability to express the knowledge in a similar way to the human perception and reasoning. Such a property allows operators, for instance, to use a linguist term such as *high* or *low* instead of providing a numerical value when defining the reference values of the controller. For this reason, in this work, controllers are based on the Fuzzy Logic theory. More details about this relatively young discipline as well as FLCs are provided in the following sections.

The second classification of approaches to face the problem of parameter self-tuning is made according to the frequency with which the self-tuning method is applied to the network. Such a frequency usually depends on the interval time with which measurements are collected, the delay to update the parameter settings and the computational time required to perform the calculation process. The tasks in which instantaneous performance indicators are used and a fast response of the algorithm is required (e.g. in the order of milliseconds or seconds) are referred to as *on-line* tuning methods. In cellular networks, this kind of tasks is known as Advanced RRM algorithms, including time and frequency domain packet schedulers, adaptive transmission bandwidth, power control, AMC, etc. In contrast, parameter changes can also be performed more slowly. For instance, the OAM system is a network entity that receives statistical performance data from the entire network, for example, every hour. After this, the new parameter settings are calculated in several minutes and immediately downloaded to the network. Hence, in this case, the optimization algorithm cannot be used to cope with fast network changes. However, as a remarkable advantage, the use of long-term statistical data leads to more robust methods. In addition, as the temporary limitation is given by the measurement periods, there is plenty of time to apply complex optimization methods, which can further improve network performance. Thus, the term that refers to this kind of tasks is *off-line* tuning methods.

From the operator perspective, the most important advantage of *off-line* methods is that they do not involve additional costs as it happens with Advanced RRM (i.e. *on-line* methods), where these algorithms are typically located in the base stations and owned by the manufacturer.

In this case, upgrading the network equipment represents an additional cost for the operator. Thus, the *off-line* approach is a more cost-effective solution and, for this reason, it has been adopted in this work.

Finally, to assess a self-tuning algorithm, there are many criteria that can be used, such as the solution quality, the convergence speed and the complexity in terms of computational load and storage requirements. The solution quality achieved by the algorithm (e.g. given by the final values of KPIs) is the most determining factor from the performance point of view, especially in complex situations (e.g. a cellular network) where the algorithm is not able to find the best solution. The computational load and storage requirements are crucial for *on-line* algorithms and those executed in the UE side, which are not the case in this thesis. Finally, the convergence speed defines how fast the algorithm approaches the final solution. This criterion is of special interest when the algorithm includes the optimizer, as this entity is typically based on an iterative approach. In this work, the proposed algorithms are *off-line* and conceived for the OAM system, whose limitations in computational load and storage requirements should not be an issue. Thus, the analysis is focused on performance indicators related to the solution quality and the convergence speed.

3.1.2 Fuzzy Logic

This section presents the theoretical basis of the computational intelligence methodology known as Fuzzy Logic. This discipline was initiated in 1965 by Lotfi A. Zadeh [111], professor at the University of California, in Berkeley. Fuzzy Logic emerged as an important tool for system control and complex industrial processes, as well as for home and entertainment electronics, diagnostic systems and other expert systems. Currently, multitude of applications based on Fuzzy Logic have been applied in many different areas, among which are control systems, robotics, medicine, pattern recognition, computer vision, information and knowledge management systems, earthquake prediction, scheduling optimization, etc. As an alternative to Classical Logic, Fuzzy Logic introduces a degree of vagueness when things are evaluated [112]. In real life, there is much knowledge that is ambiguous and imprecise, and human reasoning usually works with this kind of information. In this sense, Fuzzy Logic was designed specifically to imitate the behavior of humans. Additional benefits of Fuzzy Logic include its simplicity and its flexibility. In particular, this methodology can handle problems with imprecise and incomplete data, and it can easily model non-linear functions of arbitrary complexity.

On the one hand, classical sets arise from the need of humans to classify objects and concepts. Such sets can be defined as a well-defined set of elements or by a membership function μ that can take the values 0 or 1 from a universe of discourse for all the elements that can belong (or not) to the concerned set. Formally, let X be the universe of discourse and x the elements contained in X. In addition, let suppose that A is a set that contains some elements in the universe of discourse X. Then, the element x belongs or does not belong to the set A can be represented by the following function:

$$\mu_A(x) = \begin{cases} 1 & \text{if } x \in \text{A} \\ 0 & \text{if } x \notin \text{A} \end{cases} \tag{3.1}$$

where $\mu_A(x)$ is the membership function corresponding to the set A. On the other hand, the need to work with fuzzy sets comes from the existence of concepts with no clear boundaries in their definition. Unlike classical set theory that classifies the elements into crisp sets, fuzzy set theory has an ability to classify elements into continuous sets using the concept of degree of membership. As a result, the membership function can take values in the range between 0 and 1, and the transition between both values is gradual, unlike in classical sets. Formally, let suppose that B is a fuzzy set that contains elements in the universe of discourse X. Then, such a fuzzy set is characterized by the membership mapping function:

$$\mu_B(x) : X \to [0, 1]. \tag{3.2}$$

For all $x \in X$, $\mu_B(x)$ indicates the certainty to which element x belongs to fuzzy set B. Although the membership function for a particular fuzzy set can be of any shape or type, an appropriate membership function is typically determined by experts in the domain over which the set is defined. In this sense, some membership functions are of special interest for designers, e.g. the triangular, trapezoidal and Gaussian types.

As for crisp sets in Classical Logic, relations and operators can also be defined for fuzzy sets in Fuzzy Logic. In particular, these relations are the equality, containment, complement, intersection and union of fuzzy sets. Among these relations, the intersection of fuzzy sets plays a key role in the design of rules for fuzzy controllers, as described in the next section. By definition, the intersection of two sets, A and B, is the set of elements occurring in both sets, while the operators that implement intersection are referred to as t-norms. The result of a t-norm is a set that contain all the elements belonging to both fuzzy sets, but taking into account the degree of membership, which depends on the specific t-norm. The most popular t-norms are the following:

- *Min-operator*. Formally, it is defined as:

$$\mu_{A \cap B}(x) = \min\{\mu_A(x), \mu_B(x)\}, \forall\ x \in X. \tag{3.3}$$

- *Product operator*. It can be expressed as:

$$\mu_{A \cap B}(x) = \mu_A(x)\mu_B(x), \forall\ x \in X. \tag{3.4}$$

As previously stated, Fuzzy Logic was conceived to imitate the behavior of humans. For this reason, the concept of a linguistic variable plays an important role in Fuzzy Logic. A linguistic variable is a variable whose values are words or sentences from natural language, allowing computation with words instead of numbers. Such a linguistic variable can be a word, a linguistic label or an adjective. For example, let consider the height of the people in a country. In this case, the variable *height* is a linguistic variable. A possible value for the numeric variable

height can be *tall* or *small*, meaning that a fuzzy set is associated with a linguistic term or value. In addition, certain adverbs can also be combined with adjectives to modify fuzzy values, e.g. *very tall* would indicate a person who is "taller" than *tall*. Thus, linguistic variables allow the translation of natural language into logical, or numerical statements, which facilitates handling human reasoning at the computational level. In practice, most sensory inputs are linguistic variables, or nouns in a natural language, for instance, temperature, pressure, displacement, etc. In this work, KPIs and parameters are the inputs of the proposed algorithms, so that typical linguistic values for these inputs are *very high*, *low*, *medium*, etc.

An important feature of Fuzzy Logic is that it provides a framework for handling rules (for control or decision making) which have been expressed in an imprecise form. In this context, linguistic variables are embedded in the rules of an FLC, allowing representation of the human control expertise. More specifically, FLCs consist of a number of conditional IF-THEN rules. For the designer who understands the system, these rules are easy to write, and as many rules as necessary can be supplied to describe the system properly (although only a moderate number of rules are usually needed). Next section provides a short overview of FLCs, focusing on the components of such controllers and some types of fuzzy controllers.

3.1.3 Design of a Fuzzy Logic Controller

The design of FLCs is one of the most important application areas of Fuzzy Logic [113]. The main benefit of FLCs is that controlling a system (also called plant) can be performed by using sentences rather than equations. This means that a control strategy can be described in terms of linguistic rules, in a more similar way to human language, instead of using e.g. differential equations. Since the first one was conceived in 1975, a huge number of FLCs have been developed so far for consumer products (e.g. washing machines, video cameras and air conditioners) and industrial processes (e.g. robot control, underground trains and hydro-electrical power plants). Experience has shown that FLCs provide results superior to those obtained by conventional control algorithms. In particular, the methodology of the FLC becomes very useful when the processes are too complex for analysis by conventional quantitative techniques or when the available sources of information are interpreted qualitatively, inexactly, or uncertainly [114].

Designing an FLC includes the definition of the fuzzification and defuzzification processes and the derivation of the database and fuzzy control rules. Visually, Fig. 3.2 shows the block diagram of a generic FLC, which comprises four principal components: a fuzzifier, a defuzzifier, a knowledge base and an inference engine. Firstly, the fuzzifier converts input data into suitable linguistic values, which may be viewed as labels of fuzzy sets. Secondly, the knowledge base is a database and a collection of linguistic statements based on expert knowledge, which is usually expressed in the form of IF-THEN rules. Thirdly, the inference engine performs inference to compute a fuzzy output. Finally, the defuzzifier, which has the opposite meaning of the fuzzifier, provides a non-fuzzy control action from an inferred fuzzy control action. The remaining paragraphs of this section describe in more detail each of these blocks.

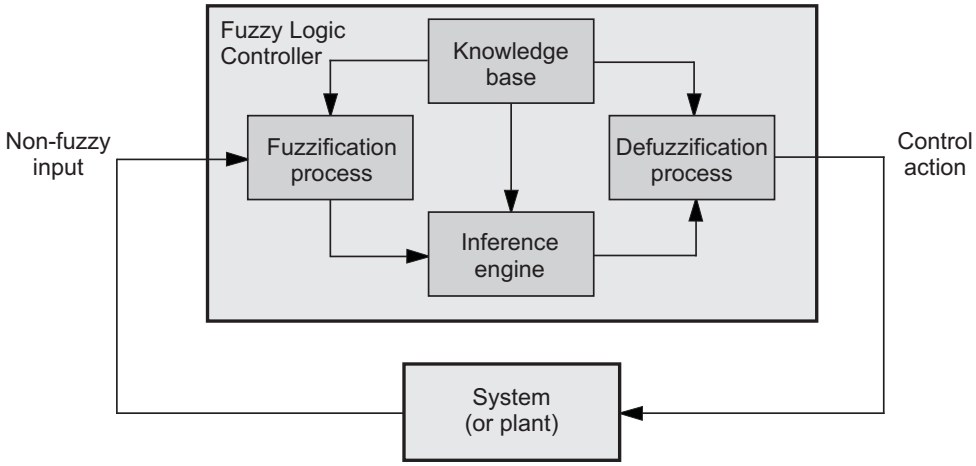

Figure 3.2: Block diagram of an FLC

Fuzzification process

The fuzzification interface involves the following tasks: (a) measuring the values of input variables, (b) performing a scale mapping that translates the range of values of input variables into the corresponding universes of discourse and (c) finding the fuzzy representation of non-fuzzy input values. In practice, this is achieved through application of the membership functions associated with each fuzzy set defined in the input space. More specifically, the fuzzification process is the assignment of membership values (one for each fuzzy value of the linguistic variable) to a numerical input value. For instance, let consider the linguistic variable "temperature of a room", which can take the fuzzy values *low*, *medium* and *high*. The input of the system is a crisp value of the temperature of the room, while the output is given by the membership value for each label, as shown in Fig. 3.3. Formally, let X denote the universe of discourse for the three fuzzy sets. Hence, the fuzzification process receives the element $a \in X$, and produces the membership degrees $\mu_{low}(a)$, $\mu_{medium}(a)$ and $\mu_{high}(a)$.

Knowledge base

The knowledge base of an FLC is divided into two different blocks: a database and a rule base. The former allows to characterize fuzzy rules and fuzzy data manipulation in the FLC, while the latter provides the dynamic behavior of the FLC through a set of linguistic rules derived from the expert knowledge.

Firstly, the database is built from concepts which are subjectively defined and based on experience and engineering judgment. The following aspects are related to the construction of the database in an FLC:

- *Discretization.* It is also referred to as quantization. Its function is to convert a continuous universe into a discrete universe, which is composed of a certain number of segments or quantization levels. In this case, a fuzzy set is defined by assigning membership values to

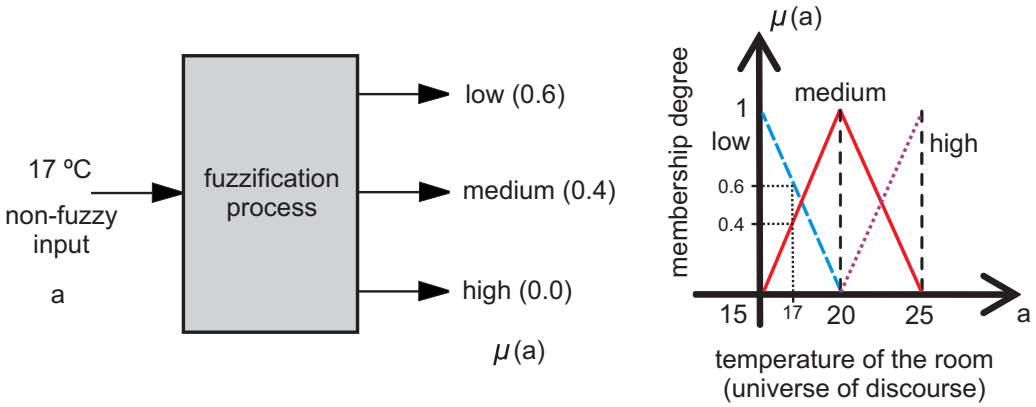

Figure 3.3: Fuzzification process through an example

each generic element of the new discrete universe. In addition, there exists a trade-off when selecting the number of quantization levels. On the one hand, it should be large enough to provide an appropriate granularity, but, on the other hand, it should be small enough to save memory storage. In this sense, the corresponding mapping that transforms measured variables into values in the discretized universe can be linear, non-linear or both.

- *Normalization.* The normalization of a universe involves a discretization of the universe of discourse into a finite number of segments, with each segment mapped into a suitable segment of the normalized universe. The mapping can also be linear, non-linear or both.
- *Partition of input and output spaces.* A fuzzy partition determines how many fuzzy sets need to be defined. This decision, which determines the granularity of the control achievable by the FLC, depends on the characteristics of the system being controlled and the quality required for the control process.
- *Completeness.* The concept of completeness is related to the fact that the FLC generates an appropriate action for every state in the system. Typically, the completeness is in connection with the design experience and engineering knowledge.
- *Membership functions.* These functions allow to assign the grades of membership to the fuzzy sets. Such an assignment is based on the subjective criteria of the decision. For example, if an input variable is affected by noise, the membership functions should be wide enough to reduce the sensitivity to noise. The membership functions are typically expressed in a functional form, among which are the bell-shaped function, triangle-shaped function and trapezoid-shaped function.

Secondly, the rule base comprises a collection of fuzzy rules following a syntax of the type IF-THEN to set the control strategy, i.e.:

$$\text{IF } (a \textit{ set of conditions are satisfied}) \text{ THEN } (a \textit{ set of consequences can be inferred}), \tag{3.5}$$

where the first part of the conditional statement is referred to as the antecedent, while the second part is known as the consequent. In particular, the antecedent is a condition in its application

domain and the consequent is a control action for the system under control. Furthermore, several linguistic variables can be included in the antecedents and the conclusions of the rules. The proper selection of the state variables included in the antecedent and the control variables included in the consequent is essential to the characterization of the operation of the FLC. An example rule would be "if pressure is very high, then open the valve very much". The main benefit of using this kind of rules is that these rules provide a natural framework for the characterization of human behavior and decisions analysis. In this sense, many experts state that fuzzy control rules provide a convenient way to express their domain knowledge. To formulate these fuzzy rules, for example, an interrogation of experienced experts or operators by using a carefully organized questionnaire can be used. This explains the fact that FLCs are implemented by using fuzzy IF-THEN rules.

Inference engine

Once the values of the input variables have been converted to fuzzy values through the fuzzification process, the inference engine identifies which rules are triggered and calculates the fuzzy values of the output variables. In other words, this process links the fuzzified inputs to the rule base in order to produce a fuzzified output for each rule. This means that, a degree of membership has to be determined for the output sets which are part of the consequents in the fuzzy rules. Such a degree of membership is calculated from the degrees of membership in the input sets and the relationships between the input sets. These relationships are established by logic operators that combine the sets in the antecedent. The output fuzzy sets in the consequent are then combined to produce one overall membership function for the output of the rule.

To explain the inferencing process, let assume that A and B are two input fuzzy sets in the universe of discourse X_1 and C is a fuzzy set in the universe of discourse X_2. Let also consider that the following rule is defined:

$$\text{IF } (A \text{ is } a \text{ and } B \text{ is } b) \text{ THEN } (C \text{ is } c). \tag{3.6}$$

The values of $\mu_A(a)$ and $\mu_B(b)$ are available for the inference engine, since they have been derived from the fuzzification process. Thus, the inferencing process starts with the calculation of the degree of truth of each rule in the rule base. The degree of truth specifies the triggering strength of a particular rule. It is calculated by combining the antecedent sets using a specific operator, among which are the *min*-operator and the product operator for the intersection relation as previously stated. In this example, assuming the *min*-operator, the degree of truth α_k for the rule k is calculated as:

$$\alpha_k = \min\{\mu_A(a), \mu_B(b)\}. \tag{3.7}$$

The following step of the inferencing process is to determine a single fuzzy value for each output $c_i \in C$ which has been activated. In general, the final fuzzy value corresponding to the output

c_i, denoted as β_i, is computed using the *max*-operator, i.e.:

$$\beta_i = \max_{\forall k}\{\alpha_{k_i}\}. \tag{3.8}$$

where α_{k_i} is the degree of truth of the rule k, which has activated the output c_i.

The final result of the inference engine is a set of fuzzified output values. In this sense, the rules that are not activated have a degree of truth equal to zero. In addition, rules can include a weighting factor in the range [0,1] to represent the degree of confidence in that rule. Such factors derived from the expert knowledge are applied when the fuzzy rules are aggregated to produce a non-fuzzy value in the defuzzification process.

Defuzzification process

This process establishes a relationship between the space of fuzzy control actions defined over the output universe of discourse and the space of crisp (non-fuzzy) control actions. The degree of truth of a rule represents the degree of membership to the sets present in the consequent. Given the degrees of truth from a set of activated fuzzy rules, the defuzzification process converts the output of the fuzzy rules into a scalar (non-fuzzy) value. To calculate such a scalar value, two different approaches can be used. The first approach, based on the well-known Mamdani-type fuzzy rule [115], implements rules in which the consequent is another fuzzy variable [e.g. see (3.6)]. The second one, known as Takagi-Sugeno approach, utilizes rules whose consequent is a polynomial function of the inputs [116].

Mamdani approach.

In this approach, there are some methods to find a scalar that represents the action to be taken:

- *Max-min method.* In this case, the rule with the highest degree of truth is selected and then, the activated consequent membership function is determined. Finally, the centroid of the area under that function is calculated and the horizontal coordinate of that centroid is the output of the FLC.
- *Averaging method.* In this approach, the average of the degrees of truth considering all the activated rules is first calculated. Then, each membership function is clipped at the average. Finally, the centroid of the composite area is calculated and its horizontal coordinate is used as the output of the FLC.
- *Root-sum-square method.* The membership functions are scaled such that the peak of each function is equal to the maximum degree of truth that corresponds to that function. Then, the centroid of the composite area under the scaled functions is computed and its horizontal coordinate is the output of the FLC.
- *Clipped center of gravity method.* In this method, the membership functions are clipped at the corresponding degree of truth of the rules. Then, the centroid of the composite area is calculated and the horizontal coordinate is the output of the FLC.

The calculation of the centroid of the trapezoidal areas depends on the domain (i.e. discrete or continuous) of the membership functions. In the discrete domain, where a finite number of values, denoted as n_x, are defined, the output of the defuzzification process is computed as:

$$output = \frac{\sum_{i=1}^{n_x} x_i \mu_C(x_i)}{\sum_{i=1}^{n_x} \mu_C(x_i)}. \tag{3.9}$$

where x_i is each possible value. In the case of a continuous domain, the output is given by the following expression:

$$output = \frac{\int_{x \in X} x\mu(x)dx}{\int_{x \in X} \mu(x)dx}. \tag{3.10}$$

where X is the universe of discourse.

Takagi-Sugeno approach.

Formally, a typical rule for this approach follows the generic expression [117]:

$$\text{IF } (X_1 \text{ is } A_1 \text{ and } ... \text{ and } X_n \text{ is } A_n) \text{ THEN } (Y = p_0 + p_1X_1 + ... + p_nX_n). \tag{3.11}$$

where X_1,...,X_n are fuzzy input variables; A_i indicates one of the fuzzy sets defined for the linguistic variable X_i; Y is the output variable, and p_0,...,p_n are parameters. Thus, the main difference between the Takagi-Sugeno approach and the Mamdani approach is that rather than having a fuzzy consequent, each rule consequent is a mathematical function. Furthermore, this method has been extended to non-linear functions. Given a set of activated rules and their corresponding degree of truth α, the output crisp value is calculated as a weighted average of the rule outputs, i.e.:

$$output = \frac{\sum_{i=1}^{N} \alpha_i \cdot f(X_1, ..., X_n)}{\sum_{i=1}^{N} \alpha_i}, \tag{3.12}$$

where N is the number of rules and $f(X_1, ..., X_n)$ is some mathematical function of the inputs.

The main benefits of the Takagi-Sugeno approach is that a more dynamic control is provided, FLCs are computationally more efficient and best suited to mathematical analysis and they work well with optimization and adaptive techniques. For these reasons, the FLCs proposed in this work are based on this approach.

Example

To conclude this section, an illustrative example of the operation of an FLC is provided. In particular, the FLC is based on the Takagi-Sugeno approach [116] previously explained. Let suppose that the controller is described by the two rules

$$\text{IF } (x \text{ is } A_1 \text{ and } y \text{ is } B_1) \text{ THEN } (z \text{ is } f_1(x,y)=k_1) \tag{3.13}$$

&

$$\text{IF } (x \text{ is } A_2 \text{ and } y \text{ is } B_2) \text{ THEN } (z \text{ is } f_2(x,y)=k_2), \tag{3.14}$$

from which the following elements can be identified:

- Two input variables, x and y, defined over the universe of discourse X and Y, respectively.
- Two fuzzy sets, A_1 and A_2, defined for the variable x.
- Two fuzzy sets, B_1 and B_2, defined for the variable y.
- One output variable, z.
- Two constant functions, f_1 and f_2, defined for the variable z.

The membership functions defined for each fuzzy set of the input variables are shown in Fig. 3.4. Then, the basic operation of the FLC is as follows:

- *Step 1.* The fuzzification process calculates the membership value for each fuzzy set by applying the associated membership function as shown in Fig. 3.5(a).
- *Step 2.* The inference engine computes the degree of truth for each fuzzy rule through the combination of the fuzzified inputs using the *min*-operator, as shown in Fig. 3.5(b). In particular, the expressions used to calculate the degrees of truth are:

$$\alpha_1 = \min\{\mu_{A_1}(x_0), \mu_{B_1}(y_0)\} \tag{3.15}$$

&

$$\alpha_2 = \min\{\mu_{A_2}(x_0), \mu_{B_2}(y_0)\}. \tag{3.16}$$

- *Step 3.* Finally, the defuzzification process calculates the non-fuzzy output as a weighted average of the rule constant outputs. In particular, the equation used to produce the output value is:

$$output = \frac{\alpha_1 \cdot k_1 + \alpha_2 \cdot k_2}{\alpha_1 + \alpha_2}. \tag{3.17}$$

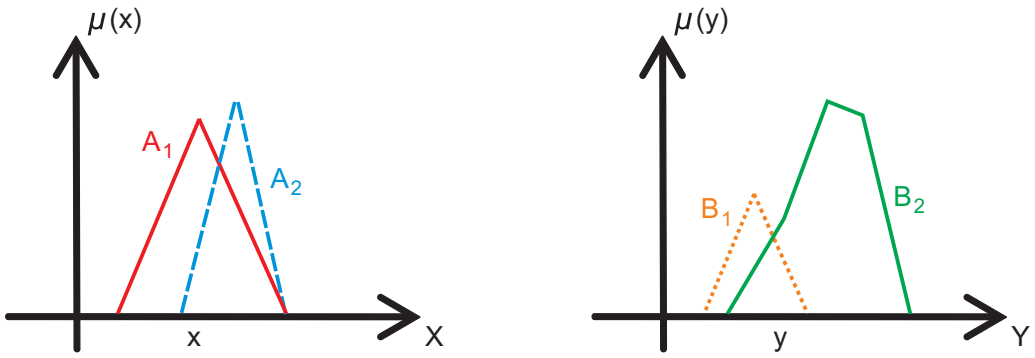

Figure 3.4: Membership functions of the input fuzzy sets in the example

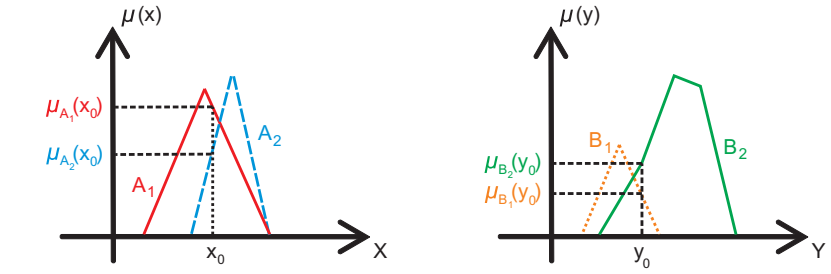

(a) Fuzzification process

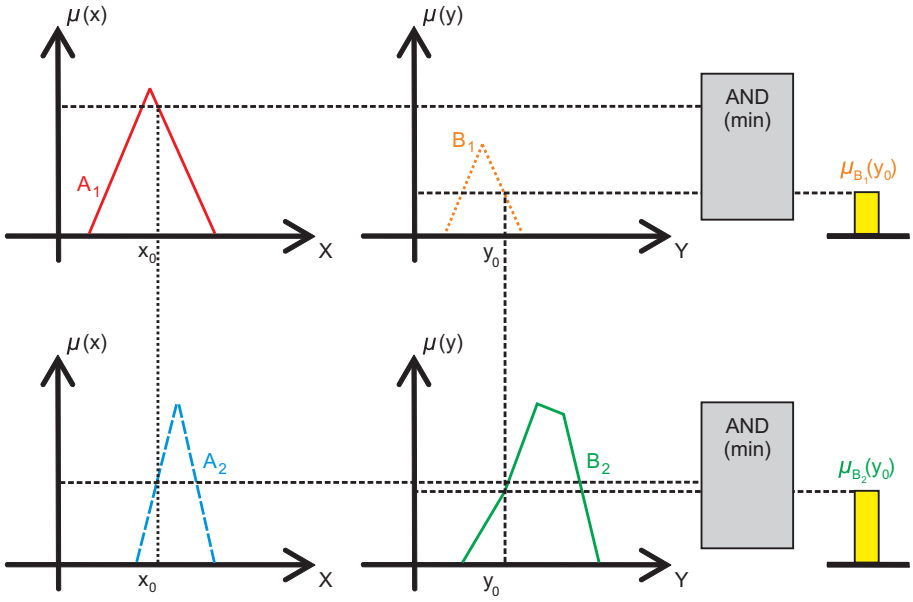

(b) Calculation of the degree of truth for each fuzzy rule

Figure 3.5: Basic operation of the FLC in the example

3.2 Optimization of the self-tuning process

3.2.1 Introduction

An important area in algorithmic development to cope with complex problems is the design of the so-called intelligent algorithms. In this context, the development of models based on biological and natural intelligence has played a key role in the last years. These algorithms include artificial neural networks, evolutionary computation, swarm intelligence and RL. Some of these techniques have recently been combined among themselves as well as with more traditional approaches to solve extremely challenging problems. Moreover, these algorithms are part of the field of Artificial Intelligence, which has been applied to a wide variety of research disciplines, for example, computer science, physiology, philosophy, sociology and biology. In principle, any of these approaches should be capable of yielding results in a relatively short time.

In this thesis, the proposed auto-tuning algorithms are based on the design of an FLC. Since wireless networks can be considered as complex systems due to the presence of a large multitude of diverse and interacting elements, the definition of the controller usually becomes a challenging task for engineers. In addition, as wireless networks involve unpredictable and highly variable context factors, which can also vary at different time-scales, the FLC needs to be reconfigured throughout the time in order to adapt to those network variations. Thus, to cope with the dynamic variations, the lack of knowledge or, simply, to refine the behavior of the controller, different strategies have been analyzed in this work, i.e. neural networks, genetic algorithms, particle swarm and RL. The objective of these mathematical techniques is to optimize the behavior of the FLC through a learning process. In this section, after providing a general overview of these techniques, a more detailed overview is devoted to RL, which is of particular interest in scenarios such as wireless networks, in which learning from interaction becomes essential. In particular, the analysis is focused on the fuzzy Q-Learning algorithm, which is one of the promising approaches in the context of RL.

3.2.2 Neural Networks

An artificial neural network is a mathematical model inspired by biological neural networks, which have the ability to learn, memorize and still generalize. In particular, a neural network consists of an interconnected group of artificial neurons. Each artificial neuron, which is in turn a model of a biological neuron, firstly receives a set of input values from the environment or other artificial neurons. Then, it modifies these values by applying the so-called synaptic weights. Finally, it transforms the values into a single output value using a specific function, called activation function. Such an output value can in turn be the input value to other artificial neurons. To illustrate this, the basic scheme of an artificial neuron is shown in Fig. 3.6(a). Mathematically, the most common computation performed by an artificial neuron j is a linear combination of the input values X, including the weights W_j in the calculation and followed by the activation function $f(\cdot)$, i.e.:

$$y_j = f(X \cdot W_j) = f\left(\sum_{i=0}^{n} x_i w_{ji}\right). \tag{3.18}$$

where $X = (x_0, x_1, ..., x_n)$ and $W_j = (w_{j0}, w_{j1}, ..., w_{jn})$. Although the possible number of activation functions is infinite, the following are regularly employed by a majority of neural networks: linear function, step function, ramp function, sigmoid function and Gaussian function. With the exception of the linear function, all of these functions introduce a nonlinearity into the network dynamics by bounding the output values within a fixed range [117].

An artificial neural network is a layered network of individual artificial neurons. Typically, it consists of an input layer, one or more hidden layers and an output layer. The artificial neurons in a specific layer can be fully or partially connected to the artificial neurons in the next layer. In addition, feedback connections to previous layers are also possible. An example artificial neural network is depicted in Fig. 3.6(b). In this sense, different structures of neural networks have been

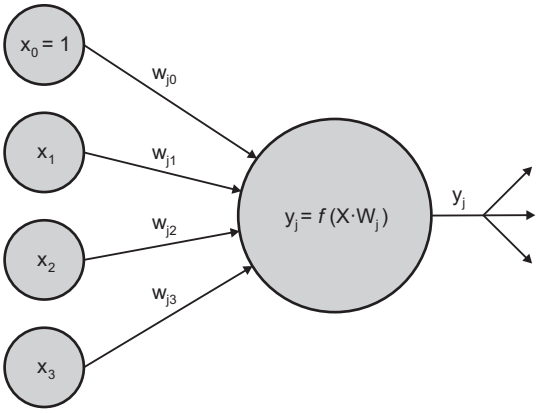

(a) An artificial neuron

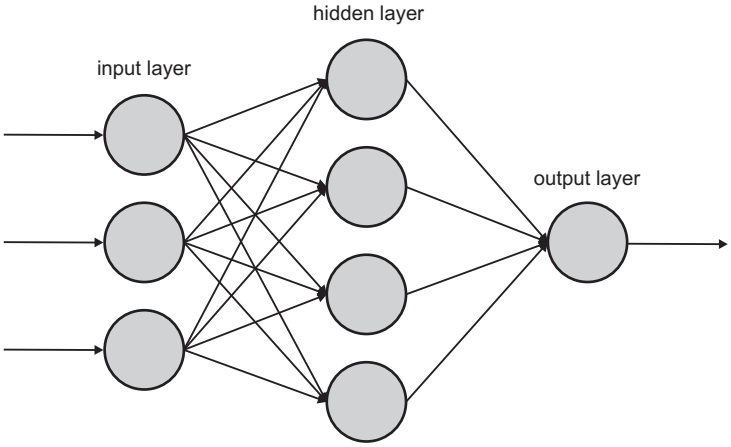

(b) An artificial neural network

Figure 3.6: Basic structures in Neural Networks [117][113]

developed, among which are single-layer, multi-layer feedforward, temporal and self-organizing neural networks.

One of the most interesting features of neural networks is the possibility of learning. There are three main types of learning: supervised learning, unsupervised learning and RL. In the first case, a data set consisting of input vectors and a target (desired output) associated with each input vector is called the training set. Such a data set is used to train a neuron (or a neural network), which means to adjust the weight values such that the error between the real output, y_j, of the neuron and the target output, $\hat{y}$, is minimized. In unsupervised learning, the objective is to find patterns or features in the input data with no assistance from an external source. Many unsupervised learning algorithms typically perform a clustering of the training patterns, i.e. grouping a set of objects so that objects in the same group are more similar. Finally, in RL, the aim is to reward the neuron for good performance, and to penalize the neuron for bad performance.

Neural Networks have been used for a wide range of applications, including diagnosis of diseases, speech recognition, data mining, composing music, image processing, forecasting, robot control, classification, pattern recognition, compression, etc. In mobile networks, several works are available in the literature, e.g. [118][119]. In this context, neural networks, which are good at pattern recognition, have also been used to effectively adjust parameters in fuzzy logic-based systems, such as those related to the definition of the membership functions [120]. As a result, hybrid solutions incorporating both fuzzy and neural methodologies have been proposed in the literature [97][98]. In [97], an FLC that integrates Neural Networks principles (known as Adaptive Network Fuzzy Inference System, ANFIS) is optimized by using historical data of the metrics involved in the controller. In [98], a learning process based on RL allows to determine appropriate membership functions for the hidden layers of the proposed fuzzy neural controller.

3.2.3 Genetic Algorithms

A genetic algorithm is an adaptive search technique that uses operations found in natural genetics to provide robust search in complex spaces [121]. Its modeling is similar to natural genetic, in which the characteristics of individuals are expressed using genotypes and the main functions are selection (i.e. survival of the fittest) and recombination (i.e. reproduction). Combined fuzzy logic and genetic algorithms provide scalability, flexibility and simplicity. In particular, this technique has been applied in various scientific applications where an FLC is designed. In those cases, genetic algorithms have been used to optimize the rule base and/or the shape of the fuzzy sets [121][122][123][99][124].

A genetic algorithm is composed of several steps. It starts with a population of randomly generated solutions named chromosomes. Then, the algorithm evolves toward better solutions by applying genetic operators, whose behavior is similar to those genetic processes present in nature. In particular, a population of solutions for the specific problem is maintained through the execution of the algorithm. Such a population experiences evolution by natural selection. At each iteration (namely generation), relatively good solutions reproduce to give offspring that replace the relatively bad solutions, which die. To distinguish what is a good or bad solution, an evaluation or fitness function playing the role of the environment needs to be previously defined.

The structure of a simple genetic algorithm is shown in Algorithm 3.1. Firstly, the initial population $P(0)$ is randomly selected. Then, the process is iterated until the system ceases to improve. Typically, the individuals in the population are represented by a fixed-length binary string which encodes values for variables. At iteration t, the algorithm maintains a population $P(t)$ of solutions, which are evaluated by the fitness function. Such a function determines the relative ability of an individual to survive and produce offspring in the next generation. At iteration $t+1$, a new population is formed by applying recombination and mutation. On the one hand, recombination is performed through application of a crossover operator, which combines the features of parent structures to form similar offspring. Crossover operators can be divided into the following three main categories based on the number of parents used:

- *Asexual*: an offspring is generated from one parent.

Algorithm 3.1. Genetic algorithm structure [121]

```
begin
    t = 0;
    initialize P(t);
    evaluate P(t);
    while (not termination-condition) do
    begin
        t = t + 1;
        select P(t) from P(t − 1);
        recombine P(t);
        mutate P(t);
        evaluate P(t);
    end
end
```

- *Sexual*: two parents are used to produce one or two offspring.
- *Multi-recombination*: more than two parents are used to produce one or more offspring.

Recombination is applied probabilistically. Each pair (or group) of parents has a probability, named the crossover probability, of producing offspring. On the other hand, the aim of mutation is to introduce new genetic material (i.e. diversity) into an existing individual. Mutation is used in support of crossover to ensure that the full range of values (alleles) is accessible for each characteristic (gene) in an individual (chromosome). Mutation is also applied at a certain probability, named the mutation probability, to each gene of the offspring.

Genetic algorithms can be used to search for a good parameter configuration for an FLC. Typically, each individual in the population is a candidate configuration of the FLC [121][122] [123][99]. In particular, a chromosome is formed by concatenating the representation of all fuzzy rules, each of which is given by a set of variables that defines the membership functions through a parametric representation. For instance, if the membership functions are trapezoidal-shaped functions, their parametric representation is given by a 4-tuple. Thus, in these cases, the membership functions are adjusted to obtain better performance results. In [124], the optimization of an FLC is divided into two steps: (a) generating an appropriate rule base and (b) tuning the fuzzy sets to optimize the performance. In the first step, a genetic algorithm that adapts the initial rule base according to the given problem is modeled. Then, after finding a rule base which is able to solve the problem to a certain degree, the fuzzy sets are tuned to obtain better performance of the FLC.

3.2.4 Particle Swarm

Particle swarm is an optimization technique that simulates the social behavior of birds within a flock. A particle swarm algorithm is a population-based search algorithm in which the individuals, referred to as particles, change their position within the search space according to the social-

psychological tendency of individuals to emulate the success of other individuals. Thus, the changes to a particle within the swarm are influenced by the experience of its neighbors. As a result, particles stochastically return toward previously successful regions in the search space.

In particle swarm algorithms, each particle represents a potential solution. Let $x_i(t)$ denote the position of particle i in the search space at time step t. Then, the position of the particle is modified by adding a velocity, $v_i(t)$, to the current position, i.e.:

$$x_i(t+1) = x_i(t) + v_i(t+1). \tag{3.19}$$

The velocity vector drives the optimization process and reflects both the experiential knowledge of the particle and socially exchanged information from the neighbors. More specifically, the velocity calculation consists of the following three terms:

- *Inertia component*: it represents the previous direction of movement (i.e. in the immediate past). This memory term prevents the particle from drastically changing direction.
- *Cognitive component*: it quantifies the performance of particle i relative to past performances. This component represents the individual memory of the position that was the best for the particle. In this sense, the tendency of individuals due to this term is to return to their own best positions.
- *Social component*: it quantifies the performance of particle i relative to neighboring particles. Conceptually, this term represents a group norm or standard that individuals attempt to achieve. Thus, the tendency of each particle due to the social component is to return to the best position found by the neighbors.

The effect of the velocity is illustrated in Fig. 3.7. For the sake of clarity, a single particle in a two-dimensional search space has been considered. The individual best position and the global best position are denoted in the figure by $y(t)$ and $\hat{y}(t)$, respectively. In addition, the positions at time steps t and $t+1$ as well as the velocity vector broken down into the different components are represented. As observed, the new position $x(t+1)$ moves closer towards the global best $\hat{y}(t)$.

As in other mathematical techniques, the optimization process in particle swarm is iterative. In particular, repeated iterations of the algorithm are executed until a stopping condition is satisfied. At each iteration, the individual and global best positions are calculated and the velocity of each particle is adjusted. To perform this, some function evaluations are carried out. A function evaluation refers to one calculation of the fitness function, which defines the optimization problem.

In mobile networks, different applications of particle swarm optimization can be found in the literature [125][126][127]. In addition, this optimization approach has been utilized to perform optimization of FLCs [128]. In that case, each particle represents an FLC. The position of a particle is given by a vector of a fixed number of parameters in the FLC. Such parameters

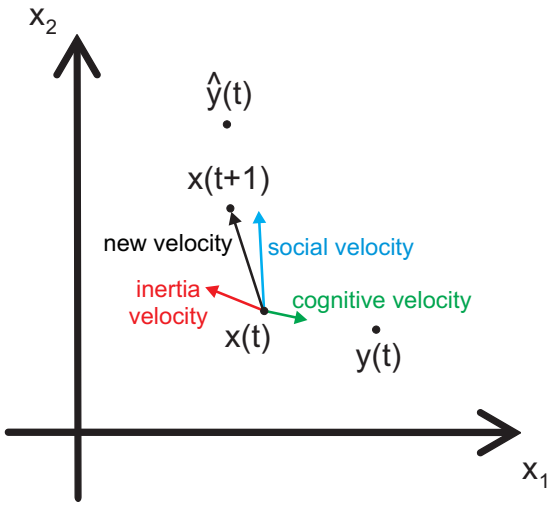

Figure 3.7: Determination of the new position of a particle in a particle swarm algorithm [113]

describe the rule base and the membership functions in the controller. The objective function used to rate the solutions is defined as a weighted sum of two filtered quality indicators in mobile networks, dropping and blocking rates. Results show that specific strategies for the auto-tuning process can be implemented by correctly choosing the cost function that guides the particle swarm optimization in the FLC.

3.2.5 Reinforcement Learning

RL is an area of machine learning based on leading an agent to take actions in an environment in order to maximize a cumulative reward. The two most important features of RL are the trial-and-error search and the fact that actions may affect not only the immediate reward but also the rewards of the successive situations [101].

RL is different from other learning approaches, for example, the supervised learning that is typically used in Neural Networks. In this latter case, learning is carried out by using previously collected examples, also called the training data set. This kind of learning is not suitable for learning from interaction. In addition, in interactive problems, it is usually very difficult to obtain a training data set that is correct and representative of all the situations in which the agent has to act. Thus, in those cases, an agent learning from its own experience remains as the only solution.

Beyond the agent and the environment, the following elements can be identified in RL: a policy, a reward function, a value function and, optionally, a model of the environment. Firstly, the policy defines how the agent has to act in a given time. In other words, it is a mapping between perceived states of the environment and actions to be taken from those states. Secondly, the reward function defines the goal in an RL problem. More specifically, it is a mapping between each perceived state and a scalar or reward that indicates the intrinsic desirability of being in that state. However, the objective of the agent is not to obtain the maximum immediate reward,

but to maximize the total reward that the agent receives in the long run. For this reason, whereas the reward function indicates what is good in an immediate sense, the value function specifies what is good in the long run. In particular, the value function is a mapping between each perceived state and the total amount of reward that an agent can expect to accumulate over the future, starting from that state. Finally, the model of the environment imitates the behavior of the environment. In this sense, RL can learn by trial-and-error and, at the same time, learn a model of the environment. To illustrate some of the previous concepts, the basic scheme of an RL problem is shown in Fig. 3.8, where a general environment responds at time $t+1$ to the action taken at time t.

A key concept in RL is the trade-off between exploration and exploitation. When the agent has to take actions, it should select those actions tried in the past which produced a lot of reward and the only way to discover them is to try actions that have not yet been selected. Thus, there exists a trade-off between exploration and exploitation as the agent must exploit the current knowledge to obtain reward, but it also has to explore other actions which could be best in the long run. In this sense, the objective of the agent is to maximize the received reward in the long run, that is, the sum of the rewards obtained from all situations or states that will be visited in the future:

$$R_t = r_{t+1} + \gamma r_{t+2} + \gamma^2 r_{t+3} + ... = \sum_{k=0}^{\infty} \gamma^k r_{t+k+1}, \tag{3.20}$$

where r is the numerical reward obtained at each time step as a consequence of taking an action and γ is the discount rate that determines the importance of future rewards.

The Markov property

As previously stated, the agent makes its decisions as a function of the state. In this context, there exists an important property of environments and their state signals which is called the Markov property. Prior to its definition, some aspects related to the state signal need to be discussed. The state signal includes all the information which is available to the agent. However,

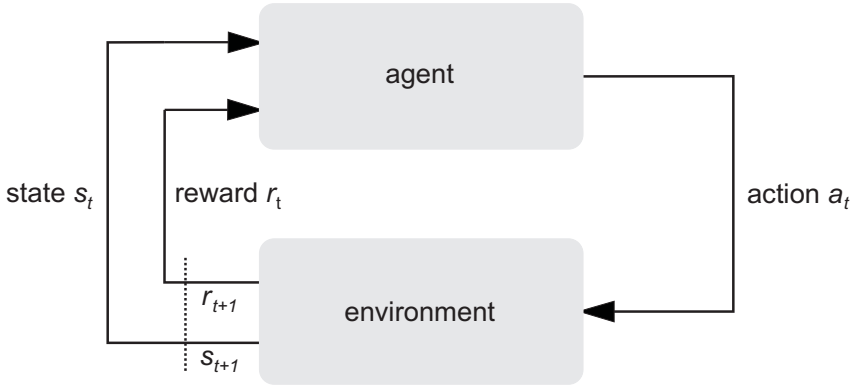

Figure 3.8: The basic elements in an RL problem

it should not be expected to inform the agent of everything about the environment, or even everything that would be useful for it in making decisions. In this sense, an appropriate state signal is the one that summarizes past information compactly, but also keeping the relevant part of the information. Roughly speaking, the Markov property is fulfilled when a state signal retains all relevant information. In this situation, the response of the environment at time step $t+1$ depends only on the state and action at time t, in which case the dynamics of the environment can be defined by specifying only:

$$Pr\left\{s_{t+1}=s', r_{t+1}=r \middle| s_t, a_t\right\}, \tag{3.21}$$

where $Pr\{\cdot\}$ denotes the probability of its argument, s the state of the environment, s' any state in the system, r the received reward and a the action taken by the agent. If an environment has the Markov property, then it is possible to predict the next state and expected next reward given the current state and action.

An RL task that satisfies the Markov property is called a Markov decision process (MDP). If the state and action spaces are finite, then it is called a finite MDP, which is defined by a set of states, a set of actions and the dynamic of the environment. The latter is specified by the so-called transition probabilities and the expected value of the next reward. Given any current state s and action a, the transition probability of each possible next state s' is:

$$P^a_{ss'} = Pr\left\{s_{t+1}=s' \middle| s_t=s, a_t=a\right\}. \tag{3.22}$$

Similarly, given any current state s and action a, together with any next state s', the expected value of the next reward is:

$$R^a_{ss'} = E\left\{r_{t+1} \middle| s_t=s, a_t=a, s_{t+1}=s'\right\}. \tag{3.23}$$

where $E\{\cdot\}$ means the expected value of its argument. These two quantities, i.e. the transition probabilities and the expected value of the next reward, define the most important aspects of the dynamics of a finite MDP.

Optimal value functions

Most RL algorithms search for value functions that estimate how beneficial it is for the agent to be in a given state. As previously stated, the value of a state s is given by the expected cumulative reward that can be received from such a state. A state-value function, named $V(s)$, is defined in RL to determine the benefit of being in a state s. The value obviously depends on the states visited by the agent, which in turn depends on the policy followed. A policy function π is a mapping from states to actions in order to determine the behavior of the agent, where $\pi(s,a)$ is the probability of taking action a from state s. In this manner, the value of a state s

following the policy π is defined by:

$$\begin{aligned} V^{\pi}(s) &= E_{\pi}\{R_t|s_t = s\} \\ &= E_{\pi}\left\{\sum_{k=0}^{\infty}\gamma^k r_{t+k+1}\middle|s_t = s\right\}, \end{aligned} \tag{3.24}$$

where $E_{\pi}\{\cdot\}$ means the expected value under policy π. Similarly, an action-value function, named $Q(s,a)$, is defined in RL to quantify the value of taking action a, when starting from state s. If the agent follows the policy π, then it is formally expressed as:

$$\begin{aligned} Q^{\pi}(s,a) &= E_{\pi}\{R_t|s_t = s, a_t = a\} \\ &= E_{\pi}\left\{\sum_{k=0}^{\infty}\gamma^k r_{t+k+1}\middle|s_t = s, a_t = a\right\}. \end{aligned} \tag{3.25}$$

The two previous functions, V^{π} and Q^{π}, can be estimated from experience. In addition, an important property of these functions is that they satisfy particular recursive relationships. More specifically, for any policy π and any state s, the following condition holds between the value of s and the value of its possible successor states:

$$\begin{aligned} V^{\pi}(s) &= E_{\pi}\{R_t|s_t = s\} \\ &= E_{\pi}\left\{\sum_{k=0}^{\infty}\gamma^k r_{t+k+1}\middle|s_t = s\right\} \\ &= \sum_a \pi(s,a)\sum_{s'} P^a_{ss'}\left[R^a_{ss'} + \gamma E_{\pi}\left\{\sum_{k=0}^{\infty}\gamma^k r_{t+k+2}\middle|s_{t+1} = s'\right\}\right] \\ &= \sum_a \pi(s,a)\sum_{s'} P^a_{ss'}\left[R^a_{ss'} + \gamma V^{\pi}(s')\right], \end{aligned} \tag{3.26}$$

which is called the Bellman equation for V^{π}. Moreover, the value function V^{π} is the unique solution to its Bellman equation.

Solving an RL problem is equivalent to find a good policy that gives a high reward in the long-term. An optimal policy always has an expected value greater (or equal) than other policies for all states. Likewise, the optimal policies share the same state-value and action-value functions, called V^* and Q^*, respectively. In particular, the optimal state-value function V^* is defined as:

$$V^*(s) = \max_{\pi} V^{\pi}(s), \tag{3.27}$$

for all $s \in S$, where S is the set of states. Similarly, the optimal action-value function Q^* is defined as:

$$Q^*(s,a) = \max_{\pi} Q^{\pi}(s,a), \tag{3.28}$$

for all $s \in S$ and $a \in A(s)$, where $A(s)$ is the set of possible actions in state s. Since the function Q^* provides the expected return for taking action a in state s and thereafter following an optimal policy, it can be expressed in terms of V^* as follows:

$$Q^*(s,a) = E\left\{r_{t+1} + \gamma V^*(s_{t+1}) | s_t = s, a_t = a\right\}. \tag{3.29}$$

The Bellman equation for V^* can be rewritten without making reference to any specific policy. In that case, it is called the Bellman optimality equation, which expresses that the value of a state under an optimal policy must be equal to the expected return for the best action taken from that state, i.e.:

$$\begin{aligned} V^*(s) &= \max_{a \in A(s)} Q^{\pi^*}(s,a) \\ &= \max_a E_{\pi^*}\left\{R_t | s_t = s, a_t = a\right\} \\ &= \max_a E\left\{r_{t+1} + \gamma V^*(s_{t+1}) | s_t = s, a_t = a\right\} \\ &= \max_a \sum_{s'} P^a_{ss'}\left[R^a_{ss'} + \gamma V^*(s')\right]. \end{aligned} \tag{3.30}$$

The Bellman optimality equation for Q^* is:

$$\begin{aligned} Q^*(s,a) &= E\left\{r_{t+1} + \gamma \max_{a'} Q^*(s_{t+1}, a') \middle| s_t = s, a_t = a\right\} \\ &= \sum_{s'} P^a_{ss'}\left[R^a_{ss'} + \gamma \max_{a'} Q^*(s', a')\right]. \end{aligned} \tag{3.31}$$

For finite MDPs, the Bellman optimality equation has a unique solution independent of the policy. In fact, the Bellman optimality equation is a system of equations, one for each state, so that if there are N states, then there are N equations with N unknown variables. If the dynamic of the environment is known (i.e. $P^a_{ss'}$ and $R^a_{ss'}$ are available), then in principle this system of equations for V^* can be solved by using any method for solving systems of non-linear equations.

Once the system of equations has been solved, it is relatively easy to find an optimal policy. If V^* is available, then those actions that appear best in the next step will be optimal actions. In other words, any policy that is *greedy* with respect to V^* is an optimal policy. The importance of V^* lies on the fact that if it used to evaluate the short-term consequences of actions, then a greedy policy is in fact optimal in the long-term, since V^* already takes into account the reward consequences of all possible future behaviors. If Q^* is available, the selection of optimal actions is still easier because the agent does not have to search for actions for the next step, but simply to find any action that maximizes $Q^*(s,a)$. Thus, at the expense of representing a function of state-action pairs [i.e. $Q^*(s,a)$], instead of just of states [i.e. $V^*(s)$], the optimal action-value function allows to select optimal actions without the need of knowing anything about possible successor states and their corresponding values (i.e. the dynamic of the environment).

By solving the Bellman optimality equation, it is possible to provide a way to find an optimal policy and, thus, to solve the RL problem. However, such a solution is rarely directly useful. In practice, there are three assumptions that are rarely satisfied: (a) accurate knowledge of the dynamic of the environment, (b) enough computational resources to complete the computation of the solution, and (c) the Markov property. To solve the problem in an approximate way, many different decision-making methods can be applied, for example, heuristic search methods and dynamic programming. In this context, many RL methods can be clearly seen as an approximate way of solving the Bellman optimality equation, using actual experienced transitions in place of knowledge of the expected transitions.

The three most important classes of methods for solving an RL problem are dynamic programming, Monte Carlo methods and temporal-difference methods. Each class of methods has both advantages and disadvantages. In particular, dynamic programming methods, which aim to solve the Bellman equation, are well developed mathematically, but a complete and accurate model of the environment is required. Monte Carlo methods attempt to estimate value functions and discover optimal policies. They are conceptually simple and a model is not required, but they are not appropriate for step-by-step incremental computation. To explain this, note that Monte Carlo methods are based on averaging sample returns, so that this kind of methods is only applicable for episodic tasks. Due to this, experience is divided into episodes and it is only upon the completion of an episode that value estimates and policies are changed. For this reason, it is said that Monte Carlo methods are incremental in an episode-by-episode sense, but not in a step-by-step sense. Finally, temporal-difference methods are fully incremental and a model is not required, but they are more complex to analyze. The three classes of methods also differ in some other aspects, such as the efficiency and speed of convergence, and they can be combined in order to obtain the benefits of each one.

Q-Learning algorithm

A mechanism for finding an optimal policy consists of following a generalized policy iteration, based on alternating two interacting processes: policy evaluation and policy improvement. The policy evaluation brings the value function closer to that for the current policy, while the policy improvement uses this new value function to enhance the policy in terms of expected value. This concept is illustrated in Fig. 3.9. The result of such an iterative process is that both policy and value function approach to optimality.

As previously stated, an RL method appropriate for step-by-step incremental computation is the temporal-difference learning. In this methodology, policy evaluation is carried out from the observed reward, r_{t+1}, and the estimate $V(s_{t+1})$. To calculate the new state-value function, the following expression can be used:

$$V(s_t) \leftarrow V(s_t) + \eta[r_{t+1} + \gamma V(s_{t+1}) - V(s_t)], \tag{3.32}$$

where η is the step-size parameter or learning rate involved in the incremental update. If the

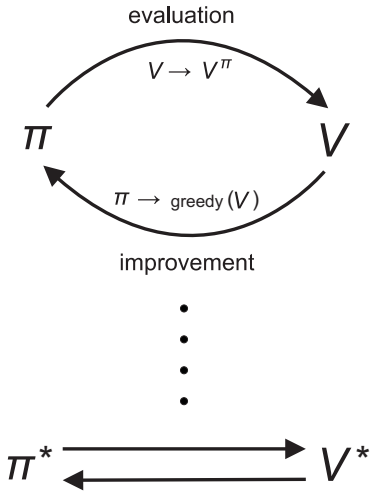

Figure 3.9: Basic scheme of a generalized policy iteration [101]

action-value function is used instead, then it is calculated by:

$$Q(s_t, a_t) \leftarrow Q(s_t, a_t) + \eta[r_{t+1} + \gamma Q(s_{t+1}, a_{t+1}) - Q(s_t, a_t)]. \tag{3.33}$$

Policy improvement is achieved by selecting actions whose current action-value is the greatest from that state, that is, making the policy greedy by:

$$a(s) = \arg\max_k Q(s, k). \tag{3.34}$$

The overall process converges to both the optimal value function and an optimal policy if all state-action pairs are visited an infinite number of times and the policy becomes greedy in the limit [101].

Q-Learning is a popular temporal-difference algorithm in which the learned $Q(s, a)$ directly approximates the optimal $Q^*(s, a)$ independently of the policy followed by the agent [129]. The update of the action-value function corresponds to the equation:

$$Q(s_t, a_t) \leftarrow Q(s_t, a_t) + \eta[r_{t+1} + \gamma \max_a Q(s_{t+1}, a) - Q(s_t, a_t)]. \tag{3.35}$$

In this case, Q approximates the optimal action-value function, Q^*, without depending on the policy followed.

Adaptation of Q-Learning to FLCs

The rule base of an FLC can be optimized by applying RL techniques. In particular, a fuzzy version of the Q-Learning algorithm is proposed in [130] to optimize the consequent part of fuzzy

rules in an FLC. Such an adaptation of Q-Learning allows to process continuous state and action spaces by a simple discretization of the action-value function. Consequently, the so-called discrete q-values can be stored in a look-up table as only a finite set of state-action values is needed. An additional advantage of this approach is that prior knowledge can be easily introduced in the fuzzy rules speeding up the learning process.

The discretization of the action space forces the agent (i.e. the FLC) to choose one action (a consequent) among J for rule i. Suppose that there are N fuzzy rules defined for the FLC. Let $a[i,j]$ be the j^{th} possible action in rule i and $q[i,j]$ its associated q-value stored in the look-up table. Hence, the representation of the continuous $Q(s,a)$ is equivalent to determine the q-values for each rule consequent, then to interpolate for the continuous input vector. More specifically, the fuzzy Q-Learning algorithm is implemented by the following steps:

1. Initialize the q-values in the look-up table. The following assignment is usually used when there is no prior knowledge:

$$q[i,j] = 0, \quad 1 \leq i \leq N \quad and \quad 1 \leq j \leq J, \tag{3.36}$$

   where $q[i,j]$ is the q-value, N is the number of rules and J is the number of actions per rule.

2. Select an action for each activated rule i with nonzero degree of truth. For instance, actions can be selected using the so-called ϵ-greedy policy, i.e.:

$$a_i = \arg\max_k q[i,k] \quad \text{with probability } 1-\epsilon, \tag{3.37}$$

   or

$$a_i = random\{a_k, k = 1, 2, ..., J\} \quad \text{with probability } \epsilon, \tag{3.38}$$

   where a_i is the consequent of rule i and ϵ is a parameter that establishes the trade-off between exploration and exploitation in the algorithm (e.g. $\epsilon = 0$ means that there is no exploration, that is, the best action is always selected).

3. Calculate the global action inferred by the FLC:

$$a(t) = \sum_{i=1}^{N} \alpha_i(s(t)) \cdot a_i(t), \tag{3.39}$$

   where $a(t)$ is the inferred action at time step t, $\alpha_i(s(t))$ is the degree of truth for rule i and $a_i(t)$ is the selected action for that rule. The degree of truth is the distance between the input state $s(t)$ and the rule i, calculated as:

$$\alpha_i(s(t)) = \prod_{j=1}^{L} \mu_{ij}(s_j(t)), \tag{3.40}$$

where L is the number of FLC inputs, $\mu_{ij}(s_j(t))$ is the membership function for the j^{th} FLC input and rule i.

4. Approximate the Q-function from the current q-values and the degree of truth of the rules:

$$Q(s(t), a(t)) = \sum_{i=1}^{N} \alpha_i(s(t)) \cdot q[i, a_i], \tag{3.41}$$

where $Q(s(t), a(t))$ is the value of the Q-function for the state $s(t)$ and the action $a(t)$ in iteration t.

5. Leave the system to evolve to the next state, $s(t+1)$.

6. Observe the reinforcement signal, $r(t+1)$, and compute the value of the new state denoted by $V_t(s(t+1))$, i.e.:

$$V_t(s(t+1)) = \sum_{i=1}^{N} \alpha_i(s(t+1)) \cdot \max_k q[i, a_k]. \tag{3.42}$$

7. Calculate the error signal:

$$\Delta Q = r(t+1) + \gamma \cdot V_t(s(t+1)) - Q(s(t), a(t)), \tag{3.43}$$

where $r(t+1)$ is the reinforcement signal, γ is a discount factor, $V_t(s(t+1))$ is the value of the new state and $Q(s(t), a(t))$ is the value of the Q-function for the previous state and the action performed from that state.

8. Update q-values by an ordinary gradient descent method:

$$q[i, a_i] \leftarrow q[i, a_i] + \eta \cdot \Delta Q \cdot \alpha_i(s(t)), \tag{3.44}$$

where η is a learning rate.

9. Repeat the above-described process starting from step 2 for the new current state until the convergence of the algorithm is achieved.

Once the Q-Learning algorithm has finished, the fuzzy rules are generated by selecting those consequents that obtained the highest q-value in the look-up table. As a summary, Algorithm 3.2 briefly describes the steps of the Fuzzy Q-Learning algorithm.

Finally, as stated in Chapter 2, several works applying both non-fuzzy and fuzzy Q-Learning algorithms in wireless network optimization problems are available in the literature, showing the effectiveness of the combination of FLCs and Q-Learning in this context.

Algorithm 3.2. Fuzzy Q-Learning

1. Initialize q-values:
$q[i,j] = 0, \quad 1 \leq i \leq N \quad and \quad 1 \leq j \leq J.$
2. Select an action for each activated rule (ϵ-greedy policy):
$a_i = \arg\max_k q[i,k]$ with probability $1-\epsilon$,
$a_i = random\{a_k, k = 1, 2, ..., J\}$ with probability ϵ.
3. Calculate the global action:
$a(t) = \sum_{i=1}^{N} \alpha_i(s(t)) \cdot a_i(t).$
4. Approximate the Q-function from the current q-values and the degree of truth of the rules:
$Q(s(t), a(t)) = \sum_{i=1}^{N} \alpha_i(s(t)) \cdot q[i, a_i].$
5. Leave the system to evolve to the next state, $s(t+1)$.
6. Observe the reinforcement signal, $r(t+1)$, and compute the value of the new state denoted by $V_t(s(t+1))$:
$V_t(s(t+1)) = \sum_{i=1}^{N} \alpha_i(s(t+1)) \cdot \max_k q[i, a_k].$
7. Calculate the error signal:
$\Delta Q = r(t+1) + \gamma \cdot V_t(s(t+1)) - Q(s(t), a(t)).$
8. Update q-values by an ordinary gradient descent method:
$q[i, a_i] \leftarrow q[i, a_i] + \eta \cdot \Delta Q \cdot \alpha_i(s(t)).$
9. Repeat the above-described process starting from step **2** for the new current state until the convergence is achieved.

3.2.6 Justification of the selected technique

Amongst the techniques explained in the previous sections, RL has been the selected one in this thesis. The main reasons for discarding the other alternatives as well as the reasons for choosing an RL method are discussed in the following paragraphs.

Firstly, although Neural Networks have been successfully applied in many applications, this artificial intelligence technique also has some limitations and disadvantages. On the one hand, neural networks are especially appropriate for prediction, function approximation, classification, pattern recognition, and clustering, which are not the problems tackled in thesis, mainly focused in developing control techniques. On the other hand, an important drawback is that neural networks require a large diversity of training for real-world operation, which can be a severe constraint in complex systems such as wireless networks. In addition, neural networks cannot be trained a second time, in the sense that it is very hard to add new data to an existing network. Finally, they require a lot of computational resources and high processing time for large neural networks.

Secondly, although genetic algorithms are a method very easy to understand which practically does not demand a high level of skills in mathematics and they are easily transferred to

existing simulations and models, they also has some important limitations and disadvantages, among which are the following:

- There is no absolute assurance that a genetic algorithm will find a global optimum, which usually happens when the population has many individuals.
- Genetic algorithms involve the problem known as *genetic drift*, which is the major problem of genetic algorithms. This issue means that the genetic algorithm may quickly lose most of its genetic diversity and the search is then made in a way that is not beneficial for recombination. This is because the random initial population quickly converges.
- Application of genetic algorithms in control problems which are performed in real-time is limited because of random solutions and convergence. In other words, this means that the entire population is improving, but this could not be extrapolated to an individual within this population. Therefore, it is unreasonable to use genetic algorithms for on-line control in real systems without testing them first on a simulation model.

It is worth mentioning that, in the context of this thesis, network operators can be reluctant to implement this kind of algorithms since the solutions found by genetic algorithms can remain at a certain distance to the optimum with higher probability, leading to suboptimal performance during an undetermined amount of time. In addition, the slow convergence of this technique can also be an issue in real systems, such wireless networks, even if an off-line control is applied.

Thirdly, in particle swarm optimization, there are some important limitations related to the optimization of an FLC in the context of cellular networks [131]. In particular, the particle swarm optimization involves loss of information in the global cost functions, since performance indicators are globally measured in the concerned network area. Thus, the situation at cell level cannot be considered. In addition, this optimization method has to compare the evolution of many particles, each of which represents a different setting of the FLC. As a result, to assess the position of each particle, the evaluation of the corresponding FLC should be carried out in many cells, thus requiring exclusive use of simulation tools. The lack of flexibility and generality in the definition of the FLC is also a constraint for particle swarm optimization. In this sense, when adding new inputs or performance indicators to the FLC, the optimization phase must be relaunched, although certain a priori knowledge can be included at the beginning. Other disadvantages of the basic particle swarm optimization algorithm are covered in [132][133] [134], among which are: (a) the algorithm experiences slow convergence in refined search stage, weak local search ability and it may lead to possible entrapment in local minimum solutions, and (b) currently, there are no mathematical proofs of the convergence and the speed of the convergence for this algorithm.

Finally, in RL, it is highlighted that the combination of FLCs and the fuzzy Q-Learning algorithm is a powerful mechanism in the context of wireless networks for the following reasons:

- Wireless networks are complex and variable systems in which obtaining a training data set that is representative of all situations becomes a difficult task. Unlike other approaches (e.g. supervised learning in Neural Networks), in RL a training data set is not required.

- Due to the complexity of network management, operators usually do not have the knowledge necessary (i.e. accurate and complete) to take proper actions in every situation. In this case, learning from interaction becomes a suitable solution, where an agent is able to learn from its own experience to perform the best actions.
- Unlike particle swarm optimization, it is possible to perform the optimization at cell level, so that many FLCs can learn in parallel. To achieve this, measurements should be taken in the area of a cell. In addition, the Q-Learning method provides operators generality to easily introduce e.g. new performance indicators in the FLC [131].

On the contrary, some limitations of this approach are that the optimization process may be sensitive to the selection of the reinforcement signal and the fact that the system states must be visited a sufficient number of times. Nevertheless, in favor of the above described advantages, the method adopted in this thesis has been based on RL.

3.3 Conclusions

In the context of SON, adaptive optimization techniques are adequate for network parameter optimization due to the complexity and dynamism of wireless networks. The main benefits of applying such techniques are cost savings and improved network performance. This chapter begins with a description of potential self-tuning approaches for wireless networks. In this analysis, the use of a network model has been discarded, since the construction of a network model that is accurate and manageable is usually a complex task that may lead to bad performance as well. Thus, the schemes adopted in this thesis are based on self-tuning entities that interact directly with the network. In those cases, a closed-loop structure is used to find the optimal parameter settings. For this reason, the next part of the chapter has been focused on controllers based on Fuzzy Logic theory, since this discipline provides a mathematical framework especially appropriate to design controllers, as its potential lies in the capability to express the knowledge in a similar way to the human perception and reasoning.

The second topic of this chapter has been devoted to mathematical approaches that can be used to optimize and adapt the behavior of FLCs. The first technique has been Neural Networks, which typically require a training data set that can be a severe constraint in wireless networks. In addition, neural networks are more suitable for other kind of problems (e.g. prediction, classification, pattern recognition, and clustering), which are different from the control problem addressed in this thesis. Secondly, the main features of Genetic Algorithms has been described, showing that their application in control problems which are performed in real-time is limited because of random solutions and convergence. Thirdly, the basic concepts of the Particle Swarm approach have been presented, highlighting that its application to FLC optimization involves some important limitations, such as the lack of flexibility and generality in the definition of the FLC. Finally, this chapter has been devoted to RL, which has been the selected method amongst the previously described ones. The main benefit of this approach is that RL algorithms learn from interaction, which becomes essential in complex systems such as wireless networks.

Chapter 4

Simulations tools

This chapter presents the simulations tools used to evaluate the different techniques proposed in this thesis. Section 4.1 is devoted to the dynamic system-level simulator for LTE macrocells, whose design has been an important part of this thesis. In particular, a physical layer abstraction is performed to predict link-layer performance with a low computational cost. At link layer, there are two important functions designed to increase the network capacity: Link Adaptation and Dynamic Scheduling. Other RRM functionalities such as Admission Control and Mobility Management are performed at network layer. It is worth noting that the simulator is conceived for large simulated network time to allow evaluation of the proposed optimization algorithms for the main network-level functionalities. Section 4.2 briefly describes the main features of the dynamic system-level simulator for LTE femtocells, whose indoor mobility model has been designed in the context of this thesis, and Section 4.3 provides a short overview of the dynamic HSPA/LTE macro/pico system-level simulator, which has been exclusively used at the user-level in this work.

4.1 The LTE macro system-level simulator

LTE is the evolution of the current UMTS mobile communication network. This 3GPP standard is the combination of the all-IP core network known as the Evolved Packet Core (EPC) and the E-UTRAN. The key benefits of LTE can be summarized in improved system performance, higher data rates and spectral efficiency, reduced latency and power consumption, enhanced flexibility of spectral usage and simplified network architecture.

This section describes the design of a dynamic system-level simulator for LTE macrocells conceived for large simulated network time. The development of the simulator has its origins in a Degree Thesis [135], whose aim was to simulate a GSM network at system-level. Since

then, several updates to include UMTS [136] and joint RRM for GSM and UMTS have been carried out. For the inclusion of LTE in the simulation tool, many people of the Mobile Network Optimization team [22] have been involved, in particular, in the design of the physical layer and the implementation phase of the simulator. In the context of this thesis, a computationally efficient link layer model has been designed for the simulator.

In the simulator, firstly, a physical layer abstraction is performed to predict link-layer performance with a low computational cost. Thus, realistic OFDM channel realizations with multi-path fading propagation conditions have been generated to obtain an accurate value of Signal-to-Interference Ratio (SIR) for each subcarrier. Then, a method is used to aggregate SIR measurements of several OFDM subcarriers into a single scalar value. Subsequently, BLER is estimated from those SIR values, which is used in the Link Adaptation and Dynamic Scheduling functions. Additionally, functions for admission control and mobility management are included in the simulator. For computational efficiency, the tool is focused on the downlink of E-UTRAN.

The design of efficient simulation tools for LTE networks has been addressed in the literature. In [137], a simple physical layer model is proposed for LTE in order to reduce the complexity of system level analysis. In [138], a link-level simulator for LTE downlink is presented as an appropriate interface to a system level simulator. In [139], an LTE downlink system-level simulator is proposed for free under an academic, non-commercial use license. The physical layer model is described in [140]. The main purpose of the MATLAB-based simulation tool presented in [139] is to assess network performance of new scheduling algorithms.

The proposed simulation tool has been designed to evaluate optimization algorithms for the main network-level functionalities, namely HO, admission control and cell reselection. For this purpose, simulations are composed of epochs or optimization loops, where the modification of network parameters can be evaluated. Each epoch is composed of a configurable number of iterations, whose duration is determined by the simulator time resolution. In addition, the size of the simulation scenario must be larger than that in most of the existing LTE simulators, which usually consider only a few cells in the network layout.

The description of the simulation tool is organized as follows. Section 4.1.1 presents the general simulator structure. Section 4.1.2 describes the Physical Layer, focusing on the calculation of the OFDM channel realizations needed for resource planning. Section 4.1.3 is devoted to the Link Layer, where link adaptation and resource planning are performed. Section 4.1.4 outlines the Network Layer, including admission control, congestion control and mobility management. Finally, in Section 4.1.5, simulation results are presented.

4.1.1 Simulator general structure

This section presents the general structure of the LTE simulator developed in MATLAB. Fig. 4.1 shows the main functional blocks of the simulator.

The first stage of a simulation is the configuration and initialization of the main simulation

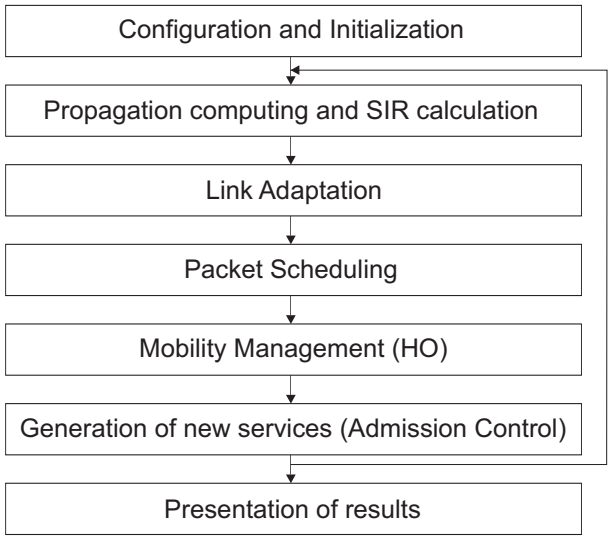

Figure 4.1: Block diagram of the simulator

parameters, defining the behavior of the main functions in the simulator. The scenario to be simulated is generated here. A warm-up distribution of users is also created by this function, which allows to obtain meaningful network statistics from the first iterations of the simulation. The next function calculates the propagation losses. This function calculates the power received by each user from the base stations of the scenario. The simulator includes a propagation loss model, a slow fading model and a fast fading model. During this phase, the interference suffered by each user is also calculated. From this information, the value of the SIR experienced by each user for different frequency subbands is obtained. Once the main parameters of interest have been obtained, the functions of RRM are executed. At link level, the simulator includes link adaptation and resource scheduling functions. The link adaptation function selects the most appropriate MCS for each user to transmit the information, maximizing spectral efficiency. This decision is based on the propagation conditions experienced by the user. The CQI indicator is used to represent the environment conditions. The radio resource scheduling function assigns available radio resources to users based on channel conditions experienced by each user for different frequency subbands. This function is also based on the CQI indicator. At network level, the simulator includes several functions. The main ones are HOs and admission control. Lastly, the main results and statistics are shown.

Macrocell scenario

This scenario models a macro-cellular environment, where the number of hexagonal cells is configurable in the simulator. Fig. 4.2 illustrates the layout for a scenario with 19 tri-sectorized sites evenly distributed.

To avoid border effects in the simulation, the simulator incorporates the wrap-around technique described in [141]. Wrap-around consists in creating replicas of the scenario surrounding the original one. Only the original scenario is considered when collecting results and statistics.

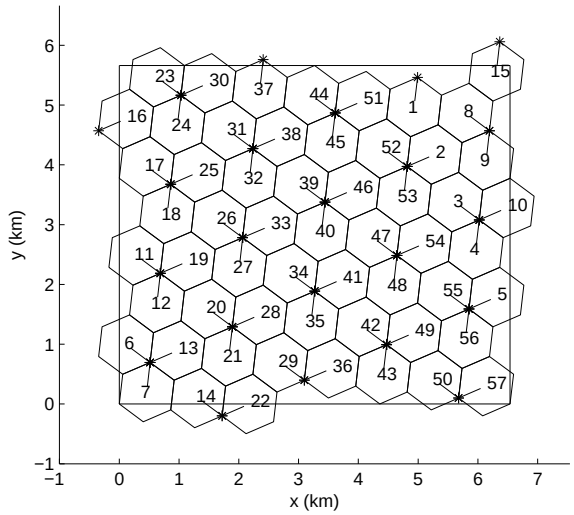

Figure 4.2: Simulation scenario

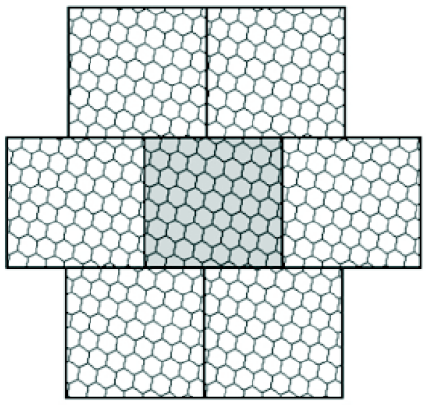

Figure 4.3: Simulation scenario with wrap-around

Fig. 4.3 shows the simulation scenario with the wrap-around technique. Finally, it is necessary to define the set of interfering cells for each cell of the scenario. For each cell, an ordered set of interfering cells are constructed in terms of power received from each interferer by static system-level simulations.

Spatial Traffic Distribution

Users can be spatially distributed in both an uniform or non-uniform way over the scenario. In the case of uniform spatial distribution, users are located in whatever point of the scenario with the same probability. However, to reproduce a realistic situation, it is recommended to use a non-uniform distribution.

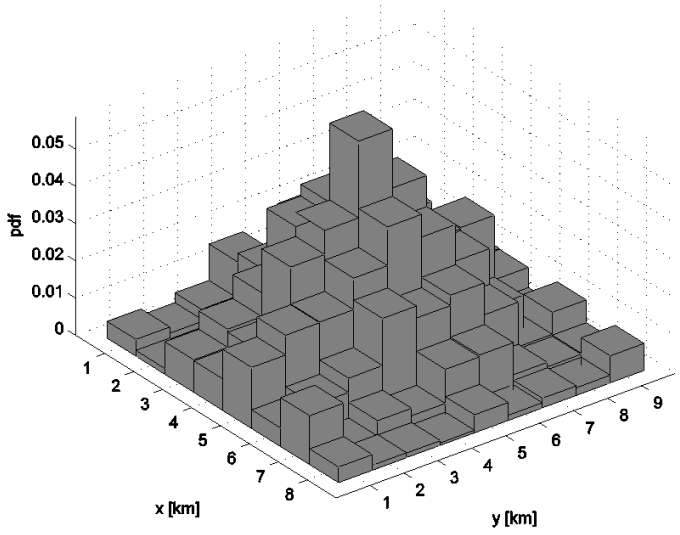

Figure 4.4: Spatial traffic distribution

The typical spatial distribution in urban areas can be described by a log-normal distribution at a cell level. The traffic is created adding to such a distribution a Gaussian random variable [142]. Fig. 4.4 shows the probability of starting a call in any location of the scenario. It is observed that the spatial traffic distribution has a central peak, creating a congested area with higher traffic density. It is noted that the spatial traffic distribution will be slightly affected by the mobility model, explained in the next section.

Mobility Model

The proposed mobility model does not define any constraint about user directions, as users can freely move over the scenario. More precisely, the mobility model considers random constant paths for the users in the simulation scenario. Users move at constant speed, set to 3, 10 or 50 km/h. This model also includes the effect of the wrap-around technique, which means that when a user reaches the limit of the original scenario, it appears in the correct position of this scenario.

Traffic Model

The service modeled in the simulator is VoIP. This service is defined as a source generating packets of 40 bytes every 20 ms [143], reaching a bit rate of 16 kbps. As it will be described later, the radio resource allocation in the simulator is performed for time intervals of 10 ms. For this reason, the voice service has been implemented as users that transmit packets of 20 bytes every 10 ms. For this service, it is also necessary to determine when a call is dropped, that is, when the service is interrupted. Such an event occurs when a user does not receive packets during a specific time interval. In particular, user packets are not scheduled when the connection quality

is below a certain threshold or there are not enough resources, so the call may be dropped.

4.1.2 Physical layer

Channel model

The mobile radio channel can be described as a time-varying linear filter [144]. Therefore, it can be represented in the time domain by its impulse response, $h(\tau, t)$, where τ stands for delay of each path in h, and the amplitude of each path varies with time t. Also, the channel can be characterized by the time-variant transfer function, $H(f, t)$, which is related with impulse response through the Fourier transform with respect to the delay variable τ.

When the behavior of the channel is randomly time variant, the above-mentioned channel functions become stochastic processes. A realistic approach to the statistical characterization of such a channel may be accomplished in terms of correlation of channel functions since it enables channel output autocorrelation to be determined. Channel autocorrelation functions are related through Fourier transform as well.

For typical physical channels, time fading statistics can be assumed stationary over short periods of time and channel correlation function is invariant under a translation in time t, thus being categorized as wide-sense stationary (WSS). In addition, frequency-selective behavior is stationary in frequency f being the autocorrelation function invariant under frequency translations. This condition is termed uncorrelated scattering (US), and most practical channels satisfy it fairly well.

Autocorrelation functions of wide-sense stationary uncorrelated scattering (WSSUS) channels exhibit the property that the time-variant transfer function autocorrelation is stationary both in time t and frequency f variables, i.e. its value does not depend on the absolute time or frequency considered but only on the time or frequency shift between time or frequency points of observation.

As a consequence, a WSSUS channel can be simulated generating the impulse response, $h(\tau, t)$, with stationary variation in time t for each path and no cross-correlation between different values of delay τ (i.e. generating independent stochastic processes for different paths). Stationarity is achieved by applying Doppler filters to the amplitude time t variation on each path. These filters perform spectrum shaping according to Doppler effect experimented by any radio signal propagating from a transmitter to a moving receiver (or vice versa). Afterwards, the frequency transfer function, $H(f, t)$, can be computed easily by applying the Fourier transform to the impulse response with respect to delay variable.

To provide the possibility of simulating non-constant speed mobiles in the future, fading realizations cannot be performed over time as an independent variable. Alternatively, space variables have to be used so that channel varies according to the current position of the mobile at each iteration of simulation. Therefore, a fading channel spatial grid has been generated. This

grid provides channel responses for every physical position in the simulated scenario, regardless of mobiles speed.

Narrow band fading grid is generated to get a Lord Rayleigh universe [145]. In other words, following Clarke's model [144], a spatial bidimensional complex Gaussian variable is filtered by a bidimensional Doppler filter. The bandwidth of 2-D Doppler filter can be obtained as a function of spatial grid resolution and wavelength size.

Once narrowband channel behavior for each spatial position is obtained, extension to wideband is possible performing the same procedure for every path in power delay profiles described in the specification for Extended Typical Urban (ETU), Extended Pedestrian A (EPA) and Extended Vehicular A (EVA) channels in [146]. Thus, different (uncorrelated) Rayleigh universes are generated for each delay in wideband channel scenario. This results in a distance-variant impulse response $h(\tau, d)$ (autocorrelation) of the channel instead of a time-variant impulse response $h(\tau, t)$ described in [144] as one of the four system functions for complete WSSUS channel characterization. The only difference is the time to distance (t to d) variable change made. A realization of the function is shown in Fig. 4.5.

Since the simulator requires channel realizations for different frequency bands (corresponding to OFDM subcarriers), the distance-variant impulse response has to be transformed into a distance-variant transfer function $H(f, d)$ at each position, by applying Fourier transform with respect to delay variable τ. An example of this function can be seen in Fig. 4.6. The only remaining step is to extend the space variable d of the generated function $H(f, d)$ to a bidimensional (x, y) space variable, obtaining $H(f, x, y)$, a tridimensional function that provides frequency response for each spatial position given by coordinates, x and y.

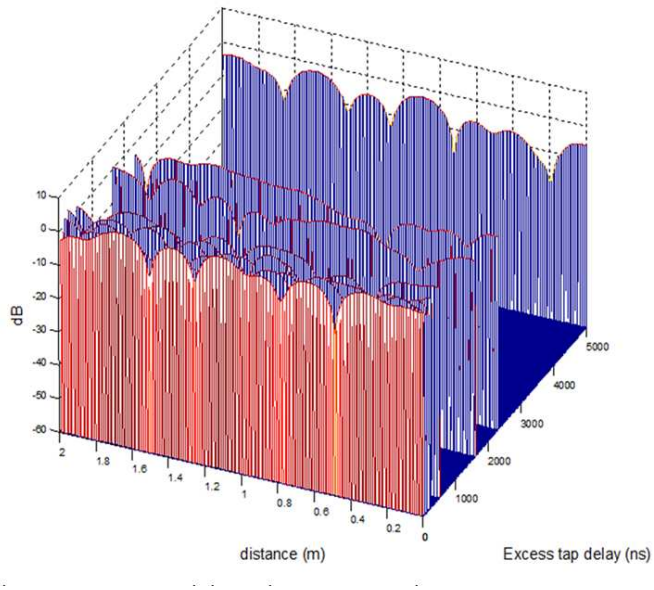

Figure 4.5: Generated bidimensional channel impulse response for ETU channel model in [146]

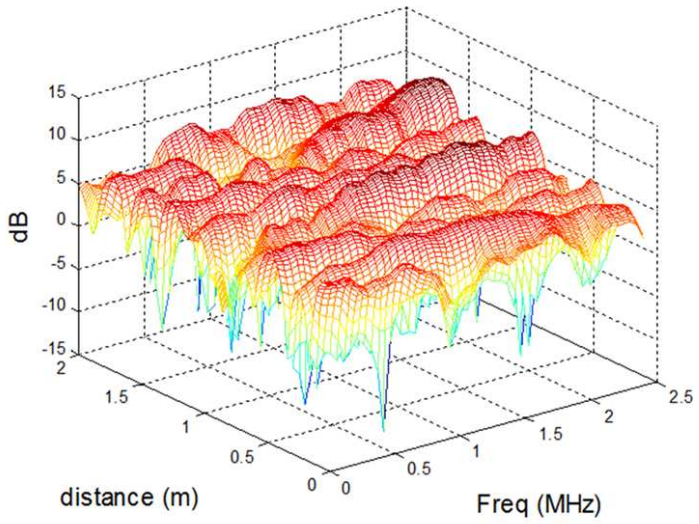

Figure 4.6: Generated distance-variant transfer function for ETU channel model in [146]

Radio propagation channel

The simulator includes two alternatives for obtaining propagation calculations. As a first option, the calculations are performed at each iteration and whenever necessary (e.g. in the function that evaluates the channel conditions of each link or in the admission control function). Alternatively, propagation calculations are made from a set of pre-computed matrices. In this case, it is not necessary to perform the calculations during the simulation.

For the definition of the pre-computed propagation matrix, the scenario is divided into a grid, whose resolution is given by the correlation distance of the slow fading (20 m). To know the values of the propagation loss a user is experiencing, it is only necessary to read the position of the matrix corresponding to the position occupied by the user in the scenario relative to every base station and then interpolate it with other values of the matrix depending on the relative position in the grid. The propagation matrices include the path loss calculations and the slow fading.

In both options, the radio propagation model is the COST 231 extension of Okumura-Hata model [147]. This model is applicable for frequencies in the range from 1500 to 2000 MHz. The effective height of the base station or eNB antenna has been set to 30 m, while the effective height of the UE antenna has been set to 1.5 m. With these assumptions and setting the operating frequency to 2 GHz, the expression for the propagation loss as a function of the distance is given by:

$$L = 134.79 + 35.22 \log d, \tag{4.1}$$

where d represents the distance in km between the UE and the eNB which the user is connected to.

In addition to the propagation loss, the simulator includes a slow fading model based on the fact that the local average of the radio signal envelope can be modeled by a log-normal distribution, i.e. the local average, in dB, is a Gaussian random variable. The standard deviation of the distribution depends on the considered environment. A typical value for the macrocell urban area analyzed is 8 dB [148].

For the choice of the propagation matrices, the value of shadowing is included in these matrices. The other alternative requires some additional calculations. The dynamic nature of the simulator leads to the implementation of a correlation model between the successive samples which represent the slow fading. An ARMA(1,1) model [149] has been selected for the simulator in this work,

$$z_t = \theta z_{t-1} + (1-\theta)a_t, \tag{4.2}$$

where z_t represents the slow fading sample at the current simulation step, z_{t-1} is the slow fading sample at the previous simulation step, a_t is a Gaussian random variable uncorrelated with z_t and θ and $(1-\theta)$ are the coefficients of the ARMA(1,1) model.

The coefficients of this model are determined from the probability that a user terminal suffers fading caused by the same obstacle at the time interval Δ/v. That probability can be modeled as an exponential distribution:

$$\theta = P(\tau < \Delta/v) = \exp(-\Delta \cdot \lambda), \tag{4.3}$$

where Δ is the distance moved by the user terminal at a time interval, v is the UE velocity and λ is the interruption rate of the line of sight. The interruption rate of the line of sight, λ, is the inverse of the correlation distance. A typical value of the correlation distance for the macrocell urban area simulated is 50 m [150].

Finally, the Gaussian random variable, a_t, must be defined based on its mean and standard deviation. This variable provides a statistical distribution of zero mean and a standard deviation, σ_a, that relates to the standard deviation of the slow fading, σ_z, as follows:

$$\sigma_z^2 = \frac{\sinh(\Delta \cdot \lambda/2)}{\cosh(\Delta \cdot \lambda/2)} \cdot \sigma_a^2. \tag{4.4}$$

Once the propagation calculations have been carried out, it is possible to study the link quality experienced by each user in terms of SIR. The next section describes the process to calculate the value of SIR for each user.

4.1.3 Link layer

SIR calculation

The SIR is a representative measurement of the link quality that the user is experiencing. To calculate the SIR in the simulator, it is first necessary to calculate the interference experienced by each user. It is assumed that intra-cell interference is negligible in LTE because the scheduler assigns different frequencies and time slots to each user. Thus, only co-channel inter-cell interference due to the interfering cells using the same subcarriers is considered. This requires knowing the signal arriving to each user from all interfering cells. To calculate the interference from each base station to the terminal, the channel response is not taken into account, but only the path loss and slow fading are considered here.

The SIR calculation for a given subcarrier k, γ_k, is computed using the expression proposed in [151],

$$\gamma_k = P(k) \times \bar{G} \times \left(\frac{N}{N + N_p}\right) \times \frac{R_D}{N_{SD}/N_{ST}}, \tag{4.5}$$

where $P(k)$ represents the frequency-selective fading power profile value for the k^{th} subcarrier, $\bar{G}$ includes the propagation loss, the slow fading, the thermal noise and the experienced interference, N is the Fast Fourier Transform size used in the OFDM signal generation, N_p is the length of the cyclic prefix, R_D indicates the percentage of maximum total available transmission power allocated to the data subcarriers, N_{SD} is the number of data subcarriers per TTI and N_{ST} is the number of total useful subcarriers per TTI.

If it is assumed that the multipath fading magnitudes and phases are constant over the observation interval, the frequency selective fading power profile value for the k^{th} subcarrier can be calculated using the expression:

$$P(k) = \left| \sum_{p=1}^{paths} M_p A_p \exp\left(j\left[\theta_p - 2\pi f_k T_p\right]\right) \right|^2, \tag{4.6}$$

where p is the multipath index, M_p and θ_p represent the amplitude and the phase values of the multipath fading respectively, A_p is the amplitude value corresponding to the long-term average power for the p^{th} path, f_k is the relative frequency offset of the k^{th} subcarrier within the spectrum, and T_p is the relative time delay of the p^{th} path. In addition, the fading profile is assumed to be normalized such that $E[P(k)] = 1$.

The value of $\bar{G}$ is calculated from the expression:

$$\bar{G} = \frac{P_{max} \frac{g_n(UE) \times g_{UE}}{PL_{UE,n} \times SH_{UE,n}}}{P_{noise} + \sum_{k=1, k \neq n}^{N} P_{max} \times \frac{g_k(UE) \times g_{UE}}{PL_{UE,k} \times SH_{UE,k}}}, \tag{4.7}$$

where $g_n(UE)$ is the antenna gain of the serving base station in the direction of the user UE, g_{UE} is the antenna gain of the user terminal, P_{noise} is the thermal noise power, $PL_{UE,k}$ is the propagation loss between the user and the eNB k, $SH_{UE,k}$ is the loss due to slow fading between the user and the eNB k and N is the number of interfering eNBs considered (set to 43 in the simulator).

A PRB is the minimum amount of resources that can be scheduled for transmission in LTE. As a PRB comprises 12 subcarriers, it is necessary to translate those SIR values previously calculated for each subcarrier into a single scalar value. This can be made using the Exponential Effective SIR Mapping, which is based on computing the effective SIR by the equation:

$$SIR_{eff} = -\beta \ln \left(\frac{1}{N_u} \sum_{k=1}^{N_u} \exp \left(-\frac{\gamma_k}{\beta} \right) \right), \tag{4.8}$$

where β is a parameter that depends on the MCS used in the PRB [152] assuming that all subcarriers of the PRB have the same modulation and N_u indicates the number of subcarriers used to evaluate the effective SIR. The values of β have been chosen so that the block error probability for all the subcarriers are similar to those obtained for the effective SIR in a additive white Gaussian noise (AWGN) channel [153]. The value of β for a particular MCS is shown in Table 4.1.

Table 4.1: Values of β depending on the Modulation and Coding Scheme

Modulation	**Coding**	β **factor**
QPSK	1/3	1.49
QPSK	2/5	1.53
QPSK	1/2	1.57
QPSK	3/5	1.61
QPSK	2/3	1.69
QPSK	3/4	1.69
QPSK	4/5	1.65
16QAM	1/3	3.36
16QAM	1/2	4.56
16QAM	2/3	6.42
16QAM	3/4	7.33
16QAM	4/5	7.68
64QAM	1/3	9.21
64QAM	2/5	10.81
64QAM	1/2	13.76
64QAM	3/5	17.52
64QAM	2/3	20.57
64QAM	17/24	22.75
64QAM	3/4	25.16
64QAM	4/5	28.38

Once the effective SIR has been calculated, the BLER showing the connection quality can be derived. There exist curves that establish the relationship between the values of SIR and BLER defined for an AWGN channel for every modulation and coding rate combination. These curves can also be used to calculate the BLER because inter-cell interference is equivalent to AWGN as the value of β has been selected for this purpose. Then, given the value of BLER and taking into account the MCS used in the transmission, it is possible to calculate the value of throughput, T_i, for each user as follows:

$$T_i = (1 - BLER(SIR_i)) \times \frac{D_i}{TTI}, \tag{4.9}$$

where D_i is the data block *payload* in bits [154], which depends on the MCS selected for the user in that time interval and $BLER(SIR_i)$ is the value of BLER obtained from the effective SIR.

Link Adaptation

Before explaining the Link Adaptation function, the 3GPP standardized parameter known as CQI needs to be described. Such an indicator represents the connection quality in a subband of the spectrum. The resolution of the CQI is 4 bits, although a differential CQI value can be transmitted to reduce the CQI signaling overhead. Thus, there is only a subset of possible MCS corresponding to a CQI value [155]. QPSK, 16QAM and 64QAM modulations may be used in the transmission scheme. In the simulator, the CQI is reported by the user to the base station each iteration (100 ms).

Based on CQI values, the link adaptation module selects the most appropriate MCS to transmit the information on the PDSCH depending on the propagation conditions of the environment. To quantify the link quality for each user and for each subband of the spectrum, the CQI index is used to provide this information. If the experienced BLER value is required to be smaller than a specific value given by the service, it is possible to establish a SIR-to-CQI mapping that allows to select the most appropriate MCS from a given value of SIR [140]. The standard 3GPP defines a 5-bit MCS field of the downlink control information to identify a particular MCS. This leads to a greater variety of possible MCSs. For simplicity, the developed LTE simulator includes only the same set of MCS given by the CQI index. From the effective SIR value, the index CQI is calculated and the MCS can be determined for the next time interval.

Resource Scheduling

The Resource Scheduling can be decomposed into a time-domain and frequency-domain scheduling. On the one hand, it is necessary to determine which user transmits at the following time interval. On the other hand, the frequency-domain scheduler selects those subcarriers within the system bandwidth whose channel response is more suitable for the user transmission. For this purpose, the channel response for each user and for each subcarrier of the system bandwidth has to be estimated. Such a piece of information is given by the channel realizations generated in

the initialization phase of the simulation, assuming a perfect estimation of the channel response. To select the most appropriate frequency subband for the user, the CQI index is used.

The developed simulator includes different strategies for radio resource scheduling. In all of them, the CQI parameter gives the information of the channel quality experienced by each user. Likewise, scheduling is done for each cell at each iteration following the configured strategy [156]. The scheduling algorithms implemented in the simulator are:

- *Best Channel Scheduler* (BC): in this scheduler, both time-domain and frequency-domain scheduling are done for a more efficient use of resources. At each iteration, all users are sorted based on the quality experienced for each PRB, which is obtained from CQI values. Once the users are sorted, the allocation will proceed until there are not available radio resources or no more users to transmit.

  The resource allocation is made following the expression:

  $$\hat{i}[n] = \arg\max_{i}\{r_{ik}[n]\}, \tag{4.10}$$

  where $\hat{i}$ is the selected user i and r_{ik} is the estimated achievable throughput for PRB k and user i obtained from the CQI.

  This scheduling algorithm maximizes the overall system efficiency because the resource allocation is done looking for the combinations PRB-user with better channel conditions. The disadvantage of this algorithm is that harms users with bad channel conditions. Thus, if a user is far from the serving eNB or it has a deep fading for prolonged periods of time, it cannot be scheduled and it can suffer significant delays.

- *Round Robin to Best Channel Scheduler* (RR-BC): this scheduler uses different strategies for time-domain and frequency-domain scheduling. For time-domain scheduling, the Round Robin method is applied. Thus, users are selected cyclically without taking into account the channel conditions experienced by each of them. Then, each PRB is assigned to the user with a higher potential transmission rate for that PRB (transmission rate is estimated based on the user's CQI value for each PRB).

  At each iteration and for each base station, the expressions to be evaluated are:

  $$\hat{i}[n+1] = (\hat{i}[n] + 1) \mod N_u \tag{4.11}$$

  and

  $$\hat{k}[n] = \arg\max_{k}\{r_{ik}[n]\}, \tag{4.12}$$

  where $\hat{i}$ is the selected user, N_u is the number of users and $\hat{k}$ represents the PRB selected. In this case, the goal is to maximize system efficiency, but trying not to harm users with unfavorable channel conditions.

- *Large Delay First to Best Channel Scheduler* (LDF-BC): this scheduler is similar to the

previous one only differing in time-domain scheduling. In this case, instead of cyclically selecting the users, they are sorted by the time they have spent without transmitting. Thus, if for some reason, such as a fading prolonged in time, the user has not been allocated in previous iterations, then he will get a higher priority in the current iteration.

In the same way as in the previous case, at each iteration and for each base station the allocation is carried out based on the following terms:

$$\hat{i}[n] = \arg\max_i \{W_i[n]\}, \tag{4.13}$$

and

$$\hat{k}[n] = \arg\max_k \{r_{ik}[n]\}, \tag{4.14}$$

where $W_i[n]$ is the number of iterations without transmitting for user i. At the end of each iteration, the value of $W_i[n]$ is updated for all the users based on whether they have been allocated or not.

- *Proportional Fair* (PF): this scheduler is an algorithm similar to BC, but it tries not to harm users with worse channel conditions. The objective of PF is to find a balance between getting the maximum possible efficiency of the channel and keeping fairness between users. To this end, scheduling is not only based on the potential transmission rate but also takes into account the average transmission rate of the user in previous iterations. The algorithm follows the expression:

$$\hat{i}[n] = \arg\max_i \left\{ \frac{r_{ik}[n]}{\bar{r}_i} \right\}, \tag{4.15}$$

where $\bar{r}_i$ is the average transmission rate experienced by user i.

4.1.4 Network layer

The success of cellular networks is based on the fact that users can obtain global support while moving (coverage, access, etc.). While physical and link level define the propagation and transmission characteristics along the UE-eNB link, network level manages all base stations, terminals and their resources as a whole.

The main network level functionalities rely on RRM processes. This section describes the Admission Control, Congestion Control and HO techniques implemented in the simulation tool. It should be pointed out that, although scheduling is also usually labeled as an RRM technique, it has been already described in previous sections since it is located at link level in the simulation tool. Another procedure implemented in the simulator is the Directed Retry, which is used when there is congestion in the network in the call set-up phase and the UE is assigned to a traffic channel in a cell other than the serving cell.

Admission Control

Once a UE decides to start a connection, a first decision is which cell will serve that connection. Such a decision is taken through two main steps:

- *Minimum RSRP*: the UE collects and sends reference signal received levels from the serving cell and its neighbors to the network. Cells are ordered from higher to lower levels and candidate cells for serving the call are those fulfilling:

$$RSRP(i) \geq MinThresholdLEV(i), \tag{4.16}$$

  where RSRP(i) is a wideband measurement meaning the received level for the reference signals in cell i and $MinThresholdLEV$ is the minimum required signal level to be accepted. Minimum level is defined on a cell basis. Finally, the best cell i in the list is initially selected.

- *Enough free resources*: the availability of free PRBs in best cell is then checked. Note that the mobile network does not know how many PRBs will require the user data connection once it is admitted. Signal level measurements are taken from the reference signals, but radio channel conditions could be quite different for the finally assigned data radio channel (e.g. fast fading, interference). That is the reason why a worst-case criterion has been taken to accept UEs. Thus, the UE is finally accepted if:

$$freePRB(i) \geq MaxPRB(serv), \tag{4.17}$$

  where $freePRB(i)$ is the number of PRBs available in cell i and $MaxPRB(serv)$ is the worst-case PRB requirement (i.e. the highest number of PRBs needed to maintain a connection) that a specific type of service, $serv$, would demand along the entire connection.

If there are not enough free PRBs, the next candidate cell in the list is checked. A user connection is blocked when no cell fulfills (4.16) and (4.17).

Congestion Control

Congestion control avoids congestion situations in the network. As a result of largely uncontrollable effects such as user mobility, traffic or propagation effects, overload situations can occur in the sense of e.g. intolerable interference levels, even if admission control aims at preventing such situations.

This technique usually defines a pool of the radio resources which will be assigned differently than by admission control. Operators give priority to ongoing connections over fresh calls [157]. If both fresh and ongoing users are in conflict for the same radio resources (e.g. an HO and a fresh connection occur simultaneously), existing users should be first scheduled. With that aim,

fresh users will not be accepted in a cell if:

$$LR(i) \geq LR_{threshold}, \tag{4.18}$$

where $LR(i)$ is the Load Ratio in cell i and $LR_{threshold}$ is the congestion threshold. There is a trade-off when selecting the $LR_{threshold}$ value. A too low value might cause call dropping from rejected incoming HOs, but a very high level could lead to unnecessary call blocking while protected resources are idle.

Handover

The HO algorithm is the main functionality to manage the connected user mobility. HO algorithms are vendor specific. Classical HO algorithms proposed for LTE and implemented in the simulator (where the execution of each HO type is configurable) are the following:

- *Quality HO* (QualHO). A QualHO is triggered when:

$$RSRQ(i) \leq RSRQ_{threshold}(i) \quad \text{for } TTT^{Qual} \text{ s}, \tag{4.19}$$

and

$$RSRP(j) - RSRP(i) \geq Margin_{Qual}(i,j), \tag{4.20}$$

where $RSRP$ is the Reference Signal Received Power, $RSRQ$ is the Reference Signal Received Quality, TTT^{Qual} is the Time-To-Trigger for this type of HO and $MarginQual$ is the level hysteresis between server and adjacent cells (i and j, respectively). This QualHO aims to re-allocate connections which are experiencing a bad quality connection to other cells. $MarginQual$ is defined on an adjacency basis.

For monitoring purposes, a QualHO is classified as an *Interference HO* (IntHO) if, in addition to fulfilling (4.19) and (4.20):

$$RSRP(i) \geq RxLEV^{Interf}_{threshold}(i) \quad \text{for } TTT^{Interf} \text{ s}, \tag{4.21}$$

i.e. the UE has a high signal level but low SIR figures.

- *Minimum Level HO* (LevHO). A LevHO is triggered when:

$$RSRP(i) \leq MinRxLEV_{LevHO}(i), \tag{4.22}$$

and

$$RSRP(j) - RSRP(i) \geq Margin_{LevHO}(i,j), \tag{4.23}$$

where $MinRxLEV_{LevHO}$ is a minimum signal level threshold. LevHO aims to re-allocate connections experiencing a very low signal level (e.g. when the UE is getting out of the coverage area). LevHO is considered an 'urgent' HO and it must be triggered as soon as

possible. Thus, no TTT parameter has been considered.

- *Power Budget HO* (PBGT_HO). A PBGT_HO is triggered when:

$$RSRP(j) - RSRP(i) \geq Margin_{PBGT}(i,j), \tag{4.24}$$

In this case, there is no first condition to be fulfilled. Eq. (4.24) is only evaluated every N^{PBGT} s, where N^{PBGT} is the length of the time period between evaluations of the condition. PBGT_HO is not considered an urgent HO, but an optimization algorithm. At the end of a PBGT_HO process, the UE should be connected to the best cell in terms of signal level (provided that $Margin_{PBGT}$ is positive).

4.1.5 Evaluation of system performance

In this section, some reference scenarios are simulated to evaluate system performance. These are termed 'reference' because network parameters (e.g. HOMs or load ratio threshold in the Admission Control) are set to a moderate default value. For voice service, system performance is evaluated by testing different levels of traffic demand and different strategies of scheduling.

Key Performance Indicators

For voice service, a KPI widely used by network operators is the Call Dropping Ratio (CDR), defined as:

$$CDR = \frac{N_{dropped}}{N_{finished}} = \frac{N_{dropped}}{N_{dropped} + N_{succ}}, \tag{4.25}$$

where $N_{dropped}$ is the number of dropped calls, N_{succ} is the number of successfully finished calls and $N_{finished}$ is the total number of finished calls. The simulation tool assumes that a call is dropped when a percentage of data packets are dropped during a specific time interval. Packet dropping may occur not only because there is no enough connection quality to be scheduled, but also because there are no available resources to be scheduled.

To quantify how efficiently resources are used, another KPI is the Call Blocking Ratio (CBR), which can be determined by the following expression:

$$CBR = \frac{N_{blocked}}{N_{offered}} = \frac{N_{blocked}}{N_{blocked} + N_{accepted}}, \tag{4.26}$$

where $N_{blocked}$ and $N_{accepted}$ are the number of blocked and accepted calls by the Call Admission Control entity respectively, and $N_{offered}$ is the total number of offered calls. Some other KPIs implemented in the simulator will be explained in the corresponding chapter where the KPI is used.

Simulation Parameters

The simulated scenarios include a macro-cellular environment whose layout consists of 19 tri-sectorized sites evenly distributed in the scenario. The main simulation parameters for the simulations are summarized in Table 4.2.

Performance Results

To assess performance, measurements of CDR, CBR and CQI are collected for different levels of traffic load and different types of schedulers. Fig. 4.7 represents the dependency of the average CQI value on the distance for several load levels. As expected, the CQI value decreases as the

Table 4.2: Simulation parameters

Parameter	Configuration
Cellular layout	Hexagonal grid, 57 cells (3x19 sites), cell radius 0.5 km
Transmission direction	Downlink
Carrier frequency	2.0 GHz
System bandwidth	5 MHz (25 PRBs)
Frequency reuse	1
Propagation model	Okumura-Hata with wrap-around Log-normal slow fading, σ_{sf}=8 dB and correlation distance=50 m
Channel model	Multipath fading, EPA model
Mobility model	Random direction, constant speed 3 km/h
Service model	Constant bit rate (voice call), poisson traffic arrival, mean call duration 120 s, 16 kbps
Base station model	Tri-sectorized antenna, SISO, $EIRP_{max}$=43 dBm
Scheduler	Round Robin - Best Channel Large Delay First - Best Channel Resolution: 1 PRB
Power control	Equal transmit power per PRB
Link Adaptation	Fast, CQI based, perfect estimation
RRM features	Directed Retry HO: QualHO, LevHO, IntHO, PBGT_HO
HO parameter settings	TTT = 100 ms HO margin = 3 dB $RSRQ_{threshold}$ = -5 dB $MinRxLEV_{LevHO}$ = -105 dBm [158]
Traffic distribution	Log-normal distribution Unevenly distributed in space
Time resolution	Iteration time = 100 TTI (100 ms) Epoch time configurable

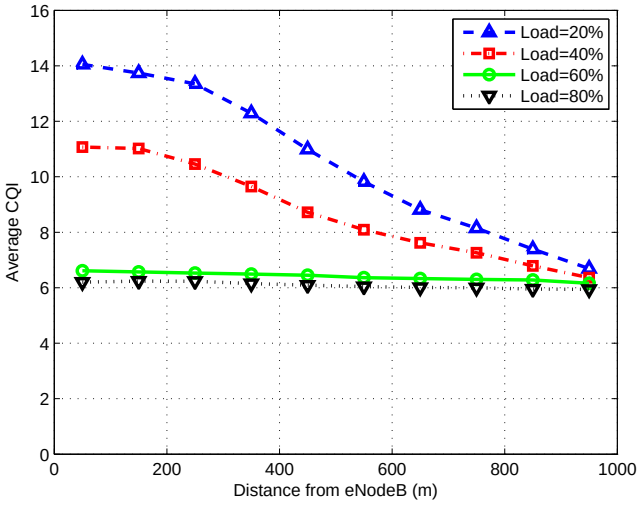

Figure 4.7: Average CQI as a function of the distance for different traffic load levels

distance from the base station is higher due to the path loss. Also it is noted that the range of variation of the CQI is much lower when the load level is higher. This is because the interference term in the expression of SIR becomes more important as the load level is increased, leading to a more restrictive set of CQI values in the cell coverage area.

Regarding call dropping, Fig. 4.8 shows the CDR for several levels of traffic load and two different scheduling schemes. The solid blue line represents the measured CDR when the scheduling strategy is RR-BC, while the dotted red line depicts the measured CDR when the scheduling strategy is LDF-BC. The difference between these two approaches is that LDF-BC sorts the users by the time they have spent without transmitting instead of cyclically sorting them according to the Round-Robin strategy. The LDF-BC scheme leads to a lower CDR for the same load level due to those users that get more priority in scheduling as they experience higher delay, avoiding call dropping.

The CBR for the two previous scheduling strategies as a function of the traffic load is illustrated in Fig. 4.9. As expected, the CBR increases as the traffic load level is higher. However, it is noted that the CBR is higher for the LDF-BC scheduling. This is because a lower CDR due to the scheduling strategy leads to a higher traffic load in the system, increasing the CBR. Logically, it is not appropriate to increase the network capacity by dropping ongoing calls. Thus, it can be concluded that the LDF-BC scheduler provides better performance than the RR-BC scheduler.

4.2 The LTE femto system-level simulator

The structure of the simulator for LTE macrocells described in the previous section has been utilized to create a hybrid scenario composed of both macrocells and femtocells. Thus, a

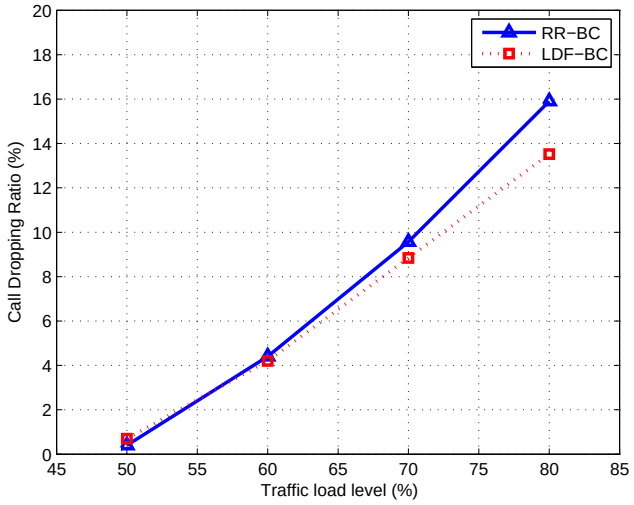

Figure 4.8: CDR as a function of the traffic load for two scheduling schemes

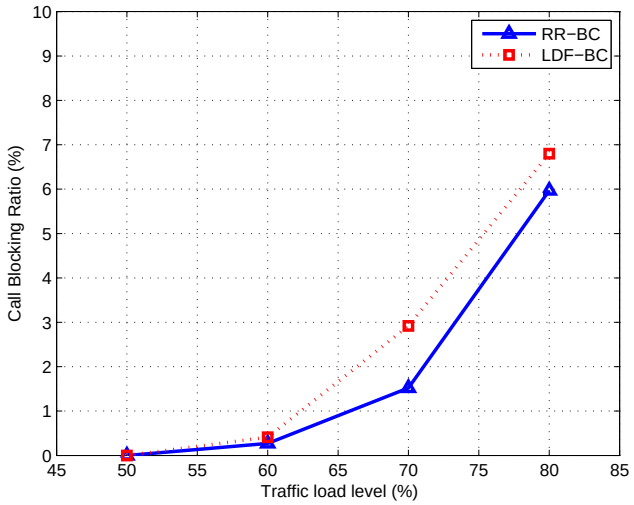

Figure 4.9: CBR as a function of the traffic load for two scheduling schemes

computationally-efficient dynamic system-level simulator for enterprise LTE femtocells has been developed, including a three-dimensional office scenario, specific mobility and traffic and propagation models for indoor environments. As part of the work in this thesis, the indoor mobility model has been designed for this simulator.

The simulation scenario is of 3×2.6 km, comprising three tri-sectorized macrocells in the same site. To avoid border effects in the simulation, the simulator incorporates the wrap-around technique [141]. Inside the coverage area of one macrocell, an office building with dimensions 50 m×50 m has been placed. The number of floors inside the building is configurable. The floor plan is the same for all floors. Fig. 4.10 shows the layout of one of the floors. Magenta circles reflect femtocells positions, lines are the walls (different colors represent their thickness), and

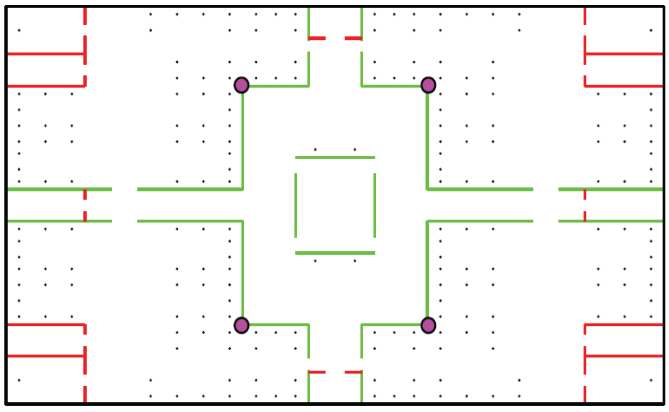

Figure 4.10: A floor diagram

black diamonds are work stations.

The outdoor mobility model adopted for the simulator is very simple, since movement only needs to be reflected in a large-scale. Users move with a random direction that does not change and a constant speed of 3 km/h. The indoor mobility model developed for the simulator as part of this thesis is described in the next section. Finally, more details about the simulator for enterprise LTE femtocell scenarios, such as the indoor propagation model, can be found in [159].

4.2.1 Indoor mobility model

Indoor environments are complex as small user movement may have a strong impact on the signal levels received from base stations. The indoor mobility model developed for the deployment scenario is an extension of the mobility model described in [160]. Users switch between stationary and moving state, but they cannot change floors. A set of location points are defined in the scenario layout so that the user can select them as destination points. Each point has a probability of keeping the user stationary in that location. The time each user spends in the stationary state follows a geometric distribution. Points located in office rooms emulate desks, so that they have associated a high probability of keeping the user there. In contrast, points located in corridors have this probability equal to zero, emulating passing locations for the users.

Unlike the approach in [160], where the user switches to the moving state leaving a desk and moving to the corridor, the destination point can be either a desk in the office room or the corridor door. The user speed in the moving state is equal to 1 km/h. If the corridor door is reached, the user selects the next destination point located in the corridor using a non-uniform distribution. Such a distribution depends on how often the user visits each room. For instance, coffee rooms, meeting rooms, and toilets should be more likely visited. Location points within these rooms are treated the same as office rooms. When the mobile reaches a destination point within a room, it is changed into the stationary state.

The user trajectory is a straight line between source and destination. Thus, there must be direct line of sight with the destination point. For this reason, some auxiliary destination points have been defined within the corridor to avoid crossing walls, as the corridor is not rectangular, as in [160].

Finally, it is noted that the user trajectories are pre-computed and stored in a file. Such a piece of information is used as an input during the simulation. Pre-computing trajectories, unlike calculating them in real time during simulation, reduces computationally load. An additional benefit is that pre-computed trajectories can be reused for different experiments, obtaining repeatability. An example of user trajectories based on the proposed mobility model is shown in Fig. 4.11.

4.3 The HSPA/LTE macro/pico system-level simulator

To assess the proposed algorithms for TS in the context of HetNets, a dynamic system-level simulator for HSPA/LTE macro/pico scenarios has been used. The utilization of the simulator in this thesis has been exclusively from the user-level perspective. The simulated scenario consists of a heterogeneous cellular environment, whose network layer structure can be configured by the user. In this sense, different RATs (HSPA, LTE), cell sizes (macrocells, picocells) and frequencies can be deployed with the aim of simulating a heterogeneous environment. The mathematical framework supporting the simulator is described in [161].

4.4 Conclusions

In this chapter, firstly, a computationally-efficient dynamic system-level simulator for LTE macrocells has been described. This simulator includes the main characteristics of the RAT as well as the RRM algorithms which provide notable improvements in the efficient use of the available

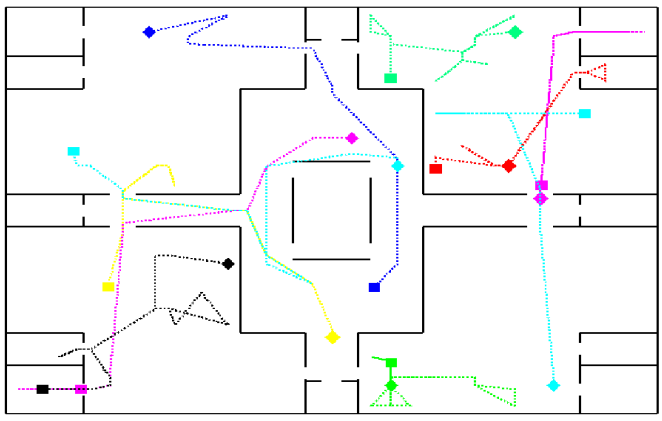

Figure 4.11: User trajectories computed by the indoor mobility model

radio resources. For this purpose, the simulator has been implemented so that simulations require a low computational cost. In addition simulations are composed of epochs to evaluate the modification of network parameters performed by optimization algorithms.

At physical and link layers, the design of the simulator has been focused on the calculation of several indicators with the purpose of evaluating the connection quality in a mobile communication. Those indicators are required in the execution of RRM functions. Hence, it is essential that these indicators reflect accurately the behavior of a real network. To achieve this goal, an OFDM channel model has been performed to characterize the temporary and frequency variation of the radio transmission environment for each user during the simulation. The main functions of RRM have also been described in this chapter. At link level, the previous calculated indicators are inputs of the Link Adaptation and Dynamic Scheduling functions. At network level, the main functions are admission control and mobility management, whose parameters can be modified to evaluate optimization algorithms. Simulation results have shown network performance in terms of several indicators for different traffic load levels and scheduling schemes.

The next part of this chapter has been devoted to a computationally-efficient dynamic system-level simulator for enterprise LTE femtocells, whose scenario has been briefly described. In addition, the indoor mobility model developed for this simulator has been explained in more detail, since it has been part of the work in this thesis.

Finally, a dynamic system-level simulator for HSPA/LTE macro/pico scenarios has also been mentioned in this chapter, as it has been used in the context of this thesis to evaluate the proposed algorithm for TS purposes.

Chapter 5

Mobility load balancing

In this chapter, different MLB algorithms are proposed. One group of these algorithms is conceived for macrocells scenarios in which the objective is to alleviate persistent congestion problems, such as a population increase in a city area. The second group of proposed MLB algorithms is designed to solve localized congestion problems in enterprise femtocell scenarios, where a thorough deployment is not typically performed. In addition, the developed algorithms are intended for voice service. Prior to describing the proposed algorithms, an introduction to the mobility parameters and procedures mainly related with the MLB algorithms is provided in Section 5.1. Then, Section 5.2 is devoted to MLB algorithms in macrocell scenarios, while Section 5.3 presents MLB algorithms in enterprise femtocell scenarios. Both sections follow a similar structure, where the specific problem, the proposed solution and its performance assessment are addressed. Finally, Section 5.4 summarizes the major findings of this work.

5.1 Introduction

Load balancing is a major issue addressed in the field of SON, which can be solved by sharing traffic between adjacent cells. This problem is tackled here as a Self-Optimizing task that can be solved by tuning specific network parameters, like those involved in the HO process. The HO process is responsible for transferring an ongoing call from one cell to another. By adjusting HO parameters settings, the service area of a cell can be modified to send users to neighboring cells. Thus, the size of the congested cell is reduced while adjacent cells increase in size taking users from the congested cell edge. As a result of a better matching between the spatial distribution of traffic demand and network resources, more users could be accepted in the crowded area so that the call blocking probability would be reduced [54].

In LTE, when a user is in connected mode, the network is responsible for deciding when

performing an HO to maintain the ongoing connection. The network also determines for how long each mobile terminal has to send signal measurements back to their serving eNBs, as well as the interval time to perform each measurement. One of the most widely used algorithms for the HO-triggering decision is the Power Budget HO, which is equivalent to the 3GPP A3 event [35]. This algorithm triggers the execution of the HO procedure if the following condition is fulfilled for a specific time period determined by the TTT parameter:

$$\overline{RSRP_j} > \overline{RSRP_i} + HOM_{i \to j}, \tag{5.1}$$

where $\overline{RSRP_i}$ and $\overline{RSRP_j}$ are the averaged values of RSRP measured for serving cell i and target cell j respectively, and $HOM_{i \to j}$ is the HOM defined between cell i and cell j. The HOM determines the area where the users connected to a cell would perform an HO toward a neighboring cell. In the context of MRO, the parameter $HOM_{i \to j}$ and the symmetric $HOM_{j \to i}$ are usually set to the same positive value so that certain symmetric region between the two cells is ensured in order to avoid unnecessary HOs. In Fig. 5.1(a), the RSRP of the neighbor and the serving cells are represented. For instance, if a user connected to cell i moves to cell j, it connects to cell j when the RSRP from cell j is equal to the RSRP from cell i plus $HOM_{i \to j}$. As in this case the HOMs are assumed to be symmetric, the same value is applied to the opposite situation (i.e. when the user moves from cell j to i, $HOM_{j \to i}$ is used). Maintaining the symmetric region, both HOMs could also be jointly tuned (e.g. $HOM_{i \to j}$ is increased while $HOM_{j \to i}$ is decreased) so that the service area of these cells is modified, for instance, for MLB purposes. In this case, both HOMs should be modified with the same magnitude to preserve the hysteresis region. However, those variations in HOM should have opposite sign to modify the service area of the two cells. In Fig. 5.1(b), it is observed that $HOM_{i \to j}$ has been increased, while $HOM_{j \to i}$ has been decreased. As a result, the service area of the cell i is larger. Finally, it is noted that, since HOMs are defined on an adjacency basis, cell service areas cannot be only re-sized but also re-shaped.

5.2 MLB algorithms for voice service in macrocells

This section is devoted to MLB algorithms developed in the context of future wireless networks. In particular, the self-optimization of an FLC to solve persistent congestion problems in macrocell scenarios is investigated. Such a congestion problem is due to an uneven spatial traffic distribution, e.g. when the center of a city becomes crowded. The optimization process is carried out by the fuzzy Q-Learning algorithm with the goal to reduce the blocking probability for voice services while the call dropping is controlled according to network operator constraints. Results are evaluated in a non-uniformly distributed traffic scenario, where the FLC is optimized to fulfill the call dropping constraint.

The rest of the section is organized as follows. Firstly, the problem is formulated, where the system model is described, including the main system measurements and involved parameters. After this, the structure of the proposed self-tuning scheme as well as the application of the fuzzy

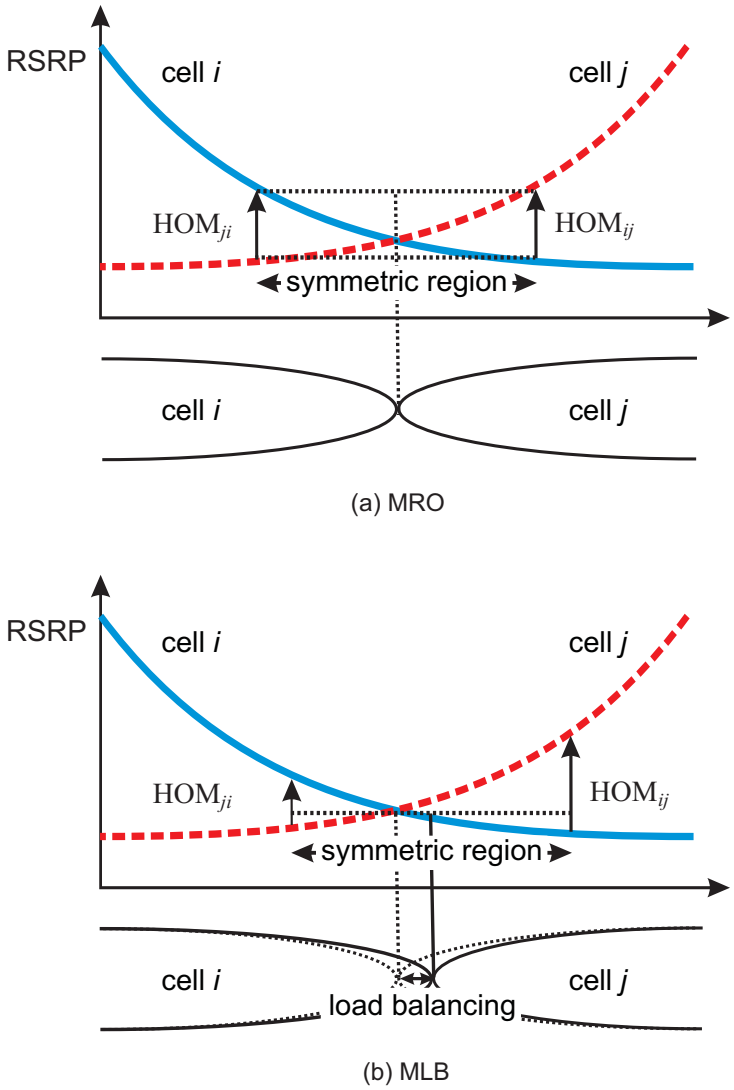

Figure 5.1: Adjustment of HOM for HO optimization and load balancing purposes

Q-Learning algorithm to the proposed FLC are explained. The last part of the section describes the simulation setup and discusses the results.

5.2.1 Problem formulation

During the last years, cellular networks have experienced a large increase in size and complexity. Generally, network planning provides proper dimensioning of radio resources during the design phase of the RAN. However, as traffic demand changes over time, both traffic demand and network resource dimensioning become misaligned, thus leading to an inefficient use of resources. To cope with such a problem in a cost-effective manner, self-optimizing techniques remains as the best solution rather than adding new resources.

To model the misalignment between traffic demand and network resources throughout the

time, an assumption made in this study is that the spatial traffic distribution during the network planning stage is uniform, leading to a deployment of cells evenly distributed in the scenario. However, as network evolves, the matching between the spatial distribution of traffic demand and network resources becomes poorer. For this reason, a different spatial traffic distribution is assumed during the operational phase, i.e. when the MLB algorithm is applied to the network. In particular, the center of the selected scenario has become more crowded than the periphery (e.g. emulating the center and the periphery of a small city), so that performance assessment has been carried out based on such a non-uniform spatial traffic distribution. It is worth mentioning that the proposed algorithm can be applied to other non-uniform spatial traffic distributions, since those distributions would be variants of that used in this work, in which the size and the number of hotspots (crowded areas) included in the scenario would be different. As results are expected to be equivalent, a simplified traffic distribution allows a better visualization of the results.

Load balancing has an impact on the GoS, which includes call accessibility and maintainability. As a result of a better exploitation of the system capacity, GoS is improved. Although HO-based load balancing is an effective method to share traffic in cellular networks, it may cause negative effects on call maintainability. If the HOM is decreased, the target cell would increase the probability to be more preferred than the serving cell (even if the connection quality is worse), so that some users could be handed over to the target cell. Those users, usually located in the cell edge, will experience worse radio conditions in the target cell as a result of applying such a traffic sharing technique. Thus, negative values of HOMs would increase the risk of dropping. The main contribution of this work is the design of an algorithm to control quality performance for real-time traffic during the load balancing process.

Typically, studies found in the bibliography addressing the load balancing problem aim to provide more capacity to a fixed number of users in the system so that they experience higher instant throughput o lower delay, but accessibility is usually not tackled. In future networks, accessibility will be an important feature as services such as VoIP calls are expected to be widely used. In addition, the connection quality loss experienced by some users when load balancing is carried out and controllability of such an effect have not been properly addressed in the literature. This work addresses how much the connection quality can be decreased when load balancing is carried out depending on the operator policy. Thus, flexibility and easiness from the network operator perspective is provided by simply adjusting a single parameter. Unlike the design in [9], the FLC proposed in this work balances traffic load in a intra-system LTE scenario where call dropping becomes a key issue. In addition, HOMs of the standard HO algorithm are adjusted in this work, instead of tuning load thresholds, as proposed in [9].

Finally, another assumption is that the voice call is the service considered in this work, since it is expected to be widely used in the future due to the successful and existing applications based on VoIP. In principle, the proposed algorithm can be applied to any real-time service (voice call, video calls, etc.) for which call dropping is defined as a KPI. For other services (e.g. data services), KPIs such as the throughput could be used to estimate the connection quality of the user.

Network model and system measurements

The proposed self-tuning scheme is applicable to any RAT for next generation cellular networks. In particular, an LTE downlink macro-cellular network providing constant bit rate service is considered here. Each cell is controlled by an eNB (i.e. a base station) and all the cells use the same frequency band. Following the 3GPP standard specifications, the eNBs are interconnected by the X2 interface, enabling direct communication between them. Thus, measurements such as traffic load can be easily exchanged between eNBs over the X2 interface and faster HOs can be performed.

The main network level functionalities are admission control and HO. The admission control is responsible for checking the availability of free PRBs in the candidate cell before accepting a call. A 'worst-case' criterion has been taken to accept calls, i.e. the user is finally accepted if the highest number of PRBs needed to maintain a connection (worst-case PRB requirement) is less or equal than the number of PRBs available in the candidate cell. If the condition is not satisfied by any candidate cell, then the user connection is blocked. On the other hand, the HO allows user mobility across the network.

The call dropping model also plays an important role because the optimization algorithm attempts to control the occurrence of this event. A call is dropped when a percentage of data packets are dropped during a specific time interval. Packet dropping may occur not only because there is a poor connection quality, but also because there are not any available resources to be scheduled.

The most important outcome derived from sharing traffic between cells is that the call blocking is reduced, especially in those cells highly loaded. To quantify the call blocking, network operators usually use the CBR, which in this work is defined as in (4.26). Additionally, the load balancing may lead to an increment in the call dropping, which is usually quantified by the CDR, defined here as in (4.25).

Since the goal is to solve persistent congestion problems, and not temporary traffic fluctuations, the previous measurements are collected during a long period (i.e. above 15 minutes). As a result, fast changes in network loading are filtered. Note that some situations can lead to a more dynamic traffic distribution, such as the half-time in a football match or a concert. In those cases, faster actions in the order of seconds or few minutes would be needed, so that the previous measurements would not be appropriate due to lack of accuracy and, instead, instantaneous measurements should be employed, for instance, the current load of the system, which is closely related to the call blocking that could be expected.

5.2.2 Optimization algorithm

Self-tuning scheme

The proposed FLC is inspired in the diffusive load balancing algorithm developed in [94], which iteratively balances the CBR between cells by adjusting the HOMs to minimize the overall CBR. The FLC computes the HOM for each pair of adjacent cells to send users from one cell to the less loaded cell in the adjacency. In particular, an adjacency consists of a pair of cells that are neighbors. Fig. 5.2 illustrates the inputs and the output of the proposed FLC. As in [94], the inputs of the FLC are the blocking difference in the adjacency and the current value of the HOM. The CBR difference is used to balance the traffic between the two adjacent cells, while the current HOM aims to reduce the magnitude of changes once margins become negative. Experience has shown that sensitivity to changes is greatly increased when margins becomes negative as a result of large parameter changes. The approach in [94] also takes into account frequency collisions, which may occur in GSM between source and target cell when an HO is carried out. However, this issue is not considered in this work as it is expected that next-generation networks usually operate in frequency reuse one [28]. Finally, the output of the proposed FLC is the increment in the HOM, as shown in Fig. 5.2.

Another requirement for the proposed FLC is that, as previously stated, HOM variations in both directions of any adjacency must have the same magnitude but opposite sign to provide a hysteresis region to ensure HO stability. Additionally, HOMs can only take values within a specific range (limited by $+/-24$dB) to avoid network instabilities due to excessive parameter changes.

For simplicity, all FLCs are based on the Takagi-Sugeno approach [116]. The design of the FLC includes the following tasks: define the fuzzy sets and membership functions of the input signals and define the linguistic rule base which determines the behavior of the FLC. The first step involved in an FLC execution is the fuzzifier, which transforms the continuous inputs into fuzzy sets. Each fuzzy set has a linguistic term, such as 'high' or 'low', associated. The membership

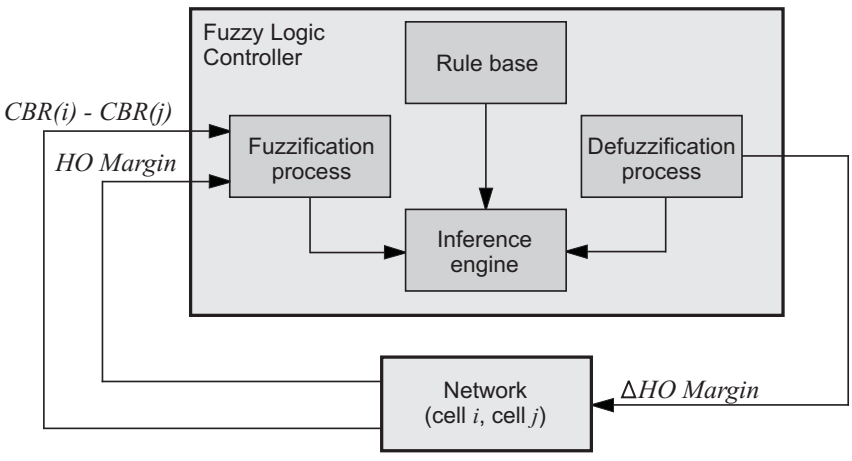

Figure 5.2: Fuzzy Logic Controller scheme for MLB in macrocells

function, $\mu(x)$, quantifies the degree of membership of an input value x to a specific fuzzy set. For simplicity, the selected input membership functions depicted in Fig. 5.3 are triangular or trapezoidal. Three fuzzy sets have been defined for the input of CBR difference between cells to represent three different situations: balanced traffic, unbalanced traffic from cell i to cell j, and unbalanced traffic from cell j to cell i. For the input of current HOM, three fuzzy sets are also identified, whose linguistic terms are 'Low' (L), 'Medium' (M) and 'High' (H). These three fuzzy sets discriminate the cases when HOM is close to saturation (i.e. $+/-24$dB) or it is around the default value (i.e. $+3$dB), which has been set to keep the hysteresis region. It is noted that a higher number of input membership functions would add complexity to the FLC (by increasing the number of rules).

Once the crisp input values are converted to fuzzy values, the next step is performed by the inference engine, which identifies the activated rules and calculates the output values. For the definition of the rule base, the knowledge and experience of a human expert is generally used although, in some cases, it is necessary to use optimization techniques. Rules follow a syntax of the type IF-THEN to set the control strategy, similar to the human knowledge. An example rule for the proposed FLC is the following: 'IF (CBR difference is $Unbalanced_{i\rightarrow j}$) AND (HOM is $High$) THEN (ΔHOM is o_i)'. The output function (Takagi-Sugeno approach) of rule i is a constant value, o_i, which can be one of the following values (each value also has an associated label): -6dB (Extremely Low, EL), -3dB (Very Low, L), -1dB (Low, L), 0dB (Zero, Z), $+1$dB (High, H), $+3$dB (Very High, VH) and $+6$dB (Extremely High, EH). Thus, the magnitude of the increment in HOM cannot be greater than 6dB. The sign of the value determines which cell in the adjacency will increase in size. The antecedent of the rule is formed from the combination of fuzzy sets using the product operator:

$$\alpha_k = \mu_x(CBR\ diff) * \mu_y(HOM), \tag{5.2}$$

where α_k is the degree of truth for the rule k.

The rule base for the proposed FLC is shown in Table 5.1. The number of rules comes from the combination of all possible fuzzy sets between the two fuzzy inputs (9 rules in total). Unlike

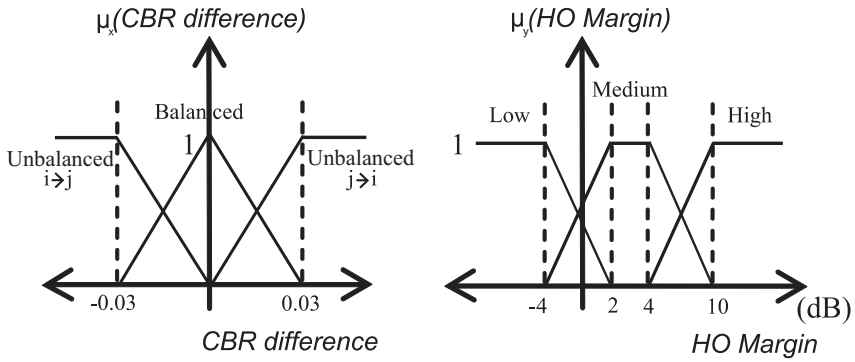

Figure 5.3: Membership functions of the FLC fuzzy sets for MLB in macrocells

Table 5.1: Set of fuzzy controller rules

Rule	CBR_i-CBR_j	HOM	Action
1	$Unbalanced_{i\rightarrow j}$	H	EL
2	$Unbalanced_{i\rightarrow j}$	M	VL
3	$Unbalanced_{i\rightarrow j}$	L	L
4	Balanced	H	Z
5	Balanced	M	Z
6	Balanced	L	Z
7	$Unbalanced_{j\rightarrow i}$	L	EH
8	$Unbalanced_{j\rightarrow i}$	M	VH
9	$Unbalanced_{j\rightarrow i}$	H	H

the design in [94], the number of input membership functions selected in this work is smaller, resulting in a lower number of fuzzy rules. A small number of rules speeds up the convergence of the Q-Learning algorithm since fewer states have to be visited during the exploration phase. The interpretation for each rule defined in this work is described as follows. Rule 1 is activated when there is a significant blocking difference from cell i to cell j and the HOM has a 'high' value, which is opposite to the desired value. A large decrement in the HOM should be necessary in this case to reduce the CBR difference. Thus, the consequent of the rule 1 is set to EL. Rule 2 is similar to rule 1 but with the difference that the HOM has a neutral ('medium') value. The consequent for that rule should be a moderate change such as VL. The activation of rule 3 occurs when there is an appreciable CBR difference in the adjacency from cell i to cell j but the HOM has an appropriate ('low') value to balance the traffic. In such a situation, HOMs could experience saturation if the HOM continues decreasing with large changes. In addition, sensitivity to changes is higher when margins become negative. For those reasons, the consequent for rule 3 is set to L. Rule 4 is activated when the CBR has been balanced in the adjacency and the HOM is not in the neutral region, but it has a 'high' value. In this case, it might be appropriate to keep the margin to the same value or try to bring it back to the default value to return users to the original cells. The selected consequent for rule 4 has been set to 'Zero' (Z), that is, no change to accelerate the load balancing process. Rule 5 is triggered when the CBR is balanced and the HOM has a neutral ('medium') value. The best action for that rule is obviously to leave the HOM at the same value. For the definition of rules 6, 7, 8 and 9, the same principles but opposite actions as in rules 4, 1, 2 and 3 are applied, respectively, due to symmetry.

The last step performed by the FLC is the aggregation of the rules into a non-fuzzy value, or a scalar (defuzzification). Given a set of activated rules and their corresponding degree of truth, the output crisp value is calculated as:

$$output = \frac{\sum_{i=1}^{N} \alpha_i \times o_i}{\sum_{i=1}^{N} \alpha_i}, \tag{5.3}$$

where N is the number of rules, α_i is the degree of truth for the rule i and o_i is the selected output constant value for the same rule.

FLCs, such as the one designed, have several limitations. The rule base defined to decrease the call blocking in the network should be successfully applied to any scenario (e.g. different traffic load levels). However, performance achieved by the FLC is not always the one desired by the operator as fuzzy rules are fixed. For instance, load balancing in a very congested network should be conservative as cell borders receive much more interference. Thus, in this case the risk of call dropping is higher when modifying HOMs. Another special situation is when there is a small overlap between cells and the FLC produces an excessive change in the HOM that significantly increases the call dropping. For these reasons, the rule base of the FLC should be particularly designed according to both the network operator policy and the current network state. The next section describes the optimization process applied to the FLC in order to deal with these issues.

Optimization of the self-tuning scheme for load balancing in macrocells

In this section, the optimization of the FLC for load balancing by using the fuzzy Q-Learning algorithm is presented. Unlike the previously designed FLC, the optimization process takes into account the call dropping constraints defined by the operator. Instead of adding a new input to the FLC, the learning algorithm enables to control this performance indicator by the 'trial-and-error' methodology with the advantage of avoiding complex rules and high number of rules. Two different approaches are proposed depending on the exploration/exploitation trade-off and results are evaluated in an LTE network. The proposed optimization scheme, showing the main elements of the RL problem, is depicted in Fig. 5.4. The FLC inputs, given by the CBR difference between cells and the current HOM, correspond to the state of the network,

$$s(t) = [CBR_{diff}(t),\ HOMargin(t)]. \tag{5.4}$$

The FLC output, given by the increment in HOM, represents the action of the agent, $a(t)$. The reinforcement signal, $r(t)$, is built from the CDR measured in both cells of the adjacency in order

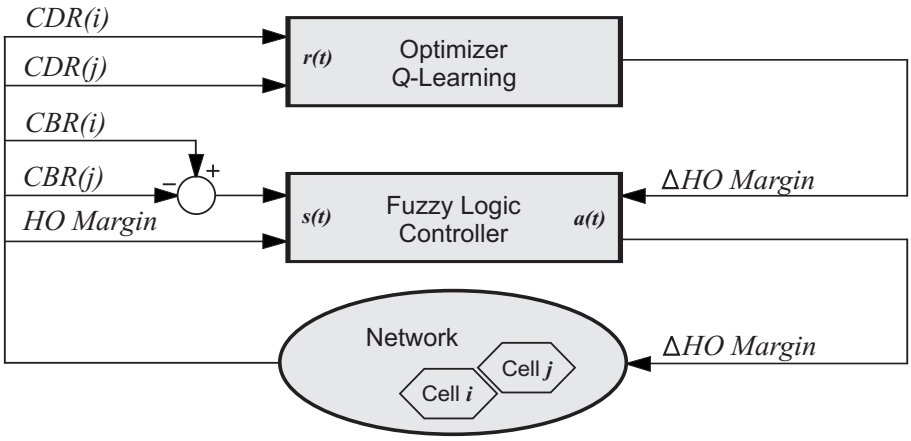

Figure 5.4: Block diagram of the optimization scheme for MLB in macrocells

to test if users are experiencing bad quality.

Several assumptions are made for the optimization process. The first assumption is that policy evaluation is shared by all cells selected for optimization, updating the same look-up table of action q-values when performing an action. Thus, the optimized inference engine will be the same in all adjacencies. Such assumption speeds up the learning process because a higher number of entries can be simultaneously updated in the look-up table. Another assumption is that policy improvement is also shared by all adjacencies, so that the same set of fuzzy rules is applied at each iteration or optimization epoch. Each epoch of the optimization process comprises a modification in HOMs. Although both policy evaluation and improvement are shared by all adjacencies, the HOM is not modified in all adjacencies at the same optimization epoch. The aim of this assumption is to accurately assess the action performed in each adjacency. This fact is illustrated in Fig. 5.5, where two congested cells, i and j, are represented in gray, while the other non-congested cells are represented in white. Let suppose that the FLC_{ij} that modifies the HOMs between both congested cells i and j performs the action of sending users towards cell i (indicated by an arrow in the figure), which is less congested than j. As observed, the assessment of this action (i.e. good match between reward r and action a) is interfered by the simultaneous actions performed by other FLCs (e.g. FLC_{ik} and FLC_{jl}), since these actions take effect in the adjacency area where the assessment takes place. Thus, to accurately evaluate actions, only one action per adjacency is carried out at each epoch, so that performance indicators measured in the adjacency would be only affected by the action performed. To avoid a significant decrease in the convergence rate, those adjacencies that do not share cells can simultaneously modify their HOM. For instance, in a hexagonal layout that defines six adjacencies per cell, HOMs (or adjacencies) could be grouped into six categories at best. At each epoch, all HOMs included in a category would be modified. Thus, the process would require six epochs to compute all HOMs. The order of modification of the categories has been decided to be sequential.

To find the optimal consequents of the fuzzy rules, the reinforcement signal, $r(t)$, must be defined. A call dropping threshold, denoted by CDR_{th}, has been introduced in the reinforcement

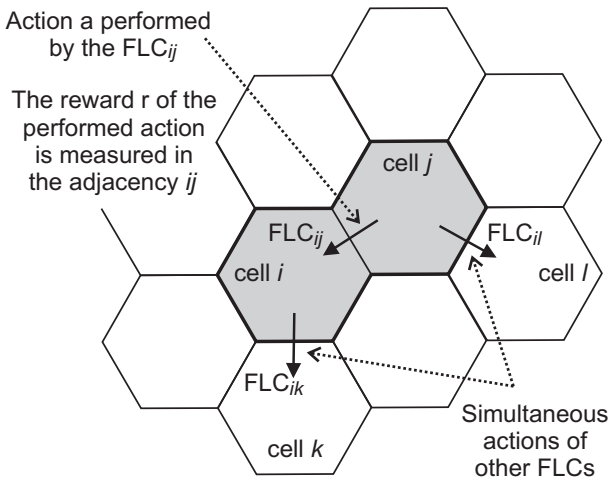

Figure 5.5: The problem of simultaneously adjusting the HOM in all adjacencies

signal to detect bad quality in terms of CDR. Network operators can adjust this parameter to fulfill their call quality constraints. Thus, those FLC actions that lead to a CDR less than CDR_{th} should be rewarded with a positive value, while those actions producing a CDR higher than CDR_{th} should be punished with a negative value. Formally, the reinforcement signal used in this work is defined by:

$$r_k(t+1) = \begin{cases} 10 & \text{if } CDR^k_{measured}(t) \leq CDR_{th} \\ -10 & \text{otherwise} \end{cases}, \tag{5.5}$$

where $r_k(t+1)$ is the reinforcement signal for the k^{th} adjacency in iteration $t+1$. The value of $CDR^k_{measured}(t)$ is calculated as the maximum value between both cells in the adjacency:

$$CDR^k_{measured}(t) = \max\{CDR^k_1(t), CDR^k_2(t)\}. \tag{5.6}$$

Note that negative values of $r(t)$ may involve a decreasing evolution of the q-values. Thus, an optimal action (given by the highest q-value) could stop of being optimal even though other candidate actions do not increase their q-value. This means that optimal actions can change along the time even if 100% exploitation is assumed (other actions are not explored).

A priori knowledge (e.g. operator experience) can be used to propose a set of consequents for a specific rule. The most unfavorable case is when there is no knowledge. The candidate consequents proposed for each rule are shown in Table 5.2. When HOMs have an intermediate value, rules 2 and 8 should always modify HOMs to decrease the service area of the congested cell. The optimization process aims to select the best magnitude of those changes (1, 3 and 6 dB are the values proposed). When HOMs have an extreme value as in rules 1, 3, 4, 6, 7 and 9, the optimization process aims to decide whether to lead the HOM to saturation, return it to the default value, or not to modify it. In this case, there is no a priori knowledge to determine the balancing direction. Finally, there is only an option for the rule 5, Z, as HOM must have the default value when the traffic is balanced.

To find the optimal fuzzy rules, two different approaches are proposed in this work by adjusting the parameter ϵ that establishes the trade-off between exploration and exploitation in the fuzzy Q-Learning algorithm. The first optimization scheme has been named Unbalanced Exploration and Exploitation (UEE). In UEE, the parameter ϵ is set to 1 in order to explore all the possible actions a large number of times. Once the optimal fuzzy rules are found, the FLC with the optimized set of fuzzy rules can be used without the optimization module in the real network. Simulation tools are preferable to be used during the optimization process instead of the real network because the FLC is continuously exploring actions while neglecting performance. Another alternative to perform this optimization method would consist of introducing test users into the network throughout the night. To avoid the need for simulation tools, which do not usually reflect reality, or decreasing performance during the night, the second optimization approach is proposed. The method named Balanced Exploration and Exploitation (BEE) can be directly used in the real network. In BEE, an appropriate ϵ is selected, e.g. $\epsilon = 0.2$ (i.e.

Table 5.2: Candidate consequents for the fuzzy rules

Rule	CBR_i-CBR_j	HOM	Candidate action
1	$Unbalanced_{i\rightarrow j}$	H	EL, VL, Z
2	$Unbalanced_{i\rightarrow j}$	M	EL, VL, L
3	$Unbalanced_{i\rightarrow j}$	L	VL, Z, VH
4	Balanced	H	VL, Z, VH
5	Balanced	M	Z
6	Balanced	L	VL, Z, VH
7	$Unbalanced_{j\rightarrow i}$	L	Z, VH, EH
8	$Unbalanced_{j\rightarrow i}$	M	H, VH, EH
9	$Unbalanced_{j\rightarrow i}$	H	VL, Z, VH

L: Low, M: Medium, H: High, EL: Extremely Low,
VL: Very Low, Z: Zero, VH: Very High, EH: Extremely High

80% of time the best action is selected). In this case, the FLC starts from a non-optimized set of rules and the Q-Learning algorithm progressively determines the best fuzzy rules for the FLC, preserving system performance.

5.2.3 Simulation setup

The dynamic system-level simulator for LTE macrocells explained in Chapter 4 has been used to perform simulations. This simulator first runs a module of parameter configuration and initialization, where a warm-up distribution of users is created to provide meaningful network statistics from the first simulation iteration. Then, several optimization loops or epochs are executed to emulate the tuning process. Each epoch comprises 14,000 simulation steps, equivalent to 23 min of actual network time. Each simulation step includes updating user positions, propagation computation, generation of new calls, and radio resource management algorithms. At the end of each epoch, measurements and reliable statistics are obtained to be used in the following optimization loop. Finally, the main statistics and final results are shown.

The simulated scenario includes a macro-cellular environment with a regular layout consisting of 19 tri-sectorized sites evenly distributed in the scenario, as shown in Fig. 4.2. The main simulation parameters are summarized in Table 5.3. Only the downlink is considered in the simulation, as it is the most restrictive link. For simplicity, the service provided to users is the voice call as it is the main service affected by the tuning process. A non-uniform spatial traffic distribution is assumed in order to generate the need for load balancing. It is assumed that, as traffic demand changes over time, both the spatial distribution of traffic demand and the network resource dimensioning have become misaligned. In this scenario, the center has become more crowded than the periphery (e.g. emulating the center and the periphery of a small city). Thus, there are several cells with a high traffic density whereas surrounding cells have a low traffic density. The average traffic load is set to 75%. It is expected that HO parameter changes performed by the FLCs manage to relieve congestion in the affected area.

Table 5.3: Simulation parameters

Parameter	Configuration
Cellular layout	Hexagonal grid, 57 cells (3x19 sites), cell radius 0.5 km
Transmission direction	Downlink
Carrier frequency	2.0 GHz
System bandwidth	1.4 MHz
Frequency reuse	1
Propagation model	Okumura-Hata with wrap-around Log-normal slow fading, $\sigma_{sf} = 8\ dB$ and correlation distance=50 m
Channel model	Multipath fading, EPA model
Mobility model	Random direction, constant 3 km/h
Service model	real-time constant bit rate service (voice call), poisson traffic arrival, mean call duration 120 s, 16 kbps
Base station model	Tri-sectorized antenna, SISO, $EIRP_{max} = 43dBm$
Scheduler	Time domain: Round-Robin Frequency domain: Best Channel
Power control	Equal transmit power per PRB
Link Adaptation	Fast, CQI based, perfect estimation
Handover	Time-To-Trigger=100 ms HOM: $[-24, 24]dB$
Traffic distribution	Unevenly distributed in space
Time resolution	100 TTI (100 ms)
Epoch time	23 min
Discount factor γ	0.95
Learning rate η	0.1

Three load balancing methods are simulated. The initial situation is common to all methods, meaning an unbalanced traffic distribution. The first approach is carried out by the non-optimized FLC and it is used as a benchmark. In this case, the inference engine is intuitively designed from the knowledge operator explained in Section 5.2.2. The other two methods are based on the optimization carried out by the fuzzy Q-Learning algorithm also described in Section 5.2.2. The first approach, named as UEE, requires two simulations as the FLC is optimized with 100% exploration ($\epsilon = 1$) in a first simulation and then used without the optimization module in a second simulation to evaluate performance. The second approach, named as BEE, requires only a simulation as the FLC is optimized while performance is enhanced. In this case, the optimization is carried out with 20% exploration ($\epsilon = 0.2$) and the Q-Learning optimizer entity is teamed with the FLC in the evaluation simulation.

Within each epoch, network and optimization parameters such as HOMs, action q-values and FLC consequents, remain unchanged. The learning rate η controls the speed of the learning process and it is set to 0.1 in order to provide a good trade-off between accumulated and fresh q-values. The discount factor γ is set to 0.95 to take into account future rewards when performing

an action.

5.2.4 Performance results

To compare the developed FLCs, a utility function named U is proposed:

$$U = [CBR + (1 - CBR) \cdot CDR] \cdot 100, \tag{5.7}$$

which is a metric that aggregates both KPIs to provide an estimation of the user dissatisfaction. Such indicators, CBR and CDR, consider the total number of blocked and dropped calls in the network, respectively.

The first experiment is related to the non-optimized FLC, which is applied to the initial unbalanced situation. As a result, the CBR is highly decreased to the disadvantage of an uncontrolled increase in the CDR, which would be unacceptable for operators, suggesting the need for a FLC optimization that finds a better trade-off between those indicators. The values of the CBR and the CDR are 1.4% and 8.0%, respectively, when such indicators remain stationary after load balancing. In this situation, the value of U is 9.3%.

The following experiment is related to the optimization approach named as UEE. To find the optimal fuzzy rules by using 100% exploration, three simulations starting from the unbalanced situation have been carried out with $\epsilon = 1$ for different values of CDR_{th}. As a result, three different sets of fuzzy rules have been extracted from the optimization process. Table 5.4 shows the optimal rule consequents determined by selecting the candidate action with the highest q-value for each rule and they are compared with the rule base for the non-optimized FLC described in Section 5.2.2. When increasing CDR_{th}, rules 3 and 9 are modified to leave the HOM at the same value, instead of returning it to the default value. As a result, lower and higher values of HOM can be achieved, increasing the risk of call dropping. Another consequence of increasing CDR_{th} is that higher changes in HOMs are allowed, as rules 2 and 8 are modified to perform larger increments in HOMs.

Table 5.4: Optimized fuzzy rules

Rule	Non-optimized FLC	Action for $CDR_{th} = 0.06$	Action for $CDR_{th} = 0.1$	Action for $CDR_{th} = 0.15$
1	EL	VL	VL	VL
2	VL	L	L	VL
3	L	VH	Z	Z
4	Z	VL	VL	VL
5	Z	Z	Z	Z
6	Z	VH	VH	VH
7	EH	VH	VH	VH
8	VH	H	H	VH
9	H	VL	Z	Z

Fig. 5.6 represents a realization of the q-value evolution of the consequents for optimized rules 1-4 during a simulation when $CDR_{th} = 0.06$ (rules 6-9 are obviated due to symmetry). As it can be observed, those consequents obtaining higher q-values are the optimal actions that can be identified in Table 5.4. The initial HOM values are set to 3 dB, i.e. the default value, corresponding to the fuzzy set named 'Medium', so that rules 2 and 8 are triggered from the first iterations, while others are triggered from iterations 10-15. In addition, the situations that trigger rules 1 and 7 are less likely to happen than others, slowing down the convergence of the algorithm for those rules. Regarding the rule 1, the algorithm converges around iterations 80-90, from which the optimal policy for the FLC can be derived. It can be seen that there is clearly one candidate action better than the others for each rule, meaning that the algorithm leads to a specific set of rules ensuring the convergence of the algorithm. In addition, the convergence time (around 32 hours) is enough to solve persistent congestion problems. The operator firstly has to identify the time frames during a day in which there exists congestion. Generally, the congestion situation is also repeated every day (e.g. from Monday to Saturday) in the same locations, so that the optimization process can be performed over days. Then, the operator performs the optimization process in the target area during the congestion periods.

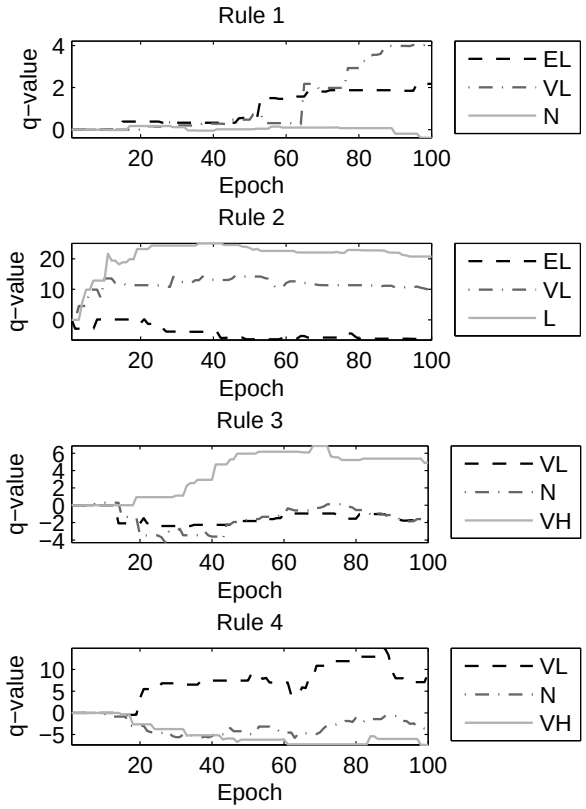

Figure 5.6: Evolution of candidate action q-values (UEE)

To compare evaluation of the three FLCs optimized by the UEE method, Fig. 5.7 and Fig. 5.8 show the temporary evolution of the global CBR and global CDR, respectively, when the optimized controller is used without the optimization module during the load balancing process (100% exploitation). Also performance of the non-optimized FLC from the first experiment is shown as a benchmark. All the simulations start from an initial situation of a global CBR close to 6% and a global CDR of 2%. After a few iterations, the network converges to a stationary state given by these indicators. The non-optimized FLC leads to the lowest CBR, but also to the highest CDR. When the FLC is optimized with a higher CDR_{th} the global CBR decreases further after load balancing, while increasing the global CDR. This is because the FLC leads to higher and lower values of HOMs in some adjacencies, so that the cell service area suffers larger variations. Regarding the CBR in Fig. 5.7, the final values are 3.5, 3.1 and 2.4% when CDR_{th} is 0.06, 0.10 and 0.15, respectively. The optimization process also has an impact on the speed of the adaptation process. When $CDR_{th} = 0.15$, the FLC achieves stationarity faster, as higher changes in HOMs are performed by the FLC (action of rules 2 is VL instead of L). In particular, stationarity in CBR is achieved around iteration 25 (9.58 hours), while the fall time (time required for the response to rise from 10% to 90% of its final value) is equal to 4.98 hours. In the case of $CDR_{th} = 0.06$ and $CDR_{th} = 0.10$, the slope of the CBR transient response is very similar (action of rule 2 is L for both cases), but stationarity is achieved before when $CDR_{th} = 0.06$ because its final value is higher. In particular, stationarity in CBR is achieved around iteration 35 (13.4 hours) and 38 (14.5 hours), and the fall time is 6.52 and 8.43 hours when CDR_{th} is equal to 0.06 and 0.10, respectively. The same reasoning could be applied to the evolution of CDR, shown in Fig. 5.8. As it can be observed, there is no overshoot or oscillation in the temporary response of these performance indicators. Note that most of the congestion is relieved in 10-12 hours, so that slow temporary changes (e.g. in the order of days) could be managed by the FLC.

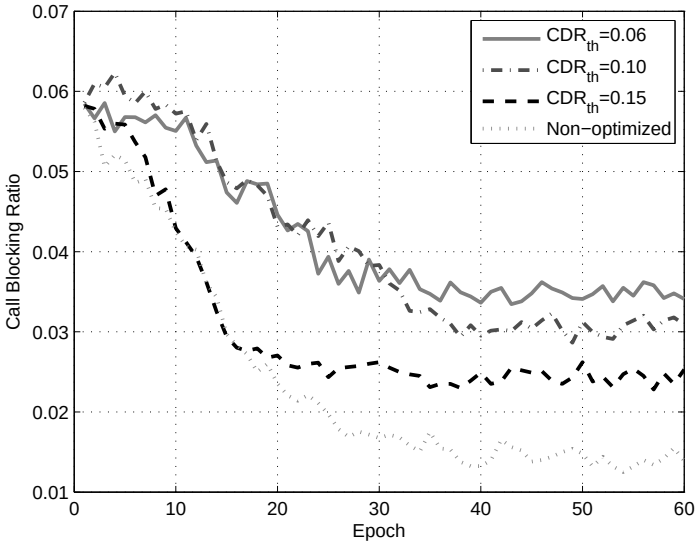

Figure 5.7: Temporary evolution of the CBR

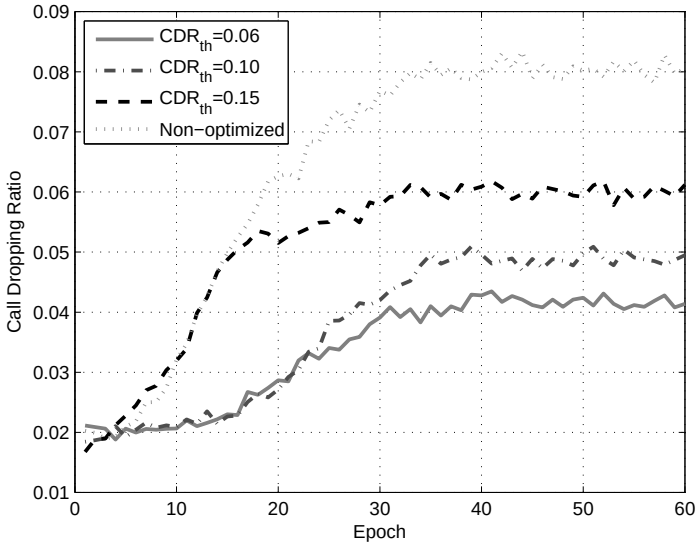

Figure 5.8: Temporary evolution of the CDR

To analyze the impact on the HO procedure, the evolution of the HOM and the number of HOs per epoch in a specific adjacency (cells 31 and 32) for two cases of UEE method ($CDR_{th} = 0.10$ and $CDR_{th} = 0.15$) are shown in Fig. 5.9 and Fig. 5.10, respectively. This adjacency is located close to the congestion situation, so that the HOM will be adjusted as part of the load balancing process. As expected, adaptation of HOM is faster when CDR_{th} is set to 0.15, because the consequent for rule 2 (rule 8) is VL (VH) instead of L (H). The impact on HOs is that the number of outgoing calls from cell 32 to cell 31 is higher than the number of incoming call to cell 32 from cell 31 after the load balancing because the algorithm attempts to offload cell 32.

The optimization process greatly simplifies the selection of fuzzy rules when the network operator imposes a GoS constraint related to the call maintainability, typically in the CDR. By adjusting the CDR_{th}, the network evolves to a new state with different trade-off between global CBR and CDR. Table 5.5 shows the evaluation of the utility function, U, for the three optimized FLCs and the non-optimized FLCs (mean and 95% confidence interval (CI) are shown). The best FLC configuration is the one with the lowest value of U (i.e. the lowest user dissatisfaction), corresponding to the FLC optimized with $CDR_{th} = 0.06$. It is noted that optimizing the FLC with a CDR_{th} lower than 0.06 leads to negative action q-values, as reinforcement signal rewards with negative values most of the time. In this case, finding the optimal fuzzy rules becomes a complicated task because all rules present similar q-values. Thus, the minimum value for U is achieved when the FLC is optimized with $CDR_{th} = 0.06$. As this configuration brings out a good trade-off between performance indicators, additional results are shown below for $CDR_{th} = 0.06$. Firstly, the CBR per cell is depicted in Fig. 5.11. The row of bars at the back corresponds to the initial situation of load imbalance, while the row of bars in the front corresponds to the end of a simulation after load balancing. It is observed that there are cells with high CBR and others with negligible CBR at the beginning of the simulation. The traffic load is shared between cells after load balancing and CBR is more equalized than the initial situation. For instance, the CBR

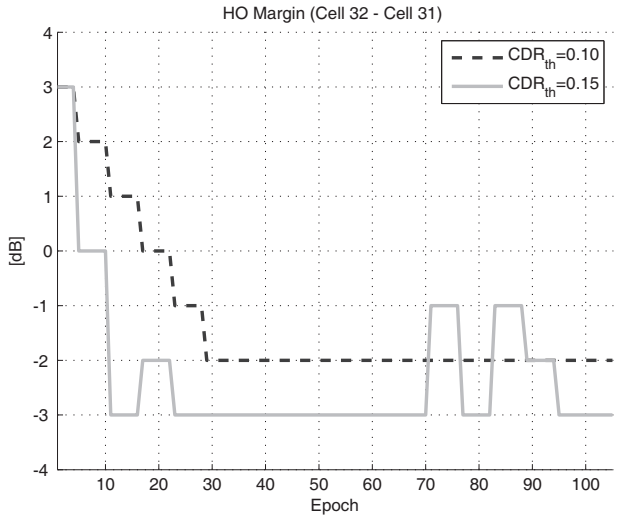

Figure 5.9: Evolution of the HOM in an adjacency for different values of CDR_{th}

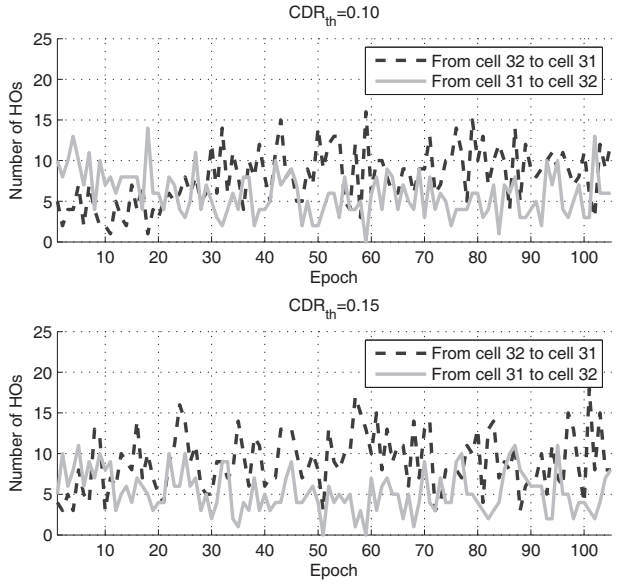

Figure 5.10: Evolution of the number of HOs in an adjacency for different values of CDR_{th}

in cells 33 and 40 is decreased from approximately 20% to 7%. This means a reduction of 65% in those highly congested cells. The CDR per cell is represented in Fig. 5.12, where both the initial and final situation are also shown. As the service area is greatly decreased in congested cells, the users connected to these cells are very close to the base station, experiencing good quality. Thus, the CDR measured in those congested cells (e.g. cells 33, 39 and 40) is decreased after load balancing. In the case of less loaded cells, the CDR is increased as they receive users from congested cells in worse quality conditions. Such an increment means a greater proportional increase taking into account that these cells have a low number of users and receive many users from congested cells.

The next experiment analyzes the BEE optimization approach, where the FLC is used

Table 5.5: Utility function for different values of CDR_{th}

CDR_{th}	CBR (mean)	CBR (95% CI)	CDR (mean)	CDR (95% CI)	U
0.06	3.48%	[3.45, 3.51]	4.17%	[4.14, 4.21]	7.5%
0.10	3.06%	[3.02, 3.10]	4.89%	[4.84, 4.93]	7.8%
0.15	2.43%	[2.40, 2.46]	6.01%	[5.97, 6.04]	8.2%
non-opt	1.44%	[1.40, 1.49]	8.04%	[7.98, 8.09]	9.3%

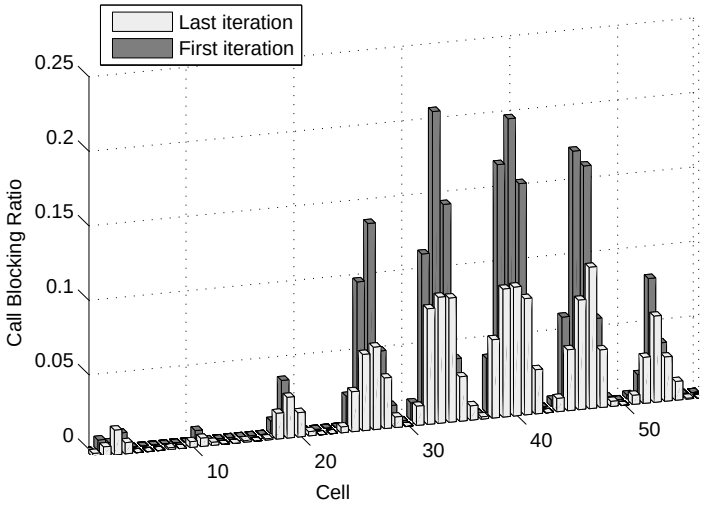

Figure 5.11: CBR per cell using the FLC optimized by UEE

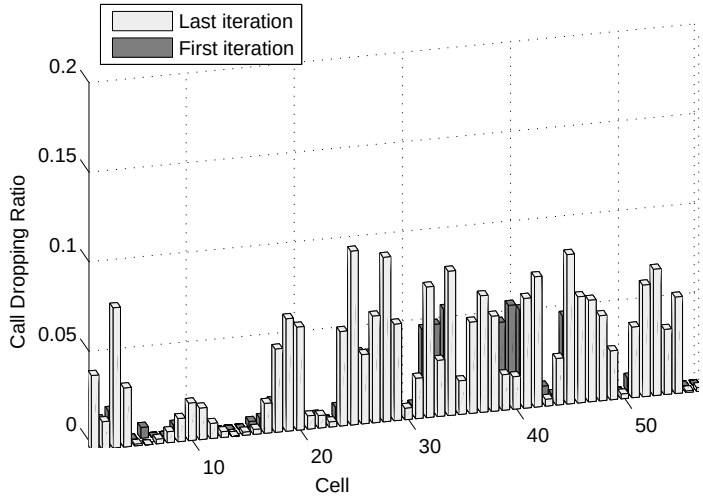

Figure 5.12: CDR per cell using the FLC optimized by UEE

starting from an unbalanced traffic distribution and the fuzzy rules are progressively modified to obtain more reward according to the reinforcement signal. The parameter ϵ is set to 0.2 in order to keep a trade-off of 20% exploration and 80% exploitation. In this case, the best action is executed most of the time and load balancing can be performed while call quality is preserved according to the specific value of CDR_{th}. Fig. 5.13 represents an example of the q-value evolution for each consequent of the rules 1-4 when $CDR_{th} = 0.06$ and $\epsilon = 0.2$. As it can be observed, the Q-Learning algorithm only needs 35-40 epochs to find the best action and use it most of the time, since low degree of exploration has been adopted. Considering that the best fuzzy rules are those receiving the highest q-value, the optimal configuration obtained from this last simulation is similar to that derived from the UEE approach with $CDR_{th} = 0.06$ and $\epsilon = 1$. This conclusion is drawn from comparing the rule base of the two approaches, where all rules of both FLC configurations match except rule 7, whose consequent is VH in the case of UEE approach and EH in the BEE approach. Such a matching suggests that both UEE and BEE optimization achieve similar system performance. The following paragraphs compare performance of the proposed methods.

In summary, Fig. 5.14 shows the performance of the proposed methods in terms of the

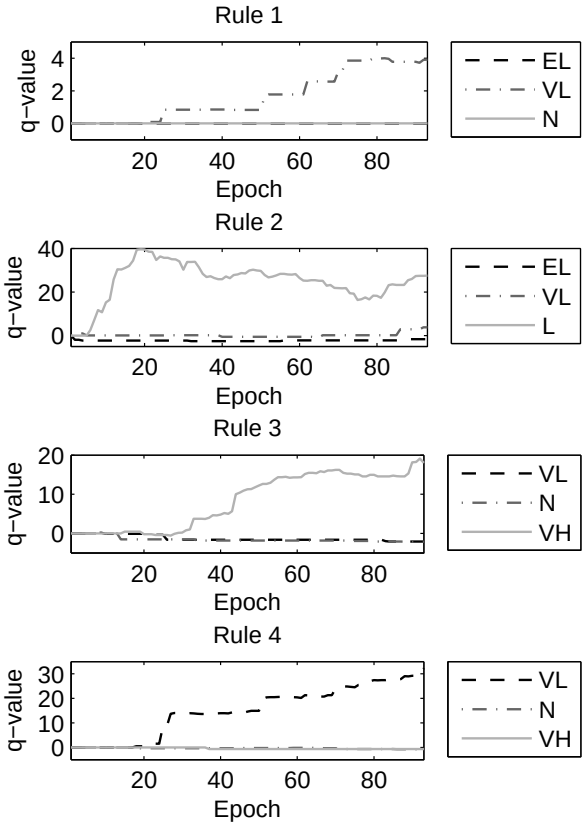

Figure 5.13: Evolution of candidate action q-values (BEE)

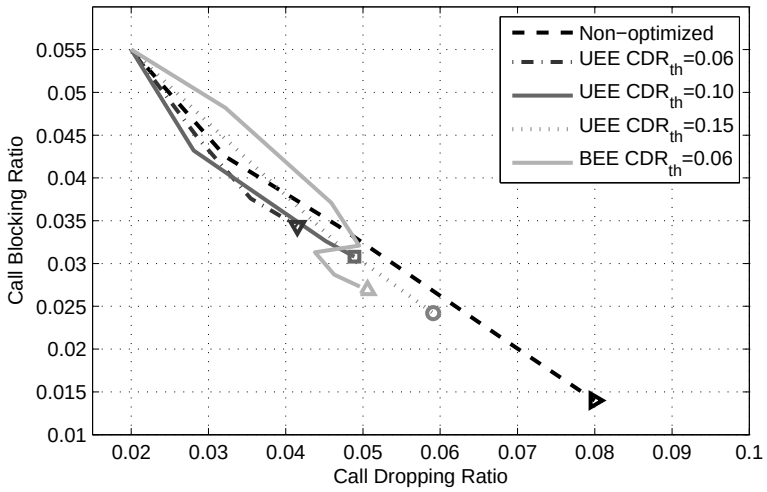

Figure 5.14: Performance of the proposed methods

global CBR and global CDR. All the simulations start from the same network state and evolve to a different state corresponding to the end of the simulation and represented by a specific symbol in Fig. 5.14. Each curve represents the intermediate states in which the HOMs are dynamically modified according to the FLC behavior. It is observed that all methods reduce CBR by increasing CDR. However, the non-optimized approach leads to an excessive CDR, highlighting the need of optimizing the FLC. Using the FLCs optimized by the UEE method, the increase in CDR can be controlled depending on the network operator constraint set by CDR_{th}. Increasing CDR_{th} leads to a higher value of global CDR, but still far from the non-optimized case. In the case of the BEE approach, non-optimal actions are explored during the load balancing process, so that the trajectory followed by the FLC is slightly worse in terms of CDR. In addition, exploration leads to small oscillations in performance once the load balancing is performed, as shown in Fig. 5.14. The utility function, U, takes the value 7.7% when BEE is performed with $CDR_{th} = 0.06$, showing that it is not a better solution than applying UEE for the same value of CDR_{th} ($U = 7.5\%$ was obtained in that case), but close to it.

The major benefit of the BEE approach is that it can be applied in any scenario without a previous (UEE) optimization phase, which usually requires the use of simulation tools. For instance, suppose that the traffic load of the scenario now is lower than in the previous simulations. More precisely, the average traffic load is set to 60% instead of 75%. Likewise, the network operator desires to keep the same quality constraint given by $CDR_{th} = 0.06$. The UEE optimized FLC with $CDR_{th} = 0.06$ would not fully exploit the FLC because the scenario now is different (i.e. the FLC would not be optimized for that traffic condition, but for the previous one). In the case of the BEE optimization approach, the FLC would select new optimal actions leading to a lower value of CBR and speeding up the load balancing process while preserving the same constraint in CDR. For instance, optimal consequent EL is selected for rule 1 instead of VL, VL is selected for rule 2 instead of L, and Z is selected for rule 3 instead of VH. Fig. 5.15 shows that the decrease in the global CBR produced by BEE is faster and greater than that

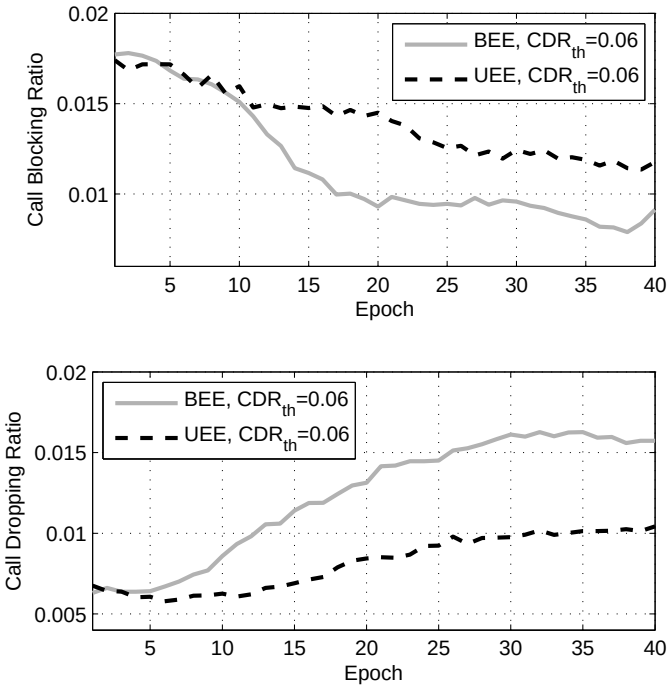

Figure 5.15: Comparison between BEE and UEE methods

produced by UEE, assuming that the increment in the global CDR is allowed by the operator, according to the defined CDR_{th}. The values of the global CBR achieved after load balancing are 0.7% (BEE) and 1.3% (UEE), while the global CDR takes a value of 1.6% and 1.0%, respectively. Both cases, BEE and UEE, share the same value of the utility function, $U = 2.3\%$. However, the BEE takes advantage of the fact that the local CBR decreases faster and further in the highly congested cells, where the traffic density is higher, leading to a more homogeneous distribution of the CBR in the scenario.

Although UEE optimization is only fully exploited when the scenario is identical to that used for optimization, it has the advantage of being easily implemented in a distributed way if all the adjacencies independently modify their HOMs. In contrast, the only way to perform BEE optimization is by using a centralized approach, because all the adjacencies share the same table of action q-values. Finally, it should be pointed out that all optimized methods do not use values of HOM higher than 9 dB, while the non-optimized FLC reaches values up to 18 dB.

5.3 MLB algorithms for voice service in enterprise femtocells

In this section, the potential of different load balancing techniques to solve localized congestion problems in enterprise LTE femtocells is investigated. Firstly, two FLCs designed in [73] are implemented for load balancing based on modifying the transmit power (TXP) and HOMs of a cell and its neighbors. Secondly, due to the fact that performance achieved by the FLCs is

limited, two Fuzzy rule-based Reinforcement Learning Systems (FRLS) based on the Q-Learning algorithm are proposed for load balancing. Thirdly, we propose to jointly use FLCs and FRLS in order to obtain the advantages of both approaches. The thorough combination of these techniques has led to different load balancing strategies which have been assessed and compared. The main contribution of this work is the proposal of an efficient mechanism for load balancing combining both the rapid response of FLCs and the improvement in performance due to the RL systems. An important issue not addressed enough in the literature is the degradation of the connection quality when the users are handed over to a worse cell at the expense of relieving the congested cell. In this work, the proposed Q-Learning algorithm considers both QoS and GoS performance indicators to solve this problem. In addition, assessment of the proposed techniques is carried out in an extreme, albeit realistic, enterprise femtocell scenario by using a dynamic system-level LTE simulator. Unlike [73][11], learning techniques are applied in this work to significantly increase performance.

The rest of the section is organized as follows. Firstly, the load balancing problem in enterprise femtocells is formulated, including the main system measurements and network parameters. Secondly, some existing self-tuning schemes are presented. After this, the design of the proposed self-optimizing schemes is described. Finally, the simulation results are discussed.

5.3.1 Problem formulation

To cope with the growing traffic demand of new services, HetNets are an attractive solution based on integrating multiple RATs, small cells and distributed antenna systems. As a result, high data rates and low latencies are provided to the end user. Femtocells are small cells whose role in HetNets is essential due to its effectiveness for increasing capacity and coverage in indoor environments [61]. Those small cells are low-power base stations using cellular technology in licensed frequency bands aimed at providing voice and data services over internet-grade backhaul under operator management. From the operator perspective, massive femtocell deployment enables to reduce the amount of traffic carried by macrocells, which should be intended for outdoor moving users. In this sense, operational and CAPEX associated to conventional macrocell sites and their backhaul network could be significantly reduced.

Most of the tasks involved in the installation, operation and maintenance of femtocells have to be done in an automatic manner, since the customer cannot be assumed to have the knowledge necessary to manage femtocells. For this reason, SON [4] is a key concept for femtocell management, where a set of principles and concepts are defined for automating network management while improving network quality.

In addition, many challenges arise from deploying femtocells in enterprise scenarios. For example, those scenarios often include three-dimensional structures, unequal distribution of traffic load is very common (e.g. crowded/uncrowded offices), the user mobility pattern is different (probably more intense) than at home and open access is usually employed instead of closed access. Thus, further study of load balancing in enterprise scenarios is necessary.

Unlike macrocell deployment, femtocells do not require thorough network planning, since they are low-cost nodes that can be relocated by the user. Thus, strategies such as uniformly distributing femtocells in an office building are expected to be a reasonable solution. However, each company or department in the building could have a different traffic demand, which usually changes over time (e.g. companies expand their staff, crowded offices, new companies move to the office building, etc.), so that the matching between the spatial distribution of traffic demand and network resources is rarely the optimal. The load balancing techniques proposed in this work aim to automatically relieve localized congestion problems due to an unequal spatial distribution of traffic demand. As a result of a better resource usage, the total traffic carried in the network is increased and the overall call blocking probability is decreased, provided that more user are accessing to the system.

Typically, load balancing techniques are based on modifying cell service areas in order to reduce or increase the traffic served by a cell. Shrinking a cell service area decreases the traffic carried in that cell by enlarging the service area of neighboring cells, provided that enough cell coverage overlapping exists. Re-sizing service areas can be easily achieved by adjusting mobility parameters, such as those used in the cell reselection or in the HO algorithm. The HO process allows user mobility across the network while the user is in connected mode. The HOM is a parameter used in the HO triggering condition to favor or penalize a neighboring cell. In LTE, the A3 event is typically used for triggering intra-system HOs. The condition for this event is equivalent to (5.1), which has to be fulfilled for a specific time period, given by the parameter TTT [35]. In addition, the service area of a cell can be modified by adjusting the transmit power, TXP. More specifically, a higher TXP_i means higher values of $RSRP_i$, so that the dominance area of cell i would be greater. Unlike HOM, TXP is defined on a cell basis, so that all neighboring cells are equally affected by variations in the transmit power of a cell. In this work, the proposed algorithms adjust both HOMs and TXPs in LTE femtocells with the purpose of load balancing.

As mentioned before, the objective of load balancing is to match network resources with traffic demand for a better exploitation of the system capacity. Obviously, this has an impact on the GoS, which includes call accessibility and maintainability. The CBR is a performance indicator directly related to call accessibility, defined as in (4.26). Note that, as a result of load balancing, more resources are free in the congested area and CBR would be decreased.

Load balancing also has an impact on call maintainability. The Outage Ratio (OR) is a performance indicator directly related to it. Unlike the CDR, the OR can be used with other types of services (i.e. not only the voice call), which can be of interest in femtocells. The OR is defined as the ratio of unserved connection time due to temporary lack of resources (OR_s) or bad Signal to Interference-plus-Noise Ratio (SINR) of users (OR_q), with $OR = OR_s + OR_q$. To calculate OR_q, the following expression is used:

$$OR_q = \frac{\sum_{i=1}^{N_{slots}} \sum_{j=1}^{N^i_{users}} X_q(i,j)}{\sum_{k=1}^{N_{slots}} N^k_{users}}, \tag{5.8}$$

where N_{slots} is the total number of slots assignable within the measurement period of OR_q,

N^i_{users} is the total number of users with data available to transmit in the slot i and $X_q(i,j)$ is a discrete variable that takes the value 1 when the active user j in the slot i cannot be scheduled due to bad SINR (its SINR is below a threshold), and otherwise it takes the value 0. Note that a similar equation is used for OR_s. In principle, it is expected that a better resource utilization would lead to a higher call maintainability (lower OR_s). However, when modifying cell service areas, some users may not be served by the 'best' cell from the radio perspective. As a result, those users would experience worse radio conditions, jeopardizing call maintainability (higher OR_q). Although AMC in LTE partly alleviates this effect, the link adaptation capability is limited. Therefore, load balancing must be performed carefully to keep call maintainability in a satisfactory level. In this work, the proposed load balancing algorithms aim to optimize GoS by finding a good trade-off between CBR and OR_q. Note that the call admission control plays the role of ensuring a good trade-off between CBR and OR_s.

5.3.2 Optimization algorithm

FLC-based load balancing techniques

The FLCs designed in this section are extracted from the diffusive load balancing algorithm developed in [73], whose aim is to solve localized congestion problems by equalizing CBR throughout the network. In that algorithm, load balancing is achieved by tuning any of these two parameters in femtocells: HOM and TXP. The former requires defining an FLC per adjacency, whereas the latter requires one per cell. Parameter tuning is carried out periodically by the FLCs, which attempt to minimize the difference in CBR (named CBR_{diff}) between adjacent cells. More specifically, the behavior of the two proposed FLCs shown in Fig. 5.16 is the following:

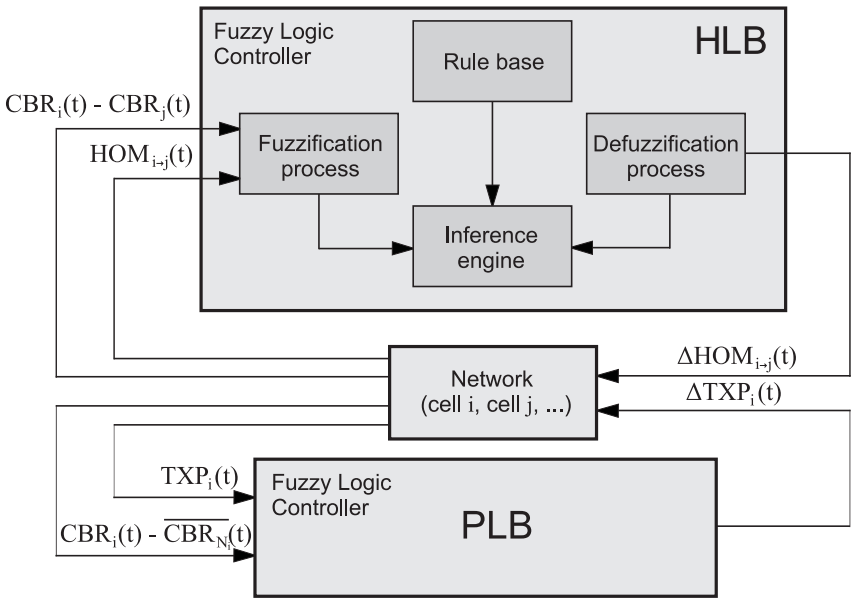

Figure 5.16: FLC scheme for HLB and PLB techniques

- *HOM Load Balancing* (HLB): the FLC adjusts $HOM_{i \to j}$ to balance the CBR between serving cell i and target cell j, where:

$$CBR_{diff}^{(ij)}(t) = CBR_i(t) - CBR_j(t). \tag{5.9}$$

  From the CBR_{diff} and the current value of HOM, the FLC calculates the change ΔHOM to be added to the HOM, that is:

$$HOM_{i \to j}(t+1) = HOM_{i \to j}(t) + \Delta HOM_{i \to j}(t). \tag{5.10}$$

  Note that changes of the same amplitude and opposite sign are performed in the symmetric margin, $HOM_{j \to i}$, to maintain the hysteresis region.

- *Power Load Balancing* (PLB): the FLC tunes TXP_i to balance the CBR of cell i against the average CBR of its neighbors, formally:

$$CBR_{diff}^{(i)}(t) = CBR_i(t) - \frac{\sum_{j \in N_i} CBR_j(t)}{|N_i|}, \tag{5.11}$$

  where N_i is the set of neighbors of cell i and $|N_i|$ is its number of neighbors. The current deviation from a reference transmit power value (e.g. maximum transmit power) is calculated as:

$$Dev_{TXP}^{(i)}(t) = TXP_i(t) - TXP_{ref}(t). \tag{5.12}$$

  Then, from the CBR_{diff} and the current deviation of transmit power Dev_{TXP}, the FLC computes the change ΔTXP to be added to the TXP, that is:

$$TXP_i(t+1) = TXP_i(t) + \Delta TXP_i(t). \tag{5.13}$$

  It is assumed that both data and pilot power are jointly tuned. For simplicity, no synchronization between neighboring cells is considered and, consequently, cell overlapping can be affected.

The previous approaches can be jointly used to improve the load balancing capability, as it can be expected that both speed and final network performance are increased.

For simplicity, the proposed FLCs are based on the Takagi-Sugeno approach [116]. In this case, the design of an FLC involves defining the fuzzy sets and membership functions of the input signals and building the linguistic rule base which determines the behavior of the FLC. Thus, the first step is to partition the input space into various fuzzy sets by means of membership functions. A membership function, denoted by $\mu_z(x)$, quantifies the degree of membership of an input value x to the fuzzy set z (this process is called *fuzzification*). Each fuzzy set has a label or linguistic term. In this work, the following labels are used: 'Very Low' (VL), 'Low' (L), 'Medium' (M), 'High' (H) and 'Very High' (VH). The fuzzy inputs of the proposed FLCs are

shown in Fig. 5.16, whereas fuzzy sets, linguistic terms and membership functions are represented in Fig. 5.17. The number of membership functions has been selected large enough to achieve a reasonable granularity in the input space, while keeping the number of states small to reduce the set of control rules. For simplicity, the selected input membership functions are triangular or trapezoidal.

Another design constraint is that a lower bound equal to -6 dB has been defined for HOM to avoid reaching very negative values, since they may cause the SINR experienced by the user to be significantly worse after the HO, increasing the risk of outage. In particular, the selected value depends on the minimum value of SINR necessary to allocate resources to the users, below which the OR would be affected. In this work, such a threshold has been set to -7 dB, according to the results shown in [140].

The rule base is formed by a set of control rules which are applied by the inference engine of the FLC to calculate the output from the input value. Rules follow a syntax of the type IF-THEN to set the control strategy, similar to the human knowledge. An example rule is the following: 'IF (CBR_{diff} is '$medium$') AND (HOM is '$very\ low$') THEN ($\Delta HOM = o$). The output function of a rule is a constant value, o, which can be one of the following values in the case of HLB (each value also has an associated label): -4 dB (VL), -2 dB (L), 0 dB (M), $+2$ dB (H) and $+4$ dB (VH). The constant values defined for PLB are: -2 dB (VL), -1 dB (L), 0 dB (M), $+1$ dB (H) and $+2$ dB (VH). The rule bases for the proposed FLCs are shown in Table 5.6. Roughly, in the case of HLB, the more positive (negative) blocking difference, the more negative (positive) margin step. The last five rules implement a slow-return mechanism to restore the default HOM value when no blocking is experienced in the network. In the case of PLB, the higher the blocking of a cell compared to its adjacencies, the higher decrease in its transmit power.

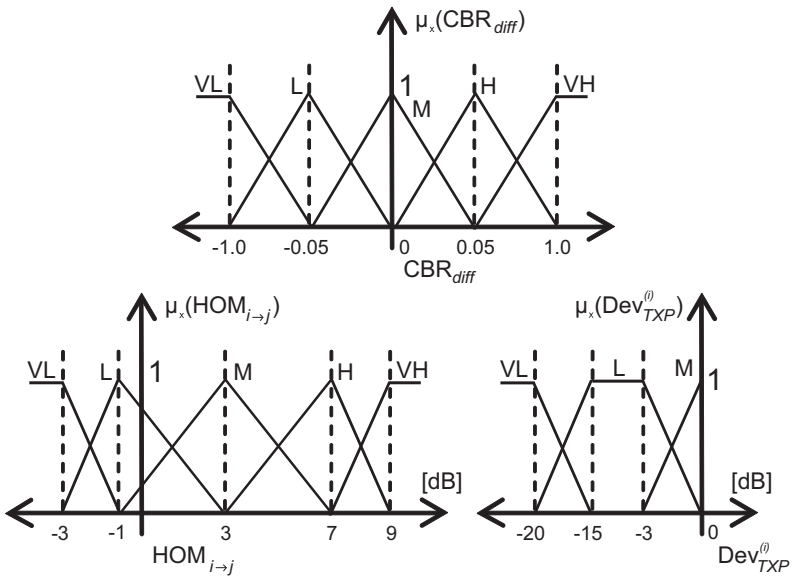

Figure 5.17: Membership functions for HLB and PLB techniques

Table 5.6: Set of fuzzy rules for HLB and PLB

$CBR_{diff}^{(ij)}$	HOM	ΔHOM	$CBR_{diff}^{(i)}$	Dev_{TXP}	ΔTXP
VH	-	VL	VH	-	VL
H	-	L	H	-	L
L	-	H	L	L	H
VL	-	VH	L	VL	H
M	VL	H	M	VL	H
M	L	H	M	L	H
M	H	L	VL	L	H
M	VH	L	VL	VL	VH
M	M	M	M	M	M

To generate the output value, the FLC firstly calculates the so-called degree of truth for each rule k, following this equation:

$$\alpha_k = \mu_x(CBR_{diff}) * \mu_y(Y), \tag{5.14}$$

where Y denotes HOM or TXP, and $*$ is the product operator related to the operation AND included in the antecedent of the rules. Once the degrees of truth are computed, the *defuzzification* process calculates the output crisp value using (5.3).

Fuzzy rule-based Reinforcement Learning systems for load balancing

The FLCs designed in the previous section integrate the knowledge necessary to perform load balancing. Likewise, performance achieved by those FLCs are limited by the knowledge transferred to them (i.e. the rule base). In this section, the designed FLCs start with no a priori knowledge. Then, they are trained with the fuzzy Q-Learning algorithm, so that the rule base is completely built from trial-and-error interactions with the network. Since knowledge is acquired directly from the environment, an increase in performance could be expected. Such FLCs teamed with fuzzy Q-Learning, whose structure is shown in Fig. 5.18, are called FRLS. As it can be observed, the input of the FLC, representing the system state $s(t)$, is the optimized network parameter, which is the HOM in the case of the proposed algorithm Q-Learning HLB (QHLB), and TXP in the case of the proposed Q-Learning PLB (QPLB). In the latter, $Dev_{TXP}^{(i)}$ also needs to be pre-calculated before the fuzzification process. The output, representing the action $a(t)$, is the increment (or the decrement) to be added to the parameter in the next optimization epoch. In this sense, the FLCs are similar to those described in the previous section, but if the signal CBR_{diff} is removed from the input side (to speed up the optimization process). The FLCs are also based on the Takagi-Sugeno approach. The input membership functions are represented in Fig. 5.19. Since only one input is defined for each FLC, the rule base needs to be redefined. In the case of the QPLB approach, the following five rules are set:

$$IF\ (Dev_{TXP}^{(i)}\ is\ very\ low)\ THEN\ (\Delta TXP_i\ is\ o_1^i), \tag{5.15}$$

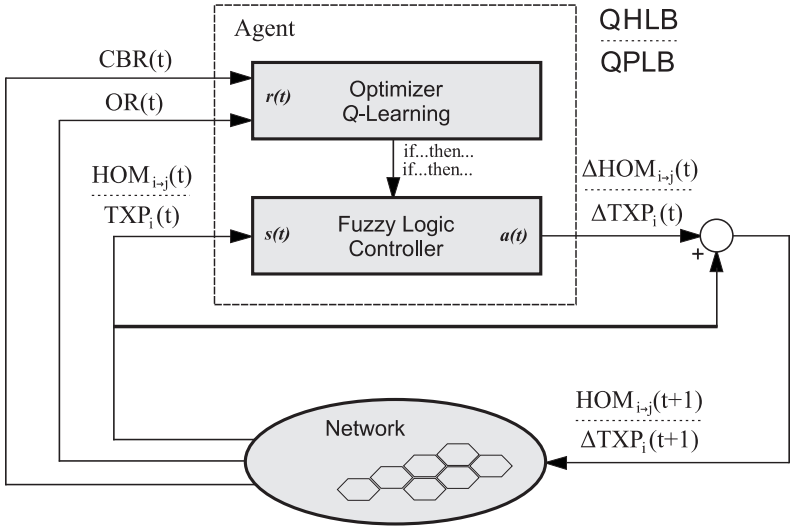

Figure 5.18: Block diagram of fuzzy rule-based RL system for QHLB and QPLB

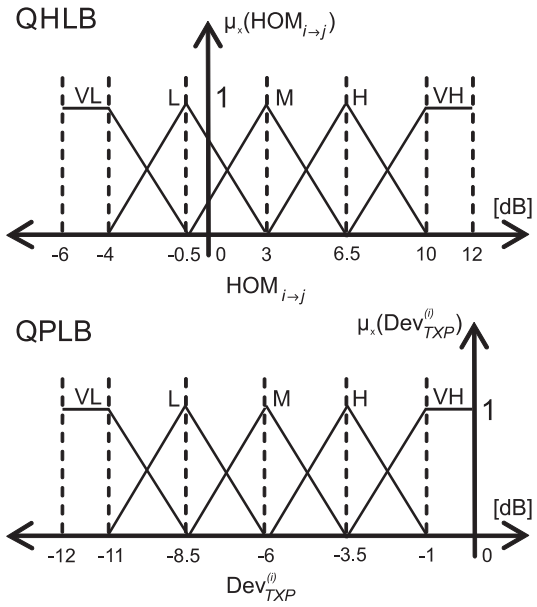

Figure 5.19: Membership functions for QHLB and QPLB techniques

$$IF\ (Dev_{TXP}^{(i)}\ is\ low)\ THEN\ (\Delta TXP_i\ is\ o_2^i), \tag{5.16}$$

$$IF\ (Dev_{TXP}^{(i)}\ is\ medium)\ THEN\ (\Delta TXP_i\ is\ o_3^i), \tag{5.17}$$

$$IF\ (Dev_{TXP}^{(i)}\ is\ high)\ THEN\ (\Delta TXP_i\ is\ o_4^i), \tag{5.18}$$

$$IF\ (Dev_{TXP}^{(i)}\ is\ very\ high)\ THEN\ (\Delta TXP_i\ is\ o_5^i). \tag{5.19}$$

Note that the consequent o_k^i of rule k applied to cell i can be either -2 dB (L), 0 dB (M) or $+2$ dB (H). The Q-Learning algorithm aims to find the optimal consequent for each rule during the optimization process. In the case of QHLB, analogous rules are defined by changing TXP by HOM. In this case, the consequent $o_k^{i \to j}$ of rule k applied to adjacency (i, j) can be either -3 dB (L), 0 dB (M) or $+3$ dB (H).

The reinforcement signal $r(t)$ (or immediate reward) shown in Fig. 5.18. has been defined as follows:

$$r(t) = k \cdot (U(t) - U(t-1)), \tag{5.20}$$

where k is a constant factor and $U(t)$ is a utility function including KPIs to be maximized. The former implies a simple scaling operation, while the latter sets the objective of the optimization process. The reinforcement signal $r(t)$ has been selected as the difference of U between two successive optimization epochs, since $r \geq 0$ would mean that the performed action was good and, otherwise, the action was bad. The negative value of $r(t)$ (action is penalized) may involve a decreasing evolution of the q-values. Thus, an optimal action (given by the highest q-value) could stop of being optimal although other candidate actions do not increase their q-value. This means that optimal actions can change along the time even if exploitation is set to 100% (other actions are not explored).

The utility function $U(t)$ has been defined with the objective of improving the GoS provided in the network. For this reason, both the overall CBR and the overall OR have been included in the function to enhance call accessibility and maintainability, respectively. In particular, the following expression for $U(t)$ has been defined:

$$U(t) = 1 - [CBR(t) + (1 - CBR(t)) \cdot OR(t)]. \tag{5.21}$$

This equation gives an estimation of the user satisfaction from the GoS perspective by calculating the ratio of blocked users and the ratio of unserved connection time for the accepted users.

Initially, the FLCs have no a priori knowledge, so that an exploration phase is needed to train the controllers. However, certain exploitation can also be maintained during this phase to ensure good performance in the network. In particular, the parameter ϵ determining the trade-off between exploration and exploitation has been set to 0.3 in order to keep only 30% exploration. After this time, the consequent whose q-value is the highest for each rule has to be used in the so-called exploitation phase. In this work, ϵ has been set to 0 during this phase (100% exploitation).

Unlike the FLCs designed in the previous section, the FLCs implemented here cannot be used independent of the Q-Learning module because there is no a priori knowledge. For this reason, they are conceived as a single entity called FRLS. As a result, these fuzzy systems have to be particularized for each cell or adjacency, because the FLC configuration will be different for each one. Another implication is that, to accurately evaluate the FLC action, only one agent

(FRLS) performs an action at each optimization epoch, so that the agents do not interfere each other. Of course, if two agents were far enough in the network, they could operate in parallel.

5.3.3 Simulation setup

Since analytical models require a high degree of complexity to provide realistic results, the dynamic system-level simulator explained in Chapter 4 has been used for assessing the proposed load balancing algorithms [11]. The simulated scenario consists of an office building with femtocells in a larger scenario of 3 x 2.6 km^2 in which a single macrocellular tri-sectorized site is deployed, as shown in Fig. 5.20. The smaller square represents the building, while the bigger one displays the area under study. The surrounding macrocells refer to the wrap-around technique implemented to avoid border effects. As it can be observed, possible interaction between macrocells and femtocells is taken into account. Propagation models are drawn from those of the Winner II project [162]. Shadowing is modeled by a spatially-correlated log-normal distribution with different standard deviation for indoor and outdoor users. Fast-fading is modeled by the Extended Indoor A (EIA) model for indoor users [163]. The building is composed of three floors, each of which includes four femtocells, whose locations are pre-fixed as shown in Fig. 5.21. To identify the femtocells in this work, they have a number associated. The layout of the floors is depicted in Fig. 5.21, where the circles represent femtocell positions, lines are walls, and small diamonds are working stations. A random waypoint mobility model is implemented for indoor users, but movements between floors are not considered. All adjacencies are considered for HO purposes inside the building. Traffic demand inside the building is unevenly distributed in order to generate the need for load balancing. In particular, the area close to femtocell 5 is very congested (high traffic demand), whereas the rest of the building has a low traffic demand. To ease the analysis, a constant-bit-rate service is provided to the users. The simulator also includes common RRM features, such HOs based on 'A3' and 'A5' events, Directed Retry (DR), cell reselection and scheduling. Finally, the main simulation parameters are summarized in Table 5.7. Note that a smaller epoch time than 30 min is not recommended because it could lead to unreliable statistics, especially in the CBR, as the number of samples obtained during that period would not be large enough to produce a reliable value. In addition, those errors due to unreliable statistics are accumulated by the Q-Learning algorithm during the learning process, affecting the convergence time.

The following assumptions are made for the proposed techniques. HLB and PLB are applied to all femtocell adjacencies and femtocells, respectively, simultaneously in the scenario. However, the algorithms based on Q-Learning, QHLB and QPLB, are only applied in relevant cells (those close to the congested area), and they are sequentially executed (only one action is performed per epoch). In particular, QHLB is applied to adjacencies (5,6), (5,7) and (5,8), since those cells are the closest to femtocell 5. In the case of QPLB, the algorithm is applied to femtocell 5 and the two closest, 6 and 8. The reason for choosing such a low number of agents is to achieve convergence faster. As agents need to be sequentially executed to accurately evaluate FLC actions, a high number of agents would need excessive time to find the optimal solution.

Load balancing techniques are assessed along 80 optimization epochs, each representing 30

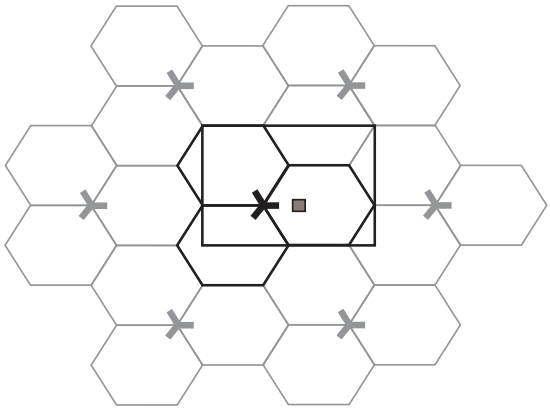

Figure 5.20: Macro/femtocell scenario

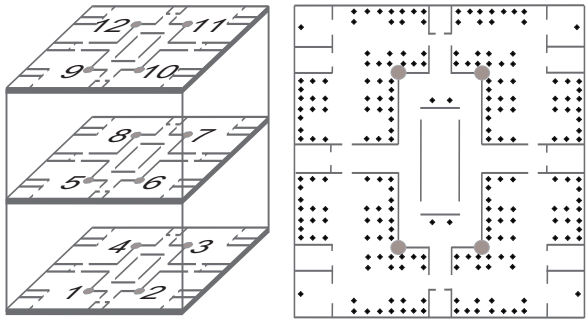

Figure 5.21: Femtocell locations and floor layout

minutes of network time. The duration of each loop is long enough to ensure robust performance statistics, while the number of epochs should ensure that the system reaches the steady state. The following paragraphs describe the proposed strategies for load balancing based on different combinations of the developed FLCs and FRLSs to overcome the limitations of individual approaches:

- *HLB&PLB*: both HLB and PLB are executed simultaneously at each epoch during the simulation.
- *HLB&QPLB*: both HLB and QPLB are alternatively executed during the simulation (at time t: HLB, $t+1$: QPLB, $t+2$: HLB, etc.).
- *QHLB&PLB*: both QHLB and PLB are alternatively executed during the simulation.
- *HLB&PLB–HLB&QPLB*: the strategy *HLB&PLB* is enabled only for the first 7 epochs, and *HLB&QPLB* is then activated for the rest of the simulation.
- *HLB&PLB–QHLB&PLB*: the strategy *HLB&PLB* is enabled only for the first 7 epochs, and *QHLB&PLB* is used hereafter.

All the proposed techniques including Q-Learning keep 30% exploration ($\epsilon = 0.3$) up to epoch 60, and then 100% exploitation ($\epsilon = 0$) is set. Note that the strategy $QHLB\&QPLB$ has not been included, since it is expected that this approach would require too much time to converge.

Table 5.7: Simulation parameters

Parameter	Configuration
Transmission direction	Downlink
Carrier frequency	2.0 GHz
System bandwidth	1.4 MHz
Frequency reuse	1
Propagation model	Indoor-indoor: Winner II A1
	Indoor-outdoor: Winner II A2
	Outdoor-outdoor: Winner II C2
	Outdoor-indoor: Winner II C4
Base station model	EIRP: 13 (femto) / 43 (macro) dBm
	Directivity: omni (femto) / tri-sector (macro)
	Access: open access (macro/femto)
Mobile station model	Noise figure: 9 dB
	Noise density: -174 dBm/Hz
Traffic model	Calls: Poisson (avg. 0.43 calls / user · h)
	Duration: exponential (avg. 100sec)
Traffic distribution	Unevenly distributed in space
Mobility model	Outdoor: 3 km/h, random direction & wrap-around
	Indoor: random waypoint
Service model	Constant-bit-rate, 16 kbps
Scheduler	Time domain: Round-Robin
	Frequency domain: Best Channel
Power control	Equal transmit power per PRB
Link Adaptation	Fast, CQI based, perfect estimation
Access control	Directed Retry ($DR_{threshold}$=−44 dBm)
Cell Reselection	Criteria S, R
Handover	Events A3, A5
Q-Learning algorithm	Discount factor: $\gamma = 0.95$
	Learning rate: $\eta = 0.1$
	Reinforcement signal: $k = 100$
Time resolution	100 TTI (100 ms)
Epoch time	30 minutes

5.3.4 Performance results

Performance assessment methodology

To compare the proposed algorithms, several indicators have been defined. Firstly, to estimate the GoS degradation in the network, the User Dissatisfaction Ratio (UDR) is calculated following a similar expression as $U(t)$ in (5.21), but expressed in the opposite sense, that is:

$$UDR(t) = CBR(t) + (1 - CBR(t)) \cdot OR(t). \tag{5.22}$$

This indicator estimates the user dissatisfaction due to blocked users and unserved connection time when the users have been accepted.

To evaluate the transient response, an infinite-horizon discounted model [164] is considered. In this model, the *overall penalty* of a trajectory, P, is calculated as:

$$P = (1-\delta)\sum_{t=0}^{\infty}\delta^t \cdot UDR(t), \tag{5.23}$$

where δ is a discount factor, fulfilling $0 \leq \delta \leq 1$. As it can be observed, the model is a weighted average of single penalties, UDR, across loops, where future penalties are given less importance according to a geometric law with δ. Typically, in live environments, early penalties are more important than delayed penalties, since congestion situations might vary along the time. To avoid an infinite number of epochs and also to reduce the computational effort, it is assumed that equilibrium is reached after h epochs. Thus, the overall penalty is calculated as:

$$P \approx (1-\delta)\sum_{t=0}^{h-1}\delta^t \cdot UDR(t) + \delta^h \cdot UDR(h). \tag{5.24}$$

The selected horizon should be large enough to ensure that the system has reached equilibrium. Hereafter, $\delta = 0.95$ and $h = 25$.

Another interesting indicator is the cell load, defined as:

$$load_i = \frac{\sum_{k=1}^{N^i_{users}} N^i_k}{N_{total}}, \tag{5.25}$$

where N^i_k is the actual number of PRBs occupied by user k connected to cell i, N^i_{users} is the number of users in cell i and N_{total} is the total number of PRBs. Note that accessibility could be improved by equalizing load between cells, but the relation between CBR and cell load is limited. For instance, full accessibility in the system (i.e. $CBR = 0$) could be achieved with partial load equalization. Finally, an important measurement from the operator perspective is the HO Ratio (HOR), defined by the ratio between the number of HOs and carried calls, as an estimation of network signaling load.

Simulation results

Assessment of the transient response.

Firstly, the evolution of the transient response for each proposed strategy has been depicted in Fig. 5.22, where the x-axis and the y-axis correspond to the CBR and the OR, respectively. All the simulations start from the same starting point, given by CBR=12.69% and OR=1.02%.

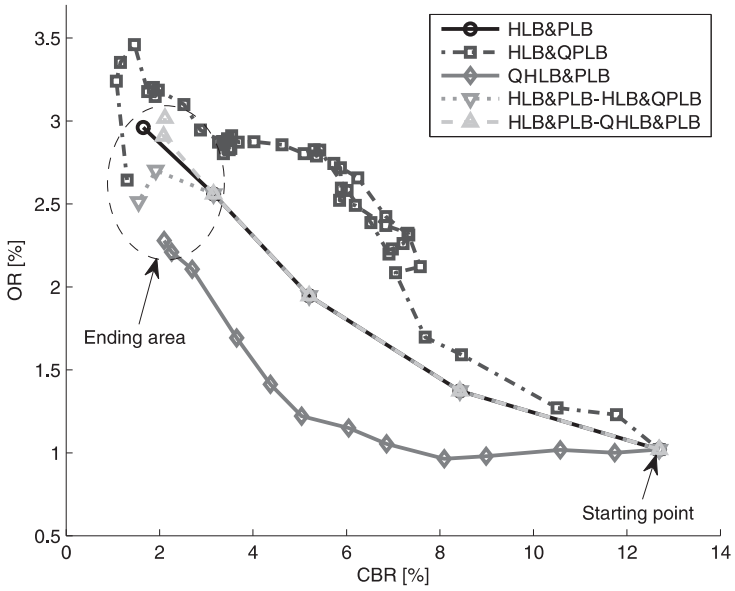

Figure 5.22: The transient response of the proposed strategies

From this point, each strategy evolves drawing a different path in the map. Each point in the curves represents a different network parameter configuration reached by the tuning process, which is determined by the HOM and TXP settings at a specific epoch. The dashed circle on the upper-left includes the ending point for all the strategies. Such an ending point is the first point in the steady state. For better readability, the remaining points in the steady state have not been depicted in the figure. Note also that those strategies starting with *HLB&PLB* share the same path during the first epochs because the same technique is being applied during that time.

The first strategy, *HLB&PLB*, is characterized by implementing only FLCs (without learning techniques). As observed, the response of this approach is very fast, since a learning stage is not necessary. Thus, most of the user dissatisfaction in terms of CBR is relieved at epoch 5. The remaining strategies are all based on the Q-Learning algorithm. In general, those strategies lead to better performance (the bottom of the dashed circle in the figure) because *HLB&PLB* tunes both HOMs and TXPs in the same direction (i.e. decreasing CBR) so that the degree of exploration is significantly low and typically, suboptimal solutions are obtained. Conversely, when Q-Learning is applied, more epochs are typically needed to achieve good performance. In this sense, the worst case is *HLB&QPLB*, which needs around 40 epochs to achieve the ending area. In the case of *QHLB&PLB*, a lower number of epochs than *HLB&QPLB* is needed to relieve most of the congestion. The reason for this is because the network is more sensitive to TXP than to HOM. As a result, CBR is decreased faster by the strategy including PLB (no learning) than the one including QPLB. In addition, not only the steady state is achieved faster by *QHLB&PLB* rather than *HLB&QPLB*, but also the trajectory (i.e. the transient response) drawn on the map is better, since it is closer to the origin of the graph.

The previous analysis highlights that FLCs are techniques with fast response time but

they usually reach suboptimal solutions. Instead, learning techniques can improve performance by carrying out some exploration. Thus, the remaining strategies shown in Fig. 5.22, that is *HLB&PLB−HLB&QPLB* and *HLB&PLB−QHLB&PLB*, include FLCs at the beginning to obtain a fast response, so that most of the call blocking is relieved at epoch 5. Then, they switch to a different technique including Q-Learning to enhance performance. The main difference lies in this second part of the strategies, i.e. when Q-Learning is applied to the network. In particular, *HLB&PLB−HLB&QPLB* leads to lower CBR and OR, while *HLB&PLB−QHLB&PLB* evolves to worse performance, which is even worse than that achieved by *HLB&PLB*.

Finally, to quantify the results of the transient response analysis, Table 5.8 shows the overall penalty, P, together with the minimum and final UDR values for the strategies analyzed in this work. This indicator assesses the transient response regarding both the response speed and the asymptotic value. As expected, *HLB&PLB−HLB&QPLB* is the strategy which combines better these two properties, thus achieving the lowest value of P. Regarding the complexity of those strategies based on Q-Learning, note that the computational cost is negligible since the epoch period of the learning algorithm is long enough (tens of minutes) to compute all the required calculations. In addition, the memory requirements given by the dimensions of the look-up table are minimal, since this table has a small size. Finally, the implementation does not involve communication with a server, since a distributed approach has been adopted.

Assessment of the steady state.

The proposed techniques achieve the steady state when the network parameters are not (or slowly) modified along the time, meaning that the optimal settings have been found, as well as the performance indicators keep more stable. To assess the performance in the steady state, some indicators have been measured and graphically represented in Fig. 5.23. In particular, the UDR, the load standard deviation of the cells mainly affected by the congestion situation, and the HOR have been depicted for each proposed strategy. Note that the y-axis represents the relative gain with respect to the reference case, *HLB&PLB*. Regarding the UDR, note that those values are derived from applying (5.22) to the CBR and the OR values corresponding to the ending points depicted in Fig. 5.22. As previously stated, those strategies including Q-Learning to optimize TXP (i.e. *HLB&QPLB* and *HLB&PLB−HLB&QPLB*) result in better performance than other approaches, since the network is more sensitive to TXP and more exploration is performed when Q-Learning is applied. On the other hand, to calculate the load standard deviation, the traffic

Table 5.8: Penalty values for all strategies

Strategy	P	$min(UDR(t))$	$UDR(80)$
No self-tuning	0.1317	0.1264	0.1330
HLB&PLB	0.0562	0.0441	0.0488
HLB&QPLB	0.0920	0.0344	0.0396
QHLB&PLB	0.0635	0.0351	0.0351
HLB&PLB−HLB&QPLB	0.0508	0.0333	0.0374
HLB&PLB−QHLB&PLB	0.0568	0.0457	0.0492

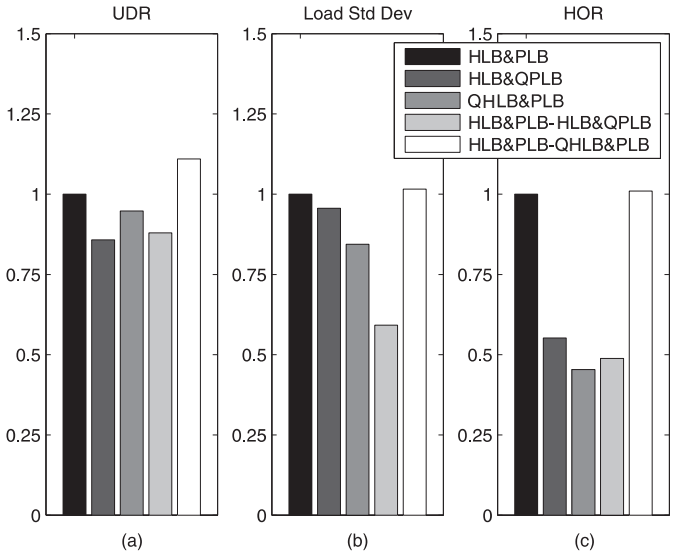

Figure 5.23: UDR, load standard deviation and HOR for proposed strategies

load of cells 1, 5, 6, 7, 8 and 9 have been considered. A lower load standard deviation means that the radio resources are more equally distributed among cells. As observed, the strategy with the lowest value is *HLB&PLB−HLB&QPLB*. Finally, the HOR estimates the impact of the strategies on network signaling load. Such an indicator includes HOs triggered by both 3GPP 'A3' and 'A5' events, so that possible *ping-pong* HOs between these two cases are counted. The strategy *HLB&PLB−HLB&QPLB* results in significantly lower HOR compared to the reference case, and similar HOR compared to other approaches based on Q-Learning. Finally, note that *HLB&PLB−QHLB&PLB* achieves the highest value on the three indicators, meaning that this approach is not recommended.

Analysis of the self-tuning and optimization process.

To further understand some of the results previously shown, the temporary evolution of the self-tuning and optimization process are now analyzed. Firstly, the temporary evolution of the HOM and Dev_{TXP} are shown in Fig. 5.24 and Fig. 5.25. As observed, all strategies decrement the transmit power of cell 5, TXP_5, from the beginning of the simulation, but *HLB&QPLB* makes it slower due to exploration. Until epoch 40 (see also Fig. 5.22), this strategy does not achieve a value of TXP_5 small enough to relieve most of the congestion. For this reason, it is highlighted that the network is more sensitive to TXP than to HOM, especially to the transmit power of cell 5, since this cell experiences congestion.

Regarding the strategies shown in Fig. 5.24, another conclusion drawn is that HOMs reach saturation early (−6 dB) when HLB is applied to the network. If saturation was not present, achieving very negative values of HOMs would involve bad connection quality, leading to an unacceptable OR. When Q-Learning is present, $HOM_{5\to6}$ and $HOM_{5\to8}$ evolve to values which are far from saturation, since TXP_5 is further decreased. This is the main difference with *HLB&PLB*, which also means an improvement in UDR, as shown in Fig. 5.23. Finally, note that

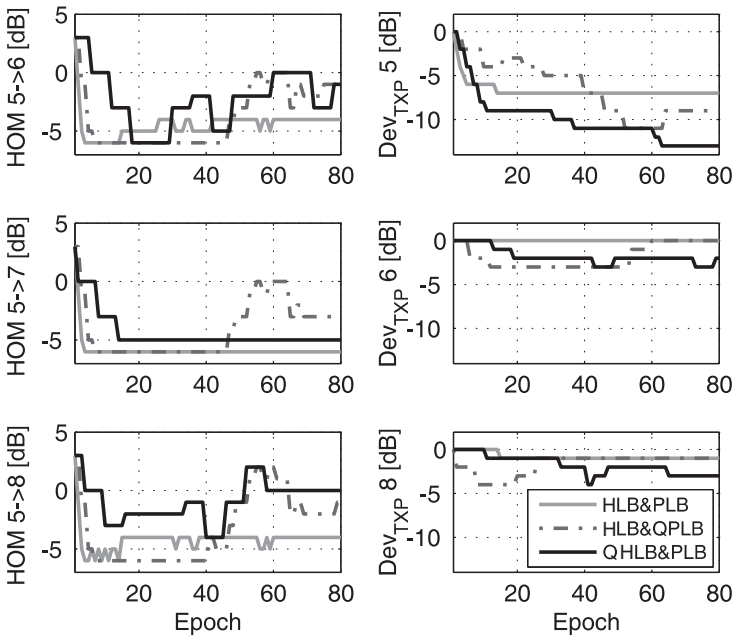

Figure 5.24: Temporary evolution of the HOM and Dev_{TXP} for single strategies

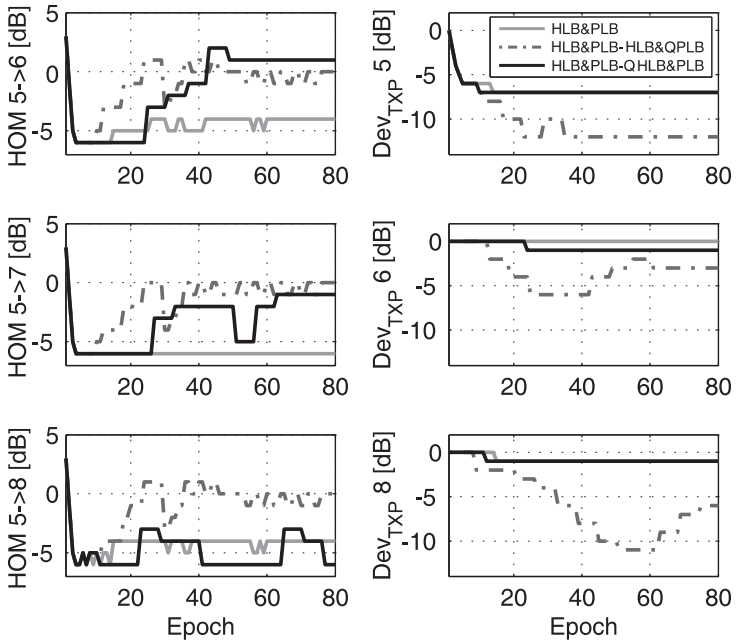

Figure 5.25: Temporary evolution of the HOM and Dev_{TXP} for combined strategies

TXP_6 and TXP_8 are close to their maximum transmit power for all strategies, which is rational from the load balancing perspective.

On the other hand, concerning the strategies shown in Fig. 5.25, note that the strategy *HLB&PLB−QHLB&PLB* continues from a value of Dev^5_{TXP} equal to −6dB after the initial stage of FLCs. As this strategy takes advantage of Q-Learning to modify HOM instead of TXP,

TXP_5 keeps suboptimal and HLB cannot find a better solution. In addition, Q-Learning leads $HOM_{5\to6}$ and $HOM_{5\to7}$ closer to the upper-bound value, but no gain in performance is obtained. The benefit of using Q-Learning here is thus hindered by the performance of PLB. In the case of *HLB&PLB−HLB&QPLB*, Q-Learning leads Dev^5_{TXP} to a lower value (−12 dB), while HLB leads HOMs to an intermediate value (∼0 dB). The main outcome of this approach is that UDR is decreased down to 3.9%.

To assess the impact of the parameter tuning on the network, the cell load of the cells mainly affected by the congestion situation is shown in Fig. 5.26. This analysis is focused on the combined strategies. As expected, cell 5 is initially close to 100% of resource utilization, while neighboring cells are less loaded. In addition, as previously stated, it is observed that the network is more sensitive to TXP than to HOM. This can be derived from the similarity in the curves between the parameters and the cell load. For instance, when *HLB&PLB−HLB&QPLB* is applied, the temporary evolution of Dev^8_{TXP} is closely linked to the load of cell 8. Regarding the *HLB&PLB−QHLB&PLB* approach, when $HOM_{5\to6}$ evolves from −3 to +2 dB, the load of cell 6 is only decreased by a 2% (from 60% to 58%), highlighting the poor relation existing between them. Note that this relation is stronger when HOM is close to the lower-bound (e.g. $HOM_{5\to6}$ and load of cell 6), but OR is highly sensitive at this point. Thus, the strategy employing Q-Learning to optimize TXP instead of HOM (i.e. *HLB&PLB−HLB&QPLB*) is more likely to improve performance. An evidence of this fact is that cell loads have a tendency to converge. It is highlighted that not only cells located in the floor suffering from congestion take part of the load balancing process, but also cells belonging to other floors (e.g. cells 1 and 9).

To estimate the impact on network signaling load throughout the time, Fig. 5.27 shows the HOR for combined strategies and reference cases. As previously stated, this indicator includes HOs triggered by both 3GPP 'A3' and 'A5' events, so that possible *ping-pong* HOs between these

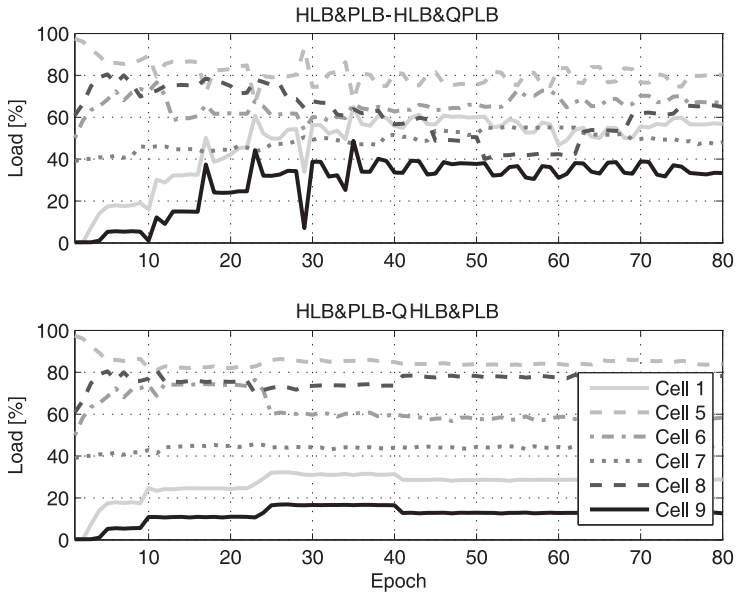

Figure 5.26: Temporary evolution of cell load for combined strategies

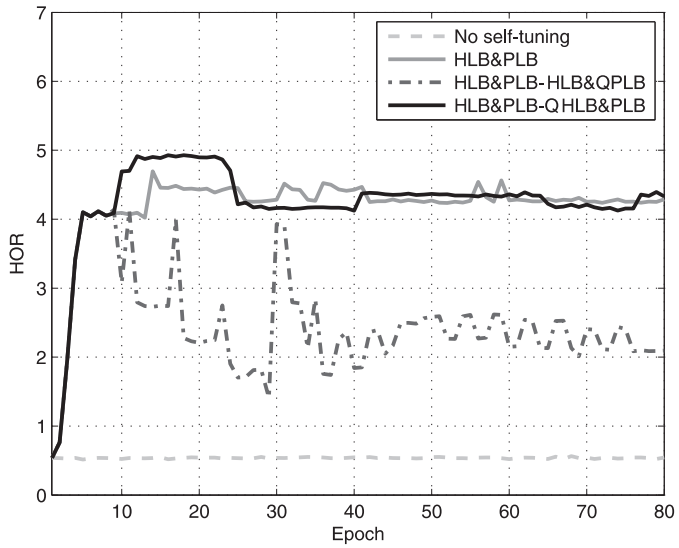

Figure 5.27: Temporary evolution of HOR for combined strategies

two cases are counted. As it is observed, *HLB&PLB−HLB&QPLB* is the strategy achieving the lowest value of HOR. Since Dev^5_{TXP} is decreased down to −12 dB and HOMs keep close to the default value (+3 dB), less *ping-pong* effect in HOs is expected. To further explain this, let consider the two overshoots in HOR around epoch 20. In Fig. 5.25, it is observed that TXP_5 is decreased by 2 dB at epochs 17 and 23. As a result, the HOR is sharply increased. However, HOMs are then increased by 2 dB at epochs 18 and 24, easing the impact of the overshoots. Thus, the strategy *HLB&PLB−HLB&QPLB* is clearly the best option from the signaling load perspective.

Once that *HLB&PLB−HLB&QPLB* has been shown as the best strategy, further analysis of this approach is covered here. Firstly, the UDR is break down into the following indicators, each of which is represented in Fig. 5.28: CBR, OR_s and OR_q. As shown, the CBR is decreased from 12.8% to 1.6%, the OR_q is increased from 0.8% to 2.1%, and OR_s keeps below 1.0%. Note that small oscillations in HOM produced by HLB (see Fig. 5.25) affect mainly to CBR. In addition, the increase in OR_q due to the fact that HOMs are close to negative values would be permitted by an operator.

Finally, Fig. 5.29 shows the temporary evolution of the q-values of each candidate action for the fuzzy rules in adjacent cells 5, 6 and 8. The q-values determine the best candidate action (i.e. the variation) to apply in TXP. Regarding cell 5, since Dev^5_{TXP} starts from −6 dB when QPLB is applied and then it is further decreased, the fuzzy rules involving high values of TXP_5 in the antecedent (rules 4 and 5) are not activated during the simulation. As a result, only candidate actions of rules 1, 2 and 3 experience changes in their q-values. The best action of those rules is mostly L (−2 dB), which means a decrease in TXP_5. For this reason, Dev^5_{TXP} is decreased down to −12 dB. A similar explanation is applied to the evolution of q-values in cells 6 and 8.

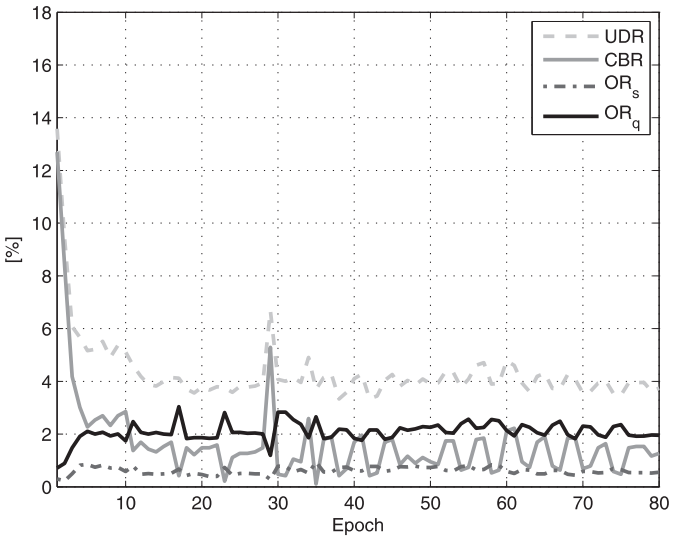

Figure 5.28: Temporary evolution of CBR, OR_s and OR_q for *HLB&PLB−HLB&QPLB* approach

5.4 Conclusions

In this chapter, the load balancing problem has been studied for two different scenarios. The first scenario consists of a macrocell environment, for which an optimized FLC for load balancing has been proposed, based on dynamically tuning HOMs. Two different optimization approaches using the fuzzy Q-Learning algorithm have been investigated. UEE approach is based on an optimization scheme that explores all the candidate FLC actions throughout the load balancing process. In this case, introducing test users into the network throughout the night or using network simulation tools are methods recommended to avoid degrading system performance when testing non-optimal actions. Once the optimal FLC configuration has been found, the FLC can be applied to the real situation. BEE is an optimization scheme that combines both exploitation and exploration to enhance performance while finding the optimal FLC actions and also to provide dynamic adaptation to system variations. The proposed methods have been compared to an FLC (with no optimization) which is used as a benchmark.

Simulations carried out in a non-uniformly distributed traffic scenario highlight that call blocking can be significantly reduced (from approximately 20% to 7% in the highest loaded cell), while at the same time keeping call dropping in neighboring cells under a certain level set by the operator. Simulation results show that the UEE optimization approach accurately preserves the call quality constraint during the load balancing by simply adjusting a call dropping threshold. It is shown that the best trade-off between CBR and CDR (given by a 7.5% of user dissatisfaction) is achieved by setting the CDR threshold to 0.06. In the case of the BEE optimization approach, performance is slightly decreased compared to UEE due to the percentage of non-optimal actions executed by the Q-Learning algorithm throughout the load balancing process (7.7% of user dissatisfaction is obtained). However, it is shown that the benefits from the BEE approach may be higher than the UEE approach because both optimization and load balancing are carried out on the same scenario at the same time, and the method can adapt to network variations.

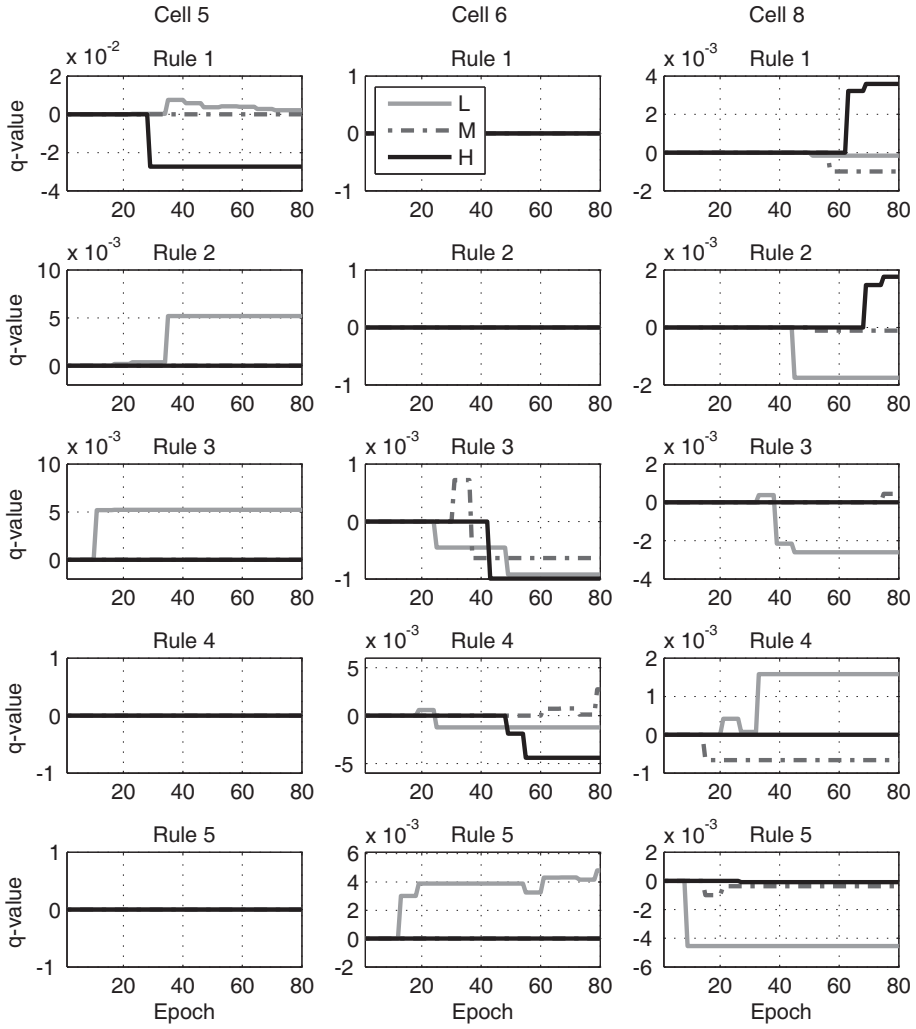

Figure 5.29: Temporary evolution of q-values for *HLB&PLB−HLB&QPLB* approach

The second investigated scenario consists of an enterprise femtocell environment, where several methods have been proposed for load balancing. These methods are based on tuning HOMs and femtocell TXP by implementing FLCs and FRLSs. Firstly, two strategies combining simultaneously FLC and FRLSs are assessed and compared to the method including only FLCs. Results show that performance in the long-term is better when the learning technique is present, but the adaptation is much slower. In particular, the strategies including Q-Learning achieve ∼4% of UDR, while the FLC-based method remains at 4.6%. However, 5 epochs are enough to relieve most of the congestion with only FLCs, while at least 12 epochs would be necessary when Q-Learning is present. Secondly, to take advantage of these strategies, they are sequentially executed to obtain both faster response and better performance in the long-term. Results show that performance is better when Q-Learning is applied to the TXP instead of HOM, since the network is more sensitive to the TXP, so that better solutions can be achieved by some exploration of the algorithm. Instead, when Q-Learning is applied to HOMs, typically suboptimal solutions are usually reached. The strategy *HLB&PLB−HLB&QPLB* has been shown as the best strategy, since it combines fast response (most of the user dissatisfaction is reduced in 5 epochs) with good

performance in the long-term (3.9% of UDR is achieved). In addition, this strategy has a lower impact on network signaling load than the reference method (around 50% reduction is obtained). Finally, note that these methods can also be applied to other scenarios with open access femtocells (e.g. airports).

Chapter 6

Mobility Robustness Optimization

The MRO is a solution whose objective is to minimize the occurrence of undesirable effects (e.g. dropped calls) due to the HO process, which is the mechanism that allows the user to freely move around the network. In this chapter, firstly, a sensitivity analysis of the two main parameters of the HO procedure, i.e. the HOM and the TTT, is carried out for different system load levels and user speeds in an LTE network. Secondly, an FLC that adaptively modifies HOMs is designed for MRO. In this case, different parameter optimization levels (network-wide, cell-wide and cell-pair-wide) as well as the impact of measurement errors have been considered. Finally, a proposal for coordination between the MLB and MRO functions designed in this thesis is also included.

Section 6.1 is devoted to the sensitivity analysis and the proposed MRO algorithm. In particular, Section 6.1.1 formulates the problem, including some aspects of the mobility management and system measurements. In Section 6.1.2, the proposed self-tuning scheme is described. Sections 6.1.3 and 6.1.4 are devoted to the sensitivity analysis and the FLC performance assessment, which are carried out based on simulations. Section 6.2 is dedicated to the method designed for SON coordination. More specifically, Section 6.2.1 explains the proposed algorithm and Section 6.2.2 describes the performance analysis. Finally, the conclusions are presented in Section 6.3.

6.1 MRO algorithm

6.1.1 Problem formulation

The significant increase in both size and complexity of current cellular networks has led to a more complex network management. For this reason, SONs has gained increasing importance in order to automate the management process and minimize the manual intervention. In the field of Self-Optimization, MRO is an important use case defined for LTE and LTE-A [43]. The

UE procedures in both idle and connected mode can be optimized to enhance user experience and to make a more efficient network resource utilization. In idle mode, no dedicated resources have been established for the UE in the radio access network and the procedure for changing of camping cell is called cell reselection. In connected mode, an HO is carried out when the UE moves between two cells to preserve the user connection. The HO is the procedure that directly affects user experience because it occurs when the UE is transmitting data packets. Due to the fact that next-generation networks, e.g. LTE, are being deployed with a frequency reuse of 1, the inter-cell interference becomes an important issue, especially in the cell-edge. Such an issue is illustrated in Fig. 6.1, where it is observed that the neighbor cell is interfering a cell-edge user in the downlink. This high interference results in dropped calls and failures related to HOs. Furthermore, sub-optimal settings of HO parameters in this situation may lead to high levels of call dropping and HO signaling load, which may result in redundant waste of network resources. Thus, the main objective of MRO should be to reduce the number of dropped calls due to suboptimal adjustment of HO parameters, while the secondary objective would be to reduce the inefficient usage of network resources due to unnecessary HOs. Finally, cell reselection parameters should be aligned with HO parameters to avoid unwanted HOs subsequent to connection setup.

In this work, the potential of adjusting HOM and TTT for HO optimization, including other factors in the analysis such as the system load and the user speed, is investigated. Firstly, a sensitivity analysis of HOM and TTT is carried out for different system load levels and user speeds. Performance is assessed by measuring the CDR and the HOR. Secondly, an FLC that adaptively modifies HOMs is proposed for HO optimization. Three different configurations of the FLC are assessed to set the optimal behavior to the proposed FLC, based on the previous KPIs, the CDR and the HOR, and regarding different system load levels and user speeds. The main contribution of this work is the performance analysis considering both HO parameters for different situations, highlighting the variation of the user speed. The impact on the GoS (e.g. call dropping and call blocking) for future services such as VoIP calls is also considered in the analysis. In addition, an FLC has been developed to optimize HO parameters, where different parameter optimization levels (network-wide, cell-wide and cell-pair-wide) have been implemented and the impact of the measurement errors has been taken into account. The main advantage of the proposed FLC is that it allows addressing numerical problems from the human

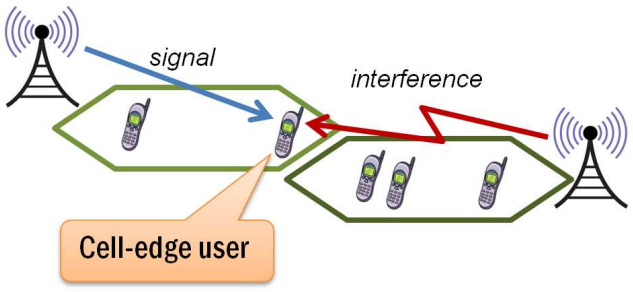

Figure 6.1: Interference problem when a frequency reuse of 1 is employed

reasoning perspective, making the translation of the network operator experience to the system control easier.

There are significant differences of the proposed scheme with respect to other existing approaches. In [15], the optimal values of the HO parameters are selected from a diagonal through the grid of HOM and TTT values, based on a previous sensitivity analysis derived from system performance simulations, thus limiting the results to the used, realistic, simulated scenario. Conversely, in this work, the proposed FLC optimizes HOM independently of the simulated scenario. Such an FLC has been thoroughly designed to provide the best response. In addition, unlike [15], the fast-fading following the 3GPP model has been considered in the simulations. This term of the received signal plays an important role in the user experience. Finally, unlike [16], the impact of the user speed has been further analyzed in this work.

Mobility management

In this work, mobility management is based on algorithms standardized by the 3GPP. In particular, the HO-triggering condition to optimize is the A3 event [35], defined as:

$$\overline{RSRP_j} > \overline{RSRP_i} + Hys + HOM_{i \to j}, \tag{6.1}$$

where $\overline{RSRP_i}$ and $\overline{RSRP_j}$ are the averaged values of RSRP measured for serving cell i and target cell j respectively, Hys is the hysteresis parameter for this event and $HOM_{i \to j}$ is the HOM defined between cell i and cell j. In practice, different parameters are optimum for different cell pairs (e.g. due to the shadowing variations), so that the parameter selected for optimization in this work has been the HOM, while Hys is set to zero. Under this assumption, the condition (6.1) is the same as (5.1), in which the parameter Hys has been omitted. In addition, to trigger the execution of the HO, the condition (6.1) needs to be fulfilled during a specific time period determined by the parameter TTT.

Thus, the A3 event forces the HO execution when the target cell (with a certain margin) becomes better than the serving cell. According to the 3GPP [35], the HOM corresponds to the Cell Individual Offset, whose possible values range from -24 to 24 dB. On the other hand, the TTT can take any of the following values: 0, 40, 64, 80, 100, 128, 160, 256, 320, 480, 512, 640, 1024, 1280, 2560 and 5120 ms.

Fig. 6.2 illustrates the HO parameters used in this work, i.e. the HOM and the TTT. The configuration of these two parameters determines the influence of the HO algorithm on network performance. Typically, $HOM_{i \to j}$ and $HOM_{j \to i}$ are set to the same positive value so that certain symmetric region between both cells is ensured to avoid unnecessary HOs. Maintaining the symmetric region, both HOMs could also be jointly tuned (achieving different values) so that the service area of these cells is modified, as explained in Section 5.1, for load balancing purposes. However, in this chapter, HOMs are modified for HO optimization, which means to determine the magnitude of the value to be equally applied to both HOMs in the adjacency. The

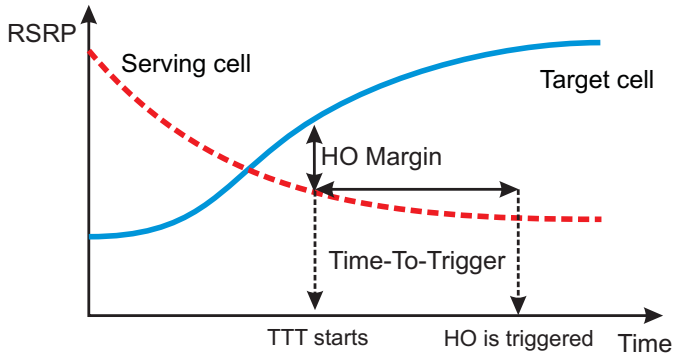

Figure 6.2: Parameters involved in the HO-triggering decision

coordination between these two ways of modifying the HOMs (i.e. HO optimization and load balancing) is covered in the last part of this chapter.

The modification of the HOM and the TTT allows the operator to meet a trade-off between HO signaling load and user experience. A decrement in either HOM or TTT favors a UE to perform an HO to a neighbor cell. This is because, in the case of decreasing the HOM, the user would need a lower received power from the target cell to trigger an HO. In the case of decreasing the TTT, the UE would need less time fulfilling that the target cell (with a certain margin) is better than the serving cell. Conversely, increasing either the HOM or the TTT makes more difficult to perform an HO, meaning that the user spends more time attached to the serving cell, while the connection quality is getting worse. However, possible unnecessary HOs due to signal fluctuations can be avoided. A compromise solution would be to decrease the number of HOs provided that the connection quality of the ongoing calls fulfills operator requirements.

System measurements

To quantify the user experience degradation due to a worse connection quality, the CDR is used in this work. The CDR will be an important indicator in future networks, since services such as VoIP calls are expected to be widely used. This KPI is defined here as in (4.25). Assuming that the Call Admission Control functionality provides enough network resources to accepted calls, the CDR is mainly given by dropped calls due to bad connection quality. In that case, a call is dropped when a Radio Link Failure (RLF) occurs, that is, the SINR is below certain threshold during a specific time interval.

On the other hand, an important measurement from the operator perspective is the HOR, defined as:

$$HOR = \frac{N_{HO}}{N_{succ}}, \tag{6.2}$$

where N_{HO} is the total number of HOs carried out in the concerned area and N_{succ} is the total number of successfully finished calls. Such a measurement gives an estimation of the network signaling load due to HOs. Another interesting KPI is the system load, ρ, used in this work

as a context factor to assess the proposed algorithm in different conditions of traffic load. It is defined in a similar way to the cell load in (5.25), but the total number of resources involves the whole network, not only a single cell. Finally, another indicator that could be affected when HO parameters are modified is the CBR. This KPI is calculated as in (4.26). In this case, the Admission Control assumes that the call needs the largest number of PRBs for the considered service (worst-case criterion) to accept or reject the call. Thus, if there are no free resources under this assumption, then the call will be blocked. Note also that only fresh (or new) calls are considered for the previous counters, meaning that incoming HOs are not included. The importance of the CBR relies on the fact that, as the call connection quality is getting worse (e.g. when HOM is increased), the Link Adaptation functionality modifies the modulation and coding scheme of the transmitted signal, meaning that more PRBs are needed to fulfill the service bit rate. As a result, the user experience of new users accessing the system could be affected.

6.1.2 Optimization algorithm

In this section, the design of the proposed FLC is described. The logic behind such a design relies on a sensitivity analysis performed by a simulation tool, which will be presented in the following section.

The designed FLC has an incremental structure, i.e. the FLC output is the increment (or the decrement) ΔHOM to be added to the HOM. The inputs defined for the FLC are the CDR and the HOR, which can be measured in the overall network, per cell or per adjacency, depending on the parameter optimization level. From these performance indicators, the HOM will be adjusted by the FLC to achieve a good trade-off between the HO signaling load and user experience. The proposed FLC has been implemented according to the Takagi-Sugeno approach [116].

The design of the FLC includes the following tasks (see Fig. 6.3): define the fuzzy sets and membership functions of the input signals and define the linguistic rule base which determines the behavior of the FLC. The first step involved in a FLC execution is the fuzzifier, which transforms the continuous inputs into fuzzy sets. Each fuzzy set has a linguistic term associated, such as high or low. In particular, two fuzzy sets have been defined for the input HOR: High (H) and Low (L). In the case of the CDR, since it is a more critical performance indicator, three fuzzy sets have been defined to have more granularity: High (H), Medium (M) and Low (L). Note that the number of input membership functions has been selected large enough to classify performance indicators as precisely as an experienced operator would do, while keeping the number of input states small to reduce the set of control rules. The translation between numerical values and fuzzy values is performed by using the so-called membership functions. A membership function, denoted by $\mu_z(x)$, quantifies the degree of membership of an input value x to the fuzzy set z, with a value between 0 and 1. The membership functions of the two inputs are depicted in Fig. 6.4. For simplicity, the selected input membership functions are triangular or trapezoidal.

Once the crisp input values are converted to fuzzy values, the next step is performed by the inference engine (Fig. 6.3), which identifies the activated rules and calculates the fuzzy output values. The inference engine maps the fuzzy inputs to the rule base, generating a fuzzy output for

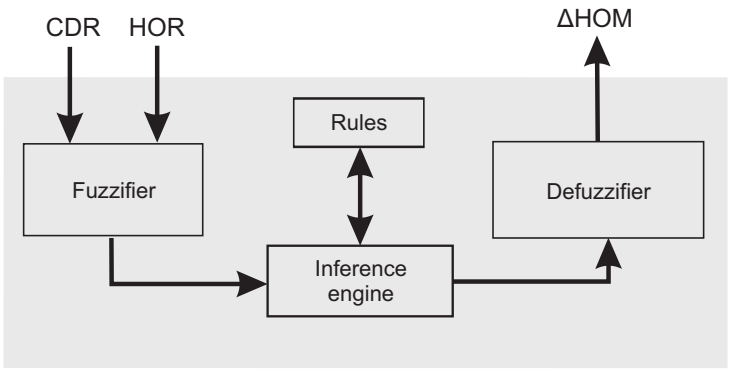

Figure 6.3: Scheme of the FLC for MRO

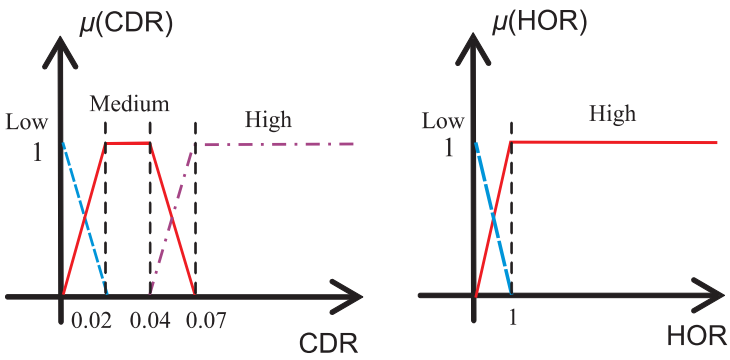

Figure 6.4: Membership functions of the inputs CDR and HOR

each rule. In other words, the rules determine situations that can occur, with the corresponding action that the FLC should execute. For the definition of the rule base, the knowledge and experience of a human expert is generally used. Rules follow a syntax of the type IF-THEN to set the control strategy, similar to the human knowledge. An example rule i for the proposed FLC is the following: 'IF (CDR is *high*) AND (HOR is *low*) THEN (ΔHOM is o_i)'. The output function (Takagi-Sugeno approach) of rule i is a constant value, o_i, which can be one of the following values (each value also has an associated label): -4 dB (Extremely Negative, EN), -2 dB (Very Negative, VN), -1 dB (Negative, N), 0 dB (Zero, Z), $+1$ dB (Positive, P), $+2$ dB (Very Positive, VP) and $+4$ dB (Extremely Positive, EP). The number of rules comes from the combination of all possible fuzzy sets between the two fuzzy inputs, as shown in the three columns on the left of Table 6.1. The configuration of the rules has been set with the aim of reducing the HOR as much as possible to achieve an acceptable value provided that the CDR is within limits defined by the operator. Prior to the definition of the rule consequents, the behavior of each rule is as follows. Rule 1 is activated when both CDR and HOR have high values. In this case, the CDR is prioritized so that the HOM should be decreased. Rule 2 is activated when CDR is narrowly within the limits set by the operator but HOR can be unnecessarily high. In principle, the HOM should be increased to lead the HOR to acceptable values, although it could be better not to change it if the CDR achieves unwanted values. Rule 3 is similar to rule 2 but, in this case, the CDR should be low enough to make greater changes in the HOM regardless of the CDR. The same reasoning is applied to rule 4. The antecedent of rule 5 matches the

Table 6.1: Proposed sets of fuzzy rules

No.	CDR	HOR	ΔHOM for RB_1	ΔHOM for RB_2	ΔHOM for RB_3
1	H	H	N	VN	N
2	M	H	P	VP	Z
3	L	H	VP	EP	VP
4	H	L	VN	EN	VN
5	M	L	Z	Z	Z
6	L	L	P	VP	P

desired network state, given by an admissible CDR and a low signaling load due to HOs. Thus, no change in the HOM would be needed. Finally, rule 6 should attempt to further decrease the HOR by increasing the HOM, provided that the CDR is negligible.

The definition of the rule base is shown in Table 6.1, where three different sets of fuzzy rules, RB_i, have been proposed in this work. Note that most of the fuzzy rules in this problem have been defined by logical reasoning. One may further refine the fuzzy rules using optimization or learning approaches such as in Chapter 5 in the expense of additional complexity. However, in this case, as the number of rules is lower and, furthermore, their candidate output values are quite limited by logical reasoning, the rules can be manually optimized. Thus, several sets of fuzzy rules have been manually defined to model different behaviors. In particular, the first rule base, named as RB_1, presents a conservative behavior, characterized by small changes in HOM. A more aggressive rule base is denoted by RB_2, whose rule consequents are greater than those in RB_1. Finally, RB_3 is a configuration similar to RB_1 in which rule 2 has a more conservative consequent (i.e. no change in HOM). In particular, this setting aims to reduce oscillations if the CDR is around the limit defined by the operator.

To calculate the output value, the FLC firstly compute the antecedent of each rule, formed from the combination of fuzzy sets using the product operator:

$$\alpha_k = \mu_x(CDR) \cdot \mu_y(HOR), \tag{6.3}$$

where α_k is the degree of truth for the rule k. The last step performed by the FLC is the conversion of the output of fuzzy rules into a non-fuzzy value, or a scalar. Given a set of activated rules and their corresponding degree of truth, the output crisp value is calculated as a weighted average of the rule outputs, using (5.3). It is noted that the range of variation of HOM is limited between 0 and 12 dB, since higher values significantly decrease the quality of the ongoing connections, increasing the CDR. In addition, the HOM value is rounded to the nearest value admissible by the 3GPP within that range [35].

6.1.3 Simulation setup

Since analytical models require a high degree of complexity to provide realistic results, the dynamic system-level simulator for LTE macrocells explained in Chapter 4 has been used to perform the sensitivity analysis and assess the FLC performance. This simulator first runs a module of parameter configuration and initialization, where a warm-up distribution of users is created. Then, several optimization loops or epochs are executed to emulate the tuning process. Each epoch comprises an adjustable number of simulation steps. Each simulation step includes updating user positions, propagation computation, generation of new calls, and radio resource management algorithms. At the end of each epoch, measurements and reliable statistics are obtained to be used in the following optimization loop. The end point of an epoch is also used as the starting point in the following epoch. After the simulation, the main statistics and final results are shown.

The simulated scenario includes a macro-cellular environment with a layout consisting of 19 tri-sectorized sites evenly distributed in the scenario, as shown in Fig. 6.5. The main simulation parameters are summarized in Table 6.2. For simplicity, only the downlink is considered in the simulation. The service provided to users is the voice call as it is the main service affected by the tuning process. The number of PRBs allocated by the scheduler to each user depends on the radio channel conditions. The spatial traffic distribution is assumed to be uniform. The epoch time comprises 1000 simulation steps, equivalent to 100 s of actual network time. This value is large enough to obtain reliable measurements of overall performance indicators (e.g. the global CDR) for the network size, the traffic model and the system load levels used in this work.

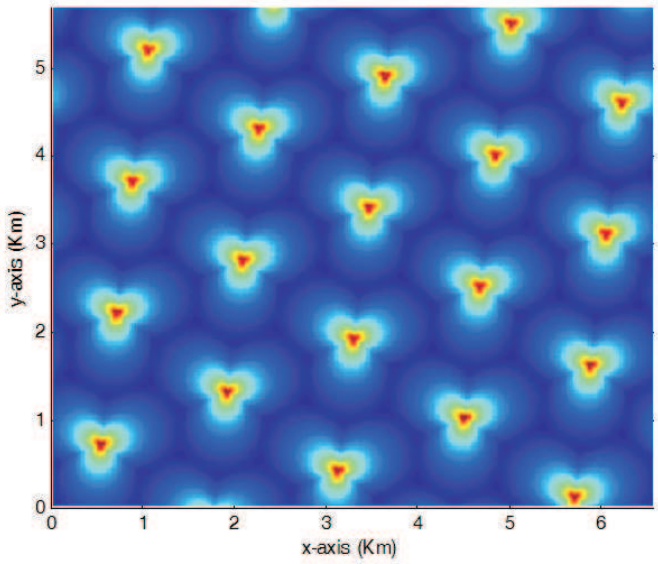

Figure 6.5: Scenario (pathloss map)

Table 6.2: Simulation parameters

Parameter	Configuration
Cellular layout	Hexagonal grid, 57 cells (3x19 sites), cell radius 0.5 km
Transmission direction	Downlink
Carrier frequency	2.0 GHz
System bandwidth	5 MHz (25 PRBs)
Frequency reuse	1
Propagation model	Okumura-Hata with wrap-around
	Log-normal slow fading, σ_{sf}=8 dB and correlation distance=50 m
Channel model	Multipath fading, EPA model
Mobility model	Random direction, 3, 10, 50 km/h
Service model	Constant bit rate (voice call), poisson traffic arrival, mean call duration 120 s, 16 kbps
Base station model	Tri-sectorized antenna, SISO, $EIRP_{max}$=43 dBm
Scheduler	Time domain: Round-Robin
	Frequency domain: Best Channel
Power control	Equal transmit power per PRB
Link Adaptation	Fast, CQI based, perfect estimation
Measurement setting	Measurement Reporting Rate = 0.1 s
Handover	Triggering event = A3
	Measurement type = RSRP
	Range of variation of HOM = [0,12] dB
Radio Link Failure	SINR < -6.9 dB for 500 ms
Traffic distribution	Evenly distributed in space
Time resolution	100 TTI (100 ms)
Epoch time	100 s
Simulation duration	4000 s

The simulations performed in this section firstly include a sensitivity analysis (or sweeping) of the two main parameters involved in the HO process (the HOM and the TTT). This analysis is carried out for different system load levels and user speeds. Then, the FLC is assessed for different parameter optimization levels, different measurement errors and the proposed sets of fuzzy rules under the same conditions than the sensitivity analysis.

6.1.4 Performance results

Performance assessment methodology

To compare the network performance achieved by each HO parameter setting, the global CDR and the global HOR are measured as an estimation of user experience and HO signaling load, respectively. In addition, when the system load is high (around 80%), the global CBR is measured

to analyze the impact of the HOM on user experience for those users accessing the network.

As in Chapter 5, to evaluate the transient response, an infinite-horizon discounted model extracted from [164], has been considered. This model is a weighted average of single penalties across loops, where future penalties have less importance according to a geometric law with the parameter γ [see (5.23)]. The advantage of this averaging method versus other approaches such as the standard averaging is that, in live environments, early penalties are typically more important than delayed penalties, since network conditions (e.g. offered traffic) might greatly vary with time. Thus, the discounted model, that gives more importance to early penalties, is more appropriate in this work. The values of the parameters involved in this model are the same as in Chapter 5.

Finally, the utility function $U(t)$ needs to be defined. To appropriately assess the trade-off between the call dropping in the network and the HO signaling cost, the following $U(t)$ has been defined:

$$U(t) = CDR(t) + k \cdot HOR(t), \tag{6.4}$$

where k is a constant weight determining the relative importance of the HOR in the equation. Since the CDR has a higher priority to fulfill the operator constraint, the factor k has been set to 0.01.

Sensitivity analysis

Firstly, the sensitivity analysis of the HOM is carried out for different system load levels. For simplicity, the HOM value is the same for all cells (i.e. network-wide level is assumed). The user speed has been set to 3 km/h in this analysis unless stated otherwise. Fig. 6.6 shows the performance obtained by sweeping HOM when TTT is set to 100 ms and 1 s. The CDR and the HOR have been measured and graphically represented for the following values of HOM: 0, 2, 4, 6, 8, 10 and 12 dB. This analysis has been carried out for the following levels of traffic load in the network: 50, 65 and 80%. It is observed that the existing trade-off between CDR and HOR is maintained for different traffic load levels. In addition, the effect of traffic load on the HOM sweeping is reflected graphically as an upward shift of the curves. A higher traffic load means a higher number of UEs (i.e. more HOs are carried out) and more interference is generated in the scenario (i.e. CDR is increased). In low-load conditions (e.g. 50% traffic load), the specific value of TTT does not significantly affect performance when sweeping HOM, resulting in approximately overlapped curves. However, with higher levels of traffic load, a TTT equal to 1 s provides worse performance than a TTT equal to 100 ms. For instance, considering an 80% traffic load and an HOM equal to 4 dB, the CDR is decreased from 0.12 to 0.07 (at the expense of a slight increase in HOR) when a TTT equal to 100 ms is used instead of 1 s. The compromise solution taken in this work is to keep the CDR under 0.05 and the HOR under approximately 0.5.

The effect on the CBR produced by the HOM variation for different traffic loads is shown in Fig. 6.7. As it can be observed, the HOM has no significant impact when the traffic load is

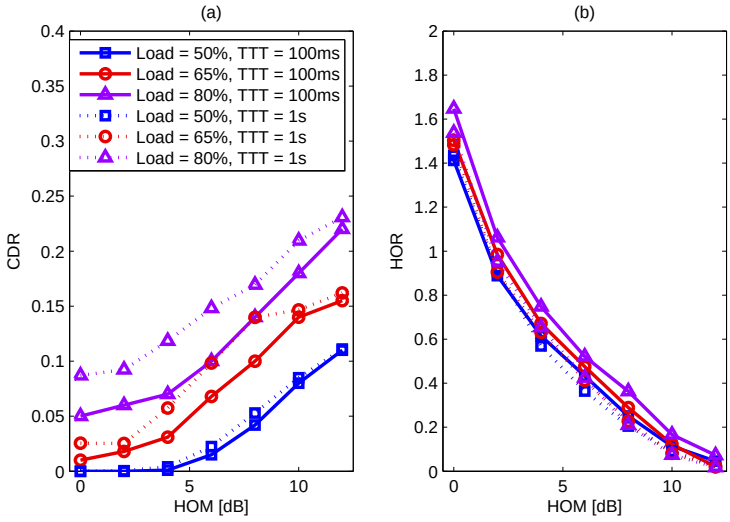

Figure 6.6: Sensitivity analysis of HOM (speed = 3 km/h)

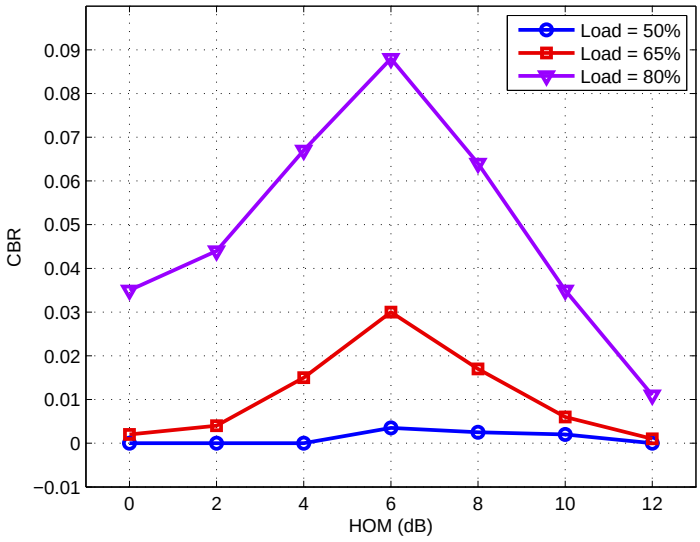

Figure 6.7: CBR as a function of the HOM

lower or equal to 50%. When the traffic load is above this value, the CBR keeps negligible for small values of HOM, while higher values of HOM would increase the CBR, since the connection quality of some calls is getting worse and more radio resources are needed to fulfill the bit rate. However, if the HOM is further increased, the CBR would be surprisingly decreased. This is because the CDR achieved at this point is above 0.10, meaning that a significant number of calls are dropped, so that more radio resources are free and the CBR is decreased. For this reason, achieving high values of HOM (e.g. greater than 8 dB) should be avoided, since it affects the ongoing calls negatively when the traffic load is substantially high.

Fig. 6.8 shows the impact of the user speed on performance when the sensitivity analysis

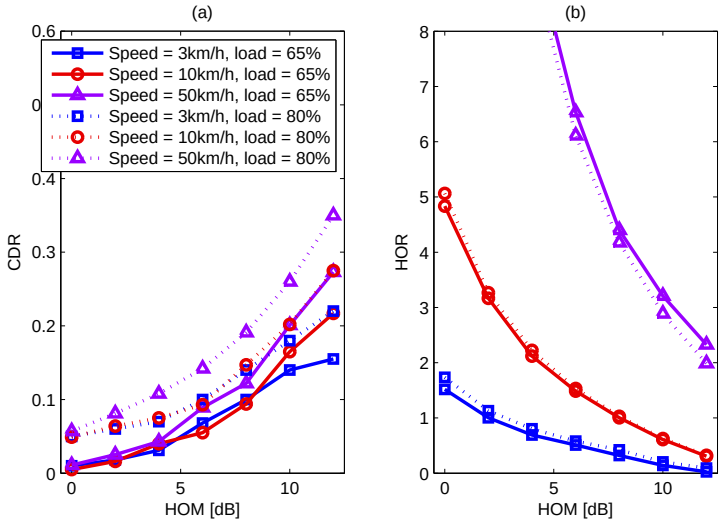

Figure 6.8: Influence of the user speed and HOM on performance

of the HOM is performed. This study has been made for different levels of traffic load and the following values of user speed: 3, 10 and 50 km/h. It is noted that the latter would be the worst case (all UEs have the highest speed), since in a real situation there would be a combination of UEs with different speeds. As it can be observed, the effect of the user speed on the HOM sweeping when the user speed is increased is mainly an upward shift of the HOR curves due to a significant increase in the number of HOs (UEs travel more distance during the call). Such a shift is extremely large for high user speeds and low values of HOM. For instance, for a user speed equal to 50 km/h, it is noted that setting an HOM below 6 dB would lead to an HOR above 8.0, that is, the number of HOs would be highly increased. In addition, there also exists an upward shift in the CDR curve, especially appreciable for high values of HOM. The reason for this is that, as the UEs travel more distance during the TTT, the risk of dropping is higher if they are moving away from the serving cell.

The evaluation of the utility function, U, for the previous analyses is depicted in Fig. 6.9. In particular, the impact of the system load is shown in Fig. 6.9(a), where the curves are very similar to those depicted in Fig. 6.6(a) because the dominant term in the utility function is the CDR (given that k is 0.01). However, if the user speed is increased [see Fig. 6.9(b)], the dominant term in the utility function becomes the HOR for low values of HOM, showing that there exists an optimal HOM with minimum value of U. As it can be observed, for user speeds above 50 km/h, the optimal HOM value is above 4 dB.

The sensitivity analysis of the TTT for a low speed (3 km/h) is represented in Fig. 6.10. The analysis has been carried out for two values of HOM: 2 dB and 8 dB. In addition, the system load has been set to 65% and 80%. The CDR and the HOR are graphically represented for the following values of TTT: 0.1, 0.3, 0.5, 1.0, 1.2, 2.5 and 5.1 s. To compare it with the previous sensitivity analysis of the HOM, both indicators are depicted in the same plot for the same user speed and system load levels. It is observed that the effect on network performance produced by

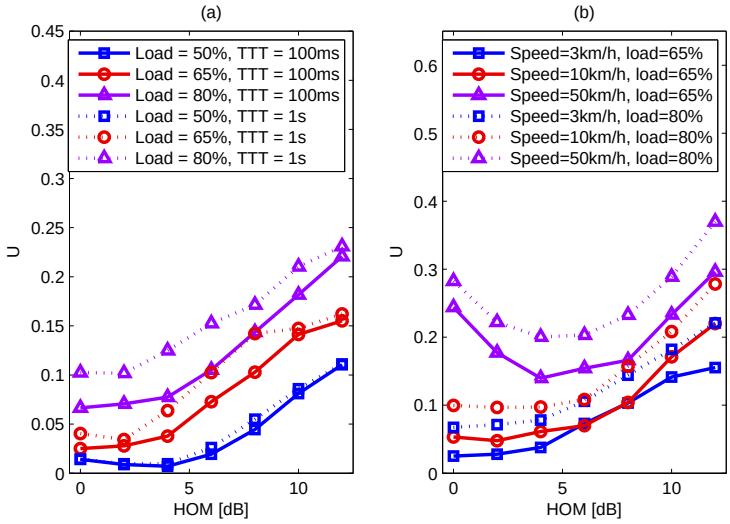

Figure 6.9: Utility function (HOM analysis)

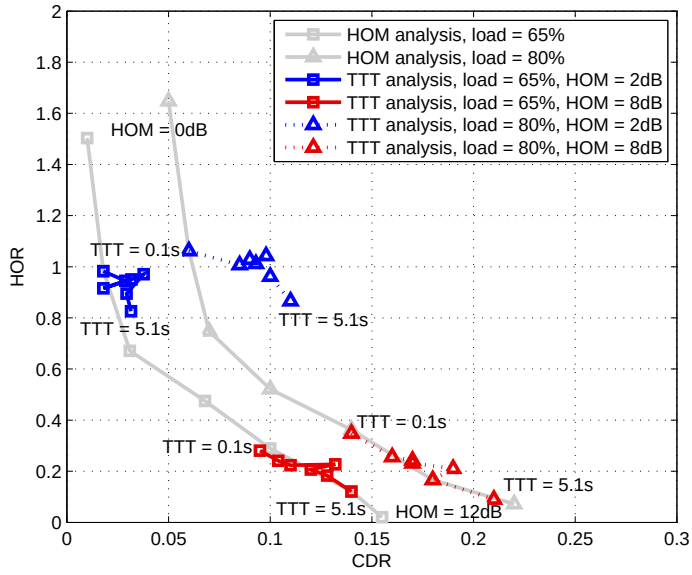

Figure 6.10: Sensitivity analysis of TTT (speed = 3 km/h)

the TTT variation is much lower than that produced by the HOM. In addition, when HOM is set to 2 dB, performance achieved by sweeping TTT is worse than keeping it to 100 ms, since CDR is increased without a significant decrease of HOR. For instance, given an 80% system load, the CDR increases from 0.06 to 0.08 when the TTT is varied from 100 to 300 ms, while the decrease in HOR is negligible. When HOM is set to 8 dB and TTT is swept, the curves are overlapped with the curves of the HOM sensitivity analysis, meaning that no gain is achieved by increasing TTT.

Fig. 6.11 shows the impact of TTT on network performance for high-speed users. The system

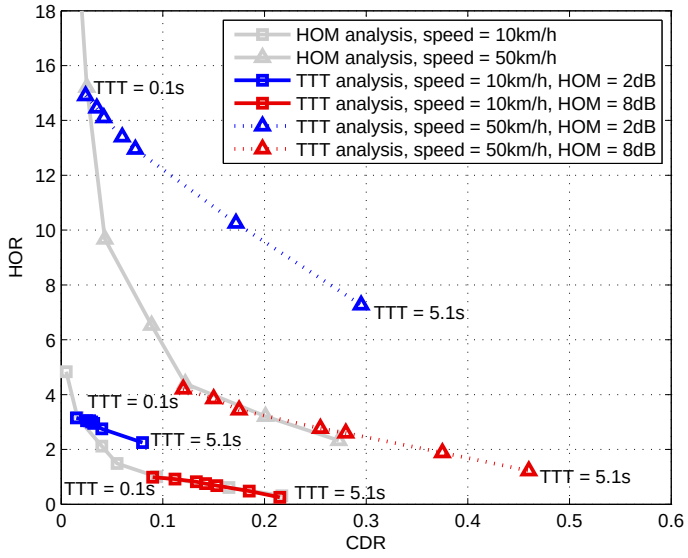

Figure 6.11: Influence of the user speed and TTT (load = 65%)

load has been set to 65%, and the sensitivity analysis of HOM is also shown as a reference case. When the UEs have a speed equal to 10 km/h, the impact of the TTT is similar to the previous case of low-speed users: performance achieved by sweeping TTT is worse than keeping it to 100 ms when HOM is set to 2 dB, and the curve of HOM is overlapped with the curve of TTT when HOM is set to 8 dB. These effects are also evident from the case with 50 km/h. For instance, suppose that a TTT equal to 100 ms and an HOM equal to 2 dB are currently set in the network. Then, if a 5% CDR is the target value imposed by the operator, it would be better to increase the HOM instead of the TTT, since HOR would experience significantly greater reduction. In addition, when the TTT sweeping is carried out with HOM=8 dB, the curves of HOM and TTT are not fully overlapped, meaning that TTT values greater than 1 s result in worse performance than the HOM sweeping (e.g. the CDR is greatly increased above 0.30).

Thus, the sensitivity analysis highlights that the parameter adaptation can be performed by simply modifying HOM and keeping TTT to 100 ms regardless the user speed, since the adjustment of TTT does not provide greater benefit than that obtained by adjusting HOM.

FLC performance assessment

In this section, the FLC tunes the HOM parameter. The first simulations have been carried out for different parameter optimization levels, assuming that RB_1 has been implemented, while the system load and the user speed have been set to 80% and 3 km/h, respectively. In the case of network-wide optimization, note that the same value of HOM is set in (6.1) for all cell-pairs. On the other hand, cell-wide optimization means that the HOM value depends on the serving cell and, finally, cell-pair-wide optimization means that this value depends on both the serving and neighboring cells, so that the output value calculated by the FLC in the adjacency is applied to

both HOMs, i.e. $HOM_{i \to j}$ and $HOM_{j \to i}$.

Initially, the simulations start with an HOM equal to 8 dB, since this allows to visualize more clearly the path of convergence drawn by the FLC. In Fig. 6.12, the global CDR and HOR for each optimization epoch are depicted, as well as the previous sensitivity analysis of HOM. On the other hand, in Fig. 6.13, the Cumulative Distribution Function (CDF) of the HOM values after the initial transient response of the FLC is shown. It is noted that cell-wide optimization provides the worst performance (around 10-15% CDR), because a symmetric margin between cells cannot be ensured, thus leading to a wide range of HOM values (see Fig. 6.13) and achieving a high CDR. The other two cases (network-wide and cell-pair-wide) have similar performance in terms of CDR, i.e. around 5% CDR is achieved. However, cell-pair-wide optimization provides fewer oscillations in the CDR, since the HOM values are adapted to the specific radio conditions of each cell-pair and, thus, the range of HOM values is greater, as shown in Fig. 6.13. According to these results, the following analyses have been carried out considering cell-pair-wide optimization.

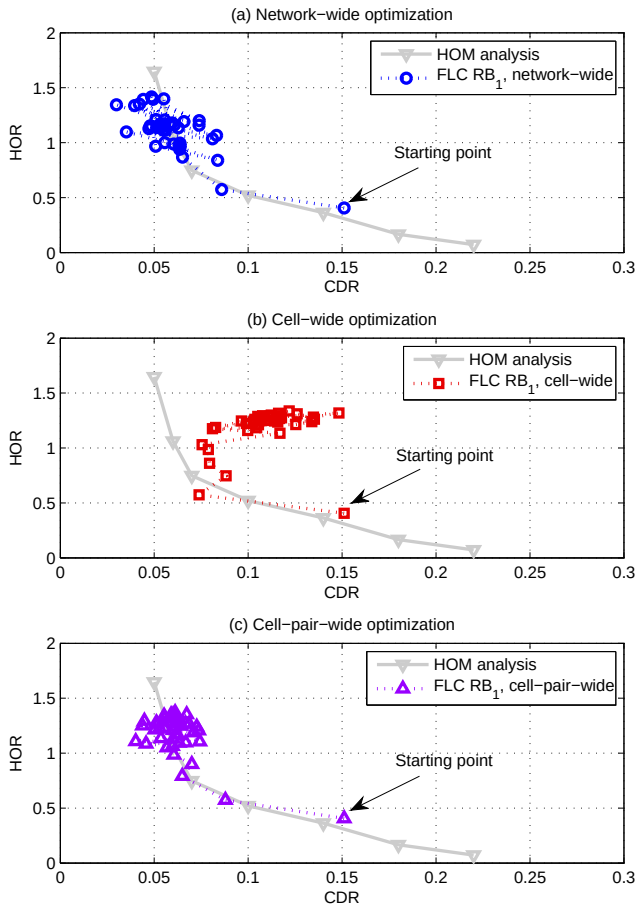

Figure 6.12: Comparison between different parameter optimization levels

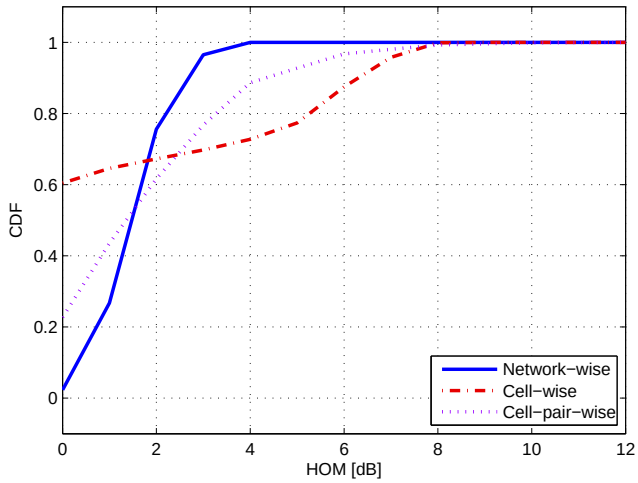

Figure 6.13: Cumulative Distribution Function of HOM

The following experiment shows the impact of the measurement error on the FLC performance. To model the noise in RSRP measurements, a Gaussian random variable (zero-mean) has been added to the reported RSRP measurement (in dB). In Fig. 6.14, different standard deviations (σ) of the Gaussian variable have been evaluated. The sensitivity analysis of HOM, as well as the previous simulation of the FLC tuning the HOM at cell-pair-wide level, are also depicted for a system load equal to 80%. It is shown that higher standard deviations of the error term lead to an increase of the HOR, since it has a direct impact on the HO triggering condition, given by (6.1). However, such a measurement error does not affect the operation of the FLC, which leads the CDR to lower values (around 5-6%) as in the case without error (σ=0), although the HOR is increased due to the noise. In principle, the noise/fluctuations in RSRP measurements can be diminished if several samples are taken at the physical layer and then filtered to generate the reported measurement. For example, in order to decrease the noise in the RSRP, instead of taking measurements every 100 ms, measurements could be taken every 10 ms and then those 10 samples would be filtered to generate the reported measurement every 100 ms. In case that the measurement error cannot be avoided, in order to diminish HOR, a compromise solution could be to increase the TTT, but at the expense of increasing the CDR.

In the following simulations, the proposed FLC configurations have been assessed for different levels of traffic load, a user speed equal to 3 km/h and a constant TTT equal to 100 ms. Results for each proposed FLC configuration, RB_1, RB_2 and RB_3, are shown in Fig. 6.15, where the measurements of CDR and HOR for each optimization epoch are depicted. As a reference case, the sensitivity analysis of HOM is also represented. Initially, the simulations start with an HOM equal to 8 dB. For those cases in which the traffic load is high (i.e. 65 and 80% load), the FLC diminishes the HOM until the CDR reaches the desired value (around 5%). From this point, the configurations RB_1 and RB_2 attempt to reduce HOR by increasing HOM (rule 2 is mainly triggered), but the constraint imposed on the CDR prevents a further increase of the HOM, leading to small oscillations in network performance. In the case of RB_2, such oscillations are more pronounced, especially when the system load is 65%, where the CDR varies between 0.01

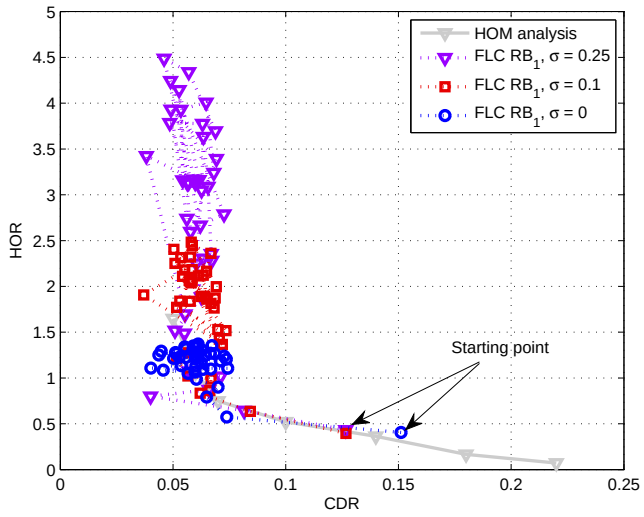

Figure 6.14: Impact of the measurement error on performance

Table 6.3: Penalty values for a speed = 3 km/h

Load	FLC	P [%]	$min(U(t))$ [%]	$max(U(t))$ [%]
65%	RB_1	5.55	2.29	7.52
65%	RB_2	6.99	2.78	11.99
65%	RB_3	4.42	2.29	6.88
80%	RB_1	11.67	9.26	15.68
80%	RB_2	11.75	7.91	20.04
80%	RB_3	10.74	7.96	15.62

and 0.11 and the HOR between 0.3 and 0.9, after the transient response. In the case of RB_1 and RB_3, both CDR and HOR achieve similar values in the steady state. However, RB_3 leads to slightly lower oscillations around the target area, since rule 2 has a more conservative setting, which aims to keep the HOM unchanged.

Table 6.3 shows the overall penalty, P, together with the minimum and maximum values of $U(t)$ for the proposed FLC configurations when the load is set to 65% and 80%, since similar performance is achieved by the FLCs when the system load is lower. This indicator, P, assesses the temporary response regarding both the response speed and the asymptotic value. As it can be observed, RB_3 gives the lowest value of P in both situations, since its response keeps lower values of CDR, which is the dominant term in the utility function for low user speeds. Note also that RB_2 leads to the worst value of P, due to the oscillations produced by greater changes in the HOM.

The impact of the user speed on network performance when the FLC is operating in the network is analyzed in the following paragraphs. Fig. 6.16 shows the evolution of CDR and HOR for each proposed rule base and different user speeds, when the system load is set to 50%. In this case, the simulations start with an HOM equal to 2 dB. It is shown that, as the user speed

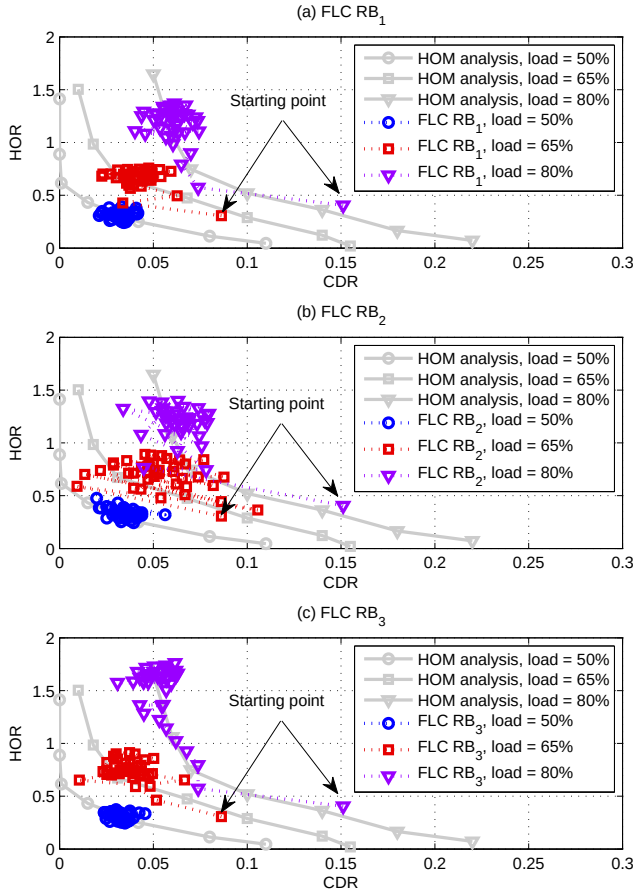

Figure 6.15: Performance of the proposed FLC (speed = 3 km/h)

increases, both performance indicators (CDR and HOR) are more sensitive to changes in HOM, especially for values above 10 km/h. In the case of RB_2 and a user speed equal to 50 km/h, oscillations in the HOM cause a strong variation in the CDR between 0.02 and 0.18, jeopardizing the operator constraint (CDR around 0.05). The differences between RB_1 and RB_3 are more pronounced in this case. As it is shown, RB_3 keeps the CDR close to the operator constraint most of the time, highlighting that this configuration is more appropriate than RB_1, which more frequently exceeds that constraint. The benefits of RB_3 comes from the more conservative variation of the HOM, which can be derived from the temporary evolution of the HOM in an example adjacency shown in Fig. 6.17, where the oscillations experienced by the HOM are the lowest. On the other hand, RB_2 produces the greatest changes in the HOM during the first optimization epochs, speeding up the adaptation process, but it also leads to higher oscillations in the HOM during the steady state, decreasing network performance. These results are in connection with the motivation of each FLC configuration defined in Section 6.1.2, where RB_2 presented a behavior less conservative than RB_1 and RB_3. The benefit of RB_2 lies in the speed of achieving the steady state, which is higher than in the case of RB_1 and RB_3.

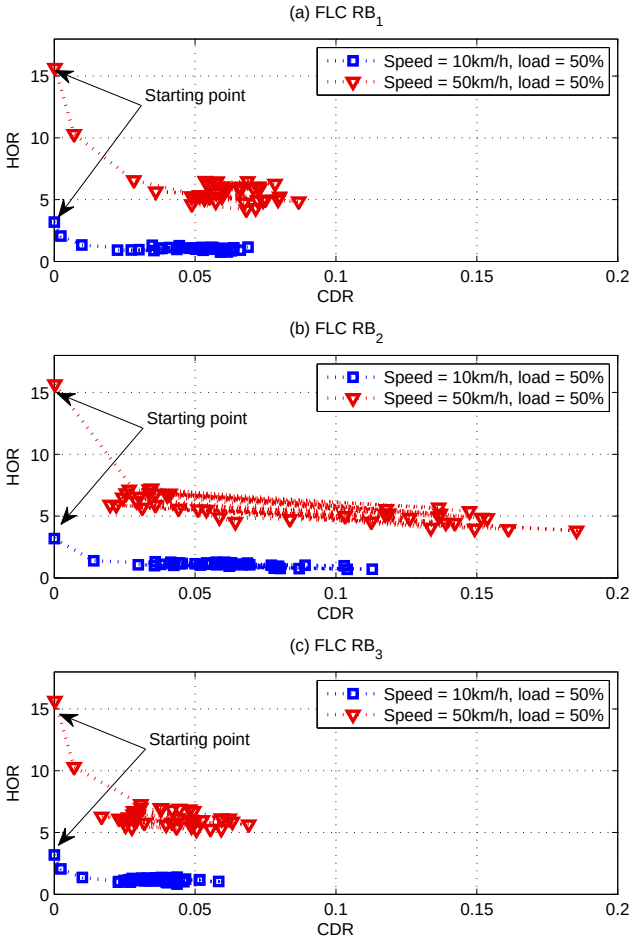

Figure 6.16: Effect of the user speed on the FLC performance

The overall penalty for the proposed FLC configurations when the user speed is set to 10 and 50 km/h and the system load is equal to 50% is shown in Table 6.4. As expected, RB_2 obtains the worst performance, given by the highest value of P and also the greatest oscillations. RB_3 provides the best performance, because the CDR is more concentrated around 0.05 (or even lower values) throughout the time, the HOR keeps similar values than other configurations and its transient response is similar to RB_1.

Thus, it is highlighted that the best proposed FLC configuration is RB_3 regardless of the system load and the user speed, since its temporary response has the best performance in terms of CDR and HOR for all cases analyzed in this work.

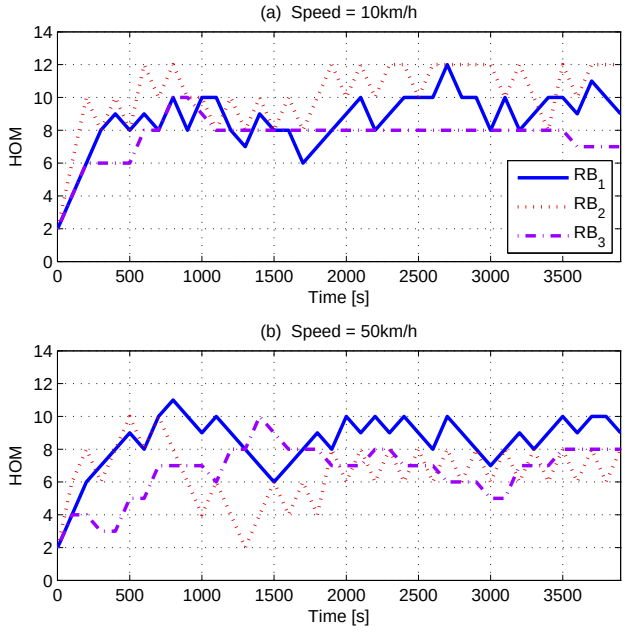

Figure 6.17: Temporary evolution of HOM when the FLC is applied

Table 6.4: Penalty values for a load = 50%

Speed	FLC	P [%]	$min(U(t))$ [%]	$max(U(t))$ [%]
10 km/h	RB_1	4.98	3.01	8.93
10 km/h	RB_2	6.17	1.52	10.93
10 km/h	RB_3	4.83	1.71	8.93
50 km/h	RB_1	7.61	5.65	15.52
50 km/h	RB_2	7.76	5.25	15.62
50 km/h	RB_3	7.21	5.63	15.57

6.2 Coordination between MRO and MLB

6.2.1 Coordination algorithm

In cellular networks, SON functionalities such as MLB, MRO, interference control and RACH optimization have been identified as important use cases [6]. In addition, since SON functionalities are numerous, a large number of SON entities might operate simultaneously in the network [80]. Due to this, there may be conflicts or dependencies between SON functions. SON coordination means preventing or resolving conflicts or negative influences between SON functions to make SON functions comply with operator's policy [6]. An example of interactions between SON functions is shown in Fig. 6.18, where there is a mesh relationship between SON functions and network parameters (or network elements) in which conflicts or negative influences may happen if SON coordination is not considered.

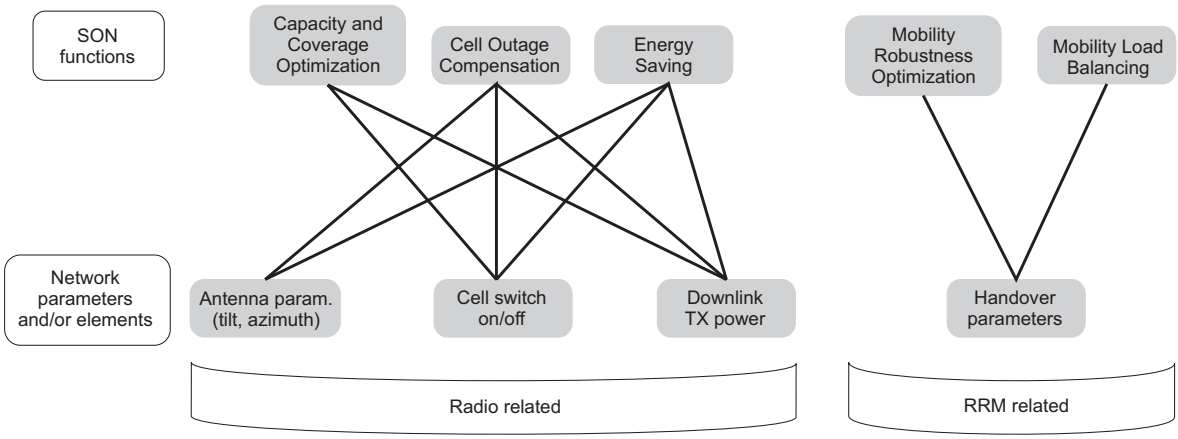

Figure 6.18: Mesh relationship between SON functions and network parameters (or elements) [6]

In this section, the conflict between the proposed MLB and MRO functions caused by a lack of coordination in the adjustment of HO parameters is studied. As previously explained, the proposed MLB and MRO functions adjust the HOMs in both directions of the adjacency. Since two variables are involved in the process, two different properties can be modified separately in the adjacency, i.e. the symmetric region and the service area (Fig. 5.1). This means that, unlike other existing approaches for MLB and MRO [82][86][87], there is no conflict when HOMs are changed in opposite direction (e.g. MLB decreases $HOM_{i\to j}$ while MRO increases it). For instance, when MLB adjusts the service areas in the adjacency, the symmetric region is maintained. Likewise, the same reasoning is applied to MRO's actions.

Due to the fact that both MLB and MRO can adjust the same mobility parameters, the simultaneous (and uncoordinated) operation of these functions may lead to sub-optimal performance. In this situation, the primary objective of the coordination scheme should be to take care of the problem of call dropping, since in the intra-frequency case (common in LTE deployments), MLB may lead to an increase in the number of dropped calls. In normal conditions, it is expected that both functionalities work well without jeopardizing the call dropping. This is because the range of the HOM values in which the MLB and MRO functions operate is not large enough. However, in more extreme situations, the fact that both functions simultaneously perform large changes in the parameter may negatively affect the network. For instance, let suppose a scenario in which most of the users have a high speed, thus leading to a high HOR. In this scenario, the MRO adjusts the HOM to lead the CDR close to the operator's constraint in order to reduce as much as possible the HO signaling (i.e. decrease the HOR). As a result, the MLB has less flexibility to perform load balancing in a congestion situation, because the HOMs may already have large values and the call dropping is close to the operator's constraint. Another situation of interest for SON coordination is the one in which the scenario is heavily congested. In this context, the MLB would lead the HOMs towards extreme values, thus achieving high values of CDR. This situation limits the normal operation of the MRO, whose increments in the HOM may lead to excessive call dropping. Hence, the avoidance of such a conflict in those situations would provide optimal network performance at any time.

The solution adopted in this thesis for those extreme situations is to switch off one function in favor of the other one. This rule avoids that both FLCs achieve (or are close to) saturation of the output at the same time. To explain this, note that the proposed FLCs have been designed to work properly when they are executed independently. For instance, the proposed MLB can operate effectively in the network if the symmetric region related with MRO is set to a reasonable default value. However, if such a symmetric region is too large and MLB further increases the HOM as well, call dropping can be highly increased. For this reason, in the adopted solution, the SON functionality that is likely to achieve saturation must be switched off. Note that the last modification made by the FLC determines the parameter setting used hereafter. Thus, while a reasonable parameter setting has been established for this function, the FLC that remains active in the network can effectively further adjust the HOM to achieve its objective. More specifically, in the extreme scenario with high-speed users, the proposed solution for this case is to switch off the MRO function when the CDR is above a threshold, which is set to avoid an excessive number of dropped calls. In the extreme scenario in which many cells are heavily congested, the adopted solution is to switch off the MLB function when the CDR is above a threshold, which is also set to avoid a high number of dropped calls.

To switch off a functionality (i.e. the MLB or MRO), firstly, the two scenarios previously explained need to be identified as "extreme" situations in the practice. For instance, the situation with high level of HO signaling (e.g. due to the presence of high-speed users) can be given by a high value of HOR. More specifically, if the HOR is above a given threshold, the situation is considered to be "extreme" from the perspective of the HO signaling load. In the other case, the situation involving a high level of congestion can be identified by a high value of CBR, for which a threshold can also be defined. Secondly, once the extreme scenarios can be identified, the other condition given by the CDR is fulfilled when this indicator is above a threshold. Thus, to switch off the MRO, the conditions related to HOR and CDR need to be fulfilled (as shown in Fig. 6.19), while to switch off the MLB, the conditions to be fulfilled are related to CBR and CDR. It is noted

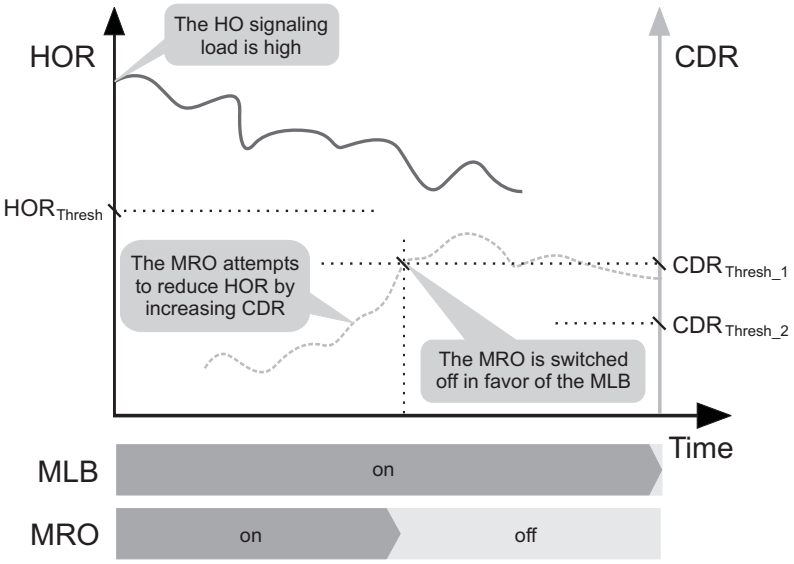

Figure 6.19: The MRO function is switched off to avoid large values of HOMs

that, although the functionalities are switched off in a situation in which their use is apparently recommended (e.g. the MLB in a heavily congestion situation, or the MRO in a scenario with high-speed users), these functionalities are switched off when their operation cannot improve the current situation (as it negatively affects the CDR). The proposed SON coordination scheme is summarized in Algorithm 6.1. It is highlighted that CDR_{Thresh_1} may depend on the system load, ρ, so that different values could be used to identify each extreme situation. In addition, to switch on the functionalities (i.e. to return to normal operation), a certain hysteresis region in the CDR is considered. Thus, the CDR must be below another threshold (Fig. 6.19) to switch on the functionalities. Note also that, if none of the above conditions is fulfilled, the normal operation (in parallel) of both functions is maintained. The next section provides specific values of the involved thresholds and analyzes the simulation results.

6.2.2 Performance results

The simulated scenario is the one used for evaluation of the proposed MLB and MRO functions in previous sections. The simulation parameters whose setting is different from previous simulations and those related to the SON coordination scheme are shown in Table 6.5. The "extreme" situation simulated here is given by the presence of high-speed users (50 km/h), which in principle would lead to a high HOR. In addition, the operator's constraint for the CDR assumed in Section 6.1 (i.e. to keep the CDR under 5%) has been modified to be 1.5% in this section. This is in line with the objective of maintaining a very low call dropping in this study. This means that the membership functions of the proposed FLC for MRO have been modified to satisfy this new constraint.

Firstly, an overview of the impact of the coordination mechanism on the observed KPIs is presented in Fig. 6.20. The coordination algorithm is compared with other approaches. In the reference case (i.e. no optimization), both the MLB and MRO functions are disabled. The MLB and MRO have also been executed separately (i.e. one of these functions has been disabled), and together in an uncoordinated way. The measured KPIs are the overall HOR, CDR and CBR. In addition to these KPIs, a utility function U that combines the previous KPIs into a scalar value

Algorithm 6.1. The SON coordination scheme for MLB and MRO

Switch on MLB, MRO
WHILE (**true**) **DO**
  IF (HOR $>$ HOR_{Thresh}) **AND** (CDR $>$ $\text{CDR}_{Thresh\_1}(\rho)$)
    Switch off MRO
  ELSE IF (CBR $>$ CBR_{Thresh}) **AND** (CDR $>$ $\text{CDR}_{Thresh\_1}(\rho)$)
    Switch off MLB
  ELSE IF (CDR $<$ CDR_{Thresh_2})
    Switch on MLB, MRO
  END IF
END

Table 6.5: Simulation parameters

Parameter	Configuration
HOR_{Thresh}	5
CBR_{Thresh}	2%
CDR_{Thresh_1}	1%
CDR_{Thresh_2}	0.5%
User speed	50 km/h
Traffic distribution	Unevenly distributed in space (the same as in Section 5.2)
Epoch time	12 min
Simulation duration	1800 min

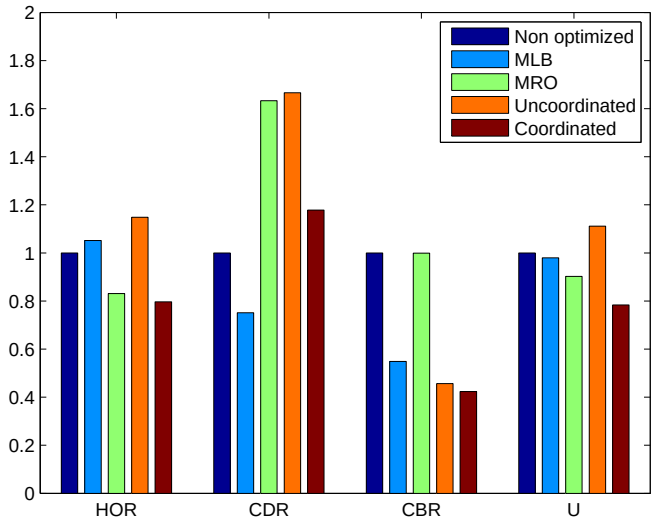

Figure 6.20: Comparison of the proposed SON coordination scheme with different approaches

has been represented in Fig. 6.20. This FoM characterizes, qualitatively, the overall performance of the evaluated approaches. Formally, U is defined as:

$$U = k \cdot (CBR[\%] + (1 - CBR[\%]/100) \cdot CDR[\%]) + HOR, \tag{6.5}$$

where k is a constant weight determining the relative importance of the CBR and CDR (both related to user dissatisfaction) compared with the HO signaling cost given by HOR. In this study, k equal to 1 is assumed. The y-axis of Fig. 6.20 represents the relative gain in each KPI/FoM with respect to the reference case. As observed, the MLB approach alleviates the congestion situation since the CBR is significantly decreased compared with the reference case, while the CDR is not negatively affected. The latter is because the MLB algorithm designed in Chapter 5 takes care of the negative impact on call dropping when the load balancing is performed. As expected, the MRO approach gives a reduction in HO signaling, which means a lower HOR, at the expense of increasing the CDR up to the operator's limit. In this case, since no load balancing is carried out,

the CBR is maintained at the same level as at the beginning. In the uncoordinated approach, both functionalities (MLB and MRO), interact in a wrong manner because both HOR and CDR achieve high values. Conversely, the coordinated approach is presented as the best alternative, since the congestion situation is alleviated at the expense of a slight increase in CDR, while a significant reduction in the HOR is also achieved. As a result, the lowest value of U is achieved by this approach.

Secondly, in the following paragraphs, a more comprehensive analysis is given by representing the KPIs evolution throughout the time and their values measured at cell level. In particular, in Fig. 6.21, the temporary evolution of the KPIs is depicted. It is observed that the HOR values are above the HOR_{Thresh}, meaning that the scenario can be considered as extreme from the perspective of the HO signaling load. In the uncoordinated approach, it is highlighted that the HOR gradually increases as a result of the bad interaction between MLB and MRO. Regarding the CDR, it is noted that the condition needed to switch off the MRO function in

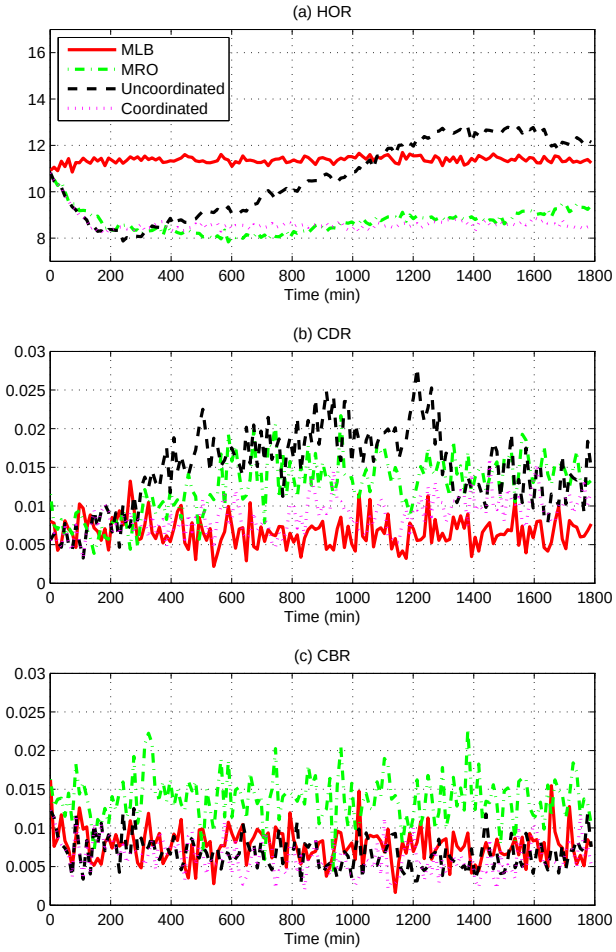

Figure 6.21: Temporary evolution of the KPIs for different approaches

the coordinated approach (i.e. CDR above a threshold) is fulfilled around t=200 min. From this point, only the MLB function is active for the rest of the simulation. In the uncoordinated approach, an undesirable increase in CDR is produced due to the bad interaction between SON functions. Regarding the CBR, all the approaches except MRO lead to a similar mitigation of the congestion (i.e. similar CBR). As expected, the MRO cannot solve by itself the congestion situation.

Fig. 6.22 shows the KPIs measured at cell level, which means that the events (e.g. a dropped call, an HO, etc.) used to calculate the KPIs are only considered in one cell. The values represented in the figure correspond to the average of the last 50 samples (one per epoch) of the simulations. Note that the simulation scenario is represented in Fig. 4.2 (showing the cell labeling), where some cells in the center have a high traffic density whereas surrounding cells have a low traffic density. Regarding the HOR, the MLB approach keeps similar HOR for all the cells, as in the reference case. Conversely, in the approaches where the MRO function is

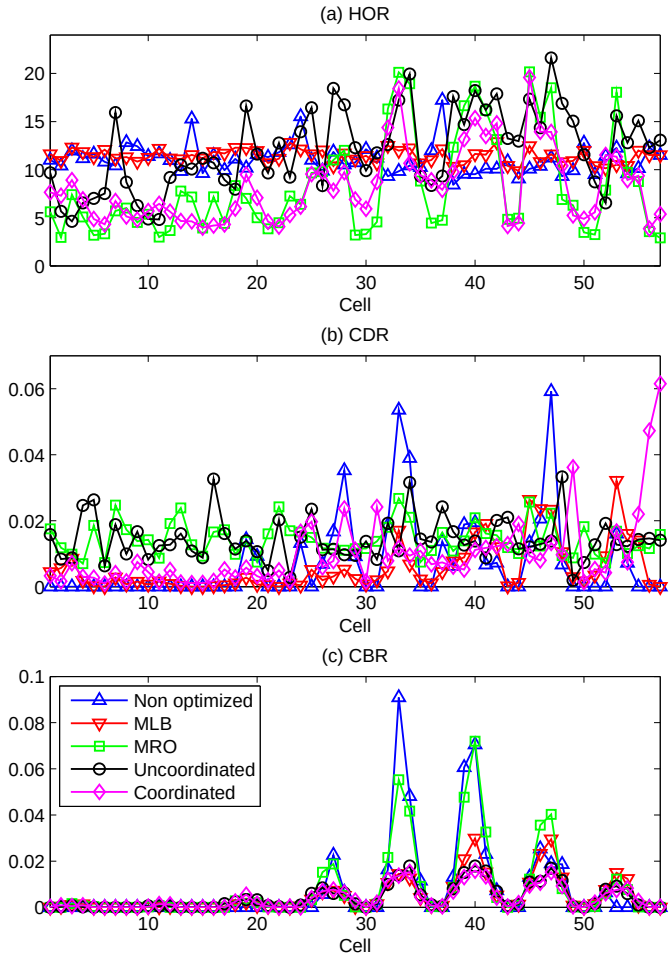

Figure 6.22: KPIs measured per cell at the end of the simulation for different approaches

included, the HOR is increased mainly in those cells experiencing high CDR (e.g. cells 33, 40 and 47), while the HOR is decreased in cells with CDR close to zero (e.g. cells on the left part of the figure), except in the uncoordinated case. The main effect of such a decrease in HOR is that the CDR [see Fig. 6.22(b)] is increased in those cells whose initial value is very low, except in the coordinated approach. Finally, regarding the CBR, it is highlighted that the CBR is initially very high in the congested area (around cells 33, 40 and 47), where the CDR is also initially high due to the strong interference existing in that area.

Finally, Fig. 6.23 shows the HOM values in each adjacency of the scenario at the end of the simulation. Note that the congested adjacencies are in the right part of the figure (for clarity, the adjacency labeling has been omitted). As it can be observed, the MLB approach keeps the HOMs to the default value of 3 dB in the non-congested cells (e.g. cells on the left part of the figure), while they are modified in the congested cells according to the measured CBR. In the MRO approach, the HOMs are decreased in the congested cells (down to zero) in order to reduce the call dropping, while they are increased in the non-congested cells with the aim of decreasing the HOR. In the uncoordinated approach, as a result of the negative interaction between SON functions, the evolution of the HOMs do not have a reasonable behavior, since the HOMs are either increased or decreased in cells with similar conditions. In the coordinated approach, the HOMs are set to $\sim$6 dB in the non-congested cells since, the MRO function is disabled when the HOMs are around this value. As a result, a good trade-off between the KPIs is achieved.

6.3 Conclusions

In this chapter, a comprehensive sensitivity analysis of the HO parameters (i.e. the HOM and the TTT simultaneously) has been carried out for different traffic load levels and user speeds. Performance has been assessed by measuring the CDR and the HOR to quantify the user experience and the HO signaling load, respectively.

Simulation results show that the network is more sensitive to variations of the HOM. In addition, the adjustment of TTT does not provide greater benefit than that obtained by adjusting HOM, meaning that a SON algorithm tuning HOM would be a simple but effective solution for MRO. For this reason, an FLC that adaptively modifies HOMs has been proposed. Such an FLC has been assessed for different parameter optimization levels (network-wide, cell-wide and cell-pair-wide) and different situations. In addition, three different FLC configurations have been assessed to set the optimal behavior, based on the CDR and the HOR, and regarding different system load levels and user speeds.

Results show that cell-pair-wide optimization provides more stable global indicators, since it can adapt to the specific radio conditions of each cell-pair. At this optimization level, the FLC improves network performance, achieving a good trade-off between CDR and HOR, even if an error model is considered in the RSRP measurements. Regarding the proposed FLC configurations, it is highlighted that RB_2 can lead to excessive values of CDR and severe oscillations due to large changes in the HOM. A more conservative approach, RB_3, is shown as the best

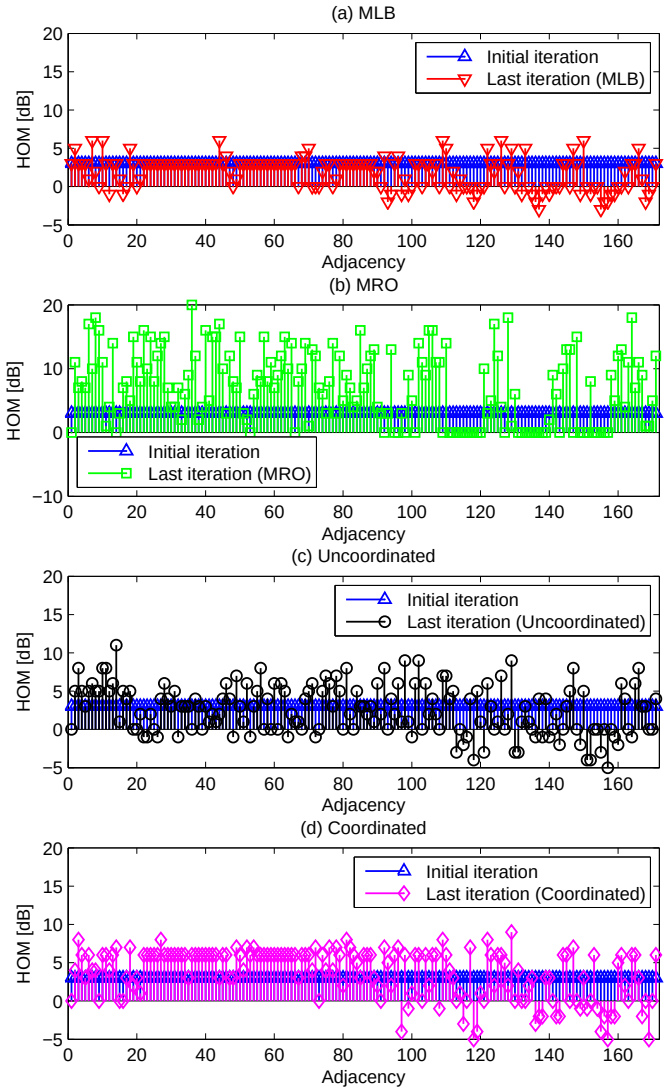

Figure 6.23: HOM values at the end of the simulation for different approaches

configuration in all situations analyzed in this work, since it provides lower values of CDR than RB_1 while keeping a similar HOR, especially for high-speed users.

To provide good operation of the proposed MLB and MRO schemes when they are simultaneously executed in the network, a coordination algorithm has also been proposed. Results show that the uncoordinated execution of both functions is far from optimal performance. Conversely, the proposed SON coordination algorithm, based on switching off the SON function that can negatively affect the operation of other functions in specific situations, has shown to be an effective solution. In particular, the coordinated approach can alleviate a congestion situation at the expense of a slight increase in CDR, while a significant reduction in the HOR is also achieved.

Chapter 7

Traffic Steering

This chapter deals with the problem of TS in HetNets. Firstly, the problem is formulated as a network parameter optimization problem, including a description of the deployment scenario used to evaluate the proposed TS techniques and a description of the involved mobility procedures and system measurements. Then, a static approach based on manually adjusting specific network parameters in both idle and connected mode is proposed. After this, a novel dynamic approach for TS in connected mode is presented. Such an approach is based on an optimized self-tuning scheme that automatically adapts to network variations, improving network performance. Finally, a comprehensive performance analysis of the proposed methods is carried out based on simulations.

7.1 Problem formulation

The infrastructure of current cellular networks must evolve to cope with the increasing demand for mobile-broadband services. This need of extra capacity comes from the increasing complexity in the mobile terminals (presently called smartphones), the growing demand for online applications (such as video and music streaming services) and the increasing number of hotspots (small areas with high demand of traffic). In this context, HetNets is a new paradigm that attempts to meet these new user demands which cannot be served by conventional cellular architectures. A HetNet is composed of several subnetworks which are individually called layers. Technically, a network layer is a set of cells with a number of features in common which depend on the specific network deployment. In this work, a network layer is given by a certain RAT, cell type (referring to the cell size) and frequency carrier. Firstly, according to the RAT, networks can be based on mature technologies (e.g. GSM, UMTS/HSPA, WiFi) and recent technologies (e.g. LTE), while technologies under investigation such as LTE-A could be included in the future. Secondly, another category is related to the cell size, so that layers can implement macrocells (the largest), microcells, picocells or femtocells (the smallest). The main advantage of deploying Small Cells

(microcells, picocells, femtocells) is that cellular coverage and capacity can be improved for both indoor and outdoor spaces, where femtocells are especially a low-cost way of providing hotspot capacity or removing coverage holes in urban areas. Thirdly, even assuming that the network layers have the same cell type and RAT, they can also be differentiated by the carrier frequency at which the layer operates, which depends on the radio spectrum licenses acquired by the operator. Finally, other differences between layers are given by the presence of new network elements (e.g. relays), alternative transmission solutions (e.g. distributed antennas), etc.

In HetNets, the UE can select the preferred network layer among several candidates, since the coverage area of those network layers is partially or totally overlapped. The concept of TS includes those decisions made by the operator to modify the user distribution across the layers according to a policy or specific objectives. Such decisions can also depend on additional issues such as the availability of technologies in the terminal or the service type. Thus, the potential of steering a user connection in HetNets brings new challenges to the operators [21] [45].

In this work, TS techniques based on both static and dynamic adjustments of mobility parameters in HetNets are investigated. On the one hand, in the static approach, a cell reselection algorithm (in idle mode) considering different layer priorities and the inter-RAT HOs (in connected mode) are used to find the optimal user distribution across the network layers according to a specific TS policy. More specifically, firstly, the problem of allocating Absolute Priorities (APs) to network layers for cell reselection is analyzed. Secondly, a procedure to select the optimal thresholds of the 3GPP events that trigger the inter-RAT HOs is proposed. In this case, the problem arising from the use of HO triggering events based on the signal level is addressed. When the events are based on the signal level instead of the signal quality, the thresholds involved in these events require a more precise adjustment, especially in multi-layer scenarios, where the location of low-power nodes within the macrocell may determine the adjustment of the thresholds. On the other hand, in the dynamic approach, a TS technique based on automatically adjusting HO parameters in HetNets is proposed. In particular, an FRLS that dynamically adapts the thresholds of the inter-RAT HO triggering condition to meet a TS policy is designed. The proposed techniques in both static and dynamic approaches are assessed in a realistic scenario thoroughly deployed to cover hotspots with LTE picocells, so that the TS policy is to offload traffic to the pico layers in order to use more efficiently the radio resources and improve service performance. The main contributions of this work are the design of an algorithm to simplify the task of adjusting the inter-RAT HO thresholds for TS purposes and the flexibility of the proposed algorithm in the dynamic approach to support different operator policies and its capability to adapt to network variations.

The rest of this section is devoted to the deployment scenario, the mobility management algorithms and the system measurements used for the TS techniques in this work. The proposed procedures for static adjustment of mobility parameters in both idle and connected mode are presented in Section 7.2. In Section 7.3, the structure of the proposed self-tuning scheme in connected mode and its optimization are explained. Section 7.4 describes the simulation setup and discusses the results. Finally, Section 7.5 draws the main conclusions of this study.

7.1.1 Deployment scenario

A key aspect to select the deployment scenario that will be used to assess the proposed algorithms is the heterogeneity expressed by the presence of different RATs, cell sizes, frequencies, hotspots, etc. in the network. However, any combination of these factors is not always a relevant deployment. Thus, the scenario must also be realistic. For these reasons, the multi-RAT macro-pico scenario described in Fig. 7.1 has been adopted in this work. Such a scenario is also representative of multiple challenges arising from HetNets scenarios, as described in the following paragraphs.

The deployment scenario is composed of four network layers, each of which comprises all the cells of the same characteristics. As previously stated, in this work, a network layer is given by a certain frequency carrier, RAT and cell type (referring to the cell size). An HSPA escape carrier, F2, has been included as another macro layer, named layer 2, which is free of interference from other layers and it is typically used by operators to provide additional capacity to macro users [41]. These two layers are co-sited (i.e. base stations are located in the same position). The presence of hotspots forces the operators to provide more capacity in those areas by deploying cells of lower sizes. Therefore, in the deployment scenario, LTE and HSPA pico layers have been deployed in areas with hotspots and these two layers are also co-sited. This configuration could be used in an early stage of LTE deployment in which LTE picocells have been deployed firstly without LTE macro coverage. In addition, there is no picocell clustering in the deployment scenario, i.e. picocells are far enough away from each other. This means that TS between non co-sited picocells cannot be properly performed in this scenario. Another feature drawn from Fig. 7.1 is that layers 1 and 3 are co-channel interferers. As a result, the interference induced by the co-channel layer would be large in the serving cell edge.

In the deployment scenario, mobility management is based on algorithms standardized by the 3GPP. Intra/inter RAT cases and intra/inter frequency cases when the user changes of cell are all covered in [165][35][166]. The following section describes the mobility management algorithms used in this work for TS.

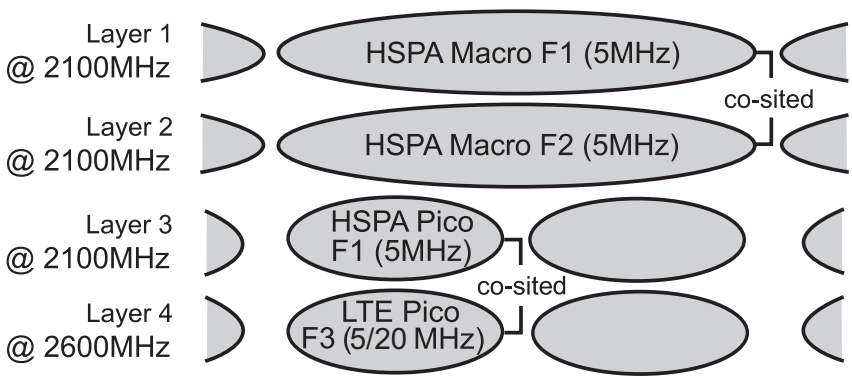

Figure 7.1: Deployment scenario

7.1.2 Mobility management

AP-based cell reselection algorithm

The idle mode is the state in which no dedicated resources have been established for the UE in the radio access network. In idle mode, the UE reselects a new cell to camp on it if the cell reselection criteria is fulfilled. Traditionally, the cell-ranking criterion R and the cell selection criterion S have been evaluated in this process [165]. However, in a context of different frequencies and RATs, AP may be provided to the UE for cell reselection.

APs is a feature that allows the operator to prioritize inter-frequency and inter-RAT network layers during the cell reselection process. Firstly, the UE finds candidate cells by checking the criterion S:

$$S_{rxlev} = Q_{rxlevmeas} - Q_{rxlevmin} > 0 \tag{7.1}$$

&

$$S_{qual} = Q_{qualmeas} - Q_{qualmin} > 0, \tag{7.2}$$

where $Q_{rxlevmeas}$ and $Q_{qualmeas}$ are the measured signal level and signal quality respectively, and $Q_{rxlevmin}$ and $Q_{qualmin}$ are the minimum required value for each of the previous measurements. Once the criterion S is fulfilled, the following condition depends on the cell priority. If the target cell has higher priority than the serving cell, the condition to be satisfied is:

$$S_{qual,t} > Thresh_{X,HighQ}, \tag{7.3}$$

where $Thresh_{X,HighQ}$ is the threshold (in dB) used by the UE on the target cell t when reselecting towards a higher priority frequency or RAT. If the priority of the target cell is lower or equal than the serving cell, then there are two conditions to be fulfilled:

$$S_{qual,s} < Thresh_{Serving,LowQ}, \tag{7.4}$$

&

$$S_{qual,t} > Thresh_{X,LowQ}, \tag{7.5}$$

where $Thresh_{Serving,LowQ}$ is the threshold (in dB) on the serving cell s and $Thresh_{X,LowQ}$ is the threshold on the target cell t. Note that the above conditions are referred to the signal quality, but they can be also based on the signal level. In LTE and HSPA, when absolute priority information for inter-RAT and inter-frequency cases is available, then the AP-based cell reselection algorithm is used. The conditions to be applied between the different cases (i.e. HSPA to HSPA, HSPA to LTE, etc.) are the same, but the signal measurements are technology-dependent. When multiple cells of different priorities are suitable for reselection by fulfilling the above conditions, cells of higher priority will take precedence over a lower priority frequency or RAT. For intra-frequency and equal priority inter-frequency cases, the criterion R is applied.

The criterion R is a cell-ranking based on either of the signal quality or the signal level.

An example of the cell reselection when APs are used in LTE is shown in Fig. 7.2, where the signal quality received by a UE from two cells with higher/lower priority is drawn. As it can be observed, the UE firstly reselects towards a cell of the lower priority layer. After this, the UE returns to the initial layer. Note that the conditions shown in this section must be fulfilled during a time interval named $T_{reselection}$. In Section 7.2.1, the cell reselection priority levels will be assigned to the network layers of the deployment scenario according to the TS policy.

Inter-RAT HO algorithm based on the B2/3A events

The connected mode is the state in which dedicated resources have been established for the UE. The HO is commonly the procedure that preserves the connection when the user moves around the network in connected mode. Inter-RAT HOs refer to those HOs carried out between cells from different RATs. An HO from LTE to HSPA is performed when the B2 event is triggered, that is, the RSRP of the LTE serving cell s becomes worse than the threshold $B2\_1$ and the RSCP of the HSPA target cell t becomes better than the threshold $B2\_2$ [35]:

$$RSRP_s < B2\_1 \quad \& \quad RSCP_t > B2\_2. \tag{7.6}$$

Similarly, an HO from HSPA to LTE is performed when the 3A event is triggered [166]. In this case, the thresholds $3A\_1$ and $3A\_2$ are used for evaluation:

$$RSCP_s < 3A\_1 \quad \& \quad RSRP_t > 3A\_2. \tag{7.7}$$

The previous measurements performed by the UE are based on the signal level. However, such measurements can be also referred to the signal quality, so that the RSRQ and the CPICH

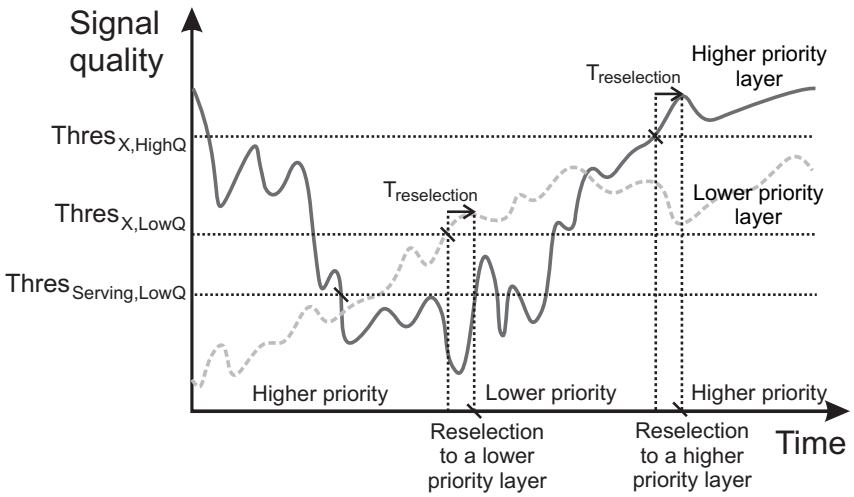

Figure 7.2: Example of the AP-based cell reselection

Ec/No are used for measuring LTE and HSPA cells, respectively. The concept of quality (e.g. the RSRQ) sometimes requires certain level of abstraction and complexity to draw inferences from the measurement analysis. Conversely, measurements based on the signal level (e.g. the RSRP) keep a closer relationship with the distance, which is usually more preferable from the operator perspective. For this reason, in this work, the measurement type for triggering HO events is based on the signal level instead of the signal quality. In a context of HetNets, this choice poses some challenges to the adjustment of the B2/3A thresholds, especially with the presence of different cell sizes in the network. Section 7.2.2 discusses more about how to define these thresholds from TS purposes.

7.1.3 System measurements

To quantify the benefits of the proposed algorithms and for comparison with reference cases, the following KPIs are used in this work:

- *#Resel*: the total number of cell reselections carried out in the overall network. It can be given per unit of time.
- *#HO*: the total number of HOs performed in the overall network. It can be given per unit of surface.
- *PP HO Ratio*: the ratio of the number of ping-pong HOs to the total number of HOs (*#HO*). A ping-pong HO occurs when the UE is handed over to a new cell and it is handed back to the source base station in less than a specific time.
- *RLF Ratio*: the number of RLFs occurred in the overall network divided by the total number of HOs (*#HO*). A RLF occurs when the radio channel signal strength is weak to keep the UE connected to the network.
- *Dropping Ratio*: the number of dropped calls to the total number of carried calls.
- *THR*: the average of the instant throughput or data transfer rate experienced by a UE, measured in bits per second.
- *PRB utilization*: the ratio of the occupied PRBs to the total number of PRBs of a network layer. A PRB is the minimum amount of radio resources that can be scheduled for transmission.
- *UE distribution*: the number of UEs connected to a network layer divided by the total number of connected UEs in the network.

The KPIs *#Resel* and *#HO* allow to estimate the signaling cost associated with a TS technique.

7.2 The static approach

7.2.1 TS in idle mode

In this section, firstly, different mechanisms in idle mode for TS purposes are briefly described, highlighting the potential of the cell reselection with absolute priorities over other techniques in HetNets. After this, some important issues arising from the adjustment of cell reselection parameters are discussed.

A survey of TS techniques in idle mode

In practice, a TS policy consists of enforcing a user distribution across the layers so that the resource utilization is optimal according to that policy. Since the HO has a signaling cost and a data transferring cost, it is important to achieve the optimal user distribution from the idle mode. A full alignment of user distributions in both idle and connected mode also avoids the ping-pong effect between layers when changing of mode.

In idle mode, the cell to which the user is attached is called the camped cell, the procedure of selecting a cell after switching on the UE is called cell selection, while the procedure of selecting a cell due to mobility is called cell reselection. Various mechanisms allow to modify the user distribution in idle mode [41]. For instance, Hierarchical Cell Structure is a feature to provide different priorities to large and small cells for cell reselection. However, this feature is intended to prioritize mobiles in high mobility to reselect towards the large cells in order to avoid continuous reselections. As a result, this functionality would be in part limited in a more heterogeneous environment where a layer is not only determined by the cell size and there can also be different objectives, not only those related to high speed users. Cell Barring is another feature that can be used by operators to bar a cell on which the UE cannot camp, but such a rigid solution could lead to sub-optimal performance. Another technique is Basic Biasing, which is based on adjusting specific offsets involved in the cell reselection process to make the cells more or less attractive to be selected during this process. In the intra-frequency case, this means that the range of the area where the cell is likely to be selected by cell-edge users can be extended or reduced. However, in recent technologies such as LTE, Basic Biasing can only be applied to cells belonging to the same RAT, which is a limitation from the TS perspective. In HetNets scenarios, the coverage areas can be fully overlapped and there can also be different RATs. In this case, the technique known as AP becomes a powerful means to steer users towards a different RAT or frequency, whether they are cell-edge users or not. In particular, this technique is based on allocating different priorities to the network layers, so that the user distribution in idle mode can be effectively modified by simply changing the priority of the layers. More details of this mechanism are provided in Section 7.1.2.

Adjustment of APs for TS purposes

In the AP-based cell reselection algorithm, both mobility parameters, i.e. the thresholds and the APs, can be tuned to perform TS strategies. For instance, the threshold used to reselect towards higher priority could be decreased to make the target cell more attractive. However, the APs can also modify the user distribution across the layers without affecting the signal level of the steered users, which is typically a more appropriate solution.

To allocate APs to networks layers, several considerations must be taken into account. First, according to the 3GPP [165], those network layers belonging to the same RAT and sharing the same frequency must have the same AP. Thus, in the deployment scenario (Fig. 7.1), layers 1 and 3, which share frequency $F1$, cannot have different AP level. Another limitation imposed by the 3GPP is that two RATs sharing the same priority level is not supported. In the deployment scenario, this implies that the pico layers cannot have the same priority, so that one layer takes higher priority for the macro offloading. As layer 1 causes co-channel interference with layer 3, the highest priority should be allocated to layer 4. Looking at the previous constraints together with the objective of offloading traffic from the macro layers, two candidate sets of AP allocation are proposed. The difference lies in the relative priority between layers 1 and 2, that is, whether the macro escape carrier takes priority over the main carrier or it is just the opposite. Thus, given that 0 is the lowest priority level, the two proposed sets of APs for the deployment scenario are:

$$AP_1 = [L1, L2, L3, L4] = [0, 1, 0, 2]; AP_2 = [1, 0, 1, 2], \tag{7.8}$$

where LX refers to layer X. In both cases, it is expected that a user located in a hotspot has higher probability of starting a connection from the LTE layer, according to the TS policy.

7.2.2 TS in connected mode

When the UE is in connected mode, TS can be performed by forced HOs, cell barring or adjusting HO parameters. Among these techniques, the latter is the simplest mechanism because it does not need to be user-specific as forced HOs and it is not as rigid as cell barring. For this reason, in this section, the HO parameters are tuned to satisfy a specific TS policy. In particular, this study is focused on the inter-RAT HO parameters corresponding to the B2/3A events defined by the 3GPP. Unlike other HO types (e.g. intra-frequency HOs), the triggering condition for inter-RAT HOs is necessarily based on comparisons of the received signal with absolute thresholds, since signal levels of different RATs cannot be compared between them. Such a constraint leads to a higher degree of freedom from the TS perspective when adjusting the HO parameters. In this section, several issues and challenges concerning the adjustment of the associated parameters are discussed. In particular, some assumptions are made to reduce the number of HO parameters needed to perform a TS strategy. In addition, a problem addressed in this example is related to the fact that, in HetNets scenarios, the location of Small Cells (e.g. picocells) within a macrocell may determine the adjustment of the HO parameters between those layers. Since up to four thresholds can be involved in the case of inter-RAT HOs, a procedure for adjusting the HO

parameters is proposed in this section.

The first challenge arising from the adjustment of HO parameters is that they are typically adjusted to avoid low signal levels or quality in order to keep the connection alive. However, in the context of HetNets, there can be many other reasons to trigger an HO assuming that the coverage areas of the network layers are overlapped. Following the 3GPP standard, it is possible to define different thresholds for the same HO triggering event according to particular policies. For instance, radio-driven HOs are concerned to those HOs carried out when the UE experiences poor signal level or quality, while TS-driven HOs are related to those HOs triggered by TS reasons, such as maximizing the user throughput. In the first case, UEs will be generally handed over to cells with better quality. In the second case, UEs will be generally handed over even under good signal conditions. Since these two cases are complementary, the operator could define two different sets of thresholds for a specific HO triggering event in the network.

TS is performed here by adjusting the thresholds of the (inter-RAT) B2 and 3A events in LTE and HSPA, respectively. As mentioned before, in the deployment scenario (Fig. 7.1), $L4$ has been selected to offload traffic from macrocells because it does not receive interference from any other layer. A thorough analysis of the concerned scenario highlights that the adjustment of the B2/3A thresholds not only affects the inter-RAT HOs between HSPA macrocells (L1, L2) and LTE picocells (L4), but also between picocells of different RATs (L3, L4). This latter case can be also divided into two different cases: inter-RAT HOs between non co-sited picocells and inter-RAT HOs between co-sited picocells. The impact of inter-RAT HOs between non co-sited picocells depends on the concentration of picocells within the macro area, meaning that a massive deployment of picocells will result in a major impact. On the other hand, the number of inter-RAT HOs between co-sited picocells is expected to be negligible because of the difficulty of fulfilling both conditions of the inter-RAT event. To explain this, consider that the serving and target base stations are located in the same position and the user is approaching or moving away from the base stations, so that the signal levels received from those cells are both increased or decreased. In this case, it is not easy to fulfill that the serving cell becomes worse than a threshold, and the target cell becomes better than a threshold. This is in contrast with the common situation for which the HO triggering condition has been defined, where the user typically leaves a cell to enter a neighboring (non co-sited) one. Thus, if it is assumed that inter-RAT HOs between pico layers have minor impact on the user distribution across the layers (in this case, due to a low deployment of picocells), the macro offloading would be mainly determined by the inter-RAT HOs between the macrocells and the pico layer L4. It is noted that, if a larger deployment of picocells were considered in the scenario, a certain hysteresis region should be considered when adjusting the B2/3A thresholds in order to avoid ping-pong HOs between non-cosited HSPA and LTE picocells due to the user mobility.

A single set of B2/3A thresholds defined in the network might be enough for TS. However, it is also possible to have the thresholds defined per layer-pair. The deployment scenario includes two macro-pico layer-pairs, as there is an additional macro layer given by the HSPA escape carrier ($F2$). Unlike the HSPA main carrier ($F1$), $F2$ does not receive interference from any other layer. This means that the optimal B2/3A thresholds are not necessarily the same for

these layers. The benefit derived from this consideration will be analyzed in Section 7.4.

A problem arising from this scenario is that, due to the fact that the cells are of different size and their coverage areas are overlapped, setting the B2/3A thresholds for TS purposes is not a simple task, especially if the HO triggering condition is based on the signal level, instead of the signal quality. For instance, suppose that the user U_1 is connected to the macrocell M_1 and is coming into a hotspot covered by a femtocell named P_1, as shown in Fig. 7.3. The TS strategy followed by the operator is to offload traffic from the macrocells towards L4 because it does not receive interference from any other layer. Thus, due to the TS policy, the thresholds $3A\_1$ and $3A\_2$ have been previously set so that U_1 fulfills that the RSCP from M_1 is lower than $3A\_1$ and the RSRP from P_1 is higher than $3A\_2$. As a result, the user U_1 is handed over to the neighboring LTE picocell P_1. Let consider now user U_2, which is located in P_2 (closer to the macrocell base station) and initially connected to the macrocell M_1. This user probably will not perform an HO to the closest LTE picocell because the condition involving $3A\_1$ would not be fulfilled (RSCP from M_1 is too high). Such a situation highlights that the adjustment of $3A\_1$ to offload the macrocell depends on the picocell location. To avoid the distance dependence, setting a very high value for $3A\_1$ is similar to removing the first condition in (7.7) related to the serving cell (i.e. macrocell will be always worse than $3A\_1$). Then, by simply adjusting the parameter related to the picocell, $3A\_2$, the amount of UEs offloaded to the picocell can be controlled.

The same approach is applied to the case in which the user is connected to an LTE picocell and he is leaving a hotspot. To send the UE to the HSPA macrocell, it is necessary to fulfill

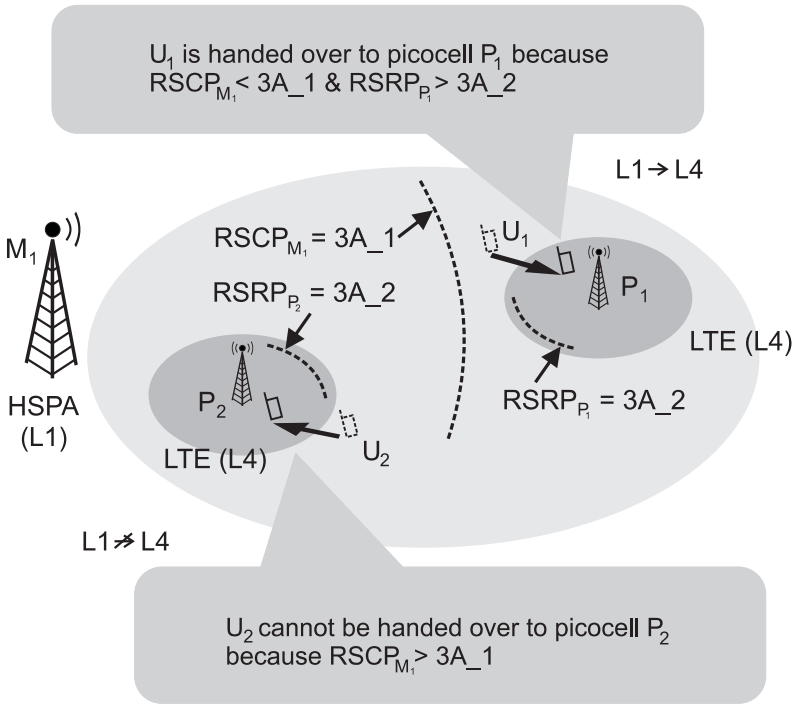

Figure 7.3: The impact of the measurement type in a multi-layer scenario

the condition in (7.6) related to the target cell that includes $B2\_2$, regardless of the picocell location. In this case, setting a very low value for $B2\_2$ would remove this dependence, so that the macrocell will be always better than $B2\_2$. It is noted that this configuration could be certainly dangerous, since the UE could be handed over to the macrocell with very poor signal level. Such a situation can be avoided if two different sets of B2/3A thresholds are defined, that is, one set for radio-driven HOs and other for TS-driven HOs. Conversely, if a single set of B2/3A thresholds is considered or, simply, a more precise adjustment of those thresholds is needed, a novel method is proposed here to adjust the thresholds of B2 and 3A events for TS. The basis of this method is summarized in Algorithm 7.1.

Algorithm 7.1 simplifies the problem to one parameter in order to determine the area where the UEs should connect to the picocell. Note that such a problem can be applied to any HetNet scenario in which the network deployment comprises cells of different size and RAT. If $B2\_2$ and $3A\_1$ have been set to be always fulfilled, $B2\_1$ and $3A\_2$ can be used to define the concerned area in both directions, i.e., moving from LTE to HSPA and vice versa. In principle, these two parameters could have the same value, but a certain hysteresis (Δ) can be also applied to avoid the ping-pong effect between RATs. Step 2 consists of a sensitivity analysis of $B2\_1$ in order to select a value that optimizes the resource utilization. A set of values selected from the normal operating range of $B2\_1$ is assessed by looking at the main KPIs in order to find the optimal value. Then, $B2\_1$ is set to this value. The remaining steps are devoted to optimize $B2\_2$ and $3A\_1$. In the case of $B2\_2$, there may exist a trade-off between keeping the optimal resource utilization achieved in step 2 and avoiding low values which jeopardize the connection quality.

In live networks, context factors such as the system load are varied frequently and dynamically. To avoid that such variations affect the analysis involved in Algorithm 7.1, the performance indicators should be collected using a measurement period long enough. For example, as there are typically two distinguished traffic patterns within a day (i.e. daily and nightly traffic patterns), the measurement period could be the hours during the day. Thus, a new control parameter

Algorithm 7.1. Adjustment of B2/3A thresholds for TS

1. Initially, set:
$B2\_2 \rightarrow -\infty$,
$3A\_1 \rightarrow +\infty$,
$3A\_2 = B2\_1 + \Delta, \quad \Delta = 4dB$ [167].
2. Sensitivity analysis of $B2\_1$
(find the optimal value according to performance indicators)
3. Set:
$B2\_1 \rightarrow$ *optimal value*.
4. Sensitivity analysis of $B2\_2$
5. Sensitivity analysis of $3A\_1$
6. Set:
$B2\_2 \rightarrow$ *optimal value*.
$3A\_1 \rightarrow$ *optimal value*.

setting would be tested every day during the same time interval to ensure similar conditions. Note that this optimization process can last several weeks, which is the typical duration of field trial campaigns performed by operators and manufacturers. Then, the optimal settings can be fixed in the network during months or even years. In addition, Algorithm 7.1 can be executed periodically to cope with long-term changes in the traffic patterns, e.g. the center of a city becomes crowded, a new shopping center is built, etc.

7.3 The dynamic approach

The dynamic approach proposed in this section is conceived to solve the problem addressed in Section 7.2.2 in a different way. In this case, the problem of adjusting the thresholds of B2 and 3A events for TS has been thoroughly reduced to one parameter, $B2\_1$. For simplicity, the other two parameters in Algorithm 7.1, $B2\_2$ and $3A\_1$, are set to the values corresponding to the 1% and 99% of the cumulative distribution function of the RSCP in the network, respectively. This configuration keeps a good trade-off between the independence with the picocell location and avoiding HOs to bad cells. Additionally, in the dynamic approach, a single set of B2/3A thresholds in the network is assumed. The motivation of this assumption is derived from the results presented in Section 7.4, where no gain is achieved by defining thresholds e.g. per layer-pair in the deployment scenario (Fig. 7.1). Thus, the basis of the proposed optimization algorithm is to adapt $B2\_1$ in order to perform the TS strategy. As previously stated, to take full advantage of the LTE picocells, the TS strategy addressed in this work is to offload as much traffic load as possible from the macro layers to L4 in order to enforce a user distribution across the layers which is optimal from the resource utilization perspective. However, such an imprecise objective can be fulfilled by optimizing one or more KPIs, e.g. the throughput, the RLF ratio, etc. The algorithm proposed in this work is an FRLS that optimizes a weighting function that combines these KPIs. The following sections describe the structure of the proposed FRLS. This scheme is based on, firstly, designing the self-tuning scheme (an FLC) and, then, applying the fuzzy Q-Learning algorithm to the self-tuning scheme.

7.3.1 Self-tuning scheme

The proposed self-tuning scheme is based on an FLC following the Takagi-Sugeno approach [116]. Such an FLC consists of one input signal and one output signal, so that the objective is to build a non-linear function in one variable. In particular, the input of the FLC is the $B2\_1$ threshold and the output is the increment (or the decrement) $\Delta B2\_1$ to be added to $B2\_1$ for the next optimization step (or epoch), so that:

$$B2\_1(t+1) = B2\_1(t) + \Delta B2\_1(t). \tag{7.9}$$

The range of variation of $B2\_1$ is considered to be from a minimum of -120 dBm to a maximum of 80 dBm, since values outside this range lead to undesired values of the KPIs. In addition, the

maximum change $\Delta B2\_1$ carried out during each optimization epoch is considered to be 4 dB. This assumption comes from the sensitivity analysis presented in Section 7.4, where performance indicators are quite sensitive to changes of higher magnitudes in that parameter.

The design of an FLC involves the following tasks: defining the fuzzy sets and membership functions of the input signals, and defining the linguistic rule base which determines the behavior of the FLC. Thus, the first step in the design process is to partition the input space into various fuzzy sets by means of membership functions. Each fuzzy set has a linguistic term, such as 'high' or 'low', associated. The membership function, denoted by $\mu_z(x)$, quantifies the degree of membership of an input value x to the fuzzy set z. Since the fuzzy membership functions are commonly overlapping, the transition between states is carried out in a smooth manner, that is, without significant abrupt changes in the FLC behavior. In this work, the membership functions, depicted in Fig. 7.4, are considered to be trapezoidal to avoid excessive overlapping between them, as it would happen if triangular functions were used. As observed, five fuzzy sets have been defined for the input to achieve a reasonable granularity in the input space, while keeping the number of states small to reduce the set of control rules. In particular, $B2\_1$ can be 'very low', 'low', 'medium', 'high' or 'very high'.

The next step consists of defining the inference engine of the FLC, which allows to express the knowledge in linguistic terms by a set of rules following a syntax of the type IF-THEN to set the control strategy. An example rule i for the proposed FLC is the following: 'IF ($B2\_1$ is *very low*) THEN ($\Delta B2\_1$ is o_i)', where the output function is a constant value, o_i, which can be one of the following values (each value also has a label associated): -4 dB ('negative'), 0 dB ('null') and 4 dB ('positive'). For the definition of the rule output functions, the knowledge and experience of a human expert is generally used, but learning techniques can be also employed to adapt or refine rules. In this work, no a priori knowledge is assumed, so that the optimal value of $B2\_1$ could be in any of the states defined for the input. For this reason, to set the constant value of each rule output function, RL will be applied to the FLC. In particular, the

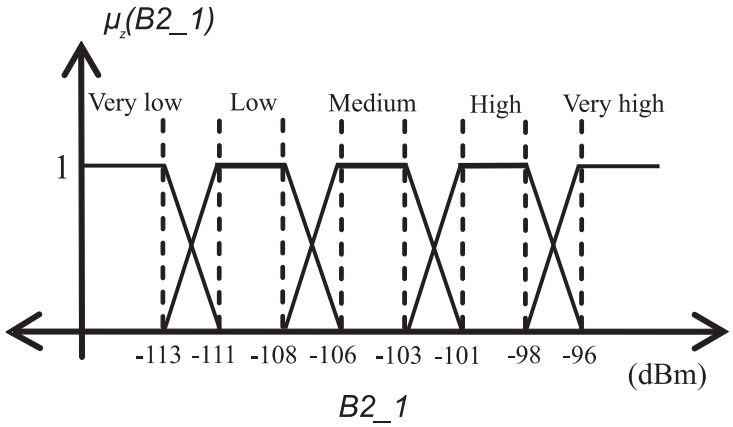

Figure 7.4: Membership functions of the input fuzzy sets

optimization algorithm will attempt to find the consequent o_i for the following rules:

$$IF\ (B2\_1\ is\ very\ low)\ THEN\ (\Delta B2\_1\ is\ o_1), \tag{7.10}$$

$$IF\ (B2\_1\ is\ low)\ THEN\ (\Delta B2\_1\ is\ o_2), \tag{7.11}$$

$$IF\ (B2\_1\ is\ medium)\ THEN\ (\Delta B2\_1\ is\ o_3), \tag{7.12}$$

$$IF\ (B2\_1\ is\ high)\ THEN\ (\Delta B2\_1\ is\ o_4), \tag{7.13}$$

$$IF\ (B2\_1\ is\ very\ high)\ THEN\ (\Delta B2\_1\ is\ o_5). \tag{7.14}$$

Note that the rule consequent, o_i, can be either 'negative', 'null' or 'positive'.

Once the FLC is designed, the execution of the FLC would involve three basic steps: fuzzification of the input, application of the inference engine and defuzzification of the output. Firstly, the fuzzifier transforms the continuous input into fuzzy sets by calculating the degree of membership to each fuzzy set. Then, the inference engine identifies the activated rules and calculates the fuzzy output values for each rule. Finally, the defuzzification process is in charge of aggregating the rules and calculating the output crisp value. The method used for calculating the output in this work is the weighted average. Thus, taking into account that the following condition is fulfilled:

$$\sum_{i=1}^{N} \mu_i(x) = 1, \tag{7.15}$$

the expression used for calculating the output is:

$$y(x) = \sum_{i=1}^{N} \mu_i(x) \times o_i, \tag{7.16}$$

where N is the number of rules, $\mu_i(x)$ is the degree of membership to the fuzzy set involved in the antecedent of rule i and o_i is the selected consequent for the same rule. Then, the output is rounded to the nearest integer, due to practical limitations when setting parameters in a real network. Finally, this value is added to the threshold $B2\_1$ and applied to the network. Note that $3A\_2$ must also be modified because of its relationship to the $B2\_1$.

7.3.2 Optimization of the self-tuning process

The optimization scheme showing the combination of the learning entity and the FLC is depicted in Fig. 7.5. For simplicity, since the network layout on which the assessment will be carried out is regular, only one agent has been defined in the concerned area, so that the modification made by the FLC affects all cells involving inter-RAT HOs. Note that, in the case of irregular networks, one agent per macrocell area modifying B2/3A thresholds within that area could be implemented. As shown in Fig. 7.5, the FLC input, given by the current value of $B2\_1$, corresponds to the

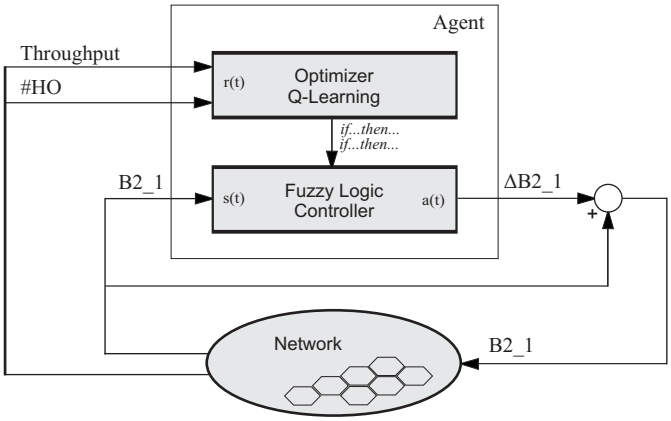

Figure 7.5: Block diagram of the reinforcement learning scheme for TS

state of the system, $s(t)$. The FLC output, given by the increment in $B2\_1$, represents the action of the agent, $a(t)$. Finally, the reinforcement signal $r(t)$ is built from various KPIs measured in the overall network to estimate the benefit or the loss obtained in performance after performing the action. This reinforcement signal or immediate reward, $r(t)$, has been defined in this work as follows:

$$r(t) = k \cdot (U(t) - U(t-1)), \tag{7.17}$$

where k is a constant factor and U is a utility function including KPIs to be maximized. The value assigned to k ($k > 0$) simply scales the q-values and it has been selected in this work to have q-values in the order of tenths. The utility function U determines the objective of the optimization process. The explanation for choosing $r(t)$ as the difference of U between two successive optimization epochs is that $r \geq 0$ would mean that the action performed was good and, otherwise, the action was bad.

The utility function U could include as many KPIs as the operator desires. In this work, the service experience for users is measured as instant throughput, while the costs for the operator are measured as signaling cost in terms of average number of HOs per UE per minute. Since the former has to be maximized and the latter minimized, the following expression for U has been defined:

$$U(t) = \rho \cdot \frac{THR\ (t)}{Ref\_THR} + \mu \cdot \left[1 - \frac{\#HO\ (t)}{Ref\_\#HO}\right], \tag{7.18}$$

where $THR(t)$ and $\#HO(t)$ are the KPI measurements (throughput and HOs, respectively) taken from the current optimization epoch, ρ and μ are constant weights determining the relative importance of each KPI in the equation, and Ref_THR and $Ref\_\#HO$ are constant reference factors to normalize each KPI in the equation. Such factors should be set so that both ratios are in the same order of magnitude (e.g. close to one) to aggregate these two quantities. For instance, they could be equal to the target values for the KPIs. Note that, in this case, the objective would not be to approximate the KPIs to the reference values, but to maximize or minimize them. On the other hand, ρ and μ could have different values depending on the

operator policy. For instance, $\rho = 1$ and $\mu = 0$ mean that the objective of the operator is to maximize the user satisfaction regardless the signaling cost. Thus, by simply modifying these weights, the proposed algorithm provides the flexibility to support different operator policies.

The proposed FRLS starts with no a priori knowledge, thus requiring some epochs to train the controller. After this time (called exploration), the consequents whose q-values are the highest for each rule are selected to be utilized in the exploitation phase. Formally, the exploration phase is given by setting $\epsilon = 1$ in the Q-Learning algorithm, while the exploitation phase is performed by setting $\epsilon = 0$. However, in live environments such as real networks, situations might vary along the time (e.g. due to traffic demand variations), so that the optimal parameter setting could be time-dependent. Since the agent can only partially observe the environment (by means of a limited number of KPIs), it would not always receive the same reward when taking an action from a given input state. Thus, there exists a need for self-adaptation to network variations, which could be achieved by simply combining the exploitation with some exploration. For instance, setting $\epsilon = 0.2$ would keep a good trade-off between exploration and exploration. The adaptation capability of the fuzzy Q-Learning algorithm will be analyzed in the next section.

7.4 Performance assessment

7.4.1 Simulation setup

The performance of the proposed TS techniques has been assessed with the dynamic system-level simulator covered in Section 4.3. Further details of the simulator implementation are found in [161]. The simulated scenario includes a macro-pico cellular environment whose macro layout consists of 7 regular hexagonal tri-sectorized sites and wrap-around is assumed. The pico layout is composed of 2 omni-directional sites per macro area, randomly located, and covering a hotspot of similar size. 68% of traffic is generated and confined within hotspots. Only the downlink is considered in the simulation, as it is the most restrictive link with the types of service used in this work for next-generation wireless networks.

Static approach

In the static approach, the service provided to the UEs is based on a realistic video streaming model, which generates traffic according to a source bit rate equal to 1024 Kbps. Considering this, the offered traffic in the network is calculated as follows:

$$\textit{Offered Traffic} = \frac{BR \cdot SL}{\overline{IAT'}}, \tag{7.19}$$

where BR is the service bit rate per session in Mbps, SL is the session length in seconds and

IAT' is the mean inter-call time in seconds in the concerned area, calculated as:

$$IAT' = \frac{IAT}{N_{users}}, \tag{7.20}$$

where IAT is the mean inter-session time per mobile in seconds and N_{users} is the number of mobiles in the concerned area. If the buffer at the UE is emptied, a re-buffering is needed and the video playout is interrupted. When the interruption time exceeds a specific threshold, the user is dropped out. The arrival rate of new connections is exponentially distributed. The main simulation parameters are summarized in Table 7.1.

In the case of the AP-based cell reselection algorithm, the following allocations of APs are evaluated: AP_0= [0 0 0 0], AP_1= [0 1 0 2] and AP_2= [1 0 1 2]. AP_0 is a reference setting allocating the same AP to the network layers and included for comparison with the proposed settings AP_1 and AP_2. The settings of B2/3A thresholds for inter-RAT HOs are the following: $B2\_1$=−104 dBm, $B2\_2$=−98 dBm, $3A\_1$=−92 dBm and $3A\_2$=−100 dBm. The motivation for setting those values is derived from the results of the inter-RAT HO study, presented later.

In the case of the inter-RAT HO algorithm, simulations have been carried out with AP_2 and 100% LTE penetration. For each parameter setting of the sensitivity analysis, an independent simulation of 150 s duration has been carried out. Note that this simulation time is large enough to obtain reliable measurements for the network size, the traffic model and the system load used in this work. In addition, network conditions remain fairly constant throughout the simulations. This situation can emulate e.g. the busy hour, the working hours in a business area, the daytime in the downtown area, etc. If the system load varies dynamically throughout the day in the real network, firstly the operator should identify the time frames in which the load remain fairly constant and then perform the optimization separately for each period. Alternatively, operators could set the parameters with the values optimized for the critical situation.

Dynamic approach

In the dynamic approach, the service provided to the UEs is based on a finite-buffer packet-based traffic model, where the source generates traffic according to a UE packet size of 400 Kb and a mean packet inter-arrival time (IAT) equal to 120 s. The main simulation parameters are summarized in Table 7.2.

The performance evaluation consists of two experiments to assess the operator policy flexibility and the adaptation capability. Such experiments are graphically described in Fig. 7.6, where two different cases per experiment have been defined: S_1 and S_2 are referred to the first experiment, while S_3 and S_4 correspond to the second experiment. To evaluate the policy flexibility, the two involved simulations are composed of three different phases, as shown in Fig. 7.6(a). In phase I (0-1500 s), the optimization algorithm explores possible consequents for the FLC rules by setting $\epsilon = 1$. Then, in phase II (1500-1600 s), the algorithm exploits the acquired knowledge ($\epsilon = 0$) to find the optimal $B2\_1$. Finally, the FLC is switched off in order to assess network

Table 7.1: Simulation parameters for TS (static approach)

Parameter	Configuration
System	HSPA, LTE
Layer	HSPA: macro, 5 Mhz @2100 MHz (F1 & F2); pico, 5Mhz @2100 MHz (F1). LTE: pico, 5 Mhz @2600 MHz (F3)
Cellular layout	Macro: hexagonal grid, 21 cells (3x19 sites), Inter-site distance = 0.5 km. Pico: 2 picocells / macro area
Propagation	Macro: 137.6 + 34.8 log10 (R) [Hata-COST 231]; 43 dBm. Pico: 140.7 + 36.7 log10 (R) [3GPP TR 36.814]; 37 dBm.
Shadowing	Gaussian, std: 8 dB (macro); 10 dB (pico) De-corr. length: 50 m (macro); 13 m (pico)
Users per macro area	100
Users per hotspot	34 (Hotspot radius = 40 m)
User speed	Hotspot: 3 km/h, Non-hotspot: 3, 50 km/h
Service model	Video streaming
Bit rate	1024 Kbps
Mean Inter-Call Time	30 s
Call duration	10 s
Dropping out	Interruption time = 10 s
Handover settings	Intra-freq: A3 (RSRP / Ec/No, offset=2 dB), A5 (RSRP / RSCP, A5_1= -111 dBm, A5_2= -109 dBm) Inter-freq: A3 (RSRQ / Ec/No, offset=4 dB) Inter-RAT: B2 / 3A (RSRP / RSCP) Time-To-Trigger=0.5 s
Reselection settings	$Thresh_{Serving,LowQ}$ = -13 dB, $Thresh_{X,LowQ}$ = -12 dB, $Thresh_{X,HighQ}$ = -10 dB, $Q_{rxlevmin}$ = -Inf, $Q_{qualmin}$ = -18 dB, $T_{reselection}$ = 1.2 s
Simulation time	150 s
Warm-up	50 s
Simulation time resolution	100 ms

performance in phase III (1600-2000 s). Initially, all the q-values are equal to zero, assuming no a priori knowledge. Two different policies have been defined for evaluation by simply modifying the KPI weights in the utility function U. S_1 defines $\rho = 1$ and $\mu = 0$ with the objective of maximizing the UE instant throughput, while S_2 sets $\rho = 1$ and $\mu = 0.5$ in order to keep a good trade-off between the throughput and the signaling cost.

The second experiment [Fig. 7.6(b)] attempts to adapt $B2\_1$ to network variations. In particular, the modeled variation is a change in the user spatial distribution, so that the net-

Table 7.2: Simulation parameters for TS (dynamic approach)

Parameter	Configuration
RATs	HSPA, LTE
Layers	HSPA: macro, 5Mhz @2100 MHz (F1 & F2); pico, 5 Mhz @2100 MHz (F1). LTE: pico, 20 Mhz @2600 MHz (F3)
Cellular layout	Macro: hexagonal grid, 21 cells (3x7 sites), ISD = 0.5 km. Pico: 2 picocells/macro-area
Propagation	Macro: 137.6 + 34.8 log10 (R) [Hata-COST 231]; 43 dBm. Pico: 140.7 + 36.7 log10 (R) [3GPP TR 36.814]; 37 dBm.
Shadowing	Gaussian, std: 8 dB (macro); 10 dB (pico) De-corr. length: 50 m (macro); 13 m (pico)
UE/macro-area	100
UE/hotspot	34 (2 hotspots/macro-area)
UE speed	Hotspot users: 3 km/h Non-hotspot users: 3 km/h and 50 km/h
Hotspot radius	40 m
Service model	Finite-buffer packet-based UE packet size = 400 Kb, mean packet IAT = 120 s
Handover settings	Intra-freq: A3 (RSRP / Ec/No, offset=2 dB), A5 (RSRP / RSCP, A5_1= -111 dBm, A5_2= -109 dBm) Inter-freq: A3 (RSRQ / Ec/No, offset=4 dB) Inter-RAT: B2 / 3A (RSRP / RSCP) B2_2=-118 dBm, 3A_1=-80 dBm Time-To-Trigger=0.5 s, $T_{HOpingpong}$=1 s
Reselection settings	$Thresh_{Serving,LowQ}$ = -13 dB, $Thresh_{X,LowQ}$ = -12 dB, $Thresh_{X,HighQ}$ = -10 dB Priorities: $P_{L1} = P_{L3}$; $P_{L1} < P_{L2} < P_{L4}$
Simulated time	2000 s (warm-up = 50 s)
Simulation step size	100 ms
Optimization algorithm	$\gamma = 0.95$, $\eta = 0.01$, $k = 100$, epoch time = 10 s Ref_THR = 1600 Kbps, Ref_#HO = 700

work abruptly changes (at t=0) from 100 UEs/macro-area and 34 UEs/hotspot (as in the first experiment) to 48 UEs/macro-area and 0 UEs/hotspot (i.e. no hotspot UEs). Note that non-hotspot UEs can be in the picocell area and that the change only affects the user distribution, i.e. picocells stay activated in both situations. Such distributions model, for instance, the daily and nightly traffic patterns, respectively. It is noted that the modeled abrupt change represents the worst case, so that the FLC needs the greatest time to adapt to the new UE distribution. For simplicity, only the policy used in S_1 has been used in this experiment, so that the objective of the TS strategy is to maximize the throughput. As shown in Fig. 7.6(b), S_3 consists of, firstly, resetting the q-values (acquired knowledge) obtained from the first experiment and then performing the three phases such as in the previous experiment: exploration ($\epsilon = 1$), exploitation

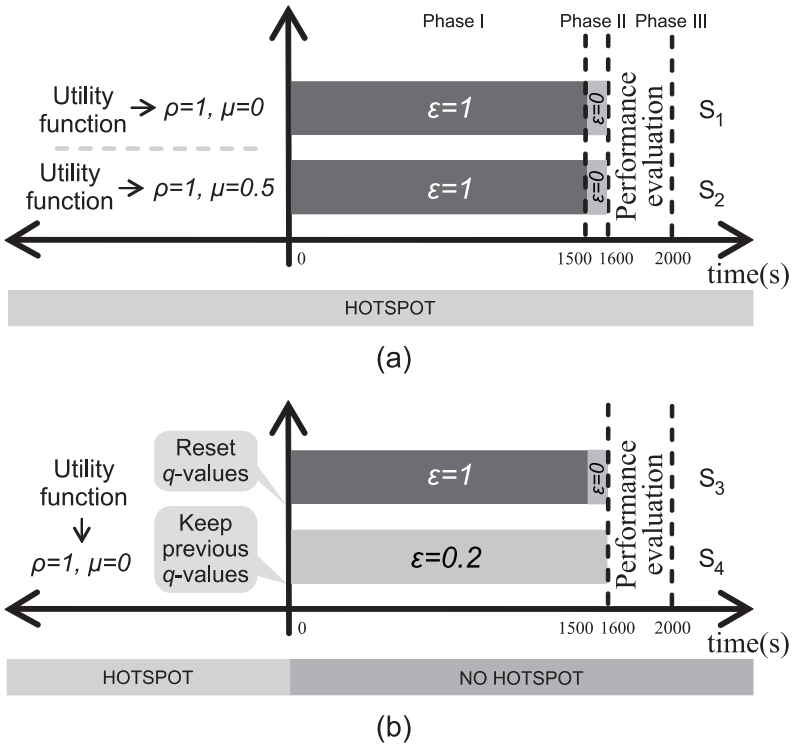

Figure 7.6: Performance evaluation of (a) the operator policy flexibility and (b) the adaptation capability

($\epsilon = 0$) and performance evaluation. S_4 initially takes the q-values from S_1 and sets $\epsilon = 0.2$ to keep 20% exploration throughout the simulation.

Finally, some additional simulations are performed to compare network performance ($\#Resel$, $\#HO$, etc.) between the proposed approaches and with other sub-optimal settings of $B2\_1$. In these cases, the simulated time is 50 s.

7.4.2 Performance results

Static approach

TS in idle mode.

For each allocation of APs, Fig. 7.7 shows the total traffic carried per macrocell area (i.e. two macrocells and four picocells), as well as the traffic carried per network layer and macrocell area. Note that, in a macrocell area, the offered traffic calculated using Eq. 7.19 with the parameter values shown in Table 7.1 is 33.333 Mbps, while in a hotspot the offered traffic is 11.333 Mbps. It is observed that, although the layers have the same bandwidth (i.e. 5 MHz), the capacity is different for each one. This is because the system capacity depends on the user distribution and how the interference affects each layer. For instance, as users are more concentrated in the picocells (i.e. closer to the base station) higher capacity for those cells (compared to macrocells) is expected. In addition, as $L1$ and $L3$ are co-channel interferers, lower capacity for those layers

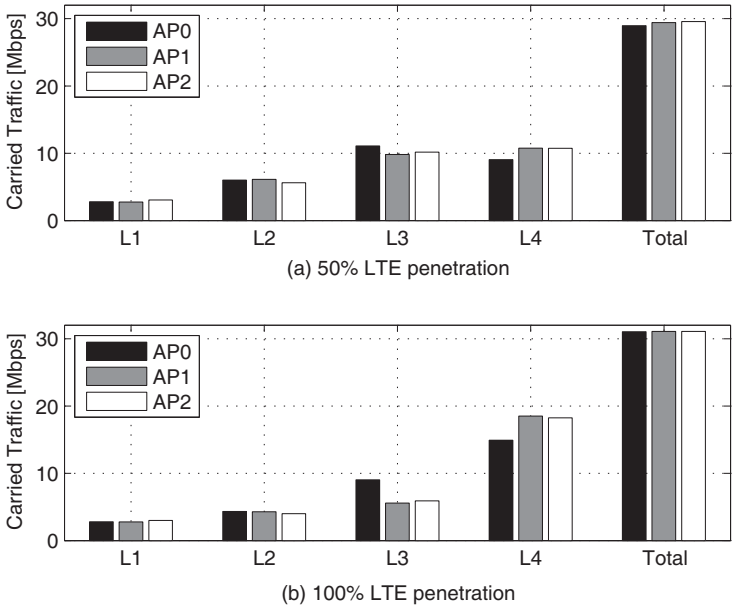

Figure 7.7: Carried traffic per macrocell area for different settings of APs

(compared to $L2$ and $L4$) is expected.

Regarding the AP settings, with 50% LTE penetration, more traffic (∼1.7 Mbps) is carried by $L4$ when AP_1 and AP_2 are used. This is because further UE offloading to $L4$ is achieved by using the AP-based cell reselection. It is also noted that AP_2 leads to a lower carried traffic in $L2$, since the priority allocated to this layer is lower. In addition, $L3$ and $L4$ carries similar traffic volume since the LTE penetration is only partial. Conversely, with 100% LTE penetration, $L4$ carries considerably more traffic since there are more LTE-compatible UEs which can be transferred to $L4$. In addition, more traffic (∼3 Mbps) is carried by $L4$ when AP_1 and AP_2 are used instead of the reference case AP_0. Note also that most of this traffic comes from the co-sited pico layer ($L3$), meaning that the macro offloading (i.e. traffic from macro to picocells) is very limited.

On the other hand, regarding the total carried traffic in Fig. 7.7, note that the differences between the AP settings are due to the dropped calls, which means that less traffic is carried by the network. The relationship between the carried traffic and the dropping ratio (i.e. the number of dropped calls to the total number of carried calls) is given by the following expression:

$$\textit{Carried Traffic} = \textit{Offered Traffic} \cdot (1 - \textit{Dropping Ratio}). \tag{7.21}$$

The dropping ratio is related in this work to resource availability rather than to bad radio conditions, i.e. a lower value for this indicator means that enough resources are available to play out the video sessions with no or few interruptions. Thus, a better optimization of mobility parameters means lower dropping ratio. The dropping ratio measured for the previous AP settings and LTE penetration levels is shown in Table 7.3. Note also that the dropping ratio

Table 7.3: KPIs for different AP settings in idle mode (total number of UEs = 2100)

Configuration				HO PP	RLF	Dropping
AP	LTE penetration	nRes/s	nHO/s	ratio	ratio	ratio
AP_0	50%	102.7	31.6	7.2	4.3	15.0
AP_1	50%	122.1	31.8	6.5	4.1	13.5
AP_2	50%	126.3	30.6	6.5	4.5	13.2
AP_0	100%	137.1	38.6	10.0	3.0	6.1
AP_1	100%	189.8	36.8	9.0	3.2	6.0
AP_2	100%	194.4	35.9	9.7	3.6	6.1

is closely related to blocking ratio. A user is blocked when it attempts to start a session but no resources are available. However, as the number of users in the simulation is fixed, all the users are accepted by the system (i.e. no measurements related to call blocking are performed). Thus, the benefits of the reselection optimization will not impact on lower call blocking or better accessibility (i.e. higher number of served users), but on user satisfaction in terms of lower dropping ratio.

With 50% LTE penetration, AP_0 leads to lower total carried traffic, since the dropping ratio is higher. This is because the traffic distribution within the pico layers for AP_0 is different from AP_1 and AP_2, as AP_0 carries more traffic in $L3$. Such a difference for the reference case causes higher interference to $L1$, increasing the dropping ratio. With 100% LTE penetration, the dropping ratio is decreased as a higher number of UEs implementing LTE can be handed over from macrocells to picocells. However, the difference in total carried traffic (and dropping ratio) between the three settings is negligible, as the two pico layers start to be overloaded when 100% LTE penetration is applied to the scenario (macro offloading is higher). This effect is drawn from the resource utilization (percentage of the total amount of resources that are being used) depicted in Fig. 7.8, where it is shown that the resource utilization in $L4$ is $\sim$50% with 50% LTE penetration and $\sim$80% with 100% LTE penetration (i.e. $\sim$30% increased). With 50% LTE penetration, the increased dropping ratio is due in part to an excessive resource utilization (99%) in $L2$. In this case, the limited macro offloading performed by settings AP_1 and AP_2 increases the resource utilization in $L4$ by only $\sim$6%. With 100% LTE penetration, this value reaches $\sim$9%. In addition, the resource utilization in $L3$ is decreased by $\sim$12%.

To compare the impact of APs on the idle mode and the connected mode, the UE distribution per network layer in these two states for different levels of LTE penetration is depicted in Fig. 7.9. With 50% LTE penetration, it is observed that APs allow to control the user distribution in idle mode, as further UE offloading to L4 is achieved when higher AP is allocated to this layer ($\sim$7% for settings AP_1 and AP_2 compared to AP_0). In addition, the UE distribution in connected mode is also modified by changing APs, as $\sim$4% UEs is transferred to L4 when AP_1 and AP_2 are used, compared to the reference case AP_0. As a result, the idle and connected mode UE distributions are aligned, avoiding ping-pong effect. It is also noted that there is no significant difference between AP_1 and AP_2 in connected mode. In idle mode, AP_2 leads to a lower UE percentage in L2, as expected. With 100% LTE penetration, not only the macro offloading is inherently higher ($\sim$10%), but also the percentage of UEs transferred to L4 for settings AP_1 and

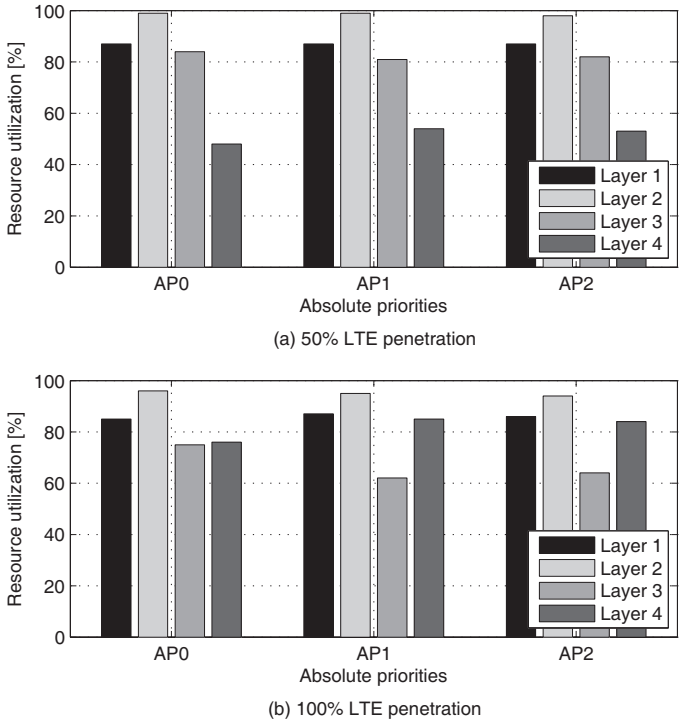

Figure 7.8: Resource utilization comparison for different settings of APs

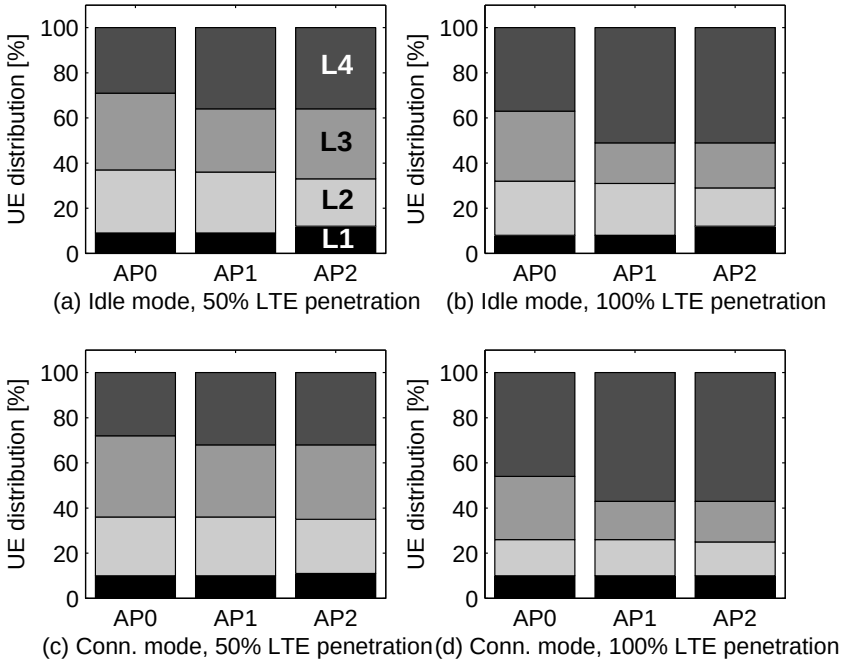

Figure 7.9: UE distribution per layer for different settings of APs

AP_2 compared to AP_0 is higher (11−14%). However, note that, although the offloading between co-sited pico layers is significantly sensitive to APs, the macro offloading performed by changing APs is, in contrast, very limited. These results are in connection with the carried traffic shown in Fig. 7.7.

Finally, Table 7.3 includes some other KPIs related to signaling and radio features. In particular, the number of reselections per second (nRes/s), the number of HOs per second (nHO/s), the HO ping-pong ratio (HO PP ratio) and the RLF ratio are shown. The main difference in signaling cost between the proposed settings (AP_1 and AP_2) and the reference case (AP_0) is that the number of reselections is increased by ∼20% and ∼40% with 50% and 100% LTE penetration, respectively. Regarding the radio aspect, there is no appreciable difference between settings, only that the RLF ratio is decreased by ∼1% when the LTE penetration changes from 50% to 100%.

The previous analysis shows that, in general, the user distribution between two layer-pairs whose coverage areas are fully overlapped (e.g. co-sited layers) can be effectively modified by allocating different APs. In this case, APs can be used for example to reduce the interference generated over other intra-frequency layers by decreasing the percentage of UEs attached to the interfering layer (e.g. $L1$ and $L3$). Such a reduction of interference would mean a lower dropping ratio in the network. Conversely, the macro offloading performed by extending the cell-edge area of small cells (e.g. picocells) is rather limited.

TS in connected mode.

In connected mode, the parameter adjustment for TS described in Algorithm 7.1 involves sweeping of B2/3A thresholds. Fig. 7.10 shows the dropping ratio drawn from sweeping $B2\_1$. Following the 3GPP specifications, the ranges of valid values for $B2\_1$ in LTE and HSPA are from -140 to -44 dBm [168] and from -120 to -25 dBm [25], respectively. However, in this work, the represented ranges have been bounded, since values outside the represented range lead to undesired values of the indicators. As the B2/3A thresholds are assumed to be defined per layer-pair, in principle there are two different sets of parameters defined for macro-pico HOs. The x-axis refers to the layer-pair involving layer 1 and 4 ($L1$, $L4$), while the y-axis corresponds to the layer-pair formed by layer 2 and 4 ($L2$, $L4$). It is observed that high values of $B2\_1$ increase the dropping ratio, since $L4$ carries out less traffic (doing the opposite of macro offloading). On the other hand, low values of $B2\_1$ also increase the dropping ratio, since more UEs connected to $L4$ stay in the cell edge experiencing very bad quality. The optimal value regarding the dropping ratio (i.e. the minimum value) is achieved by two settings: (−104, −104) dBm and (−100, −108) dBm. To select a single setting, the signaling cost in terms of total number of HOs in the overall network is depicted in Fig. 7.11. It is noted that (−96, −112) dBm leads to the highest signaling cost, since UEs are handed over from $L2$ to $L4$ and then, they are moved from $L4$ to $L1$, producing a strong ping-pong effect. The difference between the two selected points, (−104, −104) dBm and (−100, −108) dBm, is that the former gives a reduction of 25% in signaling cost. For this reason, the optimal value is (−104, −104) dBm. It is noted that both layer-pairs have the same optimal value ($B2\_1$=−104 dBm), so that a single threshold $B2\_1$ (defined per network) could be used in this case. This result supports the assumption made in Section 7.3 for the dynamic approach, meaning that a single set of B2/3A thresholds in the network can be

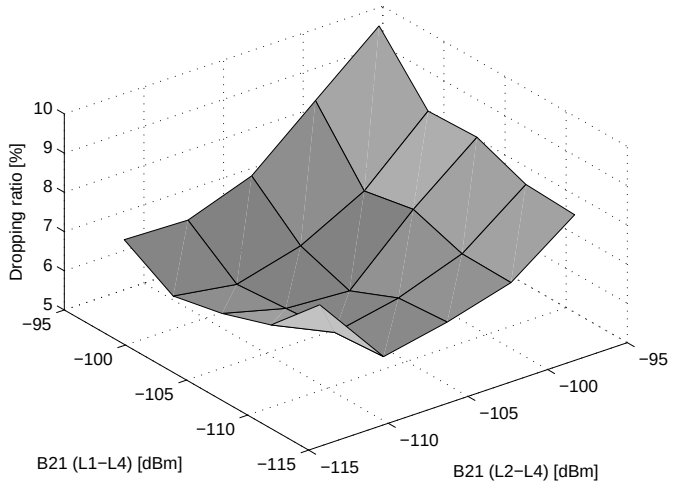

Figure 7.10: Dropping ratio versus threshold B21

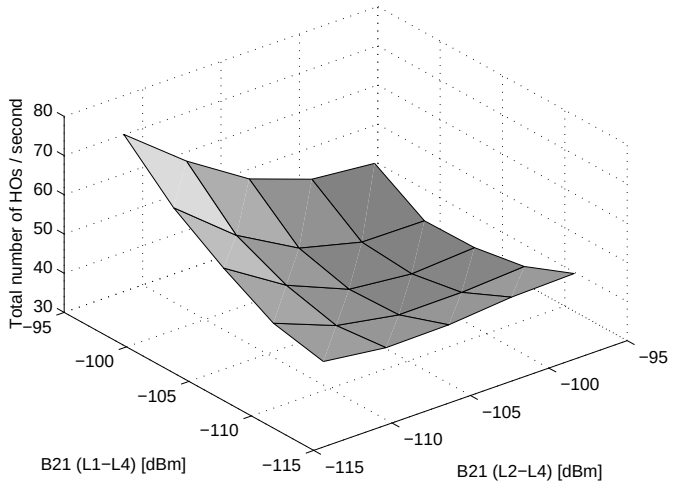

Figure 7.11: Total number of HOs per second versus threshold B21

used without degrading performance. In addition, since the adjustment of $B2\_2$ and $3A\_1$ have minor impact from the macro offloading perspective, these parameters are also assumed to be defined per network to simplify the optimization process (less sensitivity analysis are needed).

The following step from algorithm 7.1 is the sweeping of $B2\_2$. Fig. 7.12 shows the dropping ratio and the total number of HOs derived from this analysis. It is observed that increasing $B2\_2$ does not significantly affect the dropping ratio. This is because the inter-RAT HOs to bad cells are being limited while macro offloading is also being restricted, so that both effects are counteracted keeping the dropping ratio around 6%. However, there is a minimum located at $B2\_2{=}-98$ dBm. Since an acceptable signaling cost is achieved at this point (see Fig. 7.12), $B2\_2{=}-98$ dBm is selected in this work.

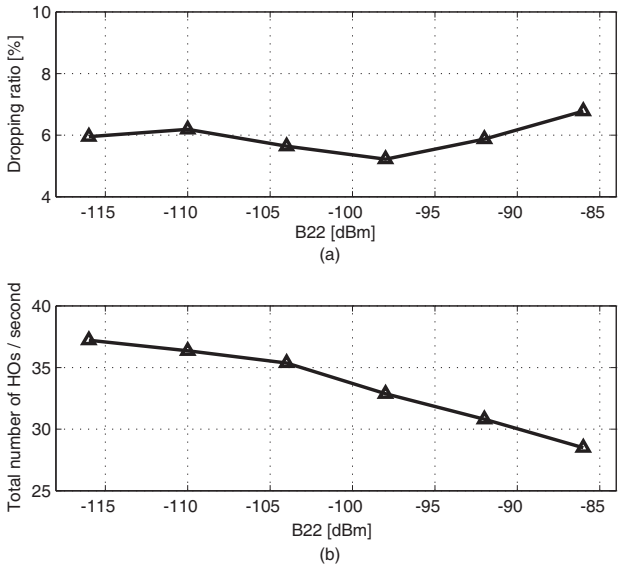

Figure 7.12: Performance evaluation of sweeping B22

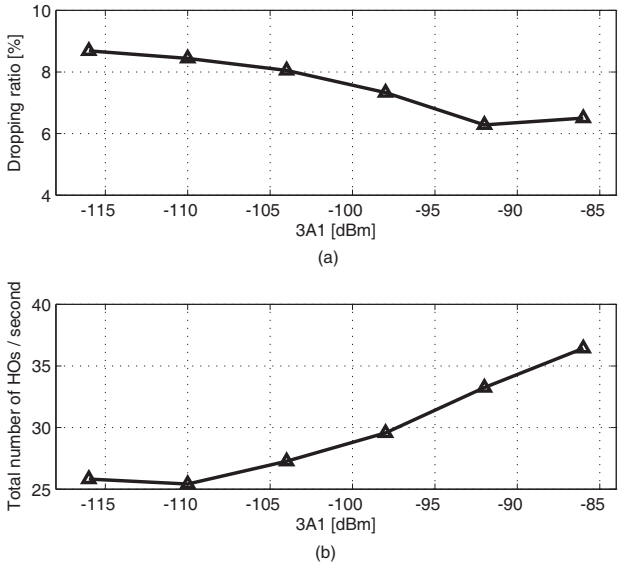

Figure 7.13: Performance evaluation of sweeping 3A1

Fig. 7.13 shows the dropping ratio and the signaling cost referred to the sweeping of $3A\_1$. It is noted that decreasing $3A\_1$ leads to an increment in the dropping ratio as a result of restricting the macro offloading (the number of inter-RAT HOs is decreased), especially in picocells close to the macrocell base station. For this reason, $3A\_1{=}-92$ dBm is the selected value since the macro offloading is not affected (dropping ratio does not increase) and a 10% signaling reduction (compared to $+\infty$) is obtained.

Once the B2/3A thresholds have been optimized, performance is assessed and compared

with reference cases. The first reference case implements inter-RAT HOs based on the 3GPP A3 event (i.e. neighbor cell becomes offset better than serving cell) with an offset equal to 4 dB and the measurement type for triggering A3 is based on the signal level. It is noted that A3 event has been typically used for intra-RAT HOs. To use A3 event for inter-RAT HOs as a reference case, the transmitted power is assumed to be the same for both HSPA and LTE in the simulations. The second reference case also uses the A3 event for inter-RAT HOs but the measurement type is based on the signal quality. Fig. 7.14 shows the carried traffic per layer and macrocell area. As observed, the use of A3 event leads to lower system capacity (i.e. higher dropping ratio), since more traffic is carried through $L3$ instead of $L4$. As $L1$ causes co-channel interference with $L3$, these configurations lead to worse performance. More specifically, the worst case leading to the lowest macro offloading is 'A3 - Level'. If the signal quality (RSRQ / Ec/No) is used instead, the macro offloading is higher (especially for $L2$) since this measurement type is load-sensitive, i.e. due to the RSRQ and Ec/No definition, such indicators also depend on the load in the serving cell, so that picocells automatically perform cell range extension when many resources are available. Conversely, the proposed setting provides the highest carried traffic, since the B2/3A thresholds have been thoroughly adjusted to offload traffic towards $L4$. It is noted that not only the macro offloading is higher (e.g. $L2$ carries less traffic), but also the traffic distribution between pico layers is different, i.e. less traffic is carried by $L3$ to avoid interfering with $L1$.

Table 7.4 shows the main KPIs to compare the proposed configuration (B2/3A - Level) with the reference cases. As a result of a better UE distribution across the layers, the proposed configuration achieves the lowest dropping ratio. Regarding the signaling cost, it is noted that the number of HOs is greatly decreased (30%) compared to the second reference case, while the number of reselections is slightly increased (2%). Thus, the proposed configuration significantly reduces the signaling cost in connected mode, where signaling is more critical. Lastly, regarding the radio aspect, it is observed that the proposed configuration increases the RLF ratio as a result of the picocell range extension, which increases the number of UEs in the cell edge, where

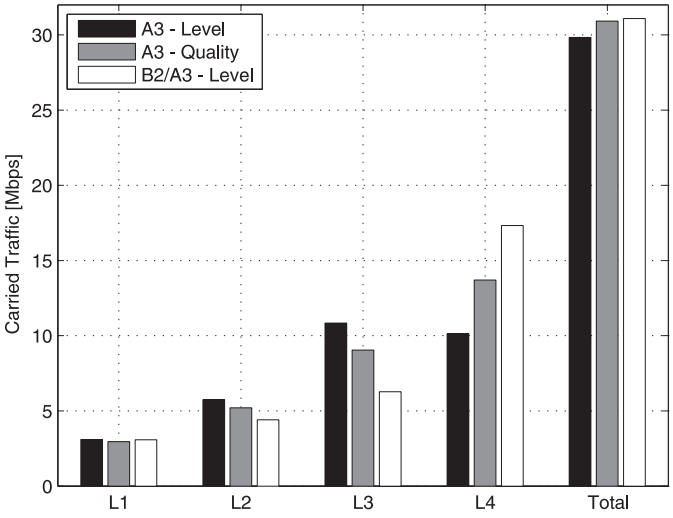

Figure 7.14: Carried traffic per layer for different settings of inter-RAT HOs

Table 7.4: KPIs for different HO settings in connected mode (total number of UEs = 2100)

Configuration	nRes/s	nHO/s	HO PP ratio	RLF ratio	Dropping ratio
A3 - Level	152.4	63.8	9.2	2.5	13.4
A3 - Quality	188.9	41.9	2.7	2.6	7.4
B2/3A - Level	192.8	29.3	6.8	6.7	5.4

the connection quality is worse.

The previous study shows that it is possible to overcome the problem of the small cell location within the macrocell by a thorough adjustment of the HO parameters for TS purposes. Let now suppose that an LTE macro layer is included as the fifth layer in the deployment scenario of this study to provide full LTE coverage. Then, the study of the inter-RAT HOs would be more complex, since there would be inter-RAT HOs between the LTE/HSPA macro layers. In addition, the B2 event would trigger not only HOs from the LTE pico layer to the HSPA macrocells (as in the previous example), but also HOs from the LTE macro layer to the HSPA picocells (the same reasoning is applied to the 3A event). In this situation, a single set of B2/3A thresholds cannot be used to further offload the macrocells, meaning that different settings for each layer-pair, as well as different settings for the same triggering event (e.g. radio-driven HOs, TS-driven HOs, etc.), should be considered in such a HetNets scenario. Otherwise, the ping-pong effect between layers would force the network to a user distribution other than the optimal. As a result, both the signaling load and the user performance would be negatively affected.

Dynamic approach

Firstly, the proposed configurations S_1 (i.e. maximizing the UE instant throughput) and S_2 (i.e. maintaining a good trade-off between the throughput and the signaling cost) have been simulated to assess the policy flexibility. The temporary evolution of the parameter and the KPIs (measured per epoch) involved in the optimization are shown in Fig. 7.15. The evolution of $B2\_1$, represented in Fig. 7.15(a), shows that most of the parameter range is covered within the training stage (phase I). Since the same random seed is used for both simulations, the random action selection and, hence, the temporary evolution of $B2\_1$ are the same for S_1 and S_2 during phase I (100% exploration). However, in phase II, each agent takes actions according to the q-values, which represent the knowledge acquired in phase I. As a result, $B2\_1$ of both configurations are not necessarily overlapped during this phase. In fact, $B2\_1$ evolves to -104 dBm and -108 dBm for S_1 and S_2, respectively. Finally, since the FLC is switched off during phase III, the parameter keeps constant throughout the time for performance evaluation.

The temporary evolution of the throughput and the number of HOs are shown in Fig. 7.15(b) and Fig. 7.15(c), respectively. During phase I, it is observed that extreme values of $B2\_1$ lead to lower values of *THR*, while intermediate values provide higher *THR*. This is because a very low $B2\_1$ means that the service area of L4 picocells is significantly enlarged, so that the number of cell-edge UEs is increased. Since the radio conditions are worse in the cell-edge, the spectral

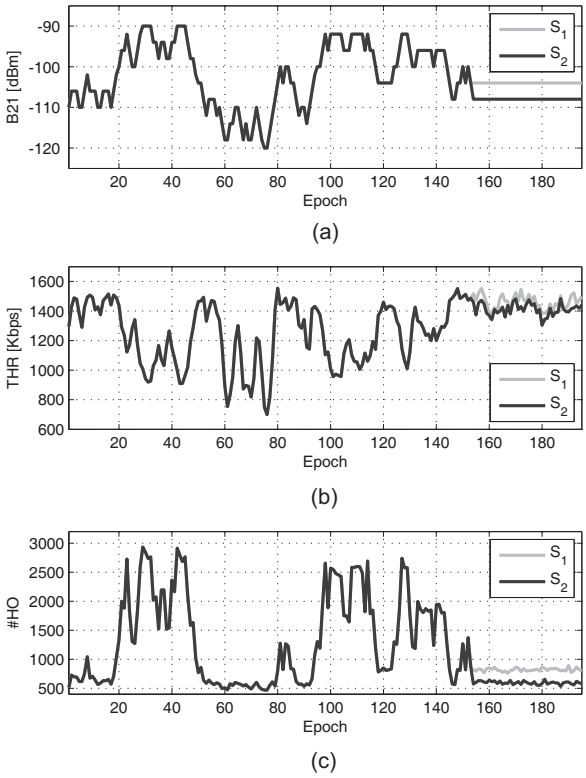

Figure 7.15: Temporary evolution of (a) B2_1, (b) THR and (c) #HO for configurations S_1 and S_2

efficiency experienced by cell-edge UEs is lower, saturating the resource usage and leading to a reduction in *THR*. Conversely, a very high value of $B2\_1$ means that L4 picocells are significantly shrunk, so that many hotspot UEs are steered to macro layers. As a result, the capacity of L4 is wasted and *THR* is decreased. Therefore, an intermediate value of $B2\_1$ within the range permitted in this work would be the optimal setting, depending on the specific operator policy. In the case of *#HO*, note that a very high value of $B2\_1$ forces hotspot UEs connected to LTE to other layers which are clearly non-optimal from the radio perspective. As a result, those UEs can trigger other HOs (e.g. from L1/L2 to L3), so that the *#HO* is highly increased. On the other hand, values of $B2\_1$ below -108 dBm do not have appreciable impact on *#HO*, since the hotspot is fully covered by the LTE picocell and only non-hotspot UEs typically could be affected by the $B2\_1$ setting. After phase II, the optimal values of *THR* and *#HO* are achieved according to the specific policy. In particular, a 6% reduction in *THR* is obtained when S_2 is used instead of S_1. Such a loss can be considered negligible compared to the gain in signaling cost, which means a 27% reduction in *#HO*.

The temporary evolution of the q-values associated to each fuzzy rule for both policies, S_1 and S_2, is shown in Fig. 7.16. Note that the variation of the q-values occurs when the corresponding rule is activated, i.e. $B2\_1$ is within the region where the membership degree to the fuzzy set involved in the rule antecedent is greater than zero. As it can be observed, during phase I, some rule consequents evolve to negative values, meaning that those actions are not appropriate. The optimal consequent for a rule is given by the highest q-value achieved at the end of phase I.

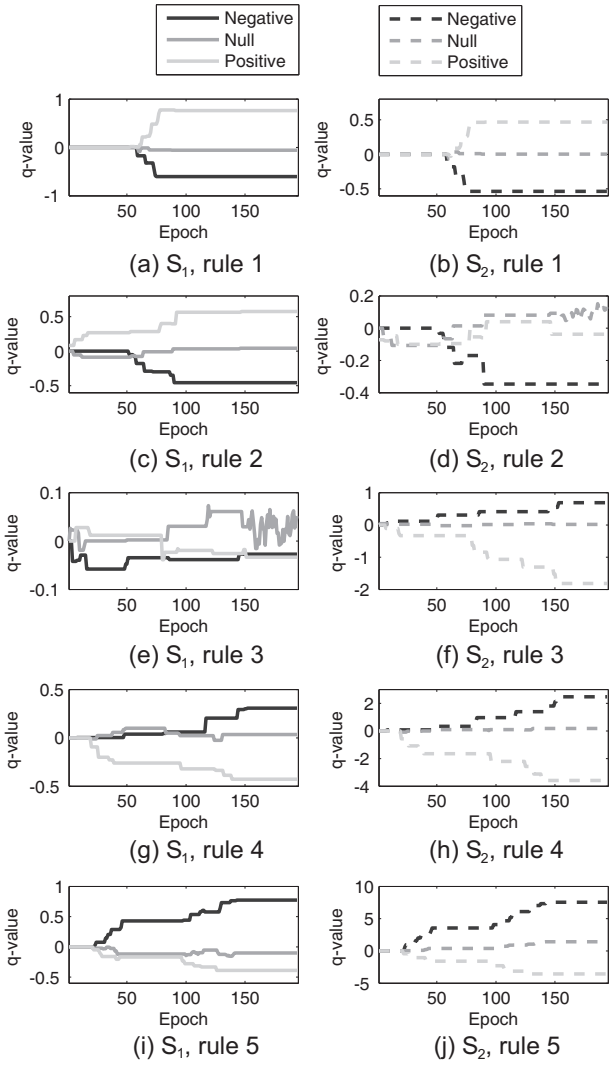

Figure 7.16: Temporary evolution of q-values for configurations S_1 and S_2

For instance, 'positive' is the best consequent for rule 1 in both approaches, S_1 and S_2. The optimal consequents have been selected by the Q-Learning algorithm so that $B2\_1$ converges to the optimal value during phase II, regardless the current value at the end of phase I. In this case, there exists a rule whose consequent is 'null', meaning that $B2\_1$ is enforced to stay at this value. More specifically, this rule is no. 3 and 2 for S_1 and S_2, respectively. Finally, note that no action is performed during phase III, since the FLC is switched off. Thus, the evolution of q-value has no meaning.

Table 7.5 summarizes the rest of KPIs measured within a time interval of 50 s for different settings of $B2\_1$, including the optimal values of $B2\_1$ achieved by S_1 and S_2 in the previous simulations. As previously explained, the higher the value of $B2\_1$, the higher the signaling cost in terms of *#Resel*, *#HO* and *PP HO Ratio*. Regarding the *RLF Ratio*, note that, although it keeps around 2%, the number of RLFs increases as the parameter $B2\_1$ is higher. This is because many hotspot UEs are steered to L1 macrocells, where the interference received from L3 picocells

Table 7.5: KPI comparison for S_1, S_2 and reference cases

B2_1 (dBm)	-112	-108 (S_2)	-104 (S_1)	-100	-96
#Resel	2209	2356	3067	4182	5707
#HO	2349	2714	3976	6434	9672
PP HO Ratio (%)	10.7	11.8	23.1	33.4	36.8
RLF Ratio (%)	2.3	2.2	2.4	2.1	1.5
THR (Kbps)	1254	1444	1587	1573	1416
PRB utilization (%)					
L1	44	54	65	73	81
L2	54	63	71	77	82
L3	8	11	22	36	53
L4	94	89	82	73	63
UE distribution (%)					
L1	5	7	10	14	18
L2	7	9	11	13	15
L3	1	2	4	8	15
L4	87	82	75	65	52

is substantially high, increasing the number of RLFs. The explanation previously given for *THR* is supported here by regarding both the PRB utilization and the UE distribution. As it can be observed, a very low $B2\_1$ (e.g. -112 dBm) implies that most of the UEs around the macro area are served by L4 (87% UEs), meaning that this layer becomes crowded (94% utilization) and, thus, *THR* is decreased. By contrast, a very high $B2\_1$ (e.g. -96 dBm) involves both less UEs connected to L4 (52%) and lower resource utilization (63%). Thus, L1 and L2 become slightly crowded (81 and 82% utilization, respectively), so that *THR* is also decreased.

The next experiment including S_3 and S_4 enables to assess the adaptation capability of the proposed algorithm. In S_3, firstly, the q-values obtained from the first experiment are resetted and then the three phases such as in the previous experiment are executed. By contrast, S_4 takes advantage of the q-values obtained from the first experiment and it performs partial exploration throughout the simulation. Fig. 7.17 shows the temporary evolution of $B2\_1$ and the main KPIs. These simulations start from a different UE distribution (with non-hotspot UEs) than the previous simulation (with hotspot UEs), S_1. For this reason, although the operator policy is the same, the optimal value of $B2\_1$ may be different. As it is shown, both approaches, S_3 and S_4, evolve to a new value of $B2\_1$, which is also different for each one. More specifically, after the adaptation phase, $B2\_1$ reaches -112 and -110 dBm for S_3 and S_4, respectively. Such values are very close, meaning that performance achieved by those approaches is very similar. In fact, during the phase of performance evaluation (epochs greater than 160), it is observed that the curves of *#HO* are overlapped, while the difference in *THR* is very small. However, there is a clear difference between S_3 and S_4 during the adaptation phase. S_3 necessarily needs the entire time interval (1600 s or 160 epochs) established for both exploration and exploitation phases to find the optimal $B2\_1$ for the new UE distribution, while S_4 lasts only 650 s (65 epochs). Since S_3 randomly explores non-optimal settings of $B2\_1$ while ϵ is equal to 1, performance are

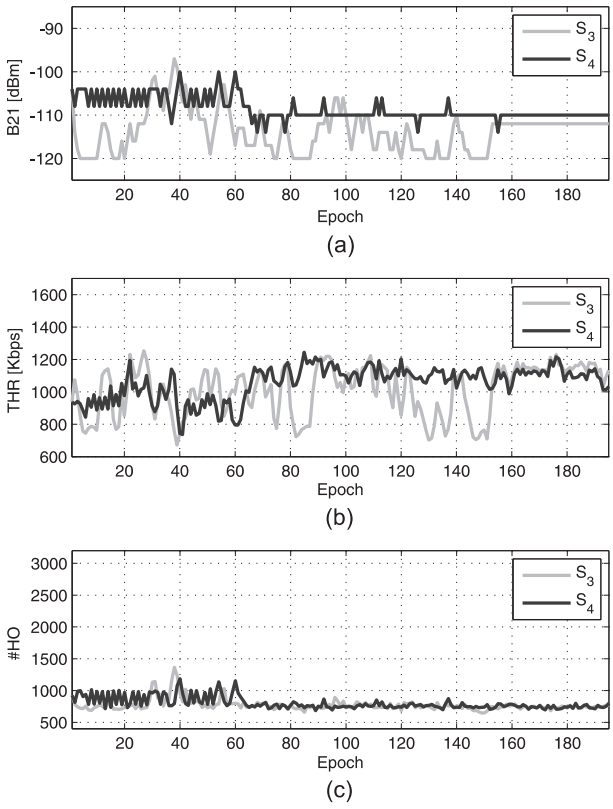

Figure 7.17: Temporary evolution of (a) B2_1, (b) THR and (c) #HO for configurations S_3 and S_4

significantly affected, as shown in Fig. 7.17(b), achieving values below 800 Kbps. However, S_4 utilizes the knowledge acquired from the previous situation and only 20% exploration is employed to adapt to the new UE distribution, obtaining better performance than S_3. This is because, after reaching the optimal $B2\_1$, the optimization algorithm has only tried ten suboptimal values [see Fig. 7.17(a)], so that performance is not really affected. Note also that *THR* is improved when the adaptation is made by either S_3 or S_4 instead of leaving the optimal $B2\_1$ obtained for the previous situation, highlighting the need for adaptation.

The temporary evolution of the q-values shown in Fig. 7.18 facilitates understanding the, previously described, evolution of $B2\_1$. In the case of S_3, the q-values start from zero because they have been reset at the beginning of the adaptation phase. As it can be observed, the q-values evolve so that $B2\_1$ keeps between 'very low' and 'low' values. The reason for this is that the optimal consequents for rules 1 and 2 are 'positive' and 'negative', respectively. Note also that the candidate actions for rule 5 are not tried because the range of values associated with this rule is far from the optimal value, meaning that their q-values remain at zero. In the case of S_4, the initial q-values are chosen from S_1 as if the simulation started from a different UE distribution. At first, 'negative' quickly becomes the best consequent for rule 3. This, together with the fact that 'positive' initially has the highest q-value for rule 2, causes that $B2\_1$ experiences some oscillations. However, since 'positive' is a bad action for rule 2, its q-value suffers a decreasing evolution. As a result, 'null' becomes the best consequent around epoch 65, so that the optimal value of $B2\_1$ is set and no oscillations take place hereafter. Finally, note that rules 1, 4 and 5

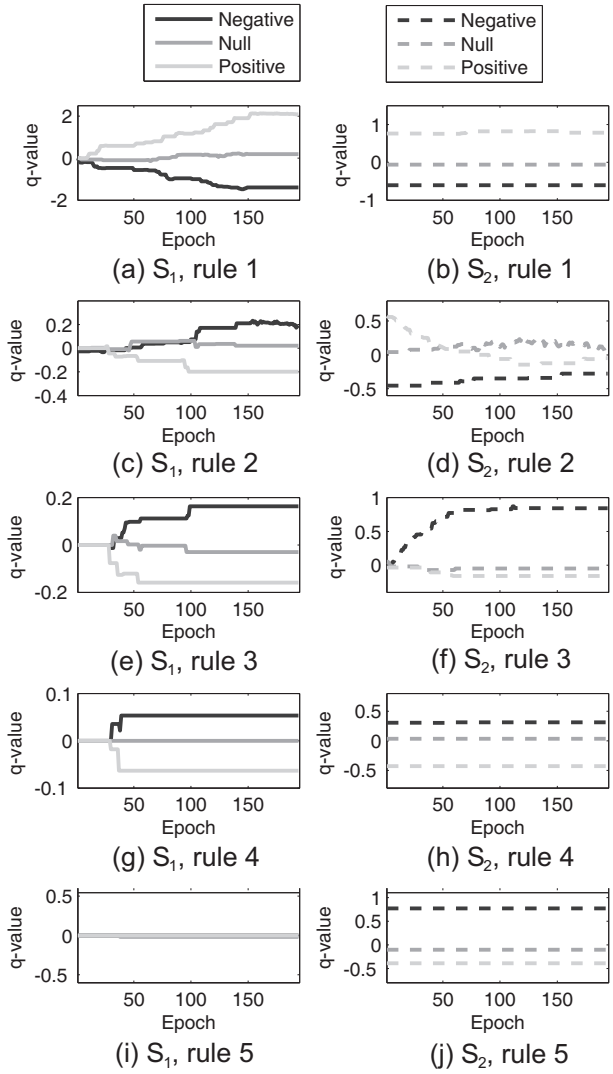

Figure 7.18: Temporary evolution of q-values for configurations S_3 and S_4

are scarcely or not triggered, since a low degree of exploration has been adopted.

The KPIs measured within a time interval of 50 s for the optimal $B2\_1$ achieved by S_3 and S_4 are shown in Table 7.6. In addition, results for $B2\_1{=}{-}104$ dBm are also presented, since it was the optimal setting for the case with hotspot UEs. As previously stated, the gain in throughput obtained by applying adaptation to the new UE distribution is very important ($\sim$25%). The KPIs *#Resel*, *#HO*, *PP HO Ratio* and *RLF Ratio* are also significantly improved. However, the difference in those KPIs between S_3 and S_4 is negligible. Thus, for similar KPIs, S_4 is better than S_3 because it achieves the optimal solution considerably faster. Finally, it is highlighted that $B2\_1{=}{-}104$ dBm makes an inefficient usage of resources, since few users are connected to L4 (only 33%), while radio resources of the macrocell layers are saturated (91% utilization).

As mentioned in Section 7.3, the FLC enables to build non-linear functions in one variable.

Table 7.6: KPI comparison for S_3, S_4 and a reference case

B2_1 (dBm)	-112 (S_3)	-110 (S_4)	-104
#Resel	2842	2885	3177
#HO	3581	3587	4580
PP HO Ratio (%)	10.0	10.2	20.8
RLF Ratio (%)	2.5	2.7	3.5
THR (Kbps)	1265	1246	1010
PRB utilization (%)			
L1	73	80	91
L2	79	83	91
L3	9	12	24
L4	68	61	40
UE distribution (%)			
L1	18	21	29
L2	23	25	31
L3	3	4	7
L4	56	50	33

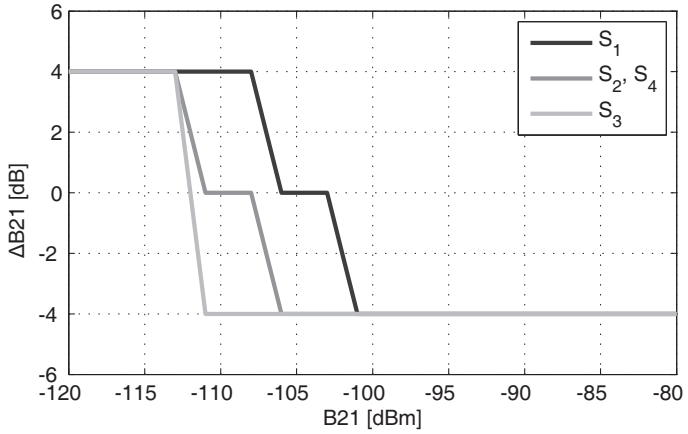

Figure 7.19: The output of the FLC as a function of the input

The input-output relationship of the FLC for each configuration is depicted in Fig. 7.19. To obtain such curves, the FLC rules (i.e. the selection of the rule consequents) have been derived from the performance evaluation phase, after the optimization phase. As it is observed, the definition of membership functions partially overlapped allows to keep certain flat region around the optimal value to ensure stability in S_1, S_2 and S_4.

7.5 Conclusions

This chapter has investigated different TS techniques in a HSPA/LTE multi-layer wireless network from two perspectives: a static approach and a dynamic approach. The purpose of these

techniques has been to offload as much traffic as possible from the macro layer to the pico layer, since extra capacity is available in picocells. To achieve this objective, in the static approach, the APs of the cell reselection algorithm in idle mode and the thresholds of B2/3A events for inter-RAT HOs in connected mode have been statically modified to further offload the macro layer. In addition, an algorithm to simplify the task of adjusting the B2/3A thresholds when the measurement type is based on the signal level has been proposed.

Simulation results show that user distributions in idle and connected mode can be controlled by adjusting the APs, although the macro offloading performed is very limited, even with 100% LTE penetration in the UEs. The user distributions between the two co-sited pico layers are more sensitive to APs, meaning that more traffic ($\sim$1.7 Mbps) can be transferred from HSPA to LTE with 50% LTE penetration, and $\sim$3 Mbps with 100% LTE penetration. The main benefit of adjusting APs is that the HSPA pico layer generates lower interference to the co-channel HSPA macro layer, decreasing the dropping ratio in the network. This is especially observable with 50% LTE penetration, where the LTE picocells are typically less loaded. In the case of performing TS in connected mode, the proposed algorithm for adjusting the B2/3A thresholds allows to control the user distribution in a more accurate way than the reference cases based on the A3 event, meaning that further offload traffic from macrocells can be achieved. In addition, a significant amount of traffic can be transferred from HSPA picocells to the LTE pico layer, thus, reducing the interference that the HSPA pico layer causes to the macro layer and increasing the total carried traffic. More specifically, the benefits of this technique are a lower dropping ratio (up to 8% decreased) and a lower signaling cost (30% decreased). The main drawback is an increase of the RLF (4%), as a result of the cell range extension.

In the dynamic approach, an FRLS that modifies the thresholds of the inter-RAT HO triggering condition has been proposed to satisfy a specific operator policy. Simulation results firstly show that the optimization algorithm can find optimal UE distributions across the network to meet a traffic steering policy. In particular, the following policies have been assessed: a) maximize the user throughput, and b) keep a good trade-off between user throughput and extra signaling load. It has been shown that the former leads to an HO threshold setting that provides the highest user throughput, while the latter obtains a 27% reduction in the number of HOs by only a 6% reduction in user throughput, compared to the former. Secondly, results show that the Q-Learning algorithm can adapt to changes in the user spatial distribution, so that network performance is significantly enhanced. In particular, two different approaches are assessed in the same scenario but both with no concentration of users in the hotspot areas. In this situation, both mechanisms achieve around 25% increase in user throughput, while around 22% reduction in the number of HOs, compared with the case in which HO thresholds are not adapted. One of the two considered approaches is considerably faster than the other, since it keeps a good trade-off between exploration and exploitation, while the other one needs different periods for independent exploration and exploitation phases.

Chapter 8

Conclusions

"As complexity rises, precise statements lose meaning and meaningful statements lose precision."
(Lofti A. Zadeh, inventor of fuzzy logic, 1965)

This chapter summarizes the major findings of the thesis. In particular, the first section of this chapter is devoted to the main results derived from the research carried out and the algorithms developed. The next section highlights the main contributions of this work. Finally, this chapter ends with a description of possible future work in the topics covered.

8.1 Results

This thesis has dealt with different use cases in the field of Self-Optimization for cellular networks, whose common basis has been that network parameters are automatically tuned to face the specific problem. In the following paragraphs, the main results are presented separately for each problem.

a) Mobility load balancing for voice service in macrocells

The proposed FLC for MLB in next-generation wireless networks has been shown to significantly reduce the call blocking in non-uniformly distributed traffic scenarios while at the same time

keeping call dropping in neighboring cells under a certain level set by the operator. Such a decrease in call blocking is especially appreciable in highly congested cells, which benefit from the spare resources of neighboring cells.

On the one hand, the approach in which unbalanced exploration and exploitation for the optimization algorithm is configured (i.e. 100% exploration and 0% exploitation during the optimization phase) has been shown to be a useful method to accurately preserve the call quality constraint during the load balancing by simply adjusting a call dropping threshold.

In the case in which a balanced exploration and exploitation is set (e.g. 20% exploration), it has been shown that the benefits from this approach can be higher than the unbalanced approach because both optimization and load balancing are carried out on the same scenario at the same time, and the method can adapt to network variations. This advantage is obtained at the expense of a slight decrease in performance compared to the unbalanced approach due to the percentage of non-optimal actions executed by the Q-Learning algorithm throughout the load balancing process.

On the other hand, the solution adopted in this problem in which a single optimization entity is shared by all cells selected for optimization has been shown to speed up the learning process. The reason for this is that a higher number of entries in the look-up table of the optimization algorithm are simultaneously updated when an action is performed. In addition, the effectiveness of the proposed optimization scheme also lies on the fact that the gain of each action performed by FLCs can be accurately measured since no more than one action is allowed in an adjacency at a given optimization epoch. This fact avoids causing interference between evaluations of actions so that the reinforcement signal, a key component in RL, becomes more reliable for the optimization process.

Finally, it is highlighted that the combination of fuzzy logic with Q-Learning simplifies the task of designing the fuzzy rules of the controller. The FLC can also be considered as a cost-effective solution to increase network capacity because hardware upgrade is not necessary and manual intervention is minimized.

b) Mobility load balancing for voice service in enterprise femtocells

In a first approach, the comparison between the proposed methods implementing Q-Learning (i.e. FLC with fuzzy Q-Learning algorithm) and those based only on FLCs has shown that FLCs are techniques with fast response time, but they usually reach suboptimal solutions. Instead, learning techniques can improve user performance by carrying out some exploration, but the adaptation is much slower.

In a second approach, the two previous strategies sequentially executed have been shown to provide both faster response and better user performance in the long term. To achieve this, the method implementing only FLCs is firstly executed to have fast response. Then, in a second

phase, the method based on Q-Learning is executed to have better user performance in the long run.

In addition, results have also shown that user performance is better when Q-Learning is applied to adjust transmit power instead of HO margins, since the network is more sensitive to the transmit power, and therefore, better solutions can be achieved by some exploration of the algorithm. Instead, when Q-Learning is applied to HO margins, typically, suboptimal solutions are usually reached.

Regarding the complexity of those strategies based on Q-Learning, it has been shown that the computational cost is negligible since the epoch period of the learning algorithm is long enough (tens of minutes) to compute all the required calculations. In addition, the memory requirements given by the dimensions of the look-up table of the fuzzy Q-Learning algorithm are minimal since this table has a small size. In addition, the implementation does not involve communication with a server since a distributed approach has been adopted.

An important difference of the learning-based methods proposed in the previous problem (i.e. MLB for macrocells) with respect to those proposed here is that the designed FLCs for optimization cannot use a priori knowledge in this latter case. The reason for this is that the input of the FLC is the actual parameter to be adjusted, i.e. no performance indicators are included as inputs. This means that an expert cannot have the knowledge necessary to initially configure the rule base of the FLC, so that Q-Learning optimization becomes mandatory to set a reasonable behavior of the FLC. Although it slows down the convergence process, the main benefit of starting with no a priori is that it avoids possible entrapment in local minimum solutions due to the particular experience of an expert.

c) Mobility robustness optimization

This study has been divided into three parts. The first one focuses on a comprehensive sensitivity analysis of the two main HO parameters, the HOM and the TTT. Results show that increasing the system load leads to an increase in both call dropping and HO signaling. This is because a higher traffic load means a higher number of users, that is, more HOs are carried out and more interference is generated, thus, call dropping is also increased. If the user speed is increased, the main effect is an increase in HO signaling due to a significant increase in the number of HOs, since users travel more distance during the call. There also exists an increase in call dropping when the users move faster. The reason for this is that, as users travel more distance during the TTT, the risk of dropping is higher if they are moving away from the serving cell.

Results of the sensitivity analysis also show that the network is more sensitive to variations in the HOM than in the TTT. In addition, the adjustment of TTT does not provide greater benefit than that obtained by adjusting HOM, meaning that a SON algorithm tuning HOM would be a simple but effective solution for MRO. For this reason, in the second part of this study, an FLC that adaptively modifies HOMs has been proposed.

The assessment of the proposed FLC has shown that cell-pair-wide optimization provides more stable global indicators than other approaches (e.g. network-wide, and cell-wide optimization). At this optimization level, the FLC improves network performance, achieving a good trade-off between call dropping and signaling cost, even if a noise model is considered in the RSRP measurements. In addition, as the user speed increases, call dropping and HO signaling indicators have been shown to be more sensitive to changes in HOM.

A configuration for the FLC has been shown as the best alternative in all situations against other FLC configurations analyzed in this study, since the proposed one provides lower values of call dropping while keeping a similar signaling cost, especially for high-speed users. A more aggressive configuration (i.e. larger changes in the HOM) of the FLC results in greater oscillations of the performance indicators, due to greater HOM variations performed by the FLC. At higher user speeds, those variations in the HOM produced by such an aggressive configuration cause strong oscillations in the call dropping indicator.

The third part of this study consists of developing a SON coordination algorithm that avoids conflicts between the proposed MLB and MRO functions when they are simultaneously operating in the network. The assessment of the proposed coordinated approach has shown that a congestion situation can be alleviated at the expense of a slight increase in call dropping, while a significant reduction in the HO signaling load can also be achieved.

d) Traffic steering

The study of TS in HetNets has been divided into two different cases: the static and the dynamic approach. In the first case, the analysis has in turn been separated into two parts: the idle and the connected mode. In idle mode, the evaluation of the AP-based cell reselection algorithm in a simulated HetNets scenario has shown that APs allow operators to control the user distribution across the network layers. Firstly, results have shown that the user distribution in idle mode between two network layers whose coverage areas are fully overlapped (e.g. co-sited layers) can be effectively modified by allocating different APs. In that case, APs can be used for example to reduce the interference generated over other (intra-frequency) network layers by decreasing the percentage of users attached to the interfering layer. Secondly, the macro offloading performed by giving higher priority to Small Cells is rather limited. Thirdly, it is highlighted that medium levels of LTE penetration (e.g. 50%) in the UEs have been shown to be already enough to observe changes in the user distribution according to the TS strategy. The main benefit of using the AP-based cell reselection algorithm for TS purposes is that, unlike the HO, the cell reselection does not have associated signaling and data transferring costs from the network perspective in most of the cases.

In connected mode, it has been shown that the adjustment of the inter-RAT HO parameters for TS purposes in a heterogeneous scenario may depend on the small cell location within the macrocell. Such an issue can be solved by a thorough adjustment of the HO parameters, as proposed in this work, where different sets of parameters for the same HO triggering event (e.g. radio-driven HOs, TS-driven HOs, etc.) could be defined to perform the TS strategy.

Another important consideration is that, in a mature stage of next-generation wireless network deployments, where fully coverage areas are typically considered, it is expected that the complexity of applying TS techniques would be significantly higher, since just adding a new network layer to the existing network deployment would involve multiple new interactions between layers and a thorough alignment of the mobility processes in idle and connected mode could be needed.

The second case in this work, the dynamic approach, has been based on a SON algorithm that is implemented with fuzzy logic and RL principles. Firstly, results has shown that the proposed algorithm can find optimal user distributions across the network to meet a TS policy. Policies such as maximizing the user throughput or keeping a good trade-off between user throughput and extra signaling load can be easily implemented with the proposed scheme.

Secondly, results have shown that the Q-Learning algorithm can adapt to changes in the user spatial distribution, so that network performance is significantly enhanced. In particular, two approaches have been assessed in this study, based on using (or not using) the acquired knowledge and setting a different trade-off between exploration and exploitation. The configuration that uses the knowledge acquired from the previous situation and only 20% exploration is employed to adapt to the new situation (given by a new user distribution) is shown to be considerably faster, since the other one needs different periods for independent exploration and exploitation phases.

8.2 Contributions

The contributions presented in this thesis can also be classified according to the problem to be solved. Thus, the following lines present the contributions separately for each problem.

a) Mobility load balancing for voice service in macrocells

The contributions in the context of load balancing for cellular networks are [169][170]:

- An FLC to solve persistent congestion problems in future wireless networks is proposed. More specifically, the congestion problem is due to an uneven spatial traffic distribution, e.g., when the center of a city becomes crowded. The optimization process is carried out by the fuzzy Q-Learning algorithm with the goal to reduce the blocking probability for voice services while the call dropping is controlled according to network operator constraints.
- The designed algorithm allows to control the degradation of the connection quality during the load balancing process, which is an issue not addressed enough in the literature. Such an issue is due to the fact that users are handed over to a worse cell at the expense of relieving the congested cell. If the HO margin is decreased, the target cell would increase the probability to be preferred than the serving cell (even if the connection quality is worse), so that some users could be handed over to the target cell. Those users, usually located in

the cell edge, will experience worse radio conditions in the target cell as a result of applying such a traffic sharing technique. For this reason, the proposed algorithm takes into account call quality constraints to avoid excessive degradation of the connection quality. In other words, this thesis addresses how much the connection quality can be decreased when load balancing is carried out depending on the operator policy. Thus, flexibility and easiness from the network operator perspective is provided by simply adjusting a single parameter.

- For the designed scheme based on the fuzzy Q-Learning algorithm, two novel approaches have also been proposed. In the first approach, the FLC is optimized with 100% exploration in a first step and then used without the optimization module. In the second approach, the FLC is optimized while performance is enhanced. In this case, the optimization is carried out with balanced exploration and exploitation.

b) Mobility load balancing for voice service in enterprise femtocells

Enterprise femtocell scenarios are particularly different from those of macrocells and residential femtocells, as there are many challenges specific to this kind of scenarios. More specifically, they often include three-dimensional structures, unequal distribution of traffic load is very common (e.g., crowded/uncrowded offices), the user mobility pattern is different (probably more intense) than at home and open access is usually employed instead of closed access. Thus, as this scenario presents particular issues, further study of load balancing in enterprise femtocell scenarios has been carried out in this thesis. The contributions derived from the research in this field are [171]:

- The potential of different load balancing techniques for voice service to solve persistent congestion problems in enterprise LTE femtocells are investigated. The proposed algorithms are assessed and compared with existing load balancing schemes based on FLCs that modify the transmit power and HO margins of a cell and its neighbors.

- In particular, two fuzzy rule-based RL systems based on the Q-Learning algorithm are proposed for load balancing. However, to obtain the advantages of both FLCs and fuzzy rule-based RL systems, these techniques are thoroughly combined across the time so that different load balancing strategies have been studied. In this sense, the main contribution of this study is the proposal of an efficient mechanism for load balancing combining both the rapid response of FLCs and the improvement in performance due to the RL systems.

- As in the previous problem (i.e. MLB for macrocells), the degradation of the connection quality when the users are handed over to a worse cell at the expense of relieving the congested cell is also addressed in this study. However, the fact that the femtocell scenario is entirely different from the previous one makes the optimization problem different.

- In addition, an important feature of the proposed fuzzy rule-based RL systems that makes them different from other previous approaches is that there is no a priori knowledge available to set the behavior of the system, meaning that both the controller and the Q-Learning algorithm must be used in a combined way. This is particularly different from the previous problem of MLB in macrocells, where an FLC is firstly designed using some a priori knowledge and then refined with Q-Learning in order to achieve a specific target.

c) Mobility robustness optimization

In this study, the potential of adjusting parameters for HO optimization has been investigated. The contributions of this work are the following [172]:

- A sensitivity analysis of the HOM and the TTT is carried out for different system load levels and user speeds. Performance is assessed by measuring CDR and HOR to estimate the degradation of the connection quality and the HO signaling cost, respectively. The impact on the GoS for voice service is also considered in the analysis, which means that not only the call dropping is measured, but also the call blocking.
- An FLC that adaptively modifies HOMs is proposed for HO optimization. Three different configurations of the fuzzy rules and their consequents are assessed to set the optimal behavior to the proposed FLC, based on the previous key performance indicators, the CDR and the HOR, and regarding different system load levels and user speeds. In this sense, the main contribution of this work is the performance analysis considering both HO parameters for different situations, highlighting the variation of the user speed. To evaluate the transient response of the FLCs, an infinite-horizon discounted model has been used.
- Different parameter optimization levels (network-wide, cell-wide and cell-pair-wide) for the proposed scheme have been investigated. In addition, the impact of the RSRP measurement errors has been taken into account in the analysis.
- A SON coordination scheme for the designed MLB and MRO functions is proposed. Such a scheme takes into account scenarios with different traffic load levels and user speeds. In addition, the method is conceived for adapting to slow changes in the environment (e.g. in terms of minutes, hours), so that its location can be on the level of the OAM system.

d) Traffic steering

Most of the TS techniques found in the literature are focused on selecting the preferred RAT, disregarding the fact that heterogeneity of future networks also means networks with different frequencies, cell sizes, etc. In addition, the RATs used as examples for assessing the TS techniques typically have been GSM, UMTS and WLAN, so that further study on future networks such as LTE and LTE-A is needed. For this reason, in this thesis, different TS techniques by static and dynamic adjustment of mobility parameters in HetNets are studied. In particular, to find the optimal user distribution across the network layers according to a TS policy, the AP-based cell reselection algorithm and the inter-RAT HOs are investigated. The contributions of this thesis in this field are [173][174]:

- The problem of allocating APs to network layers for cell reselection is analyzed. Firstly, a survey of TS techniques in idle mode is presented. Secondly, some important challenges arising from the static adjustment of cell reselection parameters from the TS perspective are discussed.
- A procedure to select the optimal thresholds of the 3GPP events that trigger the inter-

RAT HOs is proposed. In particular, the proposed algorithm simplifies the task of statically adjusting the thresholds of the inter-RAT HO when the measurement type is based on the signal level is proposed. If the events are based on the signal level instead of the signal quality, the thresholds involved in these events require a more precise adjustment, especially in multi-layer scenarios, where the location of low-power nodes within the macrocell may determine the adjustment of the thresholds. Thus, an important contribution of this work is the design of an algorithm to simplify the task of adjusting these thresholds for TS purposes.

- The proposed techniques are assessed in a realistic LTE/HSPA scenario thoroughly deployed to cover hotspots with LTE pico cells. The impact of the LTE penetration in the mobile terminals is also studied in the concerned scenario, where the LTE pico cells are deployed in areas without LTE macro coverage. This configuration would be coherent in an early stage of LTE deployment.
- A novel dynamic TS technique based on adjusting mobility parameters in HetNets is investigated. In particular, a fuzzy rule-based RL system that adapts the thresholds of the inter-RAT HO triggering condition to meet a TS policy is proposed.
- The main contributions of the proposed dynamic scheme are the flexibility to support different operator policies and the adaptation capability of the algorithm to network variations. In addition, a comparison between using and not using a priori knowledge for the optimization algorithm is performed. Finally, a singular contribution is that HetNets and SON are two paradigms jointly addressed in this work.

e) LTE simulation tools

To assess the proposed techniques in this thesis, a dynamic system-level simulator for LTE macrocells has been developed. As part of the work in this thesis, the link layer of this simulator has been designed, while the implementation has not been part of this thesis. The main contribution of this work is that, as the simulator is conceived for large simulated network time to allow evaluation of the proposed optimization algorithms, a link layer abstraction has been performed to provide low computational cost in the simulations.

In addition, an indoor mobility model, as part of a dynamic system-level simulator for LTE femtocells, has been developed in the context of this thesis. The aim of this model is to simulate realistic movements of indoor users.

8.3 Future work

Possible lines of research that might continue the work in this thesis are the following:

- The proposed algorithms in the field of load balancing and HO optimization can be applied to other types of traffic (e.g. multimedia data services), in which other QoS requirements

need to be fulfilled and other performance indicators (e.g. throughput) must be measured. In addition, the joint optimization of load balancing for various types of traffic by applying similar optimization schemes is suitable to be investigated.

- The proposed load balancing schemes aim to alleviate persistent congestion situations. In this sense, the involved KPIs (e.g. CBR and CDR) are measured over a long period of time that allows to filter the fast changes in network loading. However, as a possible line for future work, the study of load balancing can be focused on developing self-tuning schemes in order to adapt to more dynamic variations of the system load, in which KPIs should also be directly related with the network load and measured over a shorter period of time.

- Although the parameters involved in the proposed self-tuning schemes for load balancing are mainly those related to mobility, the parameter optimization could also be applied to other network parameters, such as the antenna down-tilt or the maximum transmit power. Thus, this issue can be further investigated, especially in other areas of SON, e.g. Self-Healing, where the cell outage compensation has recently become an important use case addressed in the research community.

- A relevant issue in the field of SON is the coordination of use cases. The proposed algorithms in this thesis for coordination of the MLB and MRO schemes can be further enhanced, for instance, by including a single objective function for the optimization process that takes into account performance indicators related to load imbalance, connection quality and signaling cost.

- In the field of HetNets, the proposed TS techniques can be studied in scenarios including the latest developments in technology, such as femtocells or the relays considered in the recent LTE-A standard. As these technologies are expected to provide much more capacity than the existing solutions, the impact of TS techniques on these future scenarios is a meaningful line of investigation.

- The proposed TS techniques have been analyzed in a scenario representative of an early stage of LTE deployment, i.e. partial coverage of this technology is assumed. As a future work, this study can be extended to a mature stage of next-generation wireless network deployments, where full coverage is typically provided. In that case, the study would be certainly more complex, since just adding a new network to the existing infrastructure would involve multiple new interactions between the deployed networks and a thorough alignment of the mobility processes in idle and connected mode could be needed.

- The common basis of the problems addressed in this thesis is that network parameters are automatically tuned by an FLC to deal with the specific problem. In those cases in which a mathematical approach has been required to optimize the behavior of the FLC, the selected solution has been RL. However, in the field of cellular networks, the combination of various methodologies of computational intelligence is an alternative not addressed enough in the literature. This approach may lead to better solutions or, at least, solve the problem faster. For example, a back-propagation neural network combined with a global search algorithm such as a genetic algorithm is a computational intelligence system. In this case, the neural network would be first adapted by the genetic algorithm to find a near-optimum

global solution, which can then be used as a starting point for the backpropagation learning algorithm to fine-tune the solution.

- In an FLC, both the fuzzy rule base and the membership functions can be optimized to set a specific behavior of the FLC. The optimization of the rule base involves a more coarse tuning in the sense that the environment is more sensitive to variations in the fuzzy rules than in the membership functions. Due to the complexity of cellular networks and its inherent variability, the optimization of the rule base is enough to effectively adjust network parameters. For this reason, this thesis has been exclusively focused on this approach. However, the possible benefit of the optimization of the membership functions is an issue that remains unexplored.

Appendix A

Summary (Spanish)

A.1 Introducción

A.1.1 Antecedentes y justificación

En los últimos años, las redes de comunicaciones móviles han cambiado significativamente la manera en que las personas se comunican. En particular, ha existido una clara emigración de la telefonía fija a la telefonía móvil celular, mientras que la industria móvil ha experimentado un enorme crecimiento tanto en desarrollo tecnológico como en número de abonados. Este hecho ha provocado un aumento de la demanda de tráfico, convirtiéndose en un importante problema para los operadores. Dicho problema se ha agravado por las limitaciones financieras de los operadores debidas al enorme gasto de capital y gastos operativos que requiere una red convencional. Debido a esto, los operadores no deben centrarse únicamente en invertir en nueva tecnología para incrementar la velocidad de transferencia de datos en la red, sino también en elevar el nivel de automatización de la propia red con el objetivo de reducir costes, especialmente los costes operacionales (OPEX). Como resultado de la investigación en este ámbito, ha surgido un nuevo paradigma denominado redes móviles auto-organizativas (*Self-Organizing Networks*, SON) [2]. El desarrollo de técnicas SON viene motivado por diversos factores [3]. En primer lugar, debido a la movilidad de los usuarios y a la naturaleza impredecible del canal radio, las redes celulares no son capaces de aprovechar por completo los recursos disponibles, dando lugar a posibles situaciones de congestión y otras cuyas prestaciones son sub-óptimas. En segundo lugar, el reciente despliegue de celdas más pequeñas (p.ej. femtoceldas y *relays*) para proporcionar más capacidad ha incrementado notablemente el número de elementos en la red, volviendo más tediosas las tareas de configuración y mantenimiento. En este caso, el enfoque clásico manual y el basado en pruebas de campo pueden llevar a soluciones que no son óptimas. Esto es especialmente aplicable en escenarios de femtoceldas, donde no se sigue una rigurosa planificación para este

tipo de estaciones base. Dicha práctica puede llevar a un desaprovechamiento de los recursos de red, o incluso puede elevar gravemente los niveles de interferencia a celdas vecinas de mayores tamaños, degradando las prestaciones globales de la red. En tercer lugar, teniendo en cuenta el enfoque clásico de optimización manual y periódico, la complejidad creciente de las redes futuras (en tecnología, protocolos) resultará en un número mayor de errores humanos, que a su vez darán lugar a largos tiempos de recuperación y restauración de dichos errores. Finalmente, una ventaja importante de la automatización de la gestión de red consiste en que el personal humano puede liberarse de muchas de las tareas rutinarias, de manera que sus habilidades puedan centrarse en nuevas áreas, aportando un valor añadido al operador.

Por lo tanto, la automatización de redes celulares trae consigo una disminución de costes operacionales y una mejora de la experiencia del cliente. Para conseguir esto, SON proporciona una serie de funcionalidades para automatizar la gestión de redes celulares, de manera que se consigue reducir la intervención humana en las tareas de planificación, despliegue, optimización y mantenimiento. En 2006, la Alianza *Next Generation Mobile Networks* (NGMN) identificó como un problema potencial la excesiva dependencia en las tareas operacionales llevadas a cabo de manera manual [4]. Con la idea de aumentar la eficiencia operacional, a partir del nuevo paradigma SON, se crearon funciones específicas que fueron posteriormente agrupadas por el organismo de estandarización *3rd Generation Partnership Project (3GPP)* en tres grandes categorías: auto-configuración, auto-optimización y auto-curación [5]. En particular, la auto-configuración se refiere al modo *plug and play* de las nuevas estaciones base desplegadas, cuyos parámetros radio (p.ej. la frecuencia y la potencia de transmisión) se configuran de manera automática, acelerando el proceso de planificación y despliegue celular. La auto-optimización trata de adaptar dinámicamente los parámetros de red para mejorar su calidad, incluyendo la optimización de cobertura, capacidad, traspasos e interferencia. La auto-curación está relacionada con la detección, diagnosis, compensación y recuperación de fallos con el objetivo de hacer frente a cortes y degradaciones de servicio que disminuyan de forma significativa las prestaciones de la red.

No todas las funcionalidades SON consideradas por el 3GPP han recibido la misma atención en el ámbito de la investigación. En este sentido, ciertas funciones dentro de la auto-optimización se han identificado claves, entre las que están las abordadas en esta tesis, es decir, el balance de carga mediante movilidad (MLB) y la optimización de movilidad (MRO) [6]. Como consecuencia, se ha estimulado intensamente la actividad investigadora en el campo del auto-ajuste de parámetros de red para MLB [7][8][9][10][11] y MRO [12][13][14][15][16]. MLB es una función en la que las celdas que sufren cierta congestión pueden transferir parte de la carga a celdas vecinas que posean recursos disponibles. Para llevar a cabo esto, se ajustan los parámetros de movilidad con el fin de liberar la congestión en la zona afectada. MRO es una función cuyo objetivo es la detección y corrección automática de errores en la configuración de movilidad. Dichos errores pueden dar lugar a una degradación de las prestaciones de usuario. En particular, esta función se centra principalmente en aquellos errores que provocan la caída de llamadas debido a traspasos realizados demasiado pronto o demasiado tarde cuando el usuario se mueve de una celda a otra. La coordinación entre MLB y MRO también es una función necesaria, puesto que ambas funciones pueden cooperar para mitigar el problema de la caída de llamadas, especialmente, en

aquellos escenarios intra-frecuencia en los que MLB puede llevar fácilmente a un aumento en el número de llamadas caídas.

Por otro lado, el fuerte crecimiento de la demanda de tráfico ha llevado al desarrollo de redes heterogéneas, caracterizadas por la presencia de diferentes tecnologías, tamaños de celdas, frecuencias de uso, etc. En estos escenarios, el área de cobertura de las redes se encuentra solapada, de forma que los operadores disponen de cierto grado de libertad para direccionar el tráfico entre las distintas redes con el objetivo de optimizar el uso de los recursos radio. Algunos estudios iniciales en este tema son [17][18][19][20][21]. El potencial del direccionamiento de tráfico (*Traffic Steering*, TS) en redes heterogéneas ha traído consigo nuevos desafíos a los operadores móviles, debido a que la selección de la red más apropiada para los usuarios puede realizarse de acuerdo a un objetivo o una combinación de ellos, por ejemplo, relativos al coste, la satisfacción de usuario, el consumo de potencia, la cobertura, etc. Debido a la falta de estudios relacionados con este nuevo paradigma, la presente tesis está dedicada también al estudio de TS en redes heterogéneas, centrándose en el desarrollo de técnicas automáticas basadas en el ajuste de parámetros de movilidad.

A.1.2 Objetivos

El principal objetivo de esta tesis es el diseño de técnicas de optimización para redes de comunicaciones móviles, mediante el auto-ajuste de parámetros de red. Tal objetivo se ha aplicado a diferentes problemas:

- Un método de auto-ajuste para resolver **problemas de congestión persistente en redes inalámbricas de próxima generación**, en particular, debidos a una distribución espacial de tráfico desigual, p.ej. cuando el centro de una ciudad se vuelve muy habitado. Siguiendo las directrices del 3GPP, en las que el balance de carga se denomina MLB, se utilizarán preferentemente los parámetros de movilidad en el mecanismo de auto-ajuste. Además, se estudiará la optimización del propio proceso de auto-ajuste. Tal optimización proporcionará cierta capacidad de adaptación al algoritmo de auto-ajuste.

- Un esquema para resolver **problemas de congestión persistente en escenarios de femtoceldas corporativas**, en los cuales la falta de un análisis riguroso de la etapa de planificación promueve el uso de algoritmos que hagan un uso más eficiente de los recursos. El proceso de auto-ajuste se caracterizará por ajustar parámetros específicos de femtoceldas, tales como la potencia de transmisión o los márgenes de traspaso. Además, al igual que en el problema anterior, se investigará también la optimización del proceso de auto-ajuste.

- Una propuesta para la **optimización del traspaso en redes inalámbricas de próxima generación**. El objetivo de esta función, conocida como MRO dentro de la terminología del 3GPP, es reducir el número de llamadas caídas y evitar los traspasos innecesarios. En este estudio, se incluirá el impacto de factores de contexto tales como la carga del sistema y la velocidad de usuario. Además, se considerará en el estudio la necesidad de optimizar este proceso, que depende de la complejidad del algoritmo de auto-ajuste propuesto.

- Una propuesta para la **coordinación de funciones SON**, en particular, para las dos funciones propuestas de MLB y MRO. Debido a que estas dos funciones pueden ajustar los mismos parámetros, se deberá estudiar la propuesta de un algoritmo para evitar que dichas funciones entren en conflicto.
- Un algoritmo de auto-ajuste para **direccionamiento de tráfico en redes heterogéneas**, el cual proporcione a los operadores la flexibilidad de elegir una determinada política. El escenario bajo estudio deberá ser representativo de un despliegue de red realista que incluya la presencia de diferentes tecnologías, tamaños de celdas, frecuencias de uso, *hotspots*, etc. desplegados de una manera racional. Además de la flexibilidad para soportar diferentes políticas del operador, la capacidad de adaptación a las variaciones en la red también deberá ser una característica clave del esquema propuesto.

  Con el objetivo de validar las técnicas propuestas, así mismo será necesario desarrollar una herramienta de simulación para redes inalámbricas de próxima generación, adaptada a los métodos y procedimientos propuestos. La etapa de diseño de dicho simulador será una parte importante del trabajo de esta tesis.

A.2 Estado del arte

La primera parte de la tesis presenta el marco teórico en el que se sitúa la misma. Los objetivos de esta parte son los siguientes:

- Presentar los fundamentos teóricos de las redes móviles auto-organizativas, para ubicar las técnicas desarrolladas en esta tesis.
- Revisar la literatura sobre los casos de uso que se van a estudiar en esta tesis relacionados con la auto-optimización de redes móviles, así como las técnicas adaptativas usadas para la optimización de parámetros de red.

A.2.1 Redes de comunicaciones móviles auto-organizativas

En la primera parte del Capítulo 2, se describen los fundamentos de las tecnologías de acceso radio, UMTS [23][24][27] y LTE [5][28][29], sobre las que se han desarrollado y evaluado las técnicas propuestas en esta tesis. A continuación, se presentan los principios de las redes móviles auto-organizativas, las cuales son esenciales para que los operadores posean una mayor automatización en la gestión de sus redes, con la consiguiente reducción de costes operacionales y mejora de prestaciones [2][4][6][37][38][39][40]. Se describen las tres grandes categorías en las que se clasifican las funcionalidades SON: auto-configuración, auto-optimización y auto-curación. Para cada categoría, se define su objetivo y se describen los casos de uso más relevantes. Se hace especial hincapié en el caso de la auto-optimización, puesto que los casos de uso estudiados en esta tesis están dentro de esta categoría. La importancia de la auto-optimización se debe al aprovechamiento de la infraestructura existente de red mediante la optimización de sus propios parámetros en lugar de realizar grandes inversiones para actualizar dicha infraestructura. La

auto-optimización se basa en un proceso continuo e iterativo en el que están presentes las siguientes fases: recolección de medidas de red, cálculo de la modificación de los parámetros a partir de una evaluación de prestaciones y, finalmente, actualización de los parámetros en la red real. Así mismo, los principales casos de uso de auto-optimización se han descrito con mayor detalle [44].

Una vez que se han presentado los conceptos más importantes que se utilizarán a lo largo de la investigación y los problemas a resolver en cuestión, en la segunda parte del Capítulo 2, se hace un profundo análisis de la literatura relativa a los casos de uso de auto-optimización que han sido abordados en la tesis. La primera parte del análisis se centra en los proyectos internacionales y consorcios estrechamente relacionados con la tesis, en particular, con la gestión automática de red y el concepto SON [2][47][48][49][50][51]. El resto del análisis se centra en describir el estado del arte para cada uno de los casos de uso estudiados en esta tesis. En este sentido, se destaca la importancia de los casos de uso de MLB y MRO frente a otros considerados también por el 3GPP [6]. La coordinación de las funcionalidades SON (p.ej. entre MLB y MRO) también se ha convertido en una cuestión de interés para los operadores [6]. Así mismo, debido a que se pueden obtener ganancias mayores, el direccionamiento de tráfico en redes heterogéneas es también un caso de uso de auto-optimización muy importante en la literatura [45].

El primer caso de uso estudiado, MLB, ha sido reconocido por el 3GPP como una de las funciones clave en la evolución de LTE, denominada LTE-A [53], en donde se han propuesto como objeto de investigación las mejoras para esta función. La aplicación de MLB en el contexto de redes heterogéneas y escenarios inter-tecnología también se ha incentivado en la literatura [6]. El problema de balance de carga ha sido ampliamente abordado en la literatura, donde los estudios típicamente han sido dependientes de la tecnología: GERAN [54], GSM/UMTS [55][56], UMTS [7] y LTE [8][9][10][57][58]. Sin embargo, en el análisis realizado se pone de manifiesto que la mayor parte de estas referencias investigan el balance de carga inter-frecuencia, en donde los usuarios se envían a otras celdas normalmente bajo condiciones radio adecuadas, debido a que las áreas de cobertura se encuentran solapadas. Sin embargo, en el caso intra-frecuencia (típico en LTE), cuando un usuario se envía a una celda adyacente, las condiciones de propagación pueden empeorar debido a la fuerte interferencia recibida por la celda que era anteriormente servidora. Por esta razón, se justifica la necesidad de investigar nuevas técnicas que permitan controlar el proceso de balance de carga en función de la degradación de la señal en aquellos usuarios que son enviados a otras celdas con el objetivo de liberar recursos de la celda congestionada.

A continuación, se realiza un análisis de la literatura existente sobre el balance de carga en escenarios de femtoceldas, en particular, aquellas que son corporativas. El interés en las femtoceldas se hace evidente con la existencia de varios proyectos internacionales [62][63][64]. Sin embargo, un menor número de estudios se han encontrado sobre el balance de carga en femtoceldas corporativas [72][11][73]. Estos escenarios presentan una gran cantidad de desafíos para los operadores, debido a su estructura tridimensional típica, la distribución de tráfico suele ser desigual (p.ej. oficinas poco o muy habitadas), los patrones de movilidad de usuario son más complejos que en un contexto doméstico, el acceso suele ser abierto en lugar de cerrado, etc. De esta manera, se justifica la necesidad de profundizar en el desarrollo de técnicas de balance de

carga en este tipo de escenarios, en donde además la planificación no suele seguir un riguroso análisis, por lo que se puede optimizar el uso de los recursos aportando mayores ganancias al sistema.

Al igual que MLB, MRO ha sido considerado de forma especial por el 3GPP debido a su relevancia desde el punto de vista de los operadores. Los principios básicos de MRO están definidos en [43]. Las mejoras planteadas para esta función y su aplicación en el contexto de redes heterogéneas y escenarios inter-tecnología se describen en [53]. En la comunidad investigadora, la optimización de traspasos ha ido ganando cierta atención [76][77], centrándose en el desarrollo de algoritmos SON [12][13][14][15][16] y su estudio en escenarios inter-tecnología [78][79]. Sin embargo, estas referencias no incluyen un análisis profundo sobre los principales parámetros de los traspasos (margen de traspaso y *Time-to-Trigger*) en diferentes situaciones de carga, velocidad de usuario, etc., por lo que en este sentido se requiere mayor investigación.

Dado que tanto MLB como MRO son funciones muy importantes en el contexto de SON, la coordinación de ambas funciones también juega un papel esencial y por ello se ha ganado el interés de la comunidad investigadora [85][86][87]. No obstante, debido a que la coordinación depende en cierta manera de las implementaciones de ambas funciones, la investigación llevada a cabo hasta el momento se considera escasa. En este sentido, dado que el objetivo de MLB en esta tesis es hacer frente a situaciones de congestión persistentes y adaptarse a variaciones lentas del tráfico, la coordinación de MLB y MRO actuará a un ritmo más lento que los algoritmos de coordinación propuestos en la literatura, tratándose por tanto de un problema diferente.

Posteriormente, se realiza un análisis del estado del arte en el ámbito de redes heterogéneas y direccionamiento de tráfico [17][18][19][20][21]. Sin embargo, la mayoría de las referencias son estudios previos al concepto más amplio de red heterogénea, en donde no solo existen diferentes tecnologías de acceso radio, sino también diferentes tamaños de celdas, frecuencias de uso, elementos de red (p.ej. *relays*), etc. Además, las tecnologías que se utilizan para evaluar las técnicas de direccionamiento de tráfico son típicamente GSM, UMTS y WLAN, de manera que se requiere un mayor estudio en escenarios con nuevas tecnologías de acceso radio, tales como LTE y LTE-A.

A.2.2 Técnicas adaptativas para la optimización de parámetros de red

La última parte del Capítulo 2 realiza un análisis de la literatura actual sobre los métodos de optimización que se utilizan para mejorar las prestaciones de las técnicas de auto-ajuste de parámetros. En primer lugar, se estudia el estado del arte en controladores de lógica difusa (*Fuzzy Logic Controller*, FLC) como principal método heurístico para el problema de auto-ajuste [91][94][95][96][75]. La principal razón de usar este tipo de técnicas es que son mucho más atractivas desde el punto de vista del operador debido a su bajo coste, ya que no requieren costosas herramientas de simulación para su funcionamiento. En segundo lugar, se ha realizado un análisis de la bibliografía sobre las técnicas de optimización que permiten optimizar el funcionamiento de un FLC, en particular, las reglas difusas que definen su dinámica. En el contexto de las redes móviles, es probable que los expertos tengan dificultades para ajustar estas reglas, o bien sea

necesario adaptar dinámicamente la conducta del FLC a las variaciones del entorno. Por esta razón, el uso de métodos de optimización para FLC es una cuestión muy importante que ha sido abordada en la literatura [97][98][99][9][19][100]. Entre estas técnicas, en esta tesis se ha valorado especialmente el aprendizaje por refuerzo [101], debido a que es un método particularmente apropiado para aprender mediante la interacción con el entorno, sobre todo en aquellas situaciones en las que es complicado obtener ejemplos representativos de todas las situaciones en las que el FLC debe actuar, como ocurre en los escenarios de redes móviles. Dentro del aprendizaje por refuerzo, se destaca el algoritmo de Q-Learning y sus aplicaciones en el ámbito de optimización de las redes móviles [102][103][104][105][106][107][108]. Además, la combinación de FLC y el algoritmo de Q-Learning es un potente mecanismo de optimización en donde las facilidades de modelado del FLC que ofrecen un alto nivel de abstracción se añaden a la capacidad del Q-Learning para adaptar/entrenar el controlador.

En el Capítulo 3, se realiza en primer lugar una introducción a la lógica difusa [111], centrándose posteriormente en el auto-ajuste de parámetros mediante FLC [113][116]. En segundo lugar, se realiza un estudio sobre las principales técnicas usadas para la optimización de FLC. Para cada técnica, se proporciona una breve introducción así como una descripción de cómo aplicar la técnica para optimizar FLC, incluyendo sus ventajas e inconvenientes. En particular, las técnicas estudiadas son las redes neuronales, los algoritmos genéticos, el enjambre de partículas y el aprendizaje por refuerzo [117][113]. De entre todas estas técnicas, se justifica la elección del uso de aprendizaje por refuerzo para optimizar FLC en esta tesis.

A.3 Auto-optimización de redes de comunicaciones móviles

En la segunda parte de la tesis se presentan las principales aportaciones para cada uno de los problemas abordados. El objetivo común es diseñar técnicas para el auto-ajuste de parámetros en redes de comunicaciones móviles. Para evaluar dichas técnicas, se ha desarrollado un simulador LTE dinámico de nivel de sistema. Aunque también se han hecho uso de otros simuladores, una importante parte del diseño de este simulador se ha realizado en el marco de esta tesis, de manera que el Capítulo 4 se dedica a la descripción del mismo. El resto de capítulos están dedicados a cada uno de los problemas que se abordan en la tesis. En particular, el Capítulo 5 trata el problema del balance de carga o MLB, tanto en escenarios de macroceldas como en escenarios de femtoceldas corporativas. El Capítulo 6 está dedicado al problema de la optimización de traspasos o MRO así como a la coordinación entre MLB y MRO. En el Capítulo 7 se estudian mecanismos de direccionamiento de tráfico en redes heterogéneas. En todos estos capítulos se sigue una estructura similar en la que, tras describir el problema, se presentan las técnicas propuestas y se exponen los resultados derivados de su evaluación mediante herramientas de simulación especialmente apropiadas para los algoritmos diseñados.

A.3.1 Simulador LTE dinámico de nivel de sistema

El Capítulo 4 presenta la herramienta principal de simulación que se ha utilizado en esta tesis para evaluar y validar las técnicas desarrolladas. En el proceso de diseño se ha hecho especial énfasis en desarrollar un modelo abstracto de los niveles más bajos de la arquitectura, es decir, los niveles físico y de enlace. El motivo fundamental es la necesidad de crear un simulador computacionalmente eficiente, de forma que permita simular largos períodos de tiempo en base a los problemas abordados. En particular, en esta tesis, se ha diseñado el modelo abstracto del nivel de enlace, mientras que el diseño de otros niveles del simulador, así como la parte de implementación, corresponden a otros trabajos.

El Capítulo 4 comienza describiendo el nivel físico, en donde se hace uso de una serie de realizaciones de canal OFDM generadas previamente con el fin de caracterizar fielmente el canal radio, incluyendo el desvanecimiento multicamino. Tras esto, se describe el nivel de enlace, caracterizado por los cálculos que permiten obtener la relación señal a interferencia (*Signal-to-Interference Ratio*, SIR), a partir de la cual se calcula la tasa de error de bloque (*Block Error Rate*, BLER) experimentada por el usuario. A continuación, se describen las dos funciones principales de este nivel, es decir, la adaptación de enlace y la planificación. Mientras que la primera permite seleccionar el esquema de modulación y codificación más adecuado para cada transmisión, la segunda asigna los recursos radio disponibles a los usuarios basándose en las condiciones de canal a lo largo de las diferentes sub-bandas de frecuencias. Posteriormente, se definen las funciones más importantes a nivel de red, tales como el control de admisión, el control de congestión y los traspasos. Finalmente, se presentan algunos resultados que permiten validar el simulador.

A.3.2 Balance de carga mediante movilidad

En el Capítulo 5 se describen las técnicas de balance de carga propuestas en esta tesis. El primer grupo de técnicas desarrolladas está pensado para ser aplicado en escenarios de macroceldas, mientras que el segundo grupo está diseñado para escenarios de femtoceldas corporativas. El capítulo comienza describiendo el algoritmo de movilidad y los parámetros típicamente utilizados en MLB para mitigar las situaciones de cogestión. Tras esta breve introducción, la primera parte del capítulo se dedica al problema de balance de carga en macroceldas, en particular, cuando el problema se debe a congestiones persistentes como por ejemplo las debidas a un crecimiento imprevisto de población en un área determinada. Una vez que se describe el problema, se justifica la necesidad del algoritmo propuesto y se describe tanto el modelo de red empleado como las medidas de sistema utilizadas. A continuación, se presenta el esquema de auto-ajuste (FLC) diseñado, mostrando sus entradas y salidas, así como las reglas que definen su comportamiento. Seguidamente, se describe el proceso de optimización mediante el uso del algoritmo de Q-Learning particularizado al problema en cuestión. En este sentido, se establecen una serie de supuestos prácticos que permiten aumentar la eficacia del controlador diseñado. Por último, se muestran los resultados de la evaluación y validación de las técnicas propuestas mediante el uso del simulador LTE diseñado en el Capítulo 4.

La segunda parte del Capítulo 5 trata el problema de balance de carga en escenarios de femtoceldas corporativas. Tras describir brevemente el problema y justificar la solución, se presentan dos diseños de FLC extraídos de la literatura que serán posteriormente combinados con los nuevos diseños propuestos en esta tesis para mejorar sus prestaciones. Los FLC no solo modifican los márgenes de traspaso, sino también la potencia de transmisión de las femtoceldas. Seguidamente, se explican las métodos propuestos, los cuales están basados en FLC y Q-Learning, así como la combinación con los FLC ya existentes. Finalmente, se presentan los resultados de evaluar las diferentes estrategias en un simulador específico de femtoceldas.

A.3.3 Optimización de la movilidad

El Capítulo 6 dedica una primera parte a la optimización de traspasos en redes de comunicaciones móviles, mientras que la segunda parte se dedica a la coordinación de esta función con la estudiada en el capítulo anterior, el balance de carga. El Capítulo 6 comienza con una descripción de los principales parámetros presentes en el algoritmo de traspaso y de las medidas que se utilizarán en el posterior diseño del algoritmo SON. Tras esto, se describe el diseño del FLC propuesto para la optimización de traspasos. En particular, se presentan tres configuraciones diferentes del FLC, en función de las reglas y los valores de salida que se definen. La principal diferencia entre estas configuraciones es la magnitud del cambio en el parámetro a modificar. El diseño del controlador se basa en un análisis de sensibilidad de los dos parámetros más importantes del algoritmo de traspaso, es decir, el margen de traspaso y el *Time-to-Trigger*. Dicho análisis se lleva a cabo para diferentes situaciones de carga y velocidad de usuario en una red LTE. Posteriormente, se evalúan las prestaciones del FLC y se analiza el impacto de modificar dicho parámetro según diferentes niveles de optimización, por ejemplo, a nivel de red, de celda o de adyacencia, así como el impacto del ruido en las medidas que deciden cuando se dispara un traspaso.

La segunda parte del Capítulo 6 trata el problema de la coordinación entre las funciones propuestas de MLB y MRO. La solución adoptada se basa en inhibir una de las funciones cuando su actuación (por ejemplo, valores extremos en el parámetro a modificar) puede empeorar las prestaciones de la red debido a la actuación de la otra función. Para ello, se definen una serie de umbrales que permiten detectar aquellas situaciones en las que este hecho ocurre. Finalmente, se evalúan las prestaciones del algoritmo de coordinación en una de estas situaciones que requiere resolver el conflicto entre ambas funciones.

A.3.4 Direccionamiento de tráfico en redes heterogéneas

En el Capítulo 7 se estudian diferentes técnicas para el direccionamiento de tráfico (TS) en redes heterogéneas. El estudio se divide en dos partes: la primera se centra en el desarrollo de técnicas mediante ajuste estático de los parámetro de red, es decir, a través de una serie de análisis de sensibilidad que permitan encontrar los ajustes óptimos; la segunda parte se dedica al desarrollo de técnicas mediante ajuste dinámico, las cuales modifican los parámetros de forma adaptativa para hacer frente a las variaciones de contexto en la red.

En primer lugar, se describe el problema haciendo hincapié en las principales cuestiones que surgen en un escenario de redes heterogéneas cuando el operador desea redirigir el tráfico en la red de acuerdo a una determinada política. Seguidamente, se describe el escenario bajo el cual se evaluarán las técnicas propuestas. Dicho escenario debe ser representativo de las principales características que definen una red heterogénea. Tras esto, se presentan según la terminología 3GPP dos algoritmos que son muy importantes en este tipo de escenarios, la reselección de celda mediante prioridades absolutas y el algoritmo de traspaso inter-tecnología. Así mismo, se especifican las medidas de red que se utilizarán a lo largo del capítulo. Una vez que se han introducido los conceptos previos necesarios, el capítulo se centra en el enfoque estático, comenzando por un breve estudio de las técnicas existentes para realizar TS. Tras justificar el uso de las técnicas en la presente tesis, se investiga cómo ajustar las prioridades absolutas del algoritmo de reselección de celda en función de las características del escenario. A continuación, se describe el algoritmo propuesto que optimiza los parámetros de traspaso inter-tecnología mediante una serie de análisis de sensibilidad. Una vez explicado el enfoque estático, el estudio se centra en el enfoque dinámico, el cual se basa en el diseño de un FLC optimizado por el algoritmo de Q-Learning que permite soportar diferentes políticas del operador y adaptarse a cambios en la red. Dicho algoritmo se basa en el ajuste de los parámetros de traspaso inter-tecnología. Finalmente, se muestran los resultados de evaluar los algoritmos tanto del enfoque estático como del dinámico.

A.4 Evaluación

La evaluación y comparación de las distintas alternativas propuestas en esta tesis se describe en la última parte de los Capítulos 5, 6 y 7. Para cada una de ellas, se han utilizado diversas metodologías, medidas, figuras de mérito, etc. Las pruebas se han realizado mediante el uso de simuladores dinámicos de red, adaptados a las particularidades del problema a resolver. Respecto al simulador LTE principalmente utilizado para la evaluación de los algoritmos desarrollados, los resultados de las pruebas realizadas para su validación se describen al final del Capítulo 4.

A.4.1 Resultados

Balance de carga mediante movilidad.

Para analizar los algoritmos propuestos de balance de carga en escenarios de macroceldas, se define una figura de mérito que tiene en cuenta tanto el bloqueo experimentado en la red como la caída de llamadas. De esta manera, dicha figura de mérito ofrece una medida sobre la insatisfacción de usuarios en la red. Las simulaciones presentan un tráfico espacial no uniforme con el objetivo de focalizar la carga en el centro del escenario y generar cierta congestión. Los algoritmos propuestos se comparan con un caso de referencia, caracterizado por el uso de un FLC sin optimizar para balance de carga. En los resultados, se presenta la evolución en el tiempo de un parámetro característico del algoritmo de optimización y los principales indicadores relativos al bloqueo y la caída de llamadas, así como su representación a nivel de celda. Los resultados muestran que es posible reducir significativamente el bloqueo en la red mientras se mantiene la

caída de llamadas en las celdas vecinas bajo un cierto nivel establecido por el operador.

En el caso del balance de carga en escenarios de femtoceldas corporativas, se define una figura de mérito similar al caso anterior, en la que igualmente se mide el empeoramiento de la calidad de la conexión como efecto indeseado al realizar balance de carga en la red. Además, para comparar los algoritmos propuestos, se hace uso de un modelo de horizonte infinito [164] que permite evaluar respuestas temporales en donde las muestras más lejanas en el tiempo se consideran menos importantes que las más cercanas. El estudio también incluye un análisis de la carga de señalización introducida por la modificación de los parámetros involucrados, así como la evolución temporal de estos parámetros y otros indicadores de interés. Los resultados destacan los beneficios de combinar FLCs, que proporcionan una respuesta rápida, con diseños propuestos en la tesis (basados en FLC y Q-Learning), que proporcionan buenas prestaciones a largo plazo.

Optimización de la movilidad.

La descripción de los resultados sobre optimización de la movilidad incluye en primer lugar un análisis de sensibilidad de los dos parámetros más característicos del procedimiento de traspaso. El análisis se lleva a cabo para diferentes niveles de carga de la red y diferentes velocidades de usuario. Se asume además que la distribución espacial de tráfico es uniforme. Los resultados muestran que la red es más sensible a variaciones en el margen de traspaso que en el *Time-to-Trigger*. Posteriormente, se presentan los resultados de evaluar el FLC propuesto, cuyo diseño está basado en los resultados del análisis de sensibilidad previo. Para ello, se ha considerado que la época de optimización o intervalo de tiempo que hay entre dos modificaciones del parámetro involucrado debe ser suficientemente largo para obtener medidas fiables de los indicadores de prestaciones para el tamaño de red, el modelo de tráfico y la carga de red seleccionados para las simulaciones. También se ha definido una figura de mérito que incluye un indicador relativo a las llamadas caídas y otro relativo a la carga de señalización debida a los traspasos. Para facilitar la visualización de los resultados, se presentan en una misma gráfica los dos principales indicadores de prestaciones para este problema. Los resultados muestran que la configuración propuesta para el FLC proporciona valores más bajos de caída de llamadas que otras configuraciones evaluadas, a la vez que se mantiene un coste de señalización similar. Este hecho es especialmente apreciable cuando la velocidad de los usuarios del escenario es elevada.

Para la evaluación del esquema propuesto de coordinación entre MLB y MRO se analiza la evolución temporal de los indicadores principales y se realizan medidas no solo a nivel de red sino también a nivel de celda. En este caso, la distribución espacial de tráfico es no uniforme con el objetivo de crear congestión en la red. Los resultados indican que la coordinación es necesaria, haciéndose efectiva en determinadas situaciones en las que algún indicador de la red (p.ej. de bloqueo o de señalización de traspasos en la red) provoca que el parámetro a modificar (el margen de traspaso) alcance valores grandes.

Direccionamiento de tráfico en redes heterogéneas.

Las prestaciones de los algoritmos propuestos para el direccionamiento de tráfico en redes heterogéneas se han evaluado en un simulador HSPA/LTE dinámico de nivel de sistema que incluye celdas de diferentes tamaños, en particular, macroceldas y picoceldas. En los resultados, se

definen los indicadores utilizados para la evaluación de dichos algoritmos, como por ejemplo la medida del tráfico cursado en la red, definido según el servicio proporcionado a los usuarios. Otros indicadores están relacionados por ejemplo con la distribución de usuarios a través de las redes presentes en el escenario, así como la utilización de recursos en dichas redes. El estudio también ha tenido en cuenta diferentes niveles de penetración de los terminales LTE. Además, para analizar la capacidad de adaptación del controlador propuesto, se ha incluido un cambio en la distribución espacial de usuarios que afecta al número de usuarios presentes en los *hotspots* o lugares donde existe una alta concentración de usuarios. Los resultados muestran que las técnicas propuestas son efectivas para modificar la distribución de usuarios, especialmente cuando las áreas de cobertura de las redes están completamente solapadas (p.ej. cuando las estaciones bases comparten los emplazamientos). Además, el controlador propuesto es capaz de modificar la distribución de usuarios de acuerdo a las políticas del operador, así como de adaptarse a cambios contextuales en la red.

A.4.2 Conclusiones

En el Capítulo 8 se resume el trabajo realizado durante la tesis. En particular, se describen los resultados y aportaciones para cada uno de los problemas abordados y se proponen líneas de continuación.

Las principales aportaciones de la tesis son las siguientes:

- Propuesta de algoritmos para el balance de carga mediante movilidad en macroceldas. Los diseños propuestos están basados en la optimización mediante Q-Learning de un FLC que trata de resolver problemas de congestión persistente en redes inalámbricas de próxima generación. El objetivo principal es reducir el bloqueo para servicios de voz controlando al mismo tiempo la degradación causada en la calidad de la conexión de aquellos usuarios afectados por el proceso.
- Propuesta de algoritmos para el balance de carga mediante movilidad en femtoceldas corporativas. El objetivo principal consiste en mejorar, mediante el uso de técnicas de optimización (en este caso, Q-Learning), las prestaciones de diseños existentes basados en FLC aprovechando la velocidad que poseen estos controladores. La degradación de la calidad de la conexión también es un factor clave en el desarrollo de los esquemas propuestos.
- Propuesta de algoritmos para la optimización de la movilidad. Las principales contribuciones en esta área son:
  - Un análisis de sensibilidad de los principales parámetros de traspaso realizado para diferentes niveles de carga de la red y diferentes velocidades de usuario.
  - El diseño de un FLC que modifica adaptativamente los márgenes de traspaso para la optimización de la movilidad. Para ello, se han considerado diferentes configuraciones del FLC, así como diferentes niveles de optimización (a nivel de red, de celda y de adyacencia). También se ha analizado el impacto del ruido en las medidas de nivel de señal que se utilizan para lanzar un traspaso.

  - El diseño de un esquema de coordinación entre el FLC propuesto para la optimización de la movilidad y el algoritmo (FLC combinado con Q-Learning) propuesto para el balance de carga mediante movilidad. Dicha coordinación trata de coordinar dos funciones cuyos cambios en la red se producen lentamente (en torno a minutos, horas).

- Propuesta de algoritmos para el direccionamiento de tráfico en redes heterogéneas. Las principales contribuciones en esta área son:

  - Un análisis de la asignación de prioridades absolutas a las redes de una red heterogénea en el algoritmo de reselección de celda. Se estudian algunas cuestiones que surgen del ajuste estático de los parámetros de reselección de celda desde el punto de vista del direccionamiento de tráfico.

  - Un procedimiento para seleccionar los umbrales óptimos de los eventos del 3GPP que controlan la ejecución de los traspasos inter-tecnología. Dicha selección resulta especialmente tediosa en escenarios con diferentes tamaños de celdas y cuando los eventos que controlan la ejecución de traspasos se basan en los niveles de señal recibida por el terminal.

  - El diseño de un esquema basado en FLC y optimizado mediante Q-Learning que proporciona al operador la flexibilidad de elegir diferentes políticas de direccionamiento de tráfico y permite cierta adaptación a las variaciones del entorno (p.ej. en la distribución de usuarios) de forma automática. Para ello, el algoritmo propuesto modifica los umbrales de los eventos que controlan la ejecución de los traspasos inter-tecnología.

A.5 Lista de publicaciones

La siguiente lista presenta las publicaciones relacionadas con esta tesis:

Revistas

Derivadas de la tesis

[I] P. Muñoz, R. Barco, D. Laselva y P. Mogensen. Mobility-based Strategies for Traffic Steering in Heterogeneous Networks. *IEEE Communications Magazine*, vol. 51, no. 5, pp 54-62, May 2013.

[II] P. Muñoz, R. Barco y I. de la Bandera, Optimization of Load Balancing using Fuzzy Q-Learning for Next Generation Wireless Networks, *Expert Systems With Applications* (Elsevier), vol. 40, no. 4, pp 984-994, Marzo 2013.

[III] P. Muñoz, D. Laselva, R. Barco y P. Mogensen. Adjustment of mobility parameters for traffic steering in multi-RAT multi-layer wireless networks, *EURASIP Journal on Wireless*

Communication and Networking, 2013:133, May 2013.

[IV] P. Muñoz, R. Barco e I. de la Bandera. On the Potential of Handover Parameter Optimization for Self-Organizing Networks. *IEEE Transactions on Vehicular Technology*, aceptado en 2013.

[V] P. Muñoz, R. Barco, J. M. Ruiz, I. de la Bandera y A. Aguilar. Fuzzy Rule-based Reinforcement Learning for Load Balancing Techniques in Enterprise LTE Femtocells. *IEEE Transactions on Vehicular Technology*, aceptado en 2012.

[VI] J. M. Ruiz, S. Luna-Ramírez, M. Toril, F. Ruiz, I. de la Bandera, P. Muñoz, R. Barco, P. Lázaro y V. Buenestado, Design of a Computationally Efficient Dynamic System-Level Simulator for Enterprise LTE Femtocell Scenarios, *Journal of Electrical and Computer Engineering*, vol. 2012, Diciembre 2012.

[VII] P. Muñoz, I. de la Bandera, F. Ruiz, S. Luna-Ramírez, R. Barco, M. Toril, P. Lázaro y J. Rodríguez, Computationally-Efficient Design of a Dynamic System-Level LTE Simulator, *International Journal of Electronics and Telecommunications*, vol. 57, no. 3, pp 347-358, Septiembre 2011.

Relacionadas con la tesis

[VIII] R. Barco, P. Lázaro y P. Muñoz. A Unified Framework for Self-Healing in Wireless Networks. *IEEE Communications Magazine*, Vol.50 (12), pp.134-142. Diciembre 2012.

Conferencias y *Workshops*

Derivadas de la tesis

[IX] P. Muñoz, I. de la Bandera, R. Barco, M. Toril, S. Luna-Ramírez y J.M. Ruiz, "Sensitivity Analysis and Self-Optimization of LTE Intra-Frequency Handover", *6th Scientific Meeting, COST action IC1004*, Málaga (España), Febrero 2013.

[X] P. Muñoz, R. Barco, I. de la Bandera, M. Toril y S. Luna-Ramírez, "Optimization of a Fuzzy Logic Controller for Handover-based Load Balancing", *Int. Workshop on Self-Organising Networks (IWSON), IEEE Vehicular Technology Conference (VTC) Spring*, Budapest, Hungría, Mayo 2011.

[XI] P. Muñoz, I. de la Bandera, R. Barco, F. Ruiz, M. Toril y S. Luna-Ramírez, "Estimation of Link-Layer Quality Parameters in a System-Level LTE Simulator", *5th International Conference on Broadband and Biomedical Communications* (IB2COM) 2010. Málaga (España).

Diciembre, 2010.

[XII] P. Muñoz, I. de la Bandera, R. Barco, M. Toril y S. Luna-Ramírez, "Optimización del balance de carga en redes LTE mediante el algoritmo de Q-Learning difuso", *XXVI Simposio de la Unión Científica Internacional de Radio* (URSI 2011), Leganés (España), Septiembre, 2011.

[XIII] I. de la Bandera, P. Muñoz, R. Barco, M. Toril y S. Luna-Ramírez, "Auto-ajuste del margen de handover en redes LTE", *XXVI Simposio de la Unión Científica Internacional de Radio* (URSI 2011), Leganés (España), Septiembre, 2011.

[XIV] P. Muñoz, I. de la Bandera, R. Barco, F. Ruiz, M. Toril y S. Luna-Ramírez, "Diseño del Nivel de Enlace para un Simulador LTE", *XXV Simposio de la Unión Científica Internacional de Radio* (URSI 2010), Bilbao (España), Septiembre, 2010.

Relacionadas con la tesis

[XV] J.M. Ruiz, S. Luna-Ramírez, M. Toril, F. Ruiz, I. de la Bandera y P. Muñoz, "Analysis of Load Sharing Techniques in Enterprise LTE Femtocells", *Int. Workshop on Femtocells, Wireless Advanced* 2011, Londres, Reino Unido, Junio 2011.

[XVI] J. Rodríguez, I. de la Bandera, P. Muñoz y R. Barco, "Load Balancing in a Realistic Urban Scenario for LTE Networks", *Int. Workshop on Self-Organising Networks (IWSON), IEEE Vehicular Technology Conference (VTC) Spring*, Budapest, Hungría, Mayo 2011.

[XVII] J. Rodríguez, I. de la Bandera, P. Muñoz y R. Barco, "Balance de carga en red LTE en un entorno urbano realista", *XXVI Simposio de la Unión Científica Internacional de Radio* (URSI 2011), Leganés (España), Septiembre, 2011.

[XVIII] G. Jiménez, R. Barco, P. Muñoz y M. Toril, "Optimización del Umbral de Traspaso para Femtoceldas LTE", *XXVI Simposio de la Unión Científica Internacional de Radio* (URSI 2011), Leganés (España), Septiembre, 2011.

[VI, VII, XI, XIV] se dedican a las herramientas de simulación que facilitan la evaluación de las prestaciones de los algoritmos propuestos. [II, X, XII, XVI, XVII] tratan el problema de balance de carga en escenarios de macroceldas, mientras que en escenarios de femtoceldas este problema se estudia en [V, XV, XVIII]. El problema de la optimización de los traspasos se aborda en [IV, IX, XIII]. [VIII] se dedica a la auto-curación en el campo de redes auto-organizativas. En [I, III], se describen las técnicas propuestas para el direccionamiento de tráfico en el contexto de redes heterogéneas. El autor ha sido el autor principal de todas las contribuciones "derivadas de la tesis" excepto [VI, XIII], siendo un contribuidor clave en las mismas. En [VI], el autor escribió la sección dedicada al modelo de movilidad en interiores y estuvo involucrado en el diseño de la capa de enlace del simulador. En [XIII], el autor participó activamente en las etapas de diseño

y análisis, así como en la escritura del documento. Finalmente, el autor ayudó con la escritura y revisión de las publicaciones "relacionadas con la tesis".

Todas estas contribuciones han surgido en el marco de diversos proyectos de investigación. En particular, las siguientes publicaciones fueron desarrolladas en el marco de estos proyectos:

- Proyecto P08-TIC-4052 financiado por la Junta de Andalucía: [I-VII, IX-XVIII].
- Proyecto TEC2009-13413 financiado por el Ministerio Español de Ciencia e Innovación: [II, V-VII, IX-XIV, XV, XVIII].
- Proyecto IPT-2011-1272-430000 financiado por el Ministerio Español de Ciencia e Innovación: [V].

Así mismo, [I, III] fueron desarrolladas en colaboración con Nokia Siemens Networks en Aalborg, Dinamarca.

Bibliography

[1] Information and Communication Technology (ICT) Statistics, International Telecommunication Union (ITU). The World in 2011: ICT Facts and Figures, Version 1.0, 2011. www.itu.int/ict .

[2] L.C. Schmelz et al. Self-configuration, -optimisation and -healing in wireless networks. In *Wireless World Research Forum Meeting 20*, 2008.

[3] O. G. Aliu, A. Imran, M. A. Imran, and B. Evans. A Survey of Self Organisation in Future Cellular Networks. *IEEE Communications Surveys & Tutorials*, 15(1):336–361, 2013.

[4] Next Generation Mobile Networks (NGMN) Alliance. White Paper Next Generation Mobile Networks Beyond HSPA & EVDO, Version 3.0, December 2006. www.ngmn.org .

[5] 3GPP. Evolved Universal Terrestrial Radio Access (E-UTRA) and Evolved Universal Terrestrial Radio Access Network (E-UTRAN); Overall description; Stage 2, version 11.4.0 (2012-12). TS 36.300.

[6] 3GPP. Self-Organizing Networks (SON) Policy Network Resource Model (NRM) Integration Reference Point (IRP); Information Service (IS), version 11.4.0 (2012-12). TS 32.522.

[7] J. Li, C. Fan, D. Yang, and J. Gu. UMTS Soft Handover Algorithm with Adaptive Thresholds for Load Balancing. In *Proc. of IEEE 62nd Vehicular Technology Conference (VTC)*, 2005.

[8] A. Lobinger, S. Stefanski, T. Jansen, and I. Balan. Load Balancing in Downlink LTE Self-Optimizing Networks. In *Proc. of IEEE Vehicular Technology Conference (VTC)*, 2010.

[9] R. Nasri, A. Samhat, and Z. Altman. A New Approach of UMTS-WLAN Load Balancing; Algorithm and its Dynamic Optimization. In *IEEE International Symposium on a World of Wireless, Mobile and Multimedia Networks*, 2007.

[10] R. Kwan, R. Arnott, R. Paterson, R. Trivisonno, and M. Kubota. On Mobility Load Balancing for LTE Systems. In *Proc. of IEEE Vehicular Technology Conference (VTC)*, 2010.

[11] J. Ruiz-Avilés et al. Analysis of load sharing techniques in enterprise LTE femtocells. In *Proc. of 4th International Workshop on Femtocells, Wireless Advanced (WiAd)*, 2011.

[12] A. Schröder, H. Lundqvist, and G. Nunzi. Distributed Self-Optimization of Handover for the Long Term Evolution. In *Proc. of 3rd International Workshop on Self-Organizing Systems (IWSOS)*, 2008.

[13] D. W. Lee, G. T. Gil, and D. H. Kim. A cost-based adaptive handover hysteresis scheme to minimize the handover failure rate in 3GPP LTE system. *EURASIP Journal on Wireless Communications and Networking*, 2010(6), 2010.

[14] K. Kitagawa, T. Komine, T. Yamamoto, and S. Konishi. A handover optimization algorithm with mobility robustness for LTE systems. In *Proc. of IEEE 22nd International Symposium on Personal Indoor and Mobile Radio Communications (PIMRC)*, 2011.

[15] I. Balan, T. Jansen, B. Sas, I. Moerman, and T. Kürner. Enhanced weighted performance based handover optimization in LTE. In *Proc. of Future Network Mobile Summit*, 2011.

[16] L. Ewe and H. Bakker. Base station distributed handover optimization in LTE self-organizing networks. In *Proc. of IEEE 22nd International Symposium on Personal Indoor and Mobile Radio Communications (PIMRC)*, 2011.

[17] H. J. Wang, R. H. Katz, and J. Giese. Policy-enabled handoffs across heterogeneous wireless networks. In *Proc. of IEEE Workshop on Mobile Computing Systems and Applications (WMCSA '99)*, 1999.

[18] X. Gelabert, J. Pérez-Romero, O. Salient, and R. Agustí. A 4-Dimensional Markov Model for the Evaluation of Radio Access Technology Selection Strategies in Multiservice Scenarios. In *Proc. of IEEE 64th Vehicular Technology Conference (VTC)*, 2006.

[19] L. Giupponi, R. Agustí, J. Pérez-Romero, and O. Salient. A Framework for JRRM with Resource Reservation and Multiservice Provisioning in Heterogeneous Networks. *Mobile Networks and Applications*, 11:825–846, 2006.

[20] L. Giupponi and R. Agustí and J. Pérez-Romero and O. Salient. A Fuzzy Neural Joint Radio Resource Management in a Multi-Cell Scenario Supporting a Multiservice Architecture. In *Proc. of 6th IEEE International Conference on 3G and Beyond*, 2007.

[21] A. Furuskar and J. Zander. Multiservice Allocation for Multiaccess Wireless Systems. *IEEE Transactions on Wireless Communications*, 4:174–184, 2005.

[22] www.mobilenet.ic.uma.es.

[23] H. Holma and A. Toskala. *HSDPA/HSUPA for UMTS: High Speed Radio Access for Mobile Communications*. Wiley, 2006.

[24] 3GPP. High Speed Downlink Packet Access (HSDPA); Overall description; Stage 2, version 11.3.0 (2012-12). TS 25.308.

[25] 3GPP. Requirements for support of radio resource management (FDD), version 11.3.0 (2012-12). TS 25.133.

[26] 3GPP. Physical layer; Measurements (FDD), version 11.0.0 (2011-12). TS 25.215.

[27] 3GPP. FDD Enhanced Uplink; Physical Layer Aspects, version 6.0.0 (2005-03). TR 25.808.

[28] M. Rinne and O. Tirkkonen. LTE, the radio technology path towards 4G. *Computer Communications*, 33(16):1894 –1906, October 2010.

[29] F. Khan. *LTE for 4G Mobile Broadband: Air Interface Technologies and Performance*. Cambridge University Press, 2009.

[30] 3GPP. Evolved Universal Terrestrial Radio Access (E-UTRA); Physical Channels and Modulation, version 11.1.0 (2012-12). TS 36.211.

[31] 3GPP. Evolved Universal Terrestrial Radio Access (E-UTRA); Multiplexing and channel coding, version 11.1.0 (2012-12). TS 36.212.

[32] 3GPP. Evolved Universal Terrestrial Radio Access (E-UTRA); Medium Access Control (MAC) protocol specification, version 11.1.0 (2012-12). TS 36.321.

[33] 3GPP. Evolved Universal Terrestrial Radio Access (E-UTRA); Radio Link Control (RLC) protocol specification, version 11.0.0 (2012-09). TS 36.322.

[34] 3GPP. Evolved Universal Terrestrial Radio Access (E-UTRA); Packet Data Convergence Protocol (PDCP) specification, version 11.1.0 (2012-12). TS 36.323.

[35] 3GPP. Evolved Universal Terrestrial Radio Access (E-UTRA); Radio Resource Control (RRC); Protocol specification, version 11.2.0 (2012-12). TS 36.331.

[36] 3GPP. Evolved Universal Terrestrial Radio Access (E-UTRA); Physical layer; Measurements, version 11.1.0 (2012-12). TS 36.214.

[37] R. Barco, P. Lázaro, and P. Muñoz. A Unified Framework for Self-Healing in Wireless Networks. *IEEE Communications Magazine*, 50(12):134–142, 2012.

[38] 3GPP. Self Configuration of Network Elements; Concepts and requirements, version 11.0.0 (2012-09). TS 32.501.

[39] 3GPP. Self-Organizing Networks (SON); Self-healing concepts and requirements, version 11.0.0 (2012-09). TS 32.541.

[40] 3GPP. Self-Organizing Networks (SON) Policy Network Resource Model (NRM) Integration Reference Point (IRP); Requirements, version 11.1.0 (2012-12). TS 32.521.

[41] S. Hamalainen, H. Sanneck, and C. Sartori. *LTE Self-Organising Networks (SON): Network Management Automation for Operational Efficiency*. Wiley, 2011.

[42] J. Ramiro and K. Hamied. *Self-Organizing Networks. Self-Planning, Self-Optimization and Self-Healing for GSM, UMTS and LTE*. Wiley, 2012.

[43] 3GPP. Evolved Universal Terrestrial Radio Access Network (E-UTRAN); Self-configuring and self-optimizing network (SON) use cases and solutions, version 9.3.1 (2011-03). TR 36.902.

[44] INFSO-ICT-216284 SOCRATES. Use Cases for Self-Organising Networks. Technical Report Deliverable D2.1, Version 1.0, March, 2008.

[45] N. T. K. Jorgensen, D. Laselva, and J. Wigard. On the Potentials of Traffic Steering Techniques between HSDPA and LTE. In *Proc. of IEEE 73rd Vehicular Technology Conference (VTC)*, 2011.

[46] M. Döttling and I. Viering. Challenges in mobile network operation: Towards self-optimizing networks. In *Proc. of IEEE International Conference on Acoustics, Speech and Signal Processing (ICASSP)*, 2009.

[47] Z. Altman et al. The Celtic Gandalf framework. In *Proc. of IEEE Mediterranean Electrotechnical Conference (MELECON)*, 2006.

[48] ICT-2007-216248 E3. Project Presentation Report. Technical Report Deliverable D0.2, Version 1.0, May, 2008.

[49] INFSO-ICT-224344 Self-NET. System Deployment Scenarios and Use Cases for Cognitive Management of Future Internet Elements. Technical Report Deliverable D1.1, Version 1.0, October, 2008.

[50] FP7-257513 UniverSelf. Synthesis of Use Case Requirements - Release 1. Technical Report Deliverable D4.1, Version 2.0, August, 2012.

[51] INFSO-ICT-316384 SEMAFOUR. Self-Management for Unified Heterogeneous Radio Access Networks. Technical Report Deliverable D6.1, Version 1.0, October, 2012.

[52] 3GPP. Self-Organizing Networks (SON); Concepts and requirements, version 11.1.0 (2011-12). TS 32.500.

[53] 3GPP. Feasibility study for Further Advancements for E-UTRA (LTE-Advanced), version 11.0.0 (2012-09). TR 36.912.

[54] S. Luna-Ramírez, M. Toril, M. Fernández-Navarro, and V. Wille. Optimal traffic sharing in GERAN. *Wireless Personal Communications*, 57(4):553 –574, April 2011.

[55] A. Tölli and P. Hakalin. Adaptive Load Balancing between Multiple Cell Layers. In *Proc. of IEEE Vehicular Technology Conference (VTC), Fall*, 2002.

[56] A. Pillekeit, F. Derakhshan, E. Jugl, and A. Mitschele-Thiel. Force-based Load Balancing in Co-located UMTS/GSM Networks. In *Proc. of IEEE Vehicular Technology Conference (VTC), Fall*, 2004.

[57] H. Wang, L. Ding, P. Wu, Z. Pan, N. Liu, and X. You. Dynamic Load Balancing in 3GPP LTE Multi-Cell Networks with Heterogenous Services. In *5th International ICST Conference on Communications and Networking in China (CHINACOM)*, 2010.

[58] H. Zhang, X. Qiu, L. Meng, and X. Zhang. Design of Distributed and Autonomic Load Balancing for Self-Organization LTE. In *Proc. of IEEE 72nd Vehicular Technology Conference (VTC)*, 2010.

[59] A. El-Halaby and M. Awad. A game theoretic scenario for LTE load balancing. In *Proc. of IEEE AFRICON*, 2011.

[60] Z. Li, H. Wang, Z. Pan, N. Liu, and X. You. Joint optimization on load balancing and network load in 3GPP LTE multi-cell networks. In *Proc. of International Conference on Wireless Communications and Signal Processing (WCSP)*, 2011.

[61] V. Chandrasekhar, J. Andrews, and A. Gatherer. Femtocell networks: a survey. *IEEE Communications Magazine*, 46(9):59 – 67, 2008.

[62] Z. Altman et al. Femtocells: The HOMESNET vision. In *Proc. of IEEE 21st International Symposium on Personal, Indoor and Mobile Radio Communications Workshops (PIMRC)*, 2010.

[63] A. G. Serrano, L. Giupponi, and M. Dohler. BeFEMTO's self-organized and docitive femtocells. In *Proc. of Future Network and Mobile Summit*, 2010.

[64] G. Vivier et al. Femtocells for next-G wireless systems: The FREEDOM approach. In *Proc. of Future Network and Mobile Summit*, 2010.

[65] D. López-Pérez, A. Valcarce, G. de la Roche, and J. Zhang. OFDMA femtocells: A roadmap on interference avoidance. *IEEE Communications Magazine*, 47(9):41 – 48, 2009.

[66] S. Barbarossa, S. Sardelliti, A. Carfagna, and P. Vecchiarelli. Decentralized interference management in femtocells: A game-theoretic approach. In *Proc. of Fifth International Conference on Cognitive Radio Oriented Wireless Networks & Communications (CROWNCOM)*, 2010.

[67] M. Bennis, S. Guruacharya, and D. Niyato. Distributed Learning Strategies for Interference Mitigation in Femtocell Networks. In *Proc. of IEEE Global Telecommunications Conference (GLOBECOM)*, 2011.

[68] H. Claussen and F. Pivit. Femtocell Coverage Optimization Using Switched Multi-Element Antennas. In *Proc. of IEEE International Conference on Communications (ICC '09)*, 2009.

[69] Z. Becvar and P. Mach. Adaptive Hysteresis Margin for Handover in Femtocell Networks. In *Proc. of 6th International Conference on Wireless and Mobile Communications (ICWMC)*, 2010.

[70] D. M. Rose, T. Jansen, and T. Kürner. Modeling of Femto Cells - Simulation of Interference and Handovers in LTE Networks. In *Proc. of IEEE 73rd Vehicular Technology Conference (VTC), Spring*, 2011.

[71] A. Tyrrell, F. Zdarsky, E. Mino, and M. López. Use Cases, Enablers and Requirements for Evolved Femtocells. In *Proc. of IEEE 73rd Vehicular Technology Conference (VTC Spring)*, 2011.

[72] I. Ashraf, H. Claussen, and L. T. W. Ho. Distributed Radio Coverage Optimization in Enterprise Femtocell Networks. In *Proc. of IEEE International Conference on Communications (ICC)*, 2010.

[73] J. Ruiz-Avilés, S. Luna-Ramírez, M. Toril, and F. Ruiz. Fuzzy logic controllers for traffic sharing in enterprise LTE femtocells. In *Proc. of IEEE 75th Vehicular Technology Conference (VTC)*, 2011.

[74] S. M. Tseng and W. Z. Tseng. Drop rate optimization by tuning time to trigger for WCDMA systems. In *Proc. of Second International Conference on Ubiquitous and Future Networks (ICUFN)*, 2010.

[75] C. Werner, J. Voigt, S. Khattak, and G. Fettweis. Handover Parameter Optimization in WCDMA using Fuzzy Controlling. In *Proc. of IEEE 18th International Symposium on Personal, Indoor and Mobile Radio Communications (PIMRC)*, 2007.

[76] P. Legg, G. Hui, and J. Johansson. A Simulation Study of LTE Intra-Frequency Handover Performance. In *Proc. of IEEE 72nd Vehicular Technology Conference (VTC)*, 2010.

[77] Yejee Lee, Bongjhin Shin, Jaechan Lim, and Daehyoung Hong. Effects of time-to-trigger parameter on handover performance in SON-based LTE systems. In *Proc. of 16th Asia-Pacific Conference on Communications (APCC)*, 2010.

[78] Q. Song, Z. Wen, X. Wang, L. Guo, and R. Yu. Time-Adaptive Vertical Handoff Triggering Methods for Heterogeneous Systems. *Computer Science*, 5737/2009:302–312, 2009.

[79] A. Awada, B. Wegmann, D. Rose, I. Viering, and A. Klein. Towards Self-Organizing Mobility Robustness Optimization in Inter-RAT Scenario. In *Proc. of IEEE 73rd Vehicular Technology Conference (VTC)*, 2011.

[80] R. Combes, Z. Altman, and E. Altman. Coordination of autonomic functionalities in communications networks. In *CoRR abs/1209.1236*, 2012.

[81] INFSO-ICT-216284 SOCRATES. Framework for the development of self-organisation methods. Technical Report Deliverable D2.4, Version 1.0.3, September, 2008.

[82] L. C. Schmelz, M. Amirijoo, A. Eisenblaetter, R. Litjens, M. Neuland, and J. Turk. A coordination framework for self-organisation in LTE networks. In *Proc. of IEEE International Symposium on Integrated Network Management (IM), 2011 IFIP*, pages 193–200, 2011.

[83] INFSO-ICT-216284 SOCRATES. Final Report on Self-Organisation and its Implications in Wireless Access Networks. Technical Report Deliverable D5.9, Version 1.0, December, 2010.

[84] B. Sas, K. Spaey, I. Balan, K. Zetterberg, and R. Litjens. Self-Optimisation of Admission Control and Handover Parameters in LTE. In *Proc. of IEEE 73rd Vehicular Technology Conference (VTC), Spring*, 2011.

[85] A. Lobinger, S. Stefanski, T. Jansen, and I. Balan. Coordinating Handover Parameter Optimization and Load Balancing in LTE Self-Optimizing Networks. In *Proc. of IEEE 73rd Vehicular Technology Conference (VTC), Spring*, 2011.

[86] W. Li, X. Duan, S. Jia, L. Zhang, Y. Liu, and J. Lin. A Dynamic Hysteresis-Adjusting

Algorithm in LTE Self-Organization Networks. In *Proc. of IEEE 75th Vehicular Technology Conference (VTC), Spring*, 2012.

[87] Y. Li, M. Li, B. Cao, Y. Wang, and W. Liu. Dynamic optimization of handover parameters adjustment for conflict avoidance in long term evolution. *China Communications*, 10(1):56–71, 2013.

[88] S. Horrich, S. Ben Jamaa, and P. Godlewski. Adaptive Vertical Mobility Decision in Heterogeneous Networks. In *Proc. of Third International Conference on Wireless and Mobile Communications (ICWMC)*, 2007.

[89] D. Turina and A. Furuskar. Traffic Steering and Service Continuity in GSM-WCDMA Seemless Networks. In *Proc. of the 8th International Conference on Telecommunications (ConTEL)*, 2005.

[90] I. de la Bandera, S. Luna-Ramírez, R. Barco, F. Ruiz, M. Toril, and M. Fernández-Navarro. Inter-system Cell Reselection Parameter Auto-Tuning in a Joint-RRM Scenario. In *Proc. of 5th International Conference on Broadband Communications and Biomedical Applications, IB2COM*, 2010.

[91] S. Luna-Ramírez, M. Toril, F. Ruiz, and M. Fernández-Navarro. Adjustment of a Fuzzy Logic Controller for IS-HO Parameters in a Heterogeneous Scenario. In *Proc. of the 14th IEEE Mediterranean Electrotechnical Conference, MELECON*, 2008.

[92] T. Chandra, W. Jeanes, and H. Leung. Determination of optimal handover boundaries in a cellular network based on traffic distribution analysis of mobile measurement reports. In *Proc. of 47th IEEE Vehicular Technology Conference (VTC)*, volume 1, pages 305–309, 1997.

[93] J. Steuer and K. Jobmann. The use of mobile positioning supported traffic density measurements to assist load balancing methods based on adaptive cell sizing. In *Proc. of 13th IEEE Int. Symp. on Personal Indoor and Mobile Radio Communications*, volume 3, pages 339–343, 2002.

[94] M. Toril and V. Wille. Optimization of Handover Parameters for Traffic Sharing in GERAN. *Wireless Personal Communications*, 47(3):315 –336, 2008.

[95] S.B. ZahirAzami, G. Yekrangian, and M. Spencer. Load Balancing and Call Admission Control in UMTS-RNC, using Fuzzy Logic. In *International Conference on Communication Technology Proceedings (ICCT)*, 2003.

[96] J. Rodríguez, I. de la Bandera, P. Muñoz, and R. Barco. Load Balancing in a Realistic Urban Scenario for LTE Networks. In *Proc. of IEEE 73rd Vehicular Technology Conference (VTC)*, 2011.

[97] K. C. Foong, C. T. Chee, and L. S. Wei. Adaptive Network Fuzzy Inference System (ANFIS) Handoff Algorithm. In *Proc. of the International Conference on Future Computer and Communication (ICFCC)*, 2009.

[98] L. Giupponi and R. Agustí and J. Pérez-Romero and O. Sallent. A Novel Approach for Joint

Radio Resource Management Based on Fuzzy Neural Methodology. *IEEE Transactions on Vehicular Technology*, 57(3):1789–1805, 2008.

[99] A. Çalhan and C. Çeken. An optimum vertical handoff decision algorithm based on adaptive fuzzy logic and genetic algorithm. *Wireless Personal Communications*, pages 1–18, 2010.

[100] M. Dirani and Z. Altman. Self-Organizing Networks in Next Generation Radio Access Networks: Application to Fractional Power Control. *Computer Networks*, 55(2):431–438, 2011.

[101] R. S. Sutton and A. G. Barto. *Reinforcement Learning: an Introduction*. MIT Press, 1998.

[102] Y. H. Chen, C. J. Chang, and C. Y. Huang. Fuzzy Q-Learning Admission Control for WCDMA/WLAN Heterogeneous Networks with Multimedia Traffic. *IEEE Transactions on Mobile Computing*, 8(11):1469 –1479, 2009.

[103] J. Nie and S. Haykin. A dynamic channel assignment policy through Q-learning. *IEEE Transactions on Neural Networks*, 10(6):1443 – 1455, 1999.

[104] A. Galindo-Serrano and L. Giupponi. Distributed Q-learning for aggregated interference control in cognitive radio networks. *IEEE Transactions on Vehicular Technology*, 59(4):1823 – 1834, May 2010.

[105] El-Sayed M. El-Alfy and Yu-Dong Yao. Comparing a class of dynamic model-based reinforcement learning schemes for handoff prioritization in mobile communication networks. *Expert Systems with Applications*, 38(7):8730–8737, July 2011.

[106] R. Razavi, S. Klein, and H. Claussen. A Fuzzy Reinforcement Learning Approach for Self-Optimization of Coverage in LTE Networks. *Bell Labs Technical Journal*, 15(3):153–175, 2010.

[107] A. Galindo-Serrano and L. Giupponi. Downlink femto-to-macro interference management based on Fuzzy Q-Learning. In *Proc. of International Symposium on Modeling and Optimization in Mobile, Ad Hoc and Wireless Networks (WiOpt)*, 2011.

[108] A. Galindo-Serrano, L. Giupponi, and M. Majoral. On implementation requirements and performances of Q-learning for self-organized femtocells. In *Proc. of IEEE Global Telecommunications Conference (GLOBECOM)*, 2011.

[109] M. Haddad, Z. Altman, S.E. Elayoubi, and E. Altman. A Nash-Stackelberg Fuzzy Q-Learning Decision Approach in Heterogeneous Cognitive Networks. In *Proc. of IEEE Global Telecommunications Conference (GLOBECOM)*, 2010.

[110] M. Toril. *Self-Tuning Algorithms for the Assignment of Packet Control Units and Handover Parameters in GERAN*. PhD thesis, Communications Engineering Department, ETSIT, University of Málaga, 2007.

[111] L. A. Zadeh. Fuzzy Sets. *Information and Control*, 8:338–353, 1965.

[112] T. Ross. *Fuzzy logic with engineering applications*. Wiley, 2010.

[113] A. P. Engelbrecht. *Computational Intelligence: An Introduction*. John Wiley & Sons, 2007.

[114] Chuen Chien Lee. Fuzzy logic in control systems: fuzzy logic controller. I. *IEEE Transactions on Systems, Man and Cybernetics*, 20(2):404–418, 1990.

[115] E. H. Mamdani and S. Assilian. An Experiment in Linguistic Synthesis with a Fuzzy Logic Controller. *International Journal of Man-Machine Studies*, 7:1–13, 1975.

[116] T. Takagi and M. Sugeno. Fuzzy Identification of Systems and its Application to Modeling and Control. *IEEE Transactions on Systems, Man, and Cybernetics*, 15(1):116–132, 1985.

[117] R. C. Eberhart and Y. Shi. *Computational Intelligence Concepts to Implementations*. Elsevier, 2007.

[118] K. A. Smith and M. S. Palaniswami. Static and dynamic channel assignment using neural networks. *IEEE Journal on Selected Areas in Communications*, 15(2):238–249, 1997.

[119] D. Gómez-Barquero, D. Calabuig, J. F. Monserrat, N. García, and J. Pérez-Romero. Hopfield Neural Network-Based Approach for Joint Dynamic Resource Allocation in Heterogeneous Wireless Networks. In *Proc. of IEEE 64th Vehicular Technology Conference (VTC), Fall*, 2006.

[120] C.-T. T. Lin and C.-S. G. Lee. Neural-network-based fuzzy logic control and decision system. *IEEE Transactions on Computers*, 40(12):1320–1336, 1991.

[121] F. Herrera, M. Lozano, and J. L. Verdegay. Tuning Fuzzy Logic Controllers by Genetic Algorithms. *International Journal of Approximate Reasoning*, 12:299–315, 1995.

[122] M. A. Lee and H. Takagi. Integrating design stage of fuzzy systems using genetic algorithms. In *Proc. of Second IEEE International Conference on Fuzzy Systems*, volume 1, pages 612–617, 1993.

[123] C. L. Karr and E. J. Gentry. Fuzzy control of pH using genetic algorithms. *IEEE Transactions on Fuzzy Systems*, 1(1), 1993.

[124] J. Kinzel, F. Klawonn, and R. Kruse. Modifications of genetic algorithms for designing and optimizing fuzzy controllers. In *Proc. of the First IEEE Conference on Evolutionary Computation*, volume 1, pages 28–33, 1994.

[125] S. Ghost, A. Konar, and A. K. Nagar. Dynamic Channel Assignment Problem in Mobile Networks Using Particle Swarm Optimization. In *Proc. of Second UKSIM European Symposium on Computer Modeling and Simulation (EMS)*, pages 64–69, 2008.

[126] P. Garcia-Diaz, S. Salcedo-Sanz, J. Plaza-Laina, and A. Portilla-Figueras. A discrete Particle Swarm Optimization Algorithm for Mobile Network Deployment Problems. In *Proc. of IEEE 17th International Workshop on Computer Aided Modeling and Design of Communication Links and Networks (CAMAD)*, pages 61–65, 2012.

[127] L. Su, P. Wang, and F. Liu. Particle swarm optimization based resource block allocation algorithm for downlink LTE systems. In *Proc. of 18th Asia-Pacific Conference on Communications (APCC)*, pages 970–974, 2012.

[128] H. Dubreil, Z. Altman, V. Diascorn, J.-M. M. Picard, and M. Clerc. Particle swarm optimization of fuzzy logic controller for high quality RRM auto-tuning of UMTS networks. In *Proc. of IEEE 61st Vehicular Technology Conference (VTC), Spring*, volume 3, pages 1865–1869, 2005.

[129] C. Watkins and P. Dayan. Technical Note: Q-Learning. *Machine Learning*, 8(3):279 –292, 1992.

[130] P. Y. Glorennec. Fuzzy Q-learning and dynamical fuzzy Q-learning. In *Proc. of the Third IEEE Conference on Fuzzy Systems*, volume 1, pages 474–479, 1994.

[131] H. Dubreil. *Méthodes d'optimisation de contrôleurs de logique floue pour le paramétrage automatique des réseaux mobiles UMTS*. PhD thesis, ENST - COMELEC Communication et Electronique, 2005.

[132] D.P. Rini, S. M. Shamsuddin, and S. S. Yuhaniz. Particle Swarm Optimization: Technique, System and Challenges. *International Journal of Computer Applications*, 14(1):19–27, 2011.

[133] Q. Bai. Analysis of Particle Swarm Optimization Algorithm. *Computer and Information Science*, 3(1):180–184, 2010.

[134] E. S. Ali and S. M. Abd-Elazim. Statistical Assessment of New Coordinated Design of PSSs and SVC via Hybrid Algorithm. *International Journal of Engineering and Advanced Technology (IJEAT)*, 2(3):647–654, 2013.

[135] M. I. Jiménez Vega. Simulador dinámico de red de comunicaciones móviles de segunda generación. Master's thesis, Communications Engineering Department, ETSIT, University of Málaga, 2004.

[136] M. Guerrero Navarro. Simulador dinámico de red de comunicaciones móviles de tercera generación. Master's thesis, Communications Engineering Department, ETSIT, University of Málaga, 2005.

[137] J. Wu, Z. Yin, J. Zhan, and W. Heng. Physical Layer Abstraction Algorithms Research for 802.11n and LTE Downlink. In *Proc. of International Symposium on Signals Systems and Electronics (ISSSE)*, 2010.

[138] J. Olmos, A. Serra, S. Ruiz, M. García-Lozano, and D. Gonzalez. Link Level Simulator for LTE Downlink. In *Proc. of 7th European Meeting COST-2100 - Pervasive Mobile & Ambient Wireless Communications*, TD(09)779, 2009.

[139] J. C. Ikuno, M. Wrulich, and M. Rupp. System Level Simulation of LTE Networks. In *Proc. of IEEE 71st Vehicular Technology Conference (VTC), Spring*, 2010.

[140] C. Mehlführer, M. Wrulich, J. Colom Ikuno, D. Bosanska, and M. Rupp. Simulating the Long Term Evolution Physical Layer. In *Proc. of 17th European Signal Processing Conference (EUSIPCO 2009)*, 2009.

[141] T. Hytönen. Optimal Wrap-around Network Simulation. Technical Report , Helsinki,

University of Technology Institute of Mathematics, 2001.

[142] B. Ahn, H. Yoon, and J. W. Cho. A Design of Macro-micro CDMA Cellular Overlays in the Existing Big Urban Areas. *IEEE Journal on Selected Areas in Communications*, 19(10):2094 – 2104, 2001.

[143] Next Generation Mobile Networks (NGMN) Alliance. NGMN Radio Access Performance Evaluation Methodology, Version 1.0, January 2008. www.ngmn.org .

[144] J. D. Parsons. *The Mobile Radio Propagation Channel*. Pentech, 1992.

[145] W. C. Jakes. *Microwave Mobile Communications*. Wiley, 1974.

[146] 3GPP. Evolved Universal Terrestrial Radio Access (E-UTRA); User Equipment (UE) radio transmission and reception (Release 11), version 11.4.0 (2013-03). TS 36.101.

[147] E. Bonek. Tunnels, corridors, and other special environments. In L. Correira E. Damosso, editor, *COST Action 231: Digital mobile radio towards future generation systems*, pages 190–207. European Union Publications, Brüssel, 1999.

[148] U. Gotzner, A. Gamst, and R. Rathgeber. Spatial traffic distribution in cellular networks. In *Proc. of IEEE 48th Vehicular Technology Conference (VTC), Spring*, volume 2, pages 1994–1998, 1998.

[149] D. Huo. Simulating slow fading by means of one dimensional stochastical process. In *Proc. of IEEE 46th Vehicular Technology Conference (VTC), Spring. 'Mobile Technology for the Human Race'*, volume 2, pages 620–622, 1996.

[150] M. Gudmundson. Correlation model for shadow fading in mobile radio systems. *Electronics Letters*, 27(23):2145–2146, 1991.

[151] 3GPP. Feasibility study for Orthogonal Frequency Division Multiplexing (OFDM) for UTRAN enhancement (Release 6), version 6.0.0 (2004-06). TR 25.892.

[152] 3GPP. System Analysis of the Impact of CQI Reporting Period in DL SIMO OFDMA (R1-061506). 3GPP TSG-RAN WG1 45, Shanghai, China, May 2006.

[153] E. Tuomaala and H. Wang. Effective SINR Approach of Link to System Mapping in OFDM/Multi-Carrier Mobile Network. In *Proc. of 2nd International Conference on Mobile Technology, Applications and Systems*, 2005.

[154] 3GPP. OFDM-HSDPA System level simulator calibration (R1-040500). 3GPP TSG-RAN WG1 37, Montreal, Canada, May 2004.

[155] 3GPP. Evolved Universal Terrestrial Radio Access (E-UTRA); User Equipment (UE) conformance specification Radio transmission and reception Part 1: Conformance Testing; (Release 11), version 11.0.1 (2013-03). TS 36.521.

[156] J. T. Entrambasaguas, M. C. Aguayo-Torres, G. Gomez, and J. F. Paris. Multiuser Capacity and Fairness Evaluation of Channel/QoS-Aware Multiplexing Algorithms. *IEEE Network*, 21(3):24–30, 2007.

[157] D. Hong and S. S. Rappaport. Traffic Model and Performance Analysis for Cellular Mobile Radio Telephone Systems with Prioritized and Nonprioritized Handoff Procedures. *IEEE Transactions on Vehicular Technology*, 35(3):77–92, 1986.

[158] M. Kazmi, O. Sjobergh, W. Muller, J. Wierok, and B. Lindoff. Evaluation of Inter-Frequency Quality Handover Criteria in E-UTRAN. In *Proc. of IEEE 69th Vehicular Technology Conference (VTC), Spring*, 2009.

[159] J. M. Ruiz-Avilés, S. Luna-Ramírez, M. Toril, F. Ruiz, I. de la Bandera, P. Muñoz, R. Barco, P. Lázaro, and V. Buenestado. Design of a Computationally Efficient Dynamic System-Level Simulator for Enterprise LTE Femtocell Scenarios. *Journal of Electrical and Computer Engineering*, 2012, 2012.

[160] ETSI. Universal Mobile Telecommunications System (UMTS), Selection procedures for the choice of radio transmission technologies of the UMTS, version 3.2.0 (1998-04). TR 101 112.

[161] I. Viering, M. Döttling, and A. Lobinger. A Mathematical Perspective of Self-Optimizing Wireless Networks. In *Proc. of International Conference on Communications (ICC '09)*, 2009.

[162] WINNER II. Channel Models. Part II. Radio Channel Measurement and Analysis Results. D1.1.2. v1.0, WINNER II IST project, 2007.

[163] T. Sorensen, P. Mogensen, and F. Frederiksen. Extension of the ITU channel models for wideband (OFDM) systems. In *Proc. of IEEE 62nd Vehicular Technology Conference (VTC)*, 2005.

[164] L. Kaelbling, M. Littman, and A. Moore. Reinforcement learning: a survey. *Journal of Artificial Intelligence Research*, 4:237 – 285, 1996.

[165] 3GPP. Evolved Universal Terrestrial Radio Access (E-UTRA) User Equipment (UE) procedures in idle mode, version 10.3.0 (2011-09). TS 36.304.

[166] 3GPP. Technical Specification Group Radio Access Network; Radio Resource Control (RRC); Protocol Specification, version V11.0.0 (2011-12). TS 25.331.

[167] M. N. Halgamuge, H. L. Vu, K. Ramamohanarao, and M. Zukerman. A call quality performance measure for handoff algorithms. *Int. J. Commun. Syst.*, 24:363–383, 2011.

[168] 3GPP. Evolved Universal Terrestrial Radio Access (E-UTRA); Requirements for support of radio resource management, version 11.4.0 (2013-03). TS 36.133.

[169] P. Muñoz, R. Barco, and I. de la Bandera. Optimization of load balancing using fuzzy Q-Learning for next generation wireless networks. *Expert Systems with Applications*, 40(4):984–994, 2013.

[170] P. Muñoz, R. Barco, I. de la Bandera, M. Toril, and S. Luna-Ramírez. Optimization of a Fuzzy Logic Controller for Handover-Based Load Balancing. In *Proc. of IEEE 73rd Vehicular Technology Conference (VTC)*, 2011.

[171] P. Muñoz, R. Barco, J. Ruiz-Avilés, I. de la Bandera, and A. Aguilar. Fuzzy Rule-based Reinforcement Learning for Load Balancing Techniques in Enterprise LTE Femtocells. *IEEE Transactions on Vehicular Technology*, accepted in 2012.

[172] P. Muñoz, R. Barco, and I. de la Bandera. On the Potential of Handover Parameter Optimization for Self-Organizing Networks. *IEEE Transactions on Vehicular Technology*, accepted in 2013.

[173] P. Muñoz, D. Laselva, R. Barco, and P. Mogensen. Adjustment of mobility parameters for traffic steering in multi-RAT multi-layer wireless networks. *EURASIP Journal on Wireless Communication and Networking*, 2013:133, 2013.

[174] P. Muñoz, R. Barco, D. Laselva, and P. Mogensen. Mobility-based Strategies for Traffic Steering in Heterogeneous Networks. *IEEE Communications Magazine*, 51(5):54–62, 2013.